

Geological Society Memoir No. 27

Pyroclastic Density Currents and the Sedimentation of Ignimbrites

Michael J. Branney and Peter Kokelaar



Published by the Geological Society

Pyroclastic density currents and the sedimentation of ignimbrites

Geological Society Memoirs

Society Book Editors

A. J. FLEET (CHIEF EDITOR)

P. DOYLE

F. J. GREGORY

J. S. GRIFFITHS

A. J. HARTLEY

R. E. HOLDSWORTH

A. C. MORTON

N. S. ROBINS

M. S. STOKER

J. P. TURNER

Society Publication reviewing procedures

The Society makes every effort to ensure that the scientific and production quality of its books matches that of its journals. Since 1997, all book proposals have been refereed by specialist reviewers as well as by the Society's Books Editorial Committee. If the referees identify weaknesses in the proposal, these must be addressed before the proposal is accepted.

Once the book is accepted, the Society has a team of Book Editors (listed above) who ensure that the volume editors follow strict guidelines on refereeing and quality control. We insist that individual papers can only be accepted after satisfactory review by two independent referees. The questions on the review forms are similar to those for *Journal of the Geological Society*. The referees' forms and comments must be available to the Society's Book Editors on request.

Although many of the books result from meetings, the editors are expected to commission papers that were not presented at the meeting to ensure that the book provides a balanced coverage of the subject. Being accepted for presentation at the meeting does not guarantee inclusion in the book.

Geological Society Publications are included in the ISI Science Citation Index, but they do not have an impact factor, the latter being applicable only to journals.

More information about submitting a proposal and producing a Publication can be found on the Society's web site: www.geolsoc.org.uk.

It is recommended that reference to all or part of this book should be made in the following way.

BRANNEY, M. J. & KOKELAAR, P. 2002. *Pyroclastic Density Currents and the Sedimentation of Ignimbrites*. Geological Society, London, Memoirs, 27

Pyroclastic density currents and the sedimentation of ignimbrites

Michael J. Branney¹ & Peter Kokelaar²

¹*Geology Department, University of Leicester, Leicester LE1 7RH, UK*

²*Earth Sciences Department, University of Liverpool, Liverpool L69 3BX, UK*

2002

Published by
The Geological Society
London

THE GEOLOGICAL SOCIETY

The Geological Society of London (GSL) was founded in 1807. It is the oldest national geological society in the world and the largest in Europe. It was incorporated under Royal Charter in 1825 and is Registered Charity 210161.

The Society is the UK national learned and professional society for geology with a worldwide Fellowship (FGS) of 9000. The Society has the power to confer Chartered status on suitably qualified Fellows, and about 2000 of the Fellowship carry the title (CGeol). Chartered Geologists may also obtain the equivalent European title, European Geologist (EurGeol). One fifth of the Society's fellowship resides outside the UK. To find out more about the Society, log on to www.geolsoc.org.uk.

The Geological Society Publishing House (Bath, UK) produces the Society's international journals and books, and acts as European distributor for selected publications of the American Association of Petroleum Geologists (AAPG), the American Geological Institute (AGI), the Indonesian Petroleum Association (IPA), the Geological Society of America (GSA), the Society for Sedimentary Geology (SEPM) and the Geologists' Association (GA). Joint marketing agreements ensure that GSL Fellows may purchase these societies' publications at a discount. The Society's online bookshop (accessible from www.geolsoc.org.uk) offers secure book purchasing with your credit or debit card.

To find out about joining the Society and benefiting from substantial discounts on publications of GSL and other societies world-wide, consult www.geolsoc.org.uk, or contact the Fellowship Department at: The Geological Society, Burlington House, Piccadilly, London W1J 0BG; Tel. +44 (0)20 7434 9944; Fax +44 (0)20 7439 8975; Email: enquiries@geolsoc.org.uk.

For information about the Society's meetings consult *Events* on www.geolsoc.org.uk. To find out more about the Society's Corporate Affiliates Scheme, write to enquiries@geolsoc.org.uk

Published by The Geological Society from:
The Geological Society Publishing House
Unit 7, Brassmill Enterprise Centre
Brassmill Lane
Bath BA1 3JN, UK

(Orders: Tel. +44 (0)1225 445046
Fax +44 (0)1225 442836)
Online bookshop: <http://bookshop.geolsoc.org.uk>

The publishers make no representation, express or implied, with regard to the accuracy of the information contained in this book and cannot accept any legal responsibility for any errors or omissions that may be made.

© The Geological Society of London 2002. All rights reserved. No reproduction, copy or transmission of this publication may be made without written permission. No paragraph of this publication may be reproduced, copied or transmitted save with the provisions of the Copyright Licensing Agency, 90 Tottenham Court Road, London W1P 9HE. Users registered with the Copyright Clearance Center, 27 Congress Street, Salem, MA 01970, USA: the item-fee code for this publication is 0305-8719/02/\$15.00.

British Library Cataloguing in Publication Data

A catalogue record for this book is available from the British Library.

ISBN 1-86239-097-5
ISSN 0435-4052

Typeset by Bath Typesetting, Bath, UK
Printed by Henry Ling Ltd, The Dorset Press, Dorchester, Dorset

Distributors

USA
AAPG Bookstore
PO Box 979
Tulsa
OK 74101-0979
USA
Orders: Tel. +1 918 584-2555
Fax +1 918 560-2652
E-mail bookstore@aapg.org

India
Affiliated East-West Press PVT Ltd
G-1/16 Ansari Road, Daryaganj,
New Delhi 110 002
India
Orders: Tel. +91 11 327-9113
Fax +91 11 326-0538
E-mail affiliat@nda.vsnl.net.in

Japan
Kanda Book Trading Co.
Cityhouse Tama 204
Tsurumaki 1-3-10
Tama-shi
Tokyo 206-0034
Japan
Orders: Tel. +81 (0)423 57-7650
Fax +81 (0)423 57-7651
E-mail geokanda@ma.kcom.ne.jp

Contents

Preface	vii		
Acknowledgements	viii		
Chapter 1 Introduction and key concepts	1		
Deposits of pyroclastic density currents	1		
The role of ignimbrites in ideas about pyroclastic density currents	1		
Key concepts	2		
Current steadiness and uniformity	2		
Lower flow-boundary zones: sites of segregation and variable deposition	4		
Ignimbrite architecture: a record of flow-boundary zone evolution through time and space	4		
Chapter 2 The origin, nature and behaviour of pyroclastic density currents	7		
Origin and development of pyroclastic density currents	7		
Eruption styles	7		
Current concentration and rheology	8		
Deflation reappraised	10		
The nature of pyroclastic density currents	10		
The leading part of the current	10		
Current velocity	11		
Velocity profiles and turbulence intensity	11		
Plug flow	13		
Current stratification	14		
Partitioning of mass flux in density-stratified currents	15		
The behaviour of pyroclastic density currents	16		
Inertia, buoyancy, runout distance and lofting	16		
Internal waves, hydraulic jumps and granular jumps	16		
Thalwegs (flow axes) and lateral migration	18		
Effects of topography	18		
A new twofold classification of pyroclastic density currents	20		
Chapter 3 Mechanisms of particle support and segregation	23		
Significance of current heterogeneity and pyroclast diversity	23		
Fluid turbulence	24		
Support by fluid turbulence	24		
Vertical segregation of clasts in the current during turbulent transport	24		
Segregation at the flow-boundary zone due to turbulence	24		
Support on an interface	25		
Sustained support: rolling and sliding	25		
Intermittent support: saltation	25		
Overpassing: downcurrent segregation at an interface	28		
Granular temperature and dispersive pressure	29		
Clast interactions and current mobility	29		
Segregation in granular flows	29		
Fluidization	31		
Fluidization and transport	31		
Segregation by fluidization	33		
Hindered settling, fluid escape and sedimentation-fluidization	33		
Hindered settling and current mobility	34		
Segregation by fluid escape and hindered settling	34		
Clast buoyancy	34		
Buoyancy and transport	34		
Segregation by buoyancy	34		
Acoustic mobilization	35		
Acoustic mobilization and transport	35		
Segregation by acoustic mobilization	35		
Support by strength	35		
Quasi-static grain contacts	35		
Cohesion	35		
		Segregation associated with strength	35
		Particle interlocking	35
		Chapter 4 Conceptualizing deposition: a flow-boundary zone approach	37
		Deposition from steady currents	37
		Direct fallout-dominated flow-boundary zone	37
		Traction-dominated flow-boundary zone	37
		Granular flow-dominated flow-boundary zone	39
		Fluid escape-dominated flow-boundary zone	39
		Gradational types of flow-boundary zone	41
		Selective filtering: flow-boundary zone segregation and overpassing during deposition	41
		Traction carpets	42
		Deposition during unsteadiness	43
		Fluctuating deposition	43
		Sustained gradual changes	43
		Rapid deposition	45
		En masse deposition	45
		Non-uniform deposition	47
		Interpreting ignimbrite lobes and levees	47
		Postdepositional remobilization	49
		Effects of deposition on current behaviour	49
		Chapter 5 Interpreting ignimbrite lithofacies	51
		A lithofacies scheme for ignimbrites	51
		Massive lapilli-tuff lithofacies	51
		Description	51
		Interpretation	56
		Origin of fabrics in massive lapilli-tuff lithofacies	56
		Massive to stratified lithic breccia lithofacies	57
		Description	57
		Interpretation	57
		Segregation of blocks from pumice and ash	60
		Interpretation of stratified breccias and breccia lenses	60
		Classifications of ignimbrite breccias	60
		Massive agglomerate lithofacies	61
		Description	61
		Interpretation	61
		Lithofacies with fines-poor (elutriation) pipes, sheets or pods	61
		Description	61
		Interpretation	66
		Vertical grading patterns	66
		Description	66
		Interpretation	66
		Diffuse-stratified and thin-bedded lithofacies	71
		Description	71
		Interpretation	71
		Stratified and cross-stratified tuffs	74
		Description	74
		Interpretation	74
		Pumice-rich layers, lenses and pods	76
		Description	76
		Interpretation	76
		Massive and parallel-bedded lapilli deposits	77
		Description	77
		Interpretation	77
		Parallel-bedded and parallel-laminated tuffs	83
		Description	83
		Interpretation	83
		Eutaxitic, rheomorphic and lava-like lithofacies	83
		Description	83
		Interpretation	83
		Origin of poor sorting in ignimbrites	84

Chapter 6 Ignimbrite architecture: constraints on current dynamics	87	Interpreting lithofacies at the top of ignimbrites	109
Conceptualizing architecture in a time-geometry framework	87	Transverse lithofacies variations	109
Longitudinal architectures	90	Splay-and-fade stratification	109
Transverse architectures	91	Scour splay-and-fade stratification	110
Interpreting longitudinal (proximal to distal) lithofacies variations	91	Effects of current thalwegs and braiding	111
Longitudinal coarse-tail grading	91	Gradations between massive valley-filling ignimbrite and stratified topographic veneers	111
Downcurrent lithofacies changes from stratified to massive	91	Radially symmetrical ignimbrite distributions	113
Distal lithofacies changes from massive to stratified	93	Ignimbrite fans and asymmetric ignimbrite distributions	115
Interpreting vertical lithofacies variations	95	Interpreting the shape of ignimbrites	115
Gradational versus sharp lithofacies variations	95	A classification of ignimbrite shapes	115
Bedding and flow-unit boundaries	95	Significance of aspect ratio	117
Repetitious and rhythmic lithofacies successions	98	Top surfaces of ignimbrites	118
Disordered lithofacies successions	98	Chapter 7 Overview, key implications and future research	119
Intercalated massive and stratified divisions	98	Overview and key implications	119
Complex longitudinal architectures	98	Future research	121
Interpreting lithofacies successions at bases of ignimbrites	99	Definitions of terms used	123
Stratified bases	99	References	127
Basal pumice lenses	101	Index	137
Fines-poor bases	101		
Fine-grained layers at the base of ignimbrites	101		
Some common successions of basal lithofacies	108		
Sheared or loaded substrate	108		

Preface

Ignimbrites are vast, landscape-modifying deposits composed mainly of pumice fragments and ash. They derive from the most hazardous types of explosive volcanic eruptions and record rapid sedimentation from catastrophic pyroclastic density currents that sweep across the ground. Since early work on ignimbrites by P. Marshall (1935), H. Kuno (1941), R. L. Smith (1960) and R. V. Fisher (1966), there has been a dramatic increase in research into these enigmatic deposits. Particularly instructive field studies include those of ignimbrites from the large caldera volcanoes of the western USA, from the arc volcanoes of the Mediterranean region, Japan, Southeast Asia, South America and New Zealand, and from intraplate volcanoes such as the Canary Islands. Experimental-analogue and numerical modelling of pyroclastic density current behaviour and sedimentation have recently complemented the field-based work. Now there is a bewildering plethora of ignimbrite classification schemes, emplacement models and deposit interpretations. It is therefore timely to take stock, to synthesize modern understanding, and, in particular, to consider how field investigations of ignimbrite lithofacies can best be used both to infer actual pyroclastic density current behaviour and to constrain or test the various models. A fresh look at ignimbrite emplacement is all the more important with the recognition that ignimbrites can relate to eruptions with magnitudes sufficient to impact global climate and biota.

This Memoir reviews what is known about pyroclastic density currents and presents a new *conceptual framework* for investigating the deposition of all types of ignimbrite lithofacies. After introducing some key concepts in Chapter 1, we review important observations and experiments that bear on the nature and behaviour of pyroclastic density currents (Chapter 2), and on the mechanisms by which diverse particles are supported and variously segregated within them (Chapter 3). In Chapter 4 we present the conceptual framework that we have devised to comprehend how different ignimbrite lithofacies are deposited. In this framework, ignimbrite sedimentation is treated as a sustained flow-boundary

process in which the sorting and bed-form characteristics of the deposit relate to different types of concentration and shear distributions within the *flow-boundary zone* that spans the basal part of the current and the uppermost part of the aggrading deposit. Chapter 5 describes and illustrates a wide variety of common ignimbrite lithofacies, including examples from around the world, and in it we apply the flow-boundary zone approach to provide some insights into how they may have formed. In Chapter 6, we elaborate the paradigm developed in earlier chapters to consider how the various architectures of ignimbrites may be used to reveal how flow-boundary zones of sustained currents evolved through time and space. We consider the diverse vertical and lateral lithofacies sequences exhibited by ignimbrites with reference to a temporal framework provided by time-surfaces called *deposchrons* and *entrachrons*. Such sheet-scale analysis is important because an individual lithofacies provides information primarily only about the local flow-boundary zone, whereas the properties and behaviour of the current as a whole may only be deduced when the sheet-scale depositional history is understood.

The flow-boundary zone approach to interpreting ignimbrite sedimentation, linked with the scheme for analysis of ignimbrite lithofacies architecture, provides a powerful means to constrain the overall behaviour and evolution of unseen pyroclastic density currents. The approach begs further research into the mechanisms and rates of the various processes that are inferred. It also has applications for the interpretation of deposits from lahars, turbidity currents, and other types of granular, liquefied or fluidized sediment gravity flows. We hope that this Memoir both stimulates and facilitates further research into pyroclastic density current deposits and into experimental quantification of physical conditions and process rates.

KEY WORDS: density current, sedimentation, ignimbrite, pyroclastic flow, pyroclastic surge, granular flow, fluidization, hindered settling, granular segregation.

Acknowledgements

This work was only possible because of the many excellent field studies of ignimbrites undertaken by numerous workers during the past 30 years. Our ideas have benefited from discussions on ignimbrite deposition with many colleagues, including Richard Brown, Brian Dade, Tim Druitt, Dick Fisher, Bruce Houghton, Malcolm Howells, Ben Kneller, Mauro Rosi, Steve Self, Ronnie Torres, Steve Sparks, Richard Waitt, and Colin Wilson. We particularly thank Marcus Bursik, Jocelyn McPhie, Steve Self,

Colin Wilson and Bruce Houghton for thoughtful reviews that led to significant improvements in the Memoir. Many thanks are also due to Kay Lancaster, who expertly drafted many of the line drawings and saw them tirelessly through countless iterations, and to Helen Kokelaar who sorted out and managed our reference list. We are most grateful to our wives, Tiffany Barry and Helen Kokelaar, especially for their tolerance and patience during our distraction.

Dedication

We dedicate this book to the memory of R. V. Fisher (1928–2002).

Chapter 1

Introduction and key concepts

Pyroclastic density currents are inhomogeneous mixtures of volcanic particles and gas that flow according to their density relative to the surrounding fluid (generally the atmosphere) and due to Earth's gravity. They can originate by fountain-like collapse of parts of an eruption column following explosive disintegration of magma and rock in a volcanic conduit, or from laterally inclined blasts, or from hot avalanches derived from lava domes. They can transport large volumes of hot debris rapidly for many kilometres across the ground and they constitute a lethal and destructive volcanic hazard. Ground-hugging pyroclastic density currents produce a buoyant counterpart, known as a phoenix cloud or co-ignimbrite ash plume, which can carry ash and aerosols into the stratosphere and so cause significant climatic perturbation. Most processes within pyroclastic density currents are impossible to observe and so are commonly inferred from the associated deposits.

Deposits of pyroclastic density currents

Deposits of pyroclastic density currents have been generally categorized, according to lithology and sedimentary structure, as ignimbrites, pyroclastic surge deposits and block-and-ash flow deposits. Ignimbrites typically are pumiceous and ash-rich. They predominantly comprise a poorly sorted mixture of pumice and lithic lapilli supported in a matrix of vesicle-wall-type vitric shards and crystal fragments. They may be loose and uncompact, or partly to entirely densely indurated. Some show evidence of hot deposition (e.g. $\geq 550^{\circ}\text{C}$). They generally form low-profile sheets or fans, which can cover areas as large as 45 000 km², and they tend to bury or partly drape pre-eruption topography with marked thickening into topographic depressions. Ignimbrites can vary in thickness from centimetres to many hundreds of metres, and known examples range in volume from a few thousand cubic metres up to several thousands of cubic kilometres. Many show evidence, in a higher proportion of crystals in the ash-rich matrix than exists in the pumice clasts, that the parent current was originally very rich in fine ash, and that much of this fine ash was lost during transport and deposition. Ignimbrites commonly contain subordinate pumice-poor lithofacies, such as lithic breccias and scoria agglomerates. Although many ignimbrites at first sight appear to be mainly massive (i.e. non-stratified), close examination commonly reveals a wide range of sedimentary structures, including sharp to diffuse stratification, cross-stratification, splay-and-fade stratification, erosion surfaces and elutriation pipes, as well as various grading patterns, particle fabrics and soft-state deformation structures. In many cases such features grade laterally or vertically into truly massive, structureless lithofacies. Ignimbrite sheets and fans are frequently found to comprise the deposits of several pyroclastic density currents, together with closely associated pumice-fall and ash-fall layers. Somewhat better sorted and distinctly stratified layers, sometimes referred to as pyroclastic surge deposits, are normal subordinate lithofacies in ignimbrite successions. Characteristics of ignimbrites are reviewed by Smith (1960), Fisher & Schmincke (1984), Wilson (1986), Cas & Wright (1987) and Freundt *et al.* (2000). Block-and-ash flow deposits differ from ignimbrites in that they contain a large proportion of rather dense, poorly to moderately vesicular juvenile (lava) blocks with predominantly non-pumiceous ash of similar composition. They are generally of smaller volume than ignimbrites and are normally associated with lava domes.

The role of ignimbrites in ideas about pyroclastic density currents

Ignimbrites can contain a wealth of information about their parent

pyroclastic density currents, but the transport and sedimentation processes are not well understood. Problematic issues, partly involving confused nomenclature, concern whether phenomena are discrete or intergradational, instantaneous or progressive. Early workers interpreted poorly sorted deposits and evidence of transport over hills as indicating that the pyroclastic density currents were turbulently mixed, low-concentration suspensions that were many hundreds of metres thick (Murai 1961; Yokoyama 1974; Sheridan & Ragan 1976). The poor sorting and absence of tractional stratification in ignimbrites were interpreted by Fisher (1966) to indicate that pyroclastic density currents are density stratified, with basal particle concentrations sufficiently high to inhibit turbulence and sorting during deposition. Significantly, Fisher (1966) was an early exponent of progressive aggradation for ignimbrites, viewing their deposition as a sustained, incremental process. Subsequently, however, this view was largely abandoned, even by Fisher himself (e.g. Fisher 1979, 1990b), mainly because of the seminal works of G. P. L. Walker and R. S. J. Sparks and their colleagues, who introduced the influential paradigm of a *standard ignimbrite flow-unit* related to bulk evolution of an idealized pyroclastic flow. This flow was considered to be a high-concentration, poorly expanded and partially fluidized granular flow. It was envisaged as having an inflated fluidized head and a denser, laminar body that deflated during transport to form a semi-fluidized, high-yield strength plug that moved along on a basal shear layer. It was believed that the massive layer of the 'standard ignimbrite flow-unit' was formed when such a flow finally came to a halt en masse (Sparks *et al.* 1973; Sparks 1976; Sheridan 1979; Wright & Walker 1981; Freundt & Schmincke 1986; reviews by Carey 1991 and Francis 1993). The thickness of the massive layer formed in this way was thought to be roughly 75% of the thickness of the semi-fluidized flow (e.g. Wilson 1984; Francis 1993), and its vertical organization (e.g. coarse-tail grading) was thought to reflect the vertical structure of the current just before it halted en masse (Sparks 1976; Wilson 1984, 1986; Battaglia 1993; Sparks *et al.* 1997b).

In the 1980s, the standard ignimbrite flow-unit paradigm was elaborated to account for features not previously considered, for example 'fines-depleted ignimbrite' inferred to relate to interactions with substrate (Walker *et al.* 1980), ignimbrite veneer deposits inferred to derive from the 'tail' or 'skin' of a flow (Wilson & Walker 1982; Wilson 1986), pumice-rich basal deposits inferred to have been shot forward, or 'jetted', out of the front of a current (Wilson & Walker 1982), low aspect-ratio ignimbrites inferred to record unusually energetic flows (Walker 1983) and stratified layers near the base of massive ignimbrites inferred to have formed from turbulent boundary layers beneath Bingham-type plug flows (Valentine & Fisher 1986).

More recently, ignimbrites have been treated as deposits from low-concentration currents (less than a few volume per cent (vol. %) solids) in which the particles are all fully supported by fluid turbulence virtually up to the point of deposition, which occurs progressively (e.g. Bursik and Woods 1996; Dade & Huppert 1996; Freundt 1999). These more recent models are quantitative and offer useful constraints on the possible transport behaviour of low-concentration pyroclastic density currents, and how they respond to topography. The models can reproduce some of the overall dispersal characteristics and thickness variations seen in ignimbrites, but as yet they have not succeeded in reproducing the variety and organization of ignimbrite lithofacies and sedimentary structures known from the field.

In 1992, in a paper principally concerned with ignimbrite welding and agglutination, we developed Fisher's (1966) idea that ignimbrites are deposited incrementally from density-stratified currents, the lowermost parts of which are of high concentration

and predominantly non-turbulent (Branney & Kokelaar 1992). In support, we cited evidence from fabric studies, variations in lithofacies and welding characteristics, and the presence of compositional zonation within massive flow-units. We concluded that the massive layers generally aggrade progressively from the base upwards, rather than representing plug flows that halted en masse (Branney & Kokelaar 1992, 1994a, 1997; Kokelaar & Branney 1996). We proposed that the sedimentary processes occurred virtually irrespective of the concentration and transport mechanism(s) of overriding parts of the current, which may differ from current to current. The rate of aggradation might vary from slow to extremely rapid, and because the flow-unit is assembled progressively (through time) it cannot directly record the vertical structure of the current. Instead, the vertical structure of a flow-unit (deposit) records how the processes and conditions around a current's basal flow boundary varied with time. This view of progressive aggradation of ignimbrites has been supported in some recent case studies (e.g. Capaccioni and Sarocchi 1996; Perrotta *et al.* 1996; Scott *et al.* 1996; Bryan *et al.* 1998a; Hughes & Druitt 1998; Duncan *et al.* 1999; Brown *et al.* 2003).

In this Memoir we develop a unified conceptual framework for the consideration of ignimbrite sedimentation, drawing on aspects of all of the above approaches. The emphasis is on ignimbrite sheets formed from intermediate to large-magnitude eruptions (1 km^3 to $> 1000 \text{ km}^3$); however, the approach also has implications for small-volume deposits that form from lava-dome collapses and from Vulcanian eruptions, and also for the stratified sequences, often referred to as 'pyroclastic surge' deposits, that form beyond the limits of block-and-ash flows or during phreatomagmatic explosivity.

We explore the idea that, whatever the concentration of the moving particle-gas mass, deposition is a sustained process (if sometimes only short-lived), and that the style of sedimentation must be governed by conditions and processes around the lower flow boundary of the pyroclastic density current. We investigate how changing conditions (e.g. particle concentrations and shear rates) and processes (e.g. segregation) around the lower flow boundary can account for the wide range of deposit types and their distribution. Each ignimbrite is unique, so, rather than attempt to interpret each known variation, we develop a conceptual framework involving intergradations of processes. In this framework the 'standard ignimbrite flow-unit' and the current it is inferred to have formed from constitute a particular case rather than the norm, just as a current in which transport is entirely at low concentrations constitutes another specific case. We relate vertical and lateral lithofacies distributions within ignimbrites to currents that can have various or changing source emissions, various durations and various clast-concentration profiles, and which are affected by topographies that evolve according to erosion and deposition.

The ideas in this Memoir draw both on the extensive literature that documents ignimbrite lithofacies (e.g. granulometry and fabrics) and on the results of modelling and experimental research into turbulent pneumatic and hydraulic particle transport, granular flow, stratified flow, fluidization and the settling behaviour of non-shearing polydisperse suspensions (references cited in text). We also draw attention to phenomena that remain poorly understood. The hope is that this Memoir will facilitate the interpretation of ignimbrites, and help to stimulate further field observation, laboratory experimentation and numerical simulation. The development of pyroclastic density current models that can predict, and be validated by, moderately detailed lithofacies data is crucially important for the investigation of volcanic hazards and the mitigation of associated risks.

Key concepts

Meaningful analysis of ignimbrites entails integration of four key concepts concerning pyroclastic density currents. (1) Pyroclastic

density currents are inherently inhomogeneous in both time and space, for example with respect to velocity, concentration, capacity and rheology, so that processes within them change both temporally and spatially. (2) Depositional mechanisms are fundamentally influenced by conditions and processes near the lower flow boundary, so that the lithofacies architecture of an ignimbrite essentially records temporal and spatial variations there. (3) Diverse clasts are supported and segregated in various ways so that, for example, adjacent clasts in a deposit may have had differing spatial origins and transport histories. (4) Processes and conditions near a current's depositional flow boundary can differ fundamentally from those higher in the current. These concepts are developed in the following sections.

Current steadiness and uniformity

It is important to distinguish between variations of a current that occur temporally with respect to a fixed location (the Eulerian reference frame) and variations of a current that occur spatially with respect to a point that moves with the current (the Lagrangian reference frame). A current is *steady* where material passes a fixed location with a constant velocity (dashed line on Fig. 1.1A) and direction; that is, in the Eulerian reference frame the current is invariant and acceleration is zero. Conventionally, for one-phase fluids and for low-concentration particulate currents, steadiness refers to velocity. However, with high-concentration particulate currents, other parameters also affect transport and deposition, and it is useful to apply the term 'steady' with a specification: for example, steady velocity, steady competence, steady capacity, steady mass flux and even steady composition (in the sense of the hydraulic properties of the particle population) or temperature. *Steady flow* denotes temporal invariance of all parameters. There are three main types of unsteadiness; *waxing* is when a parameter at a fixed location increases with time, *waning* is when one decreases, and *quasi-steady* is when a parameter fluctuates only slightly about some constant value with limited consequences (Fig. 1.1A).

Many researchers (e.g. Walker *et al.* 1995) have considered pyroclastic density currents to be, in effect, of single-surge type (Fig. 1.1A): that is, an individual short-lived (highly unsteady) pulse that waxes rapidly and then begins to wane almost immediately (such as the rapidly transient current formed from the May 1980 Mount St Helens blast; Druitt 1992). Clearly, all pyroclastic density currents have finite duration and thus all are inherently unsteady, but pyroclastic fountaining eruptions (Sparks *et al.* 1997a; Fig. 2.1B and C) may sustain pyroclastic density currents for periods up to several hours or more, which may include periods of quasi-steady flow (Fig. 1.1A) interspersed with periods of less steady flow. Bursik & Woods (1996) propose that the largest ignimbrites are from eruptions sustained for 10^4 – 10^5 s, and they also suggest that most deposition occurs from quasi-steady flow. Significant waxing and waning of a current during an eruption may result, respectively, from dilation of a conduit and/or vent and from the progressive depletion of volatiles in the magma chamber and conduit by eruptive withdrawal.

Spatial variability of a current at any instant, such as a change in velocity at a break of slope, is described in terms of *non-uniformity*. Uniform currents (spatial acceleration ubiquitously equals zero) do not exist naturally, but parts of some pyroclastic density currents may approach uniformity, particularly where channelled. Non-uniform, or 'varied', flow results from slope changes, sedimentation, elutriation, clast abrasion and breakage, interaction with substrate and air ingestion. Hydraulic jumps and downcurrent changes between turbulent and laminar flow (flow transformations of Fisher 1983) are types of non-uniformity. We use *accumulative* and *depletive*, respectively, to refer to downcurrent increases and decreases in a parameter (e.g. velocity) of a non-uniform current (after Kneller & Branney 1995). A pyroclastic density current is accumulative where, for example, it accelerates as a result of flow convergence or flow down a steepening slope. It is depletive where,

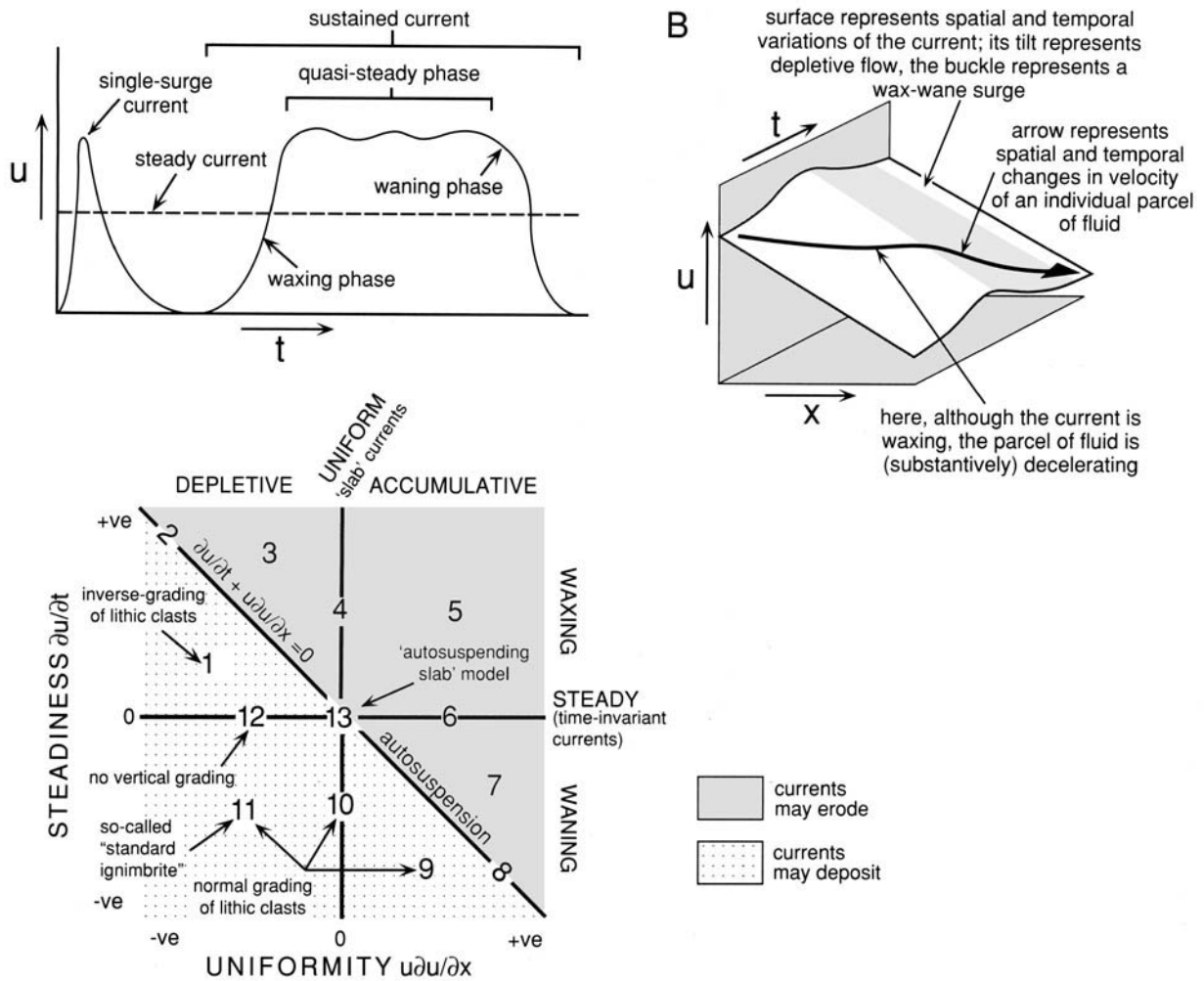


Fig. 1.1. Steadiness and uniformity in pyroclastic density currents. (A) Current velocity, u , versus time, t , at a fixed geographic location. In high-concentration currents velocity, u , may be replaced by concentration, competence or some other parameter. Pyroclastic density currents may vary from highly unsteady single-surge types (left) to more sustained currents (right) that wax and wane and may include periods of quasi-steadiness. (B) Velocity–time–distance (x) diagram for a sustained but unsteady, depletive pyroclastic density current (modified from Kneller & Branney 1995). The heavy arrow shows the deceleration of an individual parcel of fluid in the current; it may decelerate, thus causing deposition, even when the current velocity waxes. (C) Thirteen different types of pyroclastic density current classified according to their steadiness and uniformity, with consequences for grading in deposits. Currents 1–3 are waxing depletive; 4 is waxing uniform; 5 is waxing accumulative; 6 is steady accumulative; 7–9 are waning accumulative; 10 is waning uniform; 11 is waning depletive; 12 is steady depletive; and 13 is steady uniform (autosuspending). Note that the so-called standard ignimbrite flow-unit results from only currents in field 11. The classification considers only one spatial dimension (i.e. the downcurrent dimension). Most natural pyroclastic density currents migrate from one field to another, defining an evolutionary pathway across the diagram; for example, they wax then wane, and they modify the topography and hence change their uniformity by deposition and/or erosion. Grain sizes in graded sequences are subject to availability at source or within material previously deposited and then eroded by the current. Modified from Kneller & Branney (1995).

for example, it decelerates as a result of flow down a lessening (concave) slope or due to spreading radially across flat ground. Progressive infill or erosion of topography, and destruction or burial of vegetation, will cause the non-uniformity of a current to vary. As with steadiness, types of non-uniformity also can involve parameters other than velocity (e.g. competence, concentration).

Previously, ignimbrite emplacement has been considered in terms of deceleration of entire currents, but it is useful to consider the behaviour of individual local ‘parcels’ of fluid, that is, of pyroclasts plus gas. A lithic clast that has been only just fully supported in a current will tend to settle, and ultimately deposit, if the parcel of fluid in which it occurs undergoes negative net acceleration. The net acceleration experienced by a local parcel of fluid is known as the substantive acceleration, and is given by the vector relationship:

$$\frac{D\mathbf{u}}{Dt} = \frac{\partial \mathbf{u}}{\partial t} + \mathbf{u} \cdot \nabla \mathbf{u}. \quad (1.1)$$

See Tritton (1988). Useful insight can be gained by considering the simplification to one-dimensional flow, given by:

$$\frac{du}{dt} = \frac{\partial u}{\partial t} + u \frac{\partial u}{\partial x} \quad (1.2)$$

where u is the local downcurrent velocity, t is time and x is downcurrent distance. $\partial u/\partial t$ is temporal acceleration at a fixed geographical location (zero for steady currents) and $\partial u/\partial x$ is spatial downcurrent acceleration (zero for uniform currents). The equation shows that waning velocity ($\partial u/\partial t < 0$) is not a prerequisite for deposition (Kneller & Branney 1995; cf. Kieffer & Sturtevant 1988). A waning current can erode if it is sufficiently accumulative: for example accelerating down a convex slope or converging into a channel. Such currents are *simultaneously* decelerating in one sense (Eulerian reference frame) and accelerating in the other (Lagrangian reference frame). Conversely, in steady or even waxing density currents, clasts can experience spatial decelerations (Fig. 1.1B) and may tend to deposit: that is, where the current is depletive ($\partial u/\partial x < 0$), such as where it fans out across a plain. Hence, for any density current, use of the terms acceleration and deceleration without stating the reference frame is ambiguous and best avoided by using waxing, waning, accumulative and depletive.

Figure 1.1C classifies 13 conceptual types of pyroclastic density current according to their uniformity and steadiness. The classification is a considerable simplification, especially because it ignores vertical and transverse variations of currents. The 'standard ignimbrite flow-unit' (Sparks 1976) was generally assumed to have been deposited very rapidly during waning and depletive flow of a single-surge type current. Such a current is type 11, and is only one of the 13 conceptual types. Most pyroclastic density currents involve behaviour that would, in this conceptualization, involve migrations within and between some of the fields; for example changing vent emission or unsteady eruptive fountain collapse would register in migrations vertically across Fig. 1.1C, different reaches of an individual current susceptible to slope irregularities would lie horizontally distributed across the fields of Fig. 1.1C and a particular reach of a current affected by modifications to substrate and topography during emplacement would migrate in some sideways direction across the fields. Even this highly simplified conceptualization, which takes velocity to be the sole control on deposition, shows that a sustained pyroclastic density current may deposit and erode intermittently, and at varying rates at different locations, according to changes in vent emissions and changes in topographic slope. Thus we should expect diversity in the nature and organization of lithofacies within ignimbrites.

Lower flow-boundary zones: sites of segregation and variable deposition

The lower flow boundary of a pyroclastic density current is the surface between the current and its substrate. During deposition, the flow boundary must lie at the top of the aggrading deposit and each clast undergoing deposition must cross it. We propose that ignimbrite lithofacies mainly record processes and conditions in a loosely delineated *flow-boundary zone* that includes the lowermost part of the current, the boundary and the uppermost part of the forming deposit (Fig. 1.2). This zone rises relative to the former substrate as the deposit progressively aggrades (Fig. 1.2A).

The nature of the flow-boundary zone, and the rate of progressive aggradation, must vary according to the current velocity, concentration and rate of supply of particles to the flow-boundary zone (the latter is linked to spatial and temporal changes in the capacity of the current). The stratification and sorting characteristics of an ignimbrite lithofacies are largely determined by the particle concentration and velocity profiles across the flow-boundary zone from which the lithofacies aggrades. In later chapters we consider four contrasting types of flow-boundary zone, while emphasizing that each type may be continuously intergradational into another. In one type of flow-boundary zone, the clast concentration in the uppermost part of the deposit is much greater than the concentration of the lowermost levels of the current, so that the concentration and velocity profiles both have a marked step (double inflection) at the flow boundary (Fig. 1.2B). Tractional planar stratification and low-angle cross-stratification require such a flow-boundary zone type, with a high shear intensity close to the flow boundary and a marked rheological contrast across it, so that clasts are able to move freely. In another type of flow-boundary zone the clast concentration of the poorly compacted top of the forming deposit grades up into a high concentration and slowly shearing lowermost part of the current, so that the rheologies of the materials immediately above and just below the flow boundary are similar (Fig. 1.2C). In this case tractional movement and segregation are dampened, and the aggrading deposit acquires less stratification and becomes massive if traction is almost entirely inhibited. In consideration of this latter case, it is useful to define deposit as the *particle mass that has zero downcurrent velocity, irrespective of its packing density*. The aggrading deposit may continue to compact and degas, with segregation of gas-coupled fine ash (elutriation), and it may allow large dense lithic clasts to sink through it. However, once any part of the deposit starts to move downcurrent, it becomes part of the current, by definition.

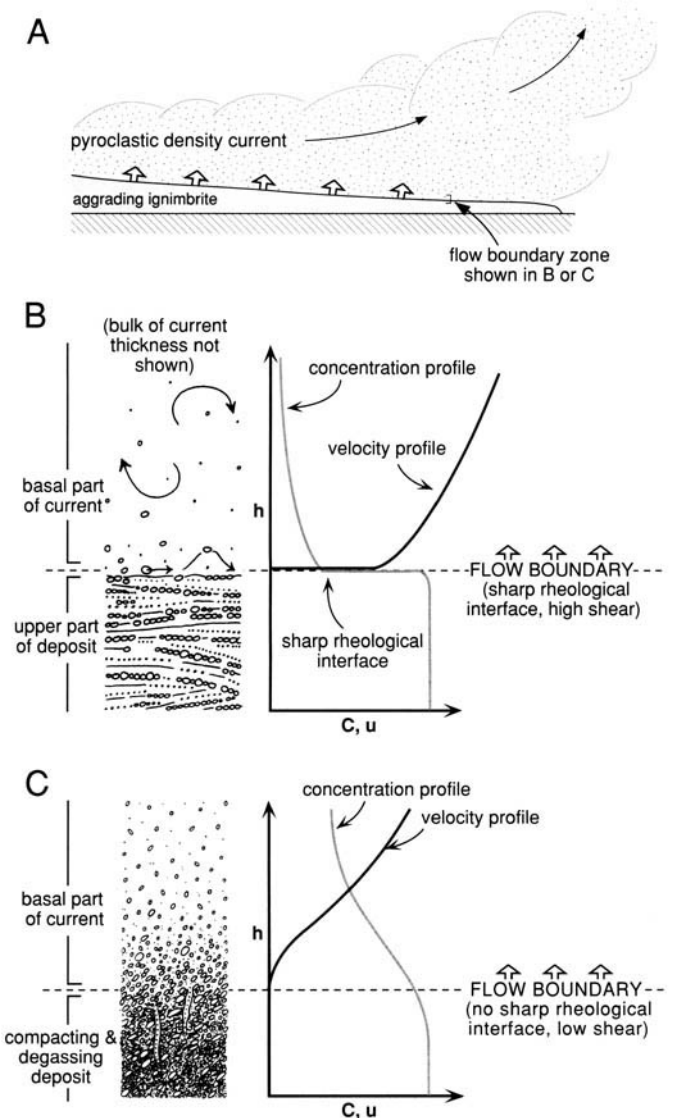


Fig. 1.2. Progressive aggradation of ignimbrite from a sustained current, showing the instantaneous position of the rising flow-boundary zone (A), which includes the lowermost part of the current, the flow boundary and the upper part of the forming deposit. (B) and (C) show two conceptual end-member types of flow-boundary zone whose thicknesses may be in the order of millimetres to decimetres; profiles further above the flow boundary are not shown because they do not directly affect the depositional mechanism. (B) Flow-boundary zone at the base of a low-concentration current, with an abrupt increase in clast concentration and a sharp decrease in velocity down towards and into the top of the deposit. Turbulence impinges close to the flow boundary so that traction occurs. (C) Flow-boundary zone at the base of a high-concentration current, with a gradational increase in clast concentration and a gradational decrease in velocity with depth through the zone. Traction, which requires a sharp interface, is inhibited at the flow boundary by concentrations approaching those of the underlying forming deposit and velocities tending to zero so that a massive deposit aggrades when the current is steady.

Ignimbrite architecture: a record of flow-boundary zone evolution through time and space

We use *architecture* to refer to the overall structure of an ignimbrite: that is, its distribution, thickness variations, and the internal arrangement of lithofacies, 'time surfaces' and any internal or bounding scour surfaces, and the relations of these features to

topography and substrate type. A *lithofacies* describes part of the deposit with a distinctive set of characteristics (e.g. granulometry, stratification, fabric anisotropy and/or composition). As pyroclastic density currents evolve in both time and space, consequent variations in conditions and processes in the flow-boundary zone determine where and how different lithofacies are formed. Thus, the vertical arrangement of lithofacies within an ignimbrite sheet records unsteadiness in the flow-boundary zone, and the horizontal variations record non-uniformity within the flow-boundary zone. Because lithofacies reflect processes and conditions in the flow-boundary zone, they do not directly record bulk properties of the overriding current. Thus, as a first step toward inferring the behaviour of an entire current, one must first interpret each

lithofacies in terms of the flow-boundary zone processes (see Table 7.1) and then analyse the vertical and horizontal lithofacies sequences across an ignimbrite sheet to determine how the flow boundary evolved overall through time and space. Ideally, an aim should be to analyse the architecture of an entire ignimbrite sheet. This is because, even though an ignimbrite may locally exhibit an apparently simple vertical organization (e.g. one that could be interpreted in terms of waning-flow-dominated deposition from a single-surge current), its overall architecture might exhibit complexities that indicate more sustained and complexly evolving currents, including switches in runout direction (e.g. Cole & Scarpati 1993; Branney & Kokelaar 1997; Wilson & Hildreth 1997; see Chapter 6).

This page intentionally left blank

Chapter 2

The origin, nature and behaviour of pyroclastic density currents

In this chapter we consider the initiation and transport behaviour of pyroclastic density currents that deposit ignimbrites. We deal with a wide range of phenomena and assess the limitations in present understanding. Some limitations considered in this chapter and the next lie in the possible differences between pyroclastic currents, which are gas-particle systems, and aqueous analogue experiments from which some understanding has been gleaned. Air has a substantially lower viscosity and density than (liquid) water, is far more compressible and shows far greater thermal expansion. Therefore flow rheologies and processes, like particle settling and sorting in pyroclastic currents, are likely to differ quantitatively from those in aqueous currents, and there may also be some more fundamental differences in behaviour, such as in fluidization, the development and propagation of shock waves and thermal effects, and in the agglomeration (clustering) behaviour of fine ash particles.

Origin and development of pyroclastic density currents

Eruption styles

Pyroclastic density currents originate in different ways and from various sources (Fig. 2.1). They may be short-lived (highly unsteady) phenomena (Fig. 2.1A, D and E) or relatively long-lived (sustained unsteady to quasi-steady; Fig. 2.1B and C). In currents that initiate explosively, the clast concentration of the erupting dispersion relates to the eruption style (e.g. high or low pyroclastic fountaining), which is a function of (1) the magma rheology and mass flux, (2) the volatile abundances, species and exsolution rates, (3) the size, abundance and timing of formation of vesicles and cracks at the time of fragmentation, and (4) the size and abundance of accidental fragments (e.g. see Sparks *et al.* 1997a; Dingwell 1998; Navon & Lyakhovskiy 1998; Alidibirov & Dingwell 2000). In most explosive eruptions the initial volatile contents of the magma are no more than a few weight per cent (wt. %), so that explosively erupting dispersions normally have bulk densities significantly greater than atmospheric density near the vent (atmosphere at sea level is typically 1.25 kg m^{-3}). Clast concentrations in the erupting dispersions are likely to be spatially and temporally heterogeneous.

Pyroclastic fountaining. Many pyroclastic density currents form directly from interior parts of gas-thrust jets in explosive eruptions, where the particulate dispersion loses momentum, fails to incorporate with, and heat, sufficient air to become buoyant, and so follows fountain-like trajectories to the ground (Sparks *et al.* 1997a and references therein). During this process, a buoyant, sub-Plinian or Plinian eruption column may develop above the pyroclastic fountain (Fig. 2.1B) and give rise to pumice-fall deposits associated with the ignimbrite. Occurrences of ignimbrites that apparently lack associated Plinian pumice-fall layers (e.g. possibly Cerro Galán ignimbrite; Sparks *et al.* 1985) may be a result of either (1) low pyroclastic fountaining without development of a tall eruption column (so-called 'boil over' eruptions), where the admixing of air and de-densification were insufficient to form a buoyant plume capable of carrying much pumice to high altitudes (Fig. 2.1C), or (2) an eruption in which Plinian fallout occurred during pyroclastic fountaining, so that pumice lapilli fell directly into widespread pyroclastic density currents and the fallout is not recorded as a pumice-fall layer. Pyroclastic density currents can also form from local instabilities within margins of jet and buoyant regions of Plinian eruption plumes, especially where densification results from re-entrainment of falling pyroclasts (e.g. Carey *et al.* 1988). Plinian fallout layers at bases of ignimbrites are common

and record that an initial convective eruption column formed prior to the onset of pyroclastic fountaining.

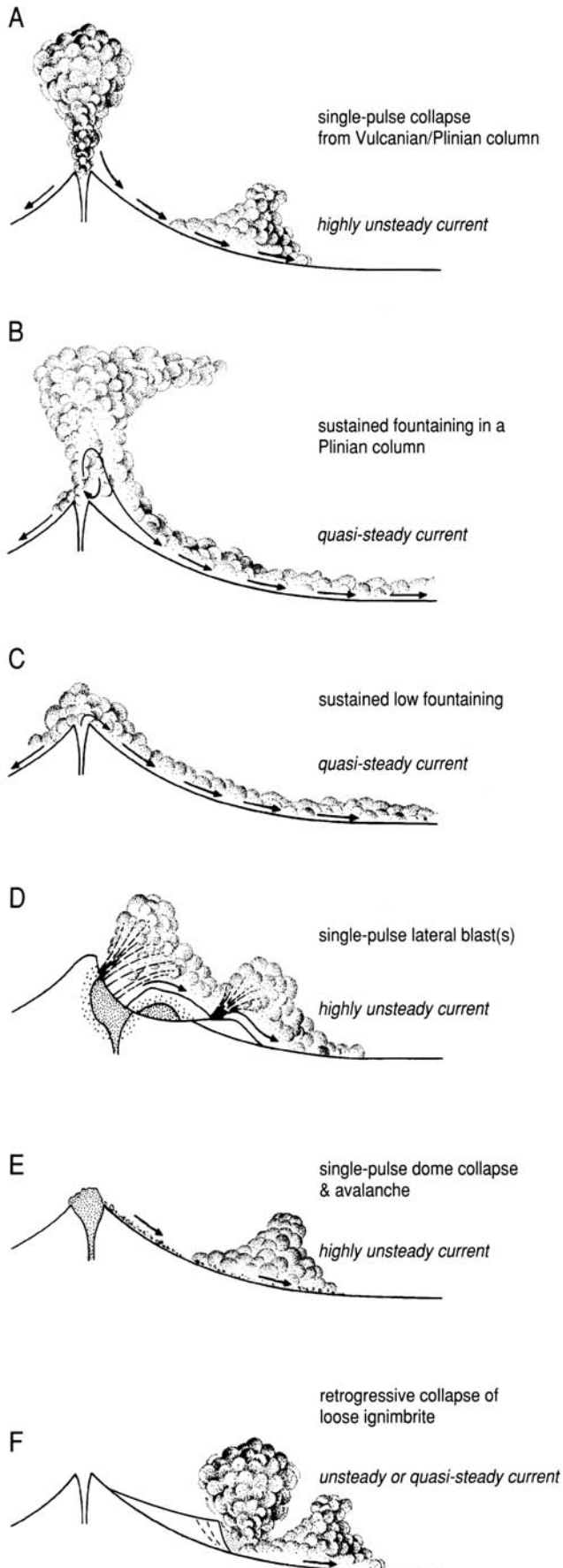
Dispersions with a volume per cent (vol. %) of solids of less than 1 are formed if the mass fraction of exsolved water exceeds 0.03 (Sparks *et al.* 1978), and most explosively derived dispersions are thought to be initially low-concentration turbulent dispersions with bulk densities of a few kg m^{-3} at 10^5 Pa . For example, 0.3 vol. % solids (Dade & Huppert 1996), which is reasonable for an *initial* dispersion at atmospheric pressure, yields a bulk density of approximately 7 kg m^{-3} . Initial dispersions more concentrated than 1% solids may arise due to various factors: (1) lithic debris is commonly entrained into the erupting dispersion from the conduit, vent or caldera walls, or from proximal rock avalanches; (2) local batches of relatively high concentration dispersion originate in convective instabilities at the margins of an eruption plume (e.g. Carey *et al.* 1988; Papanicolaou & List 1988); (3) large clasts may decouple gravitationally from the eruption column or upper parts of a pyroclastic fountain and fall back into the fountaining dispersion (e.g. Bursik 1989); (4) erupting magma commonly is heterogeneous with respect to its volatile content, volatile segregation behaviour, temperature and rheology, as indicated by diverse compositions and vesicularities of juvenile pyroclasts in many deposits (e.g. Wright & Walker 1981; Mellors & Sparks 1991); (5) the explosive decompression of magma is likely to be heterogeneous, even if the magma is initially homogeneous, as indicated by the structure of turbulent jets and by experimental shock decompression of liquids, granular solids and subsolidus magma (Anilkumar *et al.* 1993; Sugioka & Bursik 1995; Alidibirov & Dingwell 1996; Mader *et al.* 1996), and concentration heterogeneities thus formed may survive for substantial periods in turbulent flows (Papanicolaou & List 1988; Sparks *et al.* 1997a).

Models developed by Bursik & Woods (1996) suggest that many extensive ignimbrite sheets derive from eruptions with mass fluxes of 10^9 – $10^{10} \text{ kg s}^{-1}$ over durations of 10^3 – 10^5 s (i.e. 1–10 million tonnes per second for up to 28 hours). Eruption durations for the Bishop and Bandelier tuffs are estimated at about 28 hours, whereas the 10^{11} tonnes (30 km^3) of the Taupo ignimbrite is supposed to have erupted over 20–30 minutes with steady-state flow at 150 – 200 m s^{-1} . The latter figures, however, do not include the ash in the co-ignimbrite cloud, which can amount to as much as 50% of the erupted mass (Lipman 1967; Walker 1972; Sparks & Walker 1977).

Pyroclastic dispersions are compressible fluids that can exit the vent as sonic to supersonic overpressured jets. An inclined jet, producing an asymmetric fountain, may arise where the upper part of the conduit is not vertical, but even where the conduit is vertical the core of the gas thrust column can be inclined due to the effects of crater morphology. Lagmay *et al.* (1999) found that in two-dimensional simulations of small-scale explosive eruptions (their 'Soufrière-type') an over pressured (under expanded) jet tends to tilt towards any low point (e.g. a notch) in the crater rim, thus influencing the main direction of any fountain collapse. Conversely, if vent pressure becomes reduced and/or the crater widens, an over expanded jet tends to tilt towards any crater high point. With radical vent widening, as is likely with caldera collapse, any consequent subsonic gas thrust will tend to be vertical. Thus, in the course of an ignimbrite-forming eruption that initiates at a central vent, early pyroclastic density currents may be directed towards particular sectors, whereas later ones may be more radially directed. Further modelling, in three dimensions, is required to assess the possible importance of such effects during ignimbrite-forming eruptions.

Ignimbrites may be emplaced during phreatomagmatic pyroclastic fountaining (e.g. Self 1983; McPhie 1986). Such ignimbrites may

be particularly rich in fine ash, may contain some blocky phreatomagmatic shards and accretionary lapilli, and may be associated with phreatomagmatic ash-fall deposits (see pp. 74 and



83). It is likely that all gradations exist between phreatomagmatic and magmatic pyroclastic fountaining.

Lateral blasts. Some pyroclastic density currents derive from inclined or laterally directed explosive decompression jets (Fig. 2.1D), as in the 30 March 1956 eruption of Bezymianny (Bogoyavlenskaya *et al.* 1985) and in the 18 May 1980 eruption of Mount St Helens (Hoblitt 1986). Known examples were sustained for only short durations and did not produce large-volume ignimbrites. In such currents, inertial forces initially, but briefly, dominate over gravitational forces and, owing to compressibility effects and/or complex effects of turbulent mixing, the current may initiate with marked and irregular inhomogeneities of density (Papanicolaou & List 1988; Anilkumar *et al.* 1993). It remains to be explored if, and how, such near-source density fluctuations in a high-velocity pyroclastic current may affect more distal, decelerated parts of the pyroclastic current where gravitational forces have become dominant.

Collapsing lava domes. Rock avalanche-type pyroclastic density currents that are derived from collapse of lava domes or lava-flow fronts (Fig. 2.1E) tend to develop overriding low-concentration dispersions by rapid generation and segregation of relatively fine pyroclasts from underlying relatively high-concentration debris falls and granular flows (see pp. 25–30). The process involves clast comminution by breakage, abrasion and vesicle rupture, with accompanying admixture and expansion of air, as at Santiaguito (Rose *et al.* 1977), Merapi (Bardintzeff 1984), Mount Unzen (Yamamoto *et al.* 1993; Ui *et al.* 1999) and Montserrat (Cole *et al.* 1998, 2002). Stress induced by steep thermal gradients across hot fragments can cause the clasts to decrepitate spectacularly on impact, sometimes explosively, and generate abundant fines (Mellors *et al.* 1988). Similarly, elevated volatile content in mesostasis between anhydrous crystallites promotes explosive decrepitation of microcrystalline lava blocks (Sparks 1997). Most pyroclastic density currents produced in this way generate small-volume block-and-ash flow deposits (Boudon *et al.* 1993; Cole *et al.* 2002).

Current concentration and rheology

Some models of pyroclastic density currents involve low or very low clast concentrations, similar perhaps to concentrations on eruption (e.g. 0.3 vol. %, Dade & Huppert 1996; < 5 vol. %, Bursik & Woods 1996), but these cannot be reconciled with several lithofacies of ignimbrites (e.g. Wilson 1997) apparently formed from parts of currents with high clast concentration (see Chapters 5 and 6). In contrast, on the evidence of lobate deposit morphologies

Fig. 2.1. Origins of pyroclastic density currents. (A) Short single-surge current derived by momentary collapse from a Plinian eruption column. (B) Sustained current derived from prolonged pyroclastic fountaining. The height of the jet (gas thrust) that feeds the current may vary and is transitional into (C). (C) A sustained current derived from a prolonged low pyroclastic fountaining (boil over) explosive eruption. This lacks the kinetic energy derived from the potential energy of a high fountain. It may be accompanied by a buoyant eruption column (not shown) that does not feed the current. (D) Current with a single (or multiple) surge derived from lateral blasts initiated by catastrophic decompression of a magmatic and/or hydrothermal system. (E) Single-surge current derived from a collapsing lava dome or flow front. Hot rock avalanches generate turbulent density currents. (F) Deposit-derived pyroclastic density current caused by gravitational collapse and avalanching of unstable loose ignimbrite, sometimes long after the eruption has ended (see p. 49). The current may be a single-surge or more sustained where the collapse is retrogressive. Most large-volume ignimbrites derive from current types (B) and (C), which may involve periods of quasi-steady flow. Many may include significant components derived from currents of type (F).

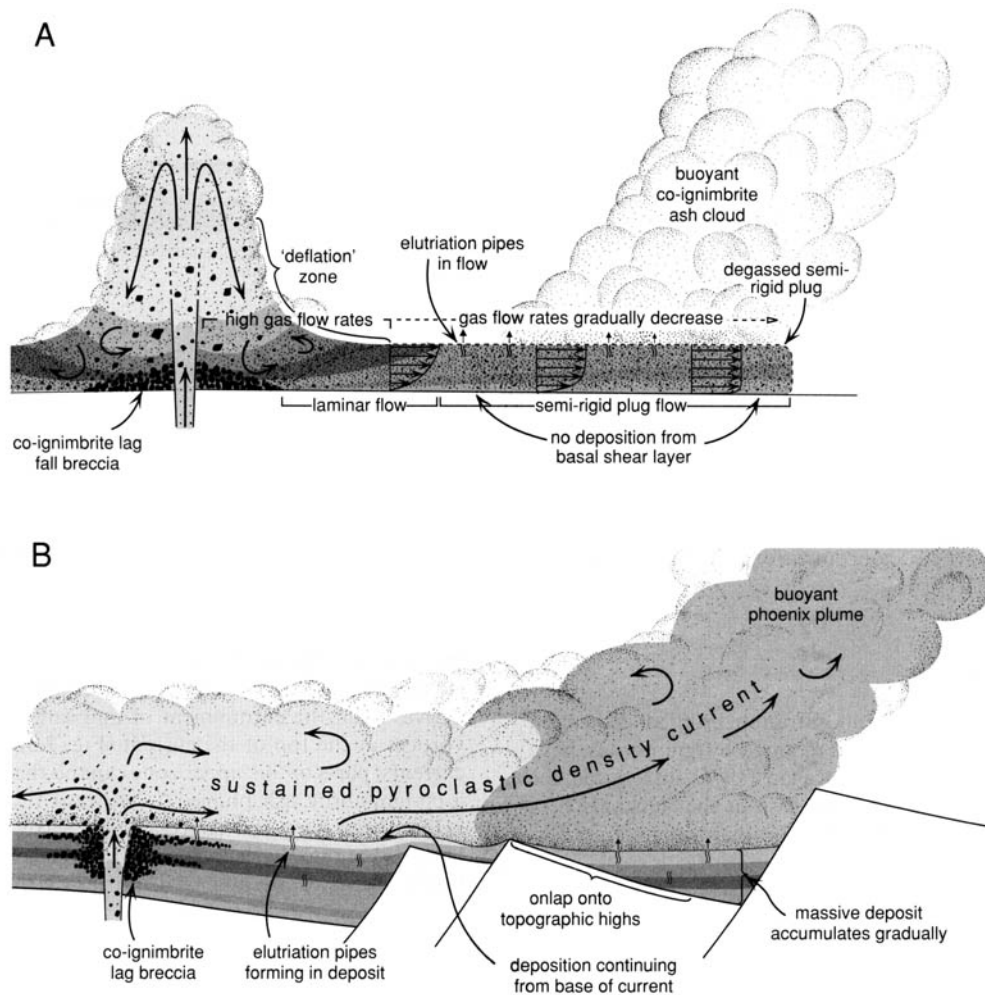


Fig. 2.2. Alternative models of ignimbrite emplacement (after Branney & Kokelaar 1997). (A) A giant, laminar, semi-fluidized flowing dispersion originates within a proximal 'deflation zone' and, during transport, evolves wholesale into a decelerating plug flow until the basal shearing layer pinches out whereupon the entire plug comes to a halt en masse. The upper turbulent low-density ash cloud is derived by elutriation from the laminar to plug-like fluidized pyroclastic flow. Velocity profiles and instantaneous time lines are indicated. Compiled from Wright & Walker (1981), Druitt & Sparks (1982) and Walker (1985). (B) A sustained density current expands and develops density stratification in which clast concentrations increase toward the base along the entire runout due to sedimentation, segregation and flow boundary effects. There is no discrete deflation zone. Elutriation pipes develop in the deposit, not in the current. Upper levels are an integral component of the density current and become progressively diluted as a result of sedimentation, and due to the ingestion, mixing and thermal expansion of air. Parts of the current that become less dense than ambient air loft buoyantly to form a co-ignimbrite, or phoenix, plume.

(see p. 48), some small pyroclastic density currents have been interpreted as having had very high concentrations, high viscosities, and high yield strengths (i.e. values similar to those of uncompacted ignimbrites; Wilson & Head 1981). It is likely that different pyroclastic density currents have different concentrations. However, determination of current concentration and rheology from deposit characteristics is less straightforward than has been supposed previously (see Kokelaar & Branney 1996). For example, matrix-supported lithic blocks in non-stratified parts of ignimbrites (often misleadingly named 'floating' blocks) have been interpreted to indicate either that the original current had a yield-strength sufficient to support the blocks high within it during transport (e.g. Francis 1993, p. 264), or that during transport the current behaved as a laminar Newtonian fluid through which the blocks gradually settled, so that their height in an ignimbrite is a function of the current viscosity, velocity and transport distance (e.g. Sparks 1975, 1976; Freundt & Schmincke 1986). We favour the alternative that such lithic blocks mainly roll, slide and/or saltate into place along the rising deposit surface during progressive aggradation (see p. 25), so that their height in an ignimbrite records the thickness of deposit that had aggraded before the blocks finally came to rest (Kokelaar & Branney 1996; this thickness may have been modified by compaction), minus any depth the blocks sank through the newly

formed loose deposit (see Fig. 5.7). Hence, coarse-tail grading of lithic clasts is more a reflection of the changing supply of clasts to a particular location through time, and varying flow-boundary conditions and segregation processes (see p. 66), than it is a measure of the overall current rheology and concentration. Similarly, inversely graded pumice concentrations towards the top of ignimbrites were thought to indicate that the pyroclastic currents were denser than the pumice clasts, which consequently floated to the top (Sparks 1976; Wilson 1980; Wilson & Head 1981). But, this only applies if the deposit represents the whole current, which stopped en masse. With progressive aggradation, any type of clast at any level in an ignimbrite must have passed through the lower flow boundary of the current when it was deposited (i.e. it was not at the top of the current), so pumice-grading patterns, like lithic-grading patterns, cannot be interpreted quite so simply in terms of the current's overall bulk density (see pp. 66–71).

Pyroclastic transport across water is indicated by occurrences of ignimbrites on land that is separated from the source volcano by a stretch of sea, which may be as much as tens of kilometres wide: for example the Koya ignimbrite of Japan (Ui 1973), the Campanian Tuff of Italy (Fisher *et al.* 1993), the Krakatau ignimbrite of Indonesia (Carey *et al.* 1996) and the Kos Plateau Tuff of Greece (Allen & Cas 1998). This evidence indicates that substantial parts of

the parent pyroclastic density currents were less dense than water, although denser parts may have entered the sea near the proximal shoreline (e.g. generating turbidity currents). Poorly sorted massive lithofacies on the distal (opposite) shore indicate that the pyroclastic currents developed denser basal parts when they crossed back onto land (for a proposed mechanism see p. 92). Shallow-marine welded ignimbrites suggest that lower levels within some pyroclastic density currents have densities of $>1020 \text{ kg m}^{-3}$, sufficient to displace and flow beneath sea water (Kokelaar & Königer 2000). This indicates a solids concentration of $\geq 40\text{--}45 \text{ vol. \%}$.

More work is needed to determine rheology and concentration distributions of pyroclastic density currents. Ignimbrite lithofacies (see Chapter 5) show that currents are, at least in part, *hyperconcentrated*, in having concentrations that are transitional between low-concentration currents in which particles are fully supported by fluid turbulence, and granular flows with negligible particle support by fluid turbulence. Moreover, lithofacies variations in ignimbrites indicate that currents typically are stratified in terms of their particle concentration (i.e. they are density stratified), and also that the particle concentrations are spatially and temporally heterogeneous.

Deflation reappraised

The processes by which a low-concentration erupted dispersion might densify on the ground, as seems required by ignimbrites, have long been problematic. Sheridan & Ragan (1976) introduced the term deflation for the 'progressive decrease in the thickness of a moving pyroclastic flow due to densification that accompanies loss of gas and kinetic energy'.

Occurrences, within a few kilometres of the vent, of typical, massive fines-rich ignimbrite with matrix-supported lapilli have been interpreted as registering development of a high-concentration semi-fluidized laminar or plug flow by 'deflation' of a low-concentration suspension that descended from a Plinian eruption column (see Fig. 2.2A; Druitt & Sparks 1982; Walker 1985). This deflation was inferred to occur in a 'deflation zone' located closer to the vent than the occurrences of fines-rich ignimbrite, and to be characterized by the deposition of lithic breccias (see fig. 3 of Walker 1985). How a low-concentration dispersion could deflate to a high concentration in a short distance from the vent, whilst retaining its fine ash, was considered problematic, mainly because it would be expected that during deflation the expelled gas would elutriate out the fine ash. It was suggested that compression of gas at the base of a collapsing tall eruption column might achieve a concentration sufficiently high to prevent the fine ash escaping (Druitt & Sparks 1982), but it is not clear that such a compressed dispersion would flow away from the impact zone in its compressed state as a laminar semi-fluidized bed; models suggest that the residence time of a dispersion in the compressed state is a matter of only tens of seconds (e.g. Wohletz & Valentine 1990). It is now thought that many pyroclastic density currents derive from fountaining of the core region of the eruptive jet (the lower 'gas-thrust' part of the eruption column), rather than from the collapse of formerly buoyant high parts of a plume (Sparks *et al.* 1997a), but the problem of densification still remains (but see p. 92).

Models and experiments involving polydisperse particulate gravity currents show that fine particles occur throughout the current thickness and can readily deposit with relatively coarse clasts, which show pronounced segregation towards the current base (e.g. García 1994; Bursik *et al.* 1998; see Fig. 3.3). We infer that massive fines-rich ignimbrite merely records high particle concentrations in a lower flow-boundary zone. Hence, proximal occurrences of massive fines-rich ignimbrite do not mean that the entire thickness of the proximal current was necessarily of high concentration, and therefore there is no need to invoke a major body transformation (*sensu* Fisher 1979) from a low-concentration current into a concentrated current via proximal 'deflation' (Fig.

2.2). We propose that, rather than a discrete proximal 'deflation zone', gravity-induced segregation occurs throughout most reaches of a depositing pyroclastic density current (see pp. 14 and 15), forming relatively high basal concentrations while the displaced gas transfers fine ash into less concentrated, higher levels of the current, which may expand. Proximally, gas compression and/or remobilization of loose deposits may also be involved. Even so, deflation is an inappropriate term; hot polydisperse pyroclastic density currents tend to inflate rather than deflate (e.g. Huppert *et al.* 1986; Sigurdsson *et al.* 1987).

The nature of pyroclastic density currents

The leading part of the current

A turbulent single-surge density current consists of a leading edge, with various possible forms, and a long trailing body (Middleton 1970; Simpson 1997; Kneller & Buckee 2000). The leading edge of the current typically has an overhanging nose and, in some cases, the part immediately behind this forms a distinct head that is thicker and travels more slowly than the body, particularly on steep slopes. Transverse vortices (Kelvin–Helmoltz billows) develop in the top of the head and trail behind it, producing a low-concentration mixing zone, or wake, above the body. This zone derives from the entrainment of ambient fluid into the transverse vortices at the top of the current (Fig. 2.3). In pyroclastic density currents, parts of this upper zone expand thermally and loft to form a co-ignimbrite ash plume. A rearward thinning 'tail' may occur below the trailing low-concentration wake in some currents. The body is commonly depositional, although it may be non-depositional or erosive. Because of its intrinsic strong non-uniformity, the leading part of a current can be erosional, non-depositional and depositional in different parts and/or at different times.

Leading parts of pyroclastic density currents are less well understood than are those of aqueous currents. Some may comprise a bulbous transverse vortex characterized by extreme non-uniformity and unsteadiness, while others may be wedge-shaped in longitudinal profile, with a rounded nose but little or no morphologically distinct head (Kieffer & Sturtevant 1984; Allen 1985; Valentine & Wohletz 1989; Simpson 1997). Various leading-edge morphologies and behaviours can be anticipated (Fig. 2.3B and C), related to: (1) styles of interaction between the current and the ambient atmosphere, for example developments of lobes and clefts (Rayleigh–Taylor instabilities) and/or billows (Kelvin–Helmoltz instabilities) with associated variations in rates of ingestion, mixing and thermal expansion of air; (2) interactions with the ground (e.g. involving combustion of vegetation or steam expansion due to rapid heating of a wet substrate, or involving drag influenced by ground roughness, erosion and sedimentation); and (3) inherent current properties, such as the nature of the particle population, density stratification and velocity profile, or the rate of leading-edge advance (see the following sub-section). Changes will occur as the current waxes and wanes, and as it crosses changes of slope. Leading edges with marked fluctuations in rates of advance of basal and overriding parts (Hoblitt 1986) are probably influenced by unsteadiness in pyroclast supply and rates of sedimentation, or ingestion and expansion of air. Thermal expansion and lofting may retard downslope advance of a current's leading edge, and promote sedimentation of coarser pyroclasts while rapidly drawing clear air inwards towards the axis of the density current (Huppert *et al.* 1986). On slopes, large 'debris fall' blocks (see p. 28) can bounce, or roll, out ahead of the leading edge of the current.

Causes for differences in sedimentation between a current's leading parts and those further behind are considered further in Chapter 6 (p. 99, 'Interpreting lithofacies successions at bases of ignimbrites').

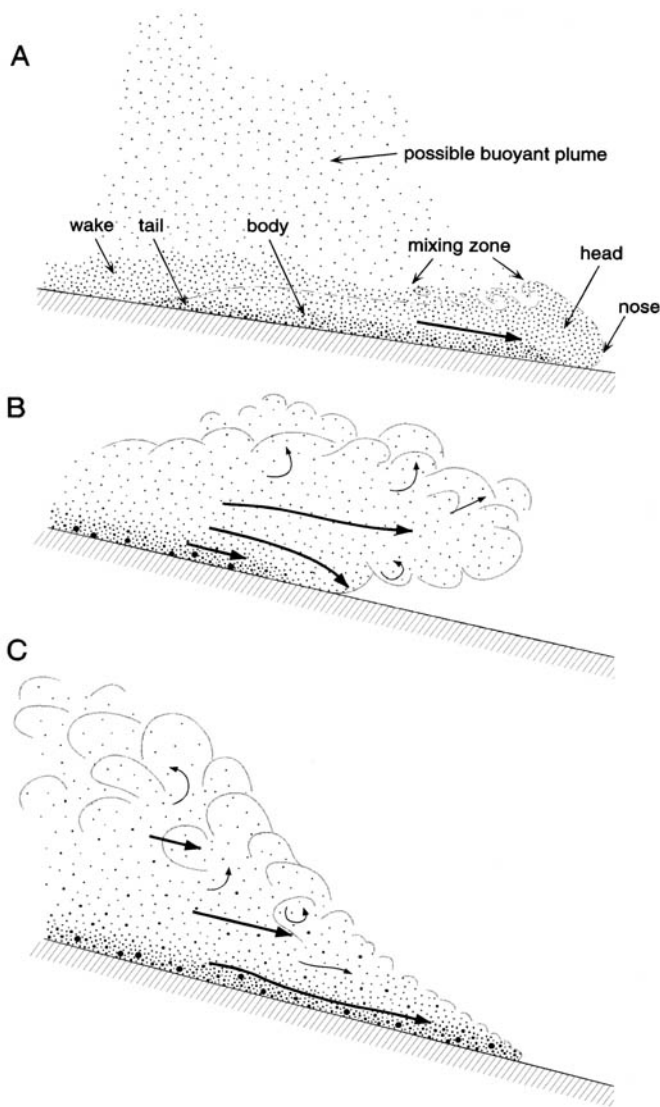


Fig. 2.3. Leading parts of density currents. **(A)** Generalized structure of a single-surge turbulent incompressible density current, with a head intergradational into a body with an overriding mixing zone and trailing wake (modified from Simpson 1997). Note that in the case of a sustained pyroclastic density current, the cumulative length of the body may far exceed the maximum runout distance. The extent to which a head develops is widely variable, and depends both upon the current properties and the substrate slope. **(B)** Overhanging head resulting from sluggish granular flow-dominated lower levels being overridden by more mobile higher levels of a density-stratified current. Velocities as for Fig. 2.4B. This current may first deposit a tractional stratified division and, later, an overlying massive division. **(C)** Advance of a density-stratified current dominated by fast-moving basal levels. The upper part of the head, expanded by air ingestion, trails behind due to air resistance. The resultant massive ignimbrite does not have a tractional stratified layer at its base, because the dilute turbulent parts of the current are not in contact with the lower flow boundary. All gradations between **(B)** and **(C)** occur, and in some cases all levels in the current may advance at a similar rate. Leading edges may fluctuate rapidly between **(B)** and **(C)** (e.g. Hoblitt 1986) so that the base of the resultant ignimbrite develops an impersistent tractional stratified layer.

Current velocity

Direct measurement of the velocity of a pyroclastic density current is difficult. The rate of advance of the leading edge of a density current cannot be taken to represent current velocity, which can be substantially faster (e.g. up to 40 % faster; Britter & Linden 1980; Allen 1994). A sustained pyroclastic density current can have a virtually stationary leading edge that is the downcurrent transport

limit of gas and particles supplying aggrading ignimbrite and a complementary buoyant phoenix plume. Material at the distal limit of an ignimbrite may have been deposited there from a high-velocity current, if it is where the ground-hugging density current left the ground to loft. Recorded leading edge advance rates are 28 (Rowley *et al.* 1981), 5–30 (Hoblitt 1986), 15–25 (Yamamoto *et al.* 1993), 64 (Moore & Melson 1969), 150 (Moore & Rice 1984), and 3–30 and 60 m s^{-1} (Cole *et al.* 2002; Loughlin *et al.* 2002a, b), although these are all for small pyroclastic currents that did not deposit extensive ignimbrite sheets.

In the absence of direct measurements of current velocities, estimates have been derived from their deposits and erosive effects using various flow models. Kieffer & Sturtevant (1988) estimated from the geometry of erosional furrows that the velocity of the 18 May 1980 blast-derived pyroclastic current of Mount St Helens at 10 km from source was 235 m s^{-1} , which is approximately twice that of the measured advance of the current's leading edge. These authors considered that this high velocity implied that the current was akin to an underexpanded jet. Although the current may have initiated as a jet, it probably transformed into a gravity current well within 10 km from source. The jet model does not resemble the gravity-dominated currents inferred to deposit large ignimbrites. The distribution and relation to topography of the 30 km^3 Taupo ignimbrite led Wilson (1985) to infer current velocities $\geq 200 \text{ m s}^{-1}$, and Freundt & Schmincke (1986) estimated 10–25 m s^{-1} based on asymmetric cross-valley profiles of Laacher See ignimbrites at valley bends. These velocity calculations, which used deposits to assess whole-current thickness and density values, in effect using the model of en masse deposition of a partly fluidized flow, may, with hindsight, be inappropriate. With progressive aggradation the top of an ignimbrite marks the *base* of the last part of the current, and does not represent the top of the current. Similarly, although channelled pyroclastic density currents will, through momentum, flow higher on the outside bank of a bend than on the inside bank, it can be difficult to determine the thickness of the current at any particular time from trim lines and the net thicknesses of aggraded deposit, especially when the current may have been sustained, depositing and unsteady. Difficulties in inferring velocities from scour lines, trim lines and swash marks on valley sides arise from: (1) current density stratification; (2) waves; (3) multiple surges; and (4) the unknown thicknesses of already aggraded deposit at the time of their formation. Velocity values deduced from deposit attributes are only as valid as the flow models on which they are based, and it is generally unrealistic to assign a single velocity value to a stratified, unsteady and non-uniform current.

Models employed by Bursik & Woods (1986) and Dade & Huppert (1996), which deduce an initial dispersion density and are then dependent on runout distance and granulometry, imply flow velocities of up to 200 m s^{-1} . If the current velocities exceed the sound speed of the dispersion, compressibility can be anticipated (see 'Lateral blasts' on p. 8). Sound speeds in particulate dispersions are considerably less than those in air (330 m s^{-1}), possibly as low as 50 m s^{-1} (Kieffer & Sturtevant 1984), but it may be simplistic to describe a pyroclastic density current as either supersonic or subsonic, because sound speed is not uniquely defined in a density-stratified dispersion.

Velocity profiles and turbulence intensity

Velocity profiles through opaque particulate currents are difficult to measure and to predict, and experimental data are sparse (Ishida & Hatano 1983; Roco & Shook 1984; Altinakar *et al.* 1996; Best *et al.* 2001). Novel laboratory techniques that use ultrasound and the Doppler frequency shift yield valuable insights into the vertical velocity and turbulence structure of experimental gravity currents (Best *et al.* 2001). The potential effects on velocity of entrainment and expansion of air, and lofting, in a pyroclastic density current have not been assessed. Aqueous particulate currents are commonly found to have a velocity maximum at approximately 0.2–0.3

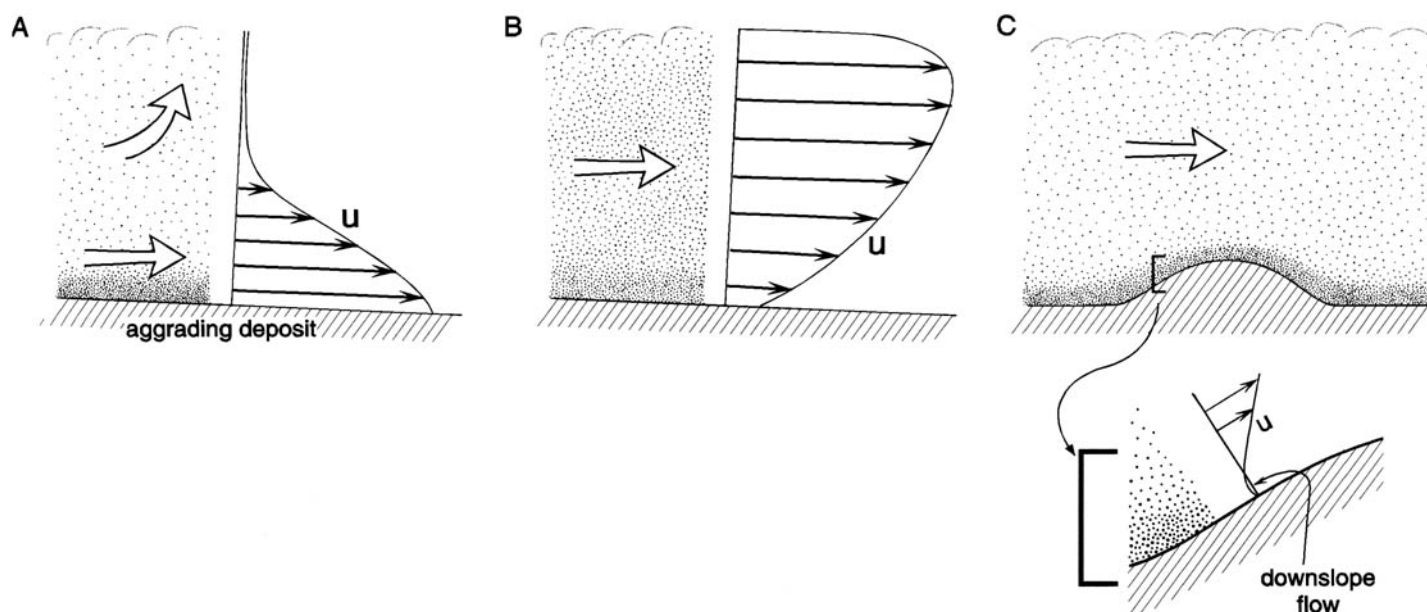


Fig. 2.4. Possible alternative velocity profiles for sustained stratified pyroclastic density currents. (A) Upper levels trail behind more rapid dense lower parts as a result of their lower densities and greater air resistance. (B) Upper levels move rapidly downslope and exert tractive stress on more sluggish, higher viscosity basal parts. (C) Clasts undergoing hindered settling decelerate gradually to a halt as they encroach the lower flow boundary (inset; compare velocity profile with that of Fig. 1.2C) and gravity causes them to settle downslope irrespective of the overall current transport direction. Although such final stages of movement may involve minimal transport, they can produce measurable anisotropy of magnetic susceptibility (AMS) or grain fabrics whose shear sense may give a misleading impression of the overall current transport direction.

of the head height above the substrate, and this region shows relatively low turbulence intensities (Kneller & Buckee 2000; Best *et al.* 2001). It is reasonable to assume that velocity profiles vary with changes in topographic slope, changes in sedimentation rate and air ingestion, and as a result of unsteady supply at source. Velocity profiles of stratified currents that have high-concentration basal parts (Fig. 2.4) are likely, in addition, to vary according to the variations in density and rheology with height (e.g. Postma *et al.* 1988). The upper levels of a current that rise buoyantly (loft) may be outrun by the lower, denser levels (Fig. 2.4A) and, conversely, rapid, low-concentration upper levels of a current may exert shear stress on a relatively sluggish (higher effective viscosity) high-concentration basal part (Fig. 2.4B). Different levels within a current can advance in different directions, such as on an upcurrent-dipping slope, either due to topographic reflection (see 'Effects of topography' p. 18) or simply due to downslope settling of clasts within the flow-boundary zone, virtually irrespective of the overriding transport direction (Fig. 2.4C).

The intensity of turbulence in pyroclastic density currents is likely to vary widely, but there are few data. All direct observations show intense turbulence, but concealed less-turbulent parts are to be expected. Turbulence is most intense where there is vigorous mixing with ambient atmosphere, especially for supercritical currents (see p. 16), and where a current that lacks a highly concentrated basal region interacts with rough ground. Although turbulence is enhanced by flow across irregular topography or rough substrates such as rocky ground and forest, which are common in subaerial volcanic terrain, progressive aggradation of ignimbrite will tend to smooth out irregularities during emplacement (Branney & Kokelaar 1997).

With Newtonian fluids the onset of turbulence in currents occurs where the Reynolds number, Re , is > 500 – 1000 , where:

$$Re = \frac{\rho U d}{\mu_s} \quad (2.1)$$

in which ρ = current bulk density, U = characteristic velocity, d = current thickness, and μ_s = current effective viscosity. On this basis, Middleton & Southard (1984) concluded that aqueous liquefied and

fluidized density currents, even of small scale, are likely to develop turbulence when they move down 'any substantial slope'. Sparks (1976) proposed that turbulence is likely in a 'high concentration' (i.e. grain interactions dominate throughout) semi-fluidized pyroclastic density current that is thicker than several metres and moving at velocities > 15 – 60 m s^{-1} . The analysis in general, however, is fraught with the practical difficulties of determining meaningful values of ρ , U , d and μ_s . In particulate fluids the particles tend to suppress turbulence because they have a different inertia to that of the interstitial fluid phase. The requirement that gas flows around particles that cannot move with it, because of inertia, constitutes an additional frictional force that dissipates energy and acts to dampen turbulence. Equation (2.1) suggests that any thin, relatively high-concentration basal parts of a pyroclastic density current will have considerably diminished turbulence at low velocities. Nevertheless, as with modified grainflows, avalanches and cohesive debris flows (Middleton 1970; Enos 1977; Middleton & Southard 1984; Nemeč 1990), pyroclastic density currents probably develop substantial turbulence when moving rapidly, even though they produce massive deposits from their lower flow boundaries. Evidence for this occurs locally within many ignimbrite sheets, where subordinate stratified lithofacies indicate that turbulence locally impinged downwards to the flow boundary from higher levels in the current, causing traction (e.g. Wilson and Walker 1982; Freundt & Schmincke 1986; Schumacher & Schmincke 1990; Cole & Scarpati 1993; Schumacher & Mues-Schumacher 1996; Branney & Kokelaar 1997).

Absence of tractional structures in massive ignimbrite is widely interpreted as indicating non-turbulent flow (e.g. Sparks 1976; Cas & Wright 1987; Carey 1991; Cole *et al.* 1993). But the deposit reflects only conditions of the flow-boundary zone, not of the rest of the current, and it only records these conditions during the period(s) of deposition, which may not be representative of the entire history of the current at that location. Vertical chemical zonation in massive ignimbrite (Fig. 6.3) also has been used as evidence for non-turbulent transport (Wright & Walker 1981; Cas & Wright 1987; Francis 1993 p. 217), but this conclusion was based on the belief that the vertical chemical zonation developed in the

current near to the vent and that this then moved as a laminar flow and a semi-rigid plug prior to coming to rest en masse (Fig. 2.5A–C). The proposition was that any turbulence would have disrupted the zonation (chemical stratification) in the current during transport (Fig. 2.2A). However, with progressive aggradation from a flow boundary, zonation within a deposit merely records changes in the composition of the material supplied to that location through time (Fig. 2.2B). The current need not have vertical chemical stratification: rather, its entire chemical composition changes with time. Therefore, compositional zonation in an ignimbrite does not bear on whether or not the current was turbulent (Branney & Kokelaar 1997).

A common assumption that pyroclastic density currents are either turbulent low-concentration currents ('pyroclastic surges') or non-turbulent, laminar to plug-like high-concentration currents ('pyroclastic flows') cannot be justified in either theoretical or experimental fluid dynamics, and is inconsistent with much field evidence of gradations between massive and traction-stratified facies (Rowley *et al.* 1985; Sigurdsson *et al.* 1987; Fierstein & Hildreth 1992; Cole & Scarpato 1993; Scott *et al.* 1996). Continuous gradations between current types are likely for the following five reasons: (1) clast-support mechanisms within currents (e.g. fluid turbulence, hindered settling, grain collisions and buoyancy) overlap and change gradationally with increasing clast concentration (see Chapter 3), so a continuous range of clast concentrations and turbulence intensities is possible; (2) any form of density stratification of a current will be linked to variations of turbulence intensity as a function of height (see 'Current stratification' p. 14); a current may be laminar where it is of relatively high-concentration near its base, but its turbulence intensity may increase with height in the successively less concentrated levels of the current; (3) changes from laminar to turbulent flow can occur along a current (e.g. 'flow transformations' of Fisher 1983) or laterally as a result of varying flow properties transverse to the current's thalweg,

and with time (unsteadiness); (4) eddies that develop spontaneously in predominantly laminar currents occur over a wide range of scales; and (5) even in homogeneous shear flows, which are much simpler than pyroclastic density currents, the transition from laminar to turbulent flow takes place over a range of conditions, for example over a range of values of Re (e.g. Massey 1989).

Plug flow

Plug flow is a type of non-turbulent flow in which an upper non-shearing layer (the 'plug zone') rides along on an underlying laminar shearing layer. Velocity does not vary with height within the plug zone (Figs 2.2A and 2.5). Plug flow occurs in flowing non-Newtonian cohesive material in which the yield strength exceeds the shear stress exerted on it in all but the lowermost part of the flow (Johnson 1970; Iverson *et al.* 1997). Plug flows are thought not to deposit by progressive aggradation during transport, apart from by accretion of lateral 'dead zones' controlled by substrate morphology (Johnson 1970) (Fig. 2.5E). Rather, as the flow decelerates (e.g. as a result of flowing onto a lower gradient), the shear stress exerted decreases and the thickness of the plug zone increases downwards at the expense of the underlying shearing layer, which correspondingly thins (Fig. 2.5A–C). Eventually the lower contact of the plug zone encroaches the substrate, so that the shearing layer disappears, whereupon the entire flow halts instantaneously (Fig. 2.5C) (Johnson 1970). When this happens, the deposit is effectively an *in situ* record of the current and any vertical variations within the deposit record variations with height in the current. In this scenario, once any post-emplacment compaction is taken into account, deposit thickness and morphology relate directly to those of the current. Although plug flow had been invoked for high-concentration parts of pyroclastic currents, such granular material has little aggregate strength (Wilson 1984; Postma 1986; see also p. 35). If normal coarse-tail-graded lithics and inverse coarse-tail-

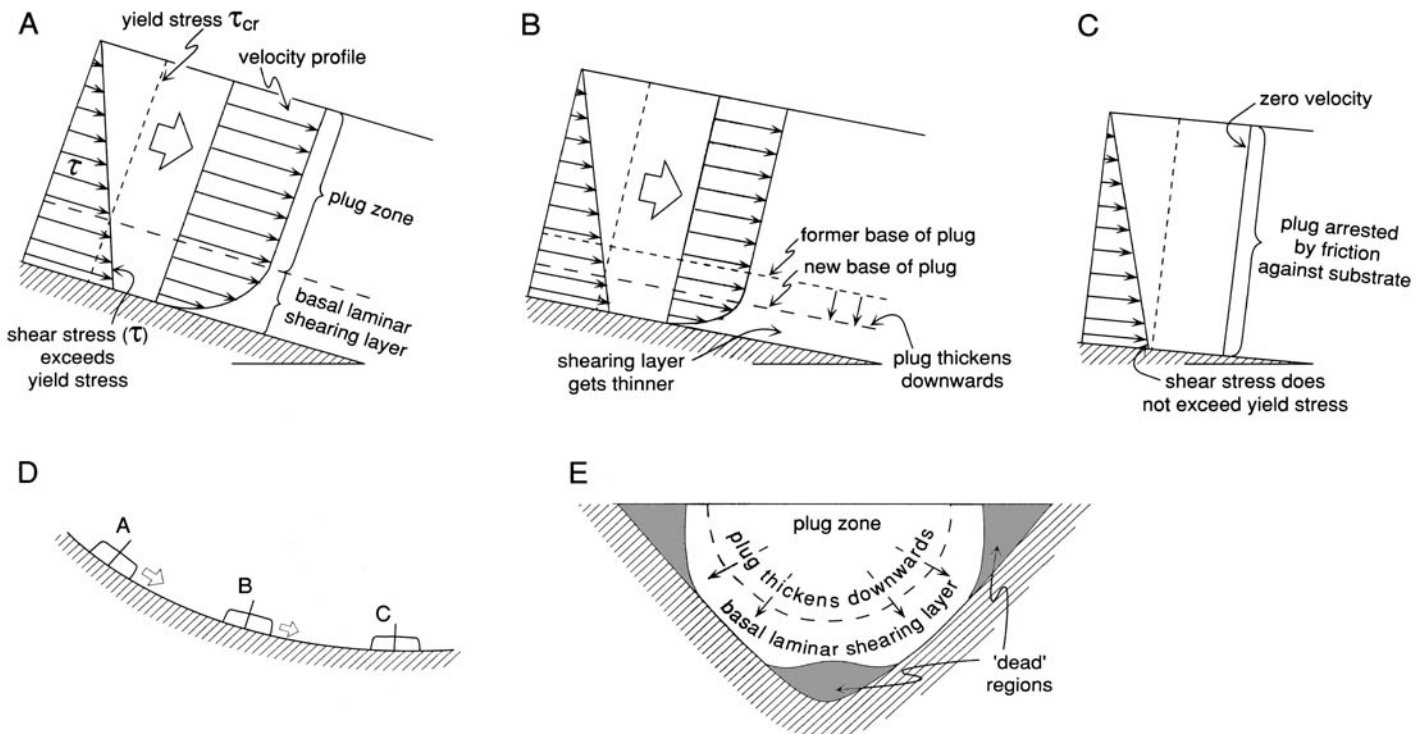


Fig. 2.5. Model of decelerating plug flow (modified from Johnson 1970). (A)–(C) Three profiles through plug flows at different locations on a concave slope (see D). (A) and (B) are non-depositional, (C) is stationary (it has come to a halt en masse). If (A), (B) and (C) were connected as a single flow the relative movements between them would cause them to interact, producing internal deformation of plug regions and possible overlap (see discussion in Branney & Kokelaar 1992). (E) Transverse section of a plug flow in a channel, showing how deposit accretes in small dead regions well before the plug halts.

graded pumices in massive ignimbrites (see p. 66) were to be the result of buoyant particle segregation within the thickness of the current (see p. 34), the currents must have had yield strengths sufficiently low to have been exceeded by the small upward and downward (sinking) forces exerted on individual lapilli; such yield strengths would be too low to give rise to (non-shearing) plug zones with thicknesses similar to thicknesses of many massive graded divisions in ignimbrites. Plug flow behaviour has neither been observed in pyroclastic density currents nor produced experimentally with pyroclasts and air. Although early computer simulations of rapid granular flows, using small numbers of 'grains', showed that shearing occurred mostly within a thin basal shear layer (e.g. Campbell & Brennen 1985), this feature did not exist during deceleration and deposition, which occurred by progressive aggradation. Subsequent more sophisticated computer simulations (Campbell *et al.* 1995; Pouliquen & Vallance 1999) suggest that granular flows shear throughout rather than developing non-shearing plug zones. We propose that the relevance of plug flow to pyroclastic density currents is mostly limited to slow-moving terminal pumice dams and levees, as well as possibly accounting for some attributes of lithofacies deposited from thin granular fluid-dominated basal parts of some stratified currents (see p. 43 and Fig. 4.5B). Evidence for and against en masse deposition of ignimbrite is discussed on pages 45 to 46.

Current stratification

A current is said to be stratified if its properties (e.g. density, rheology, clast population) vary with height above the base. There is no connotation of distinct stratal discontinuities, although these may be present in some cases. A wide range of stratification types has been envisaged (e.g. Einstein & Chien 1955; Hsü 1959; Coleman 1969; Middleton 1970; Carter 1975; Wasp *et al.* 1977; Turner 1979; Yih 1980; Roco & Shook 1984; Postma *et al.* 1988; Chun & Chough 1992; Nishimura & Ito 1997; Felix 2001), including laminar stratified currents (Schaflinger *et al.* 1990), stratified turbulent currents with laminar basal parts (Fisher 1966; Hein 1982; Todd 1989; Vrolijk & Southard 1998), turbulent dilute currents overriding granular fluid basal levels with an intervening transition zone (Hanes & Bowen 1985) and turbulent stratified currents with gradational vertical changes of concentration or density (Sigurdsson *et al.* 1987; Valentine 1987; Cole & Scarpati 1993). In density stratification, gravity acts to increase the clast concentration towards the base of the current and/or segregate clasts vertically according to their sizes, shapes and densities (pneumatic equivalence). Concentration gradients through pyroclastic density currents have not been measured, but certainly exist, especially near the upper and lower flow boundaries. The concept of stratified flow can apply to low- or high-concentration particulate currents, to currents with any type(s) of particle support mechanisms and to the near-flow-boundary parts of otherwise non-stratified currents. It encompasses a spectrum of pyroclastic density current types in a way that the traditional surge versus flow dichotomy did not. In most stratified currents, clast support and segregation mechanisms vary with height above the lower flow boundary, which is one reason why lithofacies deposited from the base of a current do not necessarily reflect the overall character of the current.

A complete and realistic description of the structure and behaviour of a turbulent stratified density current has been elusive. One suggested approach to describing a low-concentration, steady, turbulent stratified current in which the entire particle population is fully suspended by turbulence (i.e. a non-depositional current) has been to treat turbulence as a diffusive-advective process, in which clast concentration, S , as a function of height is:

$$S = S_0 \left[\frac{\eta_0(1-\eta)}{\eta(1-\eta_0)} \right]^{Pn} \quad (2.2)$$

where S_0 is the particle volume concentration at a non-dimensional

reference level, η_0 (close to the base of the current) and η is y/d , the non-dimensional height, with y and d being the height above the base and the current's total thickness, respectively (Rouse 1937; Valentine 1987). The particle Rouse number, Pn_i , is the ratio of the settling velocity, w_i , of a given population of clasts, i , to the turbulence intensity, ku_* ($k \approx 0.4$ is von Kármán's coefficient and u_* is the shear velocity), that is:

$$Pn_i = \frac{w_i}{ku_*} \quad (2.3)$$

or, for suspensions with clast populations of more than one settling velocity, the distribution Rouse number, Pn is given by:

$$Pn = \frac{1}{\bar{S}} \sum_i S_i \left(\frac{w_i}{ku_*} \right) \quad (2.4)$$

where \bar{S} is the height-averaged volume concentration of all clasts and S_i is the height-averaged concentration of clast population i ('population' here means all clasts of a given settling velocity, w_i ; clasts of different sizes, densities and shapes may constitute a single population if their settling velocities are equal). The relations in Equation 2.2 predict clast-concentration (and hence density) gradients that have maximum concentrations at the base of the current, declining to zero at the top (Fig. 2.6). The way in which concentration increases toward the base of the current depends on the Rouse number. Low Rouse numbers correspond to small particles and efficient suspension by turbulence, and result in gradual downward increases in concentration, whereas high Rouse numbers (e.g. $Pn > 1$) result in steep concentration gradients near the base of the current (Fig. 2.6). Any batch of suspension rising from a low level to a higher level in such a current is placed in lower density surroundings and, conversely, any descending batch of suspension moves into a denser environment. Thus, any batch of fluid that is displaced vertically experiences a buoyancy force that tends to return it to its original level; the stronger the density gradient, the stronger the restoring force, and the stronger the stability of the stratification. Steep density gradients of high Pn currents act to suppress turbulence by inhibiting the vertical movement of batches of suspension (Middleton & Southard 1984; Valentine 1987), and mechanisms of clast support other than turbulence (Chapter 3) may be required to support the clasts within the basal part of the current.

Application of the Rouse number in consideration of pyroclastic

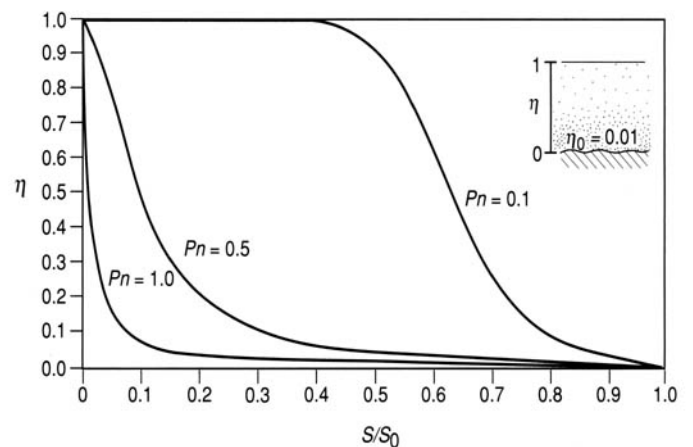


Fig. 2.6. Relative concentration S/S_0 as a function of dimensionless height (η) in a turbulent density current (after Rouse 1937). The model is based on open-channel flow and it ignores shearing at the top of the current, bed loads and deposition. Valentine (1987) took $\eta = 1$ as the top of the current, although this is generally not appropriate for density currents, whereas Hiscott (1994a) took it as the height to the maximum on the current velocity profile and ignored overlying parts of the current. S_0 is the particle volume concentration at reference level $\eta_0 = 0.01$. Profiles are shown for three values of the distribution Rouse number (Pn).

density currents has several limitations. The first is that it was developed (Rouse 1937) for open-channel flows (like rivers) with negligible flow retardation towards their upper boundaries, whereas, in contrast, upper boundaries of pyroclastic density currents (as with turbidity currents) undergo significant shear due to drag and mixing effects with the overlying ambient fluid. This significantly affects turbulence and the corresponding shear-stress and particle-concentration profiles (see García and Parker 1993; García 1994; Kneller & Buckee 2000). Valentine's (1987) analysis assumed the top of a pyroclastic density current to have the maximum velocity, which is unlikely to be true. Hiscott (1994a) attempted to deal with this problem, in his application of the Rouse number treatment to turbidity currents, by assuming that levels of the current above the maximum in the velocity profile have negligible transport capability and exert negligible gravitational driving force. However, the upper flow boundaries of hot pyroclastic density currents also are modified by thermal convection, which draws in cold air across the top of the current (Huppert *et al.* 1986), causing boundary layer shear, mixing, thermal expansion and buoyancy. Furthermore, the Rouse number approach is not appropriate for any current undergoing sedimentation (or for that matter erosion) because the suspended load is then no longer in equilibrium with the bed (see Dobbins 1944). Similarly, the approach cannot account for pyroclastic currents in which velocity maxima and/or dominant mass transport lie at a level in the current where mechanisms other than turbulence dominate clast support (for example support from grain interactions, saltation or fluid escape; see p. 21 and pp. 25–35).

A significant part, and in some cases the greater part, of some density currents is not *fully* supported by fluid turbulence. Even in low-concentration currents (e.g. so-called 'pyroclastic surges') many of the clasts are only intermittently supported, in that they pause on the substrate or deposit surface for a while before being re-entrained, or they saltate or roll (see 'Support on an interface', p. 25). With increasing clast concentration near the lower flow boundary, clast interactions and saltation are likely to cause significant departures from the velocity and concentration profiles predicted by the Rouse number approach. Such departures apparently occur at concentrations well below those at which grain interactions (p. 29) replace fluid turbulence as the *dominant* grain-support mechanism (Einstein & Chien 1955; Coleman 1969; Middleton & Southard 1984). Within a polydisperse current dominated by fluid turbulence, the various support mechanisms themselves cause current stratification, as diverse clasts segregate vertically according to their dominant mode of support (see Fig. 3.3); clasts with the highest settling velocities spend most time closer to the lower flow boundary and are not fully supported by turbulence.

Recent modelling (e.g. Bursik & Woods 1996) distinguishes subcritical and supercritical flow regimes that correspond with contrasting mixing and hence stratification profiles. It also indicates that the contrasting amounts of mixing along the upper flow boundary fundamentally influence overall flow behaviour (see p. 16). García (1994) applied layer averaging to modelling of turbidity currents laden with poorly sorted sediment and found good agreement with observations of depositional laboratory flows that were sustained for up to 1 hour as they flowed down a slope onto a flat surface. On the slope he produced supercritical turbulent currents with concentration and velocity maxima close to the bed and strong admixture of ambient fluid along the top. Beyond the slope change, the currents underwent a jump to subcritical, with negligible mixing along the top, and the residual sediment became more fully mixed, with no steep concentration gradient and with a velocity maximum near or just beneath the middle of the current depth. The experimental currents tended to segregate coarser material towards the lower boundary, and to produce deposits that thinned exponentially and became finer grained downstream, while remaining poorly sorted. Although García's experimental currents differ in several ways from pyroclastic density currents, they show:

(1) that depositional currents develop variable stratification and grain-size segregation according to slope and flow regime, while at the same time producing deposit trends that are not grossly dissimilar to those predicted by models of fully mixing low-concentration currents; and (2) that models that fail to account for evolving polydisperse sedimentation, changing stratification and influence of flow regime will be of limited use in accounting for detailed features of most ignimbrites.

Currently, there is little theoretical or experimental basis for predicting concentration profiles through turbulent flows in which clast support and hindered settling are aided within lower levels by clast buoyancy, fluidization, and/or grain collisional interactions. Their profiles may be stepped (Middleton 1967; Shook *et al.* 1982) or smoothly gradational (Shook & Daniel 1965; Shook *et al.* 1982; Roco & Shook 1984; Denlinger 1987; Ibad-zade 1987; Pugh & Wilson 1999). Pronounced density stratification is commonly evident from observations and deposits of small-volume pyroclastic density currents, wherein the lowermost levels are strongly guided by topography while the higher levels spread more widely, inflate and/or rise buoyantly (e.g. at Mt Pelée, Anderson & Flett 1903; Mount St Helens, Hoblitt 1986; Unzen, Yamamoto *et al.* 1993; Soufrière Hills, Cole *et al.* 2002; Loughlin *et al.* 2002a, b).

It is not clear to what extent large pyroclastic currents that deposit extensive ignimbrites may comprise a lower high-concentration level sharply overlain by an upper relatively low-concentration level of differing behaviour (Fig. 2.9F), in contrast to having more gradual variations of concentration with height (Fig. 2.9E). Concentration profiles in ignimbrite-forming pyroclastic density currents have not been measured or observed, and bipartite division has been invoked for modelling convenience and simplicity. Sharp transitions in deposit lithofacies up valley sides have been interpreted as evidence that some pyroclastic currents are bipartite with a lower, laminar basal part sharply overlain by a low-concentration turbulent current. This conceptualization may be correct in some cases, but lithofacies up valley sides may reflect lateral (i.e. current marginal) transitions in the current's lower flow boundary, and these may not exactly mimic the vertical concentration profile at the valley axis. Elsewhere (see p. 111) lithofacies transitions at valley sides are gradational.

Partitioning of mass-flux in density-stratified currents

The transport of mass within a density-stratified pyroclastic current may occur: (1) predominantly in lower, concentrated levels of the current; (2) predominantly within upper low-concentration levels; or (3) fairly evenly partitioned between various levels. In non-uniform currents, significant transfer of pyroclasts from one level to another is likely (see p. 93), and the partitioning of the mass flux between different levels in a single current is likely to vary between different reaches.

Early models of pyroclastic density currents were bipartite, with an upper 'co-ignimbrite' ash cloud generated by elutriation from a largely obscured, high-momentum, high-concentration, fluidized laminar flow, within which the majority of the mass was transported (e.g. Sparks 1976) (see Fig. 2.2A). More recently the concept of a bipartite current has continued with loosely defined, lower, more concentrated levels being referred to as an 'underflow' or, in the cases of some small currents, as a 'basal avalanche'. The term underflow does not account for the fact that, by convention, the entire pyroclastic density current that flows under the atmosphere (see the next section) constitutes an underflow, while the second term is confusing because many avalanches *include* upper levels with gradationally decreasing particle concentration and increasing turbulence (e.g. Scheiwiller 1986; Nishimura & Ito 1997) and hence more closely resemble entire pyroclastic density currents than just some discrete basal part.

Recent models have envisioned mass transport as occurring predominantly in a low-concentration turbulent current that sediments pyroclasts into a relatively dense mobile layer, referred

to as a 'depositional system' (Fisher 1990a; Fisher *et al.* 1993) or 'underflow' (Bursik & Woods 1996; Druitt 1998). Bursik & Woods (1996) considered that the low-concentration turbulent levels of the current determined the large-scale characteristics of an ignimbrite sheet, such as proximal to distal decreases in maximum and mean grain sizes and exponential thinning. In this modelling the lower, more concentrated levels that deposit massive ignimbrite are of second-order importance in transport and segregation. For example, Bursik & Woods (1996) modelled the emplacement of the Taupo ignimbrite as an extremely high mass-flux ($2 \times 10^{10} \pm 1 \times 10^{10} \text{ kg s}^{-1}$), short-duration (approximately $2 \times 10^3 \pm 1 \times 10^3 \text{ s}$ or 17–50 min) and high-velocity ($150\text{--}200 \text{ m s}^{-1}$) low-concentration current, which probably took at least 400–500 s (7–8 min) to reach its distal limit in contact with the ground. If this is correct (the durations derive from the model), and a dense lower part developed and persisted for not much longer than the eruption, the proximal massive ignimbrite, which is *c.* 100 m thick, must have aggraded at an average rate of about 33–100 mm s^{-1} . In contrast, the Valley of Ten Thousand Smokes ignimbrite, erupted in 1912 from Novarupta with an eruptive mass flux of $5 \times 10^8 \pm 2.5 \times 10^8 \text{ kg s}^{-1}$ over a period of 8 ± 4 hours, apparently aggraded up to 250 m at an average rate of about 6–17 mm s^{-1} .

In the modelling that takes mass transport to be predominantly via a low-concentration suspension, reasonable initial conditions are derived, and both runout and gross ignimbrite granulometry are linked to eruptive mass flux (Bursik and Woods 1996; Dade and Huppert 1996). The models utilize parameters and sedimentation laws that are moderately well constrained for low-concentration dispersions. However, controls on the capacity of, and sedimentation from, more concentrated levels of a current are less well understood, particularly where levels are intergradational rather than discrete. The present consensus is that ignimbrite can be deposited from a spectrum of current types, ranging from ones in which most mass transport occurs within a fast, turbulent, low-concentration current to currents in which most transport is within more concentrated, lower levels. Recent models (e.g. Bursik & Woods 1996) relate this spectrum to the flow regime and related transport capacity of the low-concentration part of the current. They indicate that subcritical low-concentration currents tend to become strongly density-stratified, and rapidly transfer much of their mass to lower, high-concentration levels.

The match of deposit attributes to predictions from models of low-concentration currents remains somewhat problematic, and the possibility that similar deposits develop from currents in which significant mass flux occurs within more concentrated levels, or dispersed across many levels of a density-stratified current, is not precluded. Quantitative models of this type are lacking, and it is too early to know whether the latest models realistically describe the essential physics of pyroclastic density currents. The approach in this Memoir focuses on the behaviour of the depositional flow-boundary zone, which provides information about whether, where and when basal high-concentration levels actually developed in pyroclastic currents.

The behaviour of pyroclastic density currents

Inertia, buoyancy, runout distance and lofting

A pyroclastic density current consists of two essential and intergradational counterparts: an underflow and a phoenix plume. The underflow is denser than the atmosphere and flows underneath it, whereas the phoenix (or co-ignimbrite) plume is less dense than the lower atmosphere and so lofts convectively (Dobran *et al.* 1993; Sparks *et al.* 1997a). Pyroclastic density currents may flow primarily along the ground for a distance, the runout distance, beyond which they loft wholesale into the atmosphere as a result of de-densification by deposition and/or by turbulent mixing with and thermal expansion of air. In addition, upper parts of a density-

stratified current may become buoyant and loft above considerable reaches of the ground-hugging current. Such lofting is commonly pronounced where a slope change induces sedimentation, or enhances mixing with air, or where the current is affected by a change in substrate (e.g. surface roughness or standing water).

Runout distance is controlled by the current mass flux, density and pyroclast granulometry, by topography, and by the rates of air entrainment and pyroclast sedimentation during transport. In models of low-concentration currents (Bursik & Woods 1996) runout distance is a function of mass eruption rate and grain-size distribution, and it decreases with entrainment of air. In sustained currents, head and compressibility effects can be neglected and flow can be quasi-steady (Fig. 1.1A), either with substantial entrainment of air along the upper flow boundary or with little such entrainment, according to the ratio of buoyancy forces to inertial forces in the current (expressed as the Richardson number, $Ri = gD\Delta\rho/\rho v^2$, where D is the current thickness, v is velocity, ρ is current density and $\Delta\rho$ is the density contrast with the atmosphere). The buoyancy forces act to stabilize the relatively dense layer beneath the atmosphere whereas the inertial forces tend to result in turbulent mixing. Relatively slow ($10\text{--}100 \text{ m s}^{-1}$) and deep ($1000\text{--}3000 \text{ m}$) subcritical or 'tranquil' currents (see next section) entrain little air ($Ri > 1$), whereas relatively fast ($100\text{--}200 \text{ m s}^{-1}$) and shallow ($500\text{--}1000 \text{ m}$) supercritical or 'rapid' currents entrain considerable air ($Ri < 1$). (The figures are taken from Bursik & Woods's 1996 models of low-concentration non-stratified pyroclastic currents with mass fluxes in the range of $10^9\text{--}10^{10} \text{ kg s}^{-1}$). Thus, subcritical currents tend to propagate with practically constant volume-flux, apart from the effects of sedimentation, whereas supercritical currents entrain air along their length and become progressively more voluminous, less dense and cooler, with more elutriation of ash into a buoyant cloud (Fig. 2.7B). However, in a density-stratified current, values of v , ρ and $\Delta\rho$ vary with height, so that designation of a single Richardson number for the entire current is not appropriate. Furthermore, vertical mixing between different levels of the current may vary considerably with height above the base.

Internal waves, hydraulic jumps and granular jumps

Density currents with sharp interfaces of fluid density may develop internal waves, standing waves and hydraulic jumps (Middleton 1967; Hand 1974; Turner 1979; Yih 1980; Simpson 1997; Woods *et al.* 1998). Hydraulic jumps relate to a shift in the balance between inertial and gravity forces (expressed by the Froude number, $Fr = u/\sqrt{gh}$) and are downcurrent changes from relatively shallow, rapid flow (supercritical, $Fr > 1$) to deeper, slower flow (subcritical, $Fr < 1$). Jumps typically occur where currents transgress a decrease in slope, and/or where they debouch onto a plain from a channel (canyon) or chute (Fig. 2.7).

Jumps have been postulated in pyroclastic density currents presumed to have a sharp density interface, although this was not clearly observed (Clark 1984; Levine & Kieffer 1991). Jumps have been produced experimentally with continuously stratified currents (lacking pronounced interfaces), although they are not predicted in such currents by theory (Yih 1980). García & Parker (1989) and García (1993) produced experimental turbidity currents that developed a jump across a change of slope designed to simulate a canyon-to-fan transition. Downstream of the jump, a marked change in velocity and particle-concentration profiles occurred, with the deeper, slower flow having its velocity maximum relatively higher in the current. The resultant reduced bed shear stress caused deposition from the bed load. In experimental simulations of surge-like aqueous density currents, Mulder & Alexander (2001) showed that increased sedimentation just downstream of breaks of various angles of slope was related to flow thickening and velocity decrease, possibly related to hydraulic jumps. The velocity decrease led to an abrupt loss of flow competence and bed shear stress, leading to relatively rapid sediment aggradation. Valentine (1987) proposed

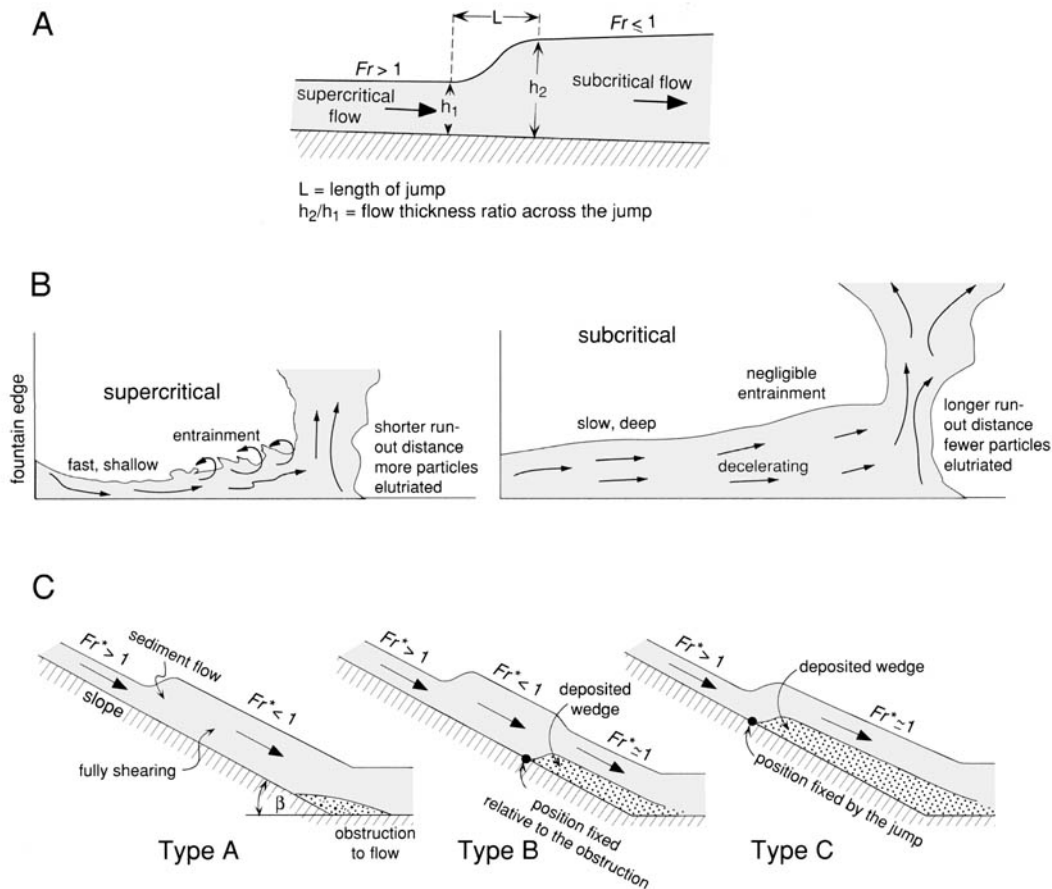


Fig. 2.7. (A) A hydraulic jump. (B) Comparison between models of supercritical and subcritical pyroclastic density currents (after Bursik & Woods 1996). See text for the explanation. (C) A granular jump, with three types of behaviour dependent on slope angle, β . Type A: slope near repose angle for the granular flow; type B: slope up to 8° steeper than repose angle; type C: slope between 8° and 38° above repose angle (from experiments of Brennen *et al.* 1983). $Fr^* = Fr/(\cos\beta)^{1/2}$. Modified from Savage (1979), Brennen *et al.* (1983) and Nemeč (1990).

that downcurrent changes in the lithofacies of some 'pyroclastic surge deposits' may relate to gradual transitions from supercritical to subcritical flow in a smoothly stratified fully turbulent current, but the nature of such putative transitions and how they may influence depositional processes in the flow-boundary zone of a pyroclastic density current are unknown. Jumps to subcritical may: (1) decrease the turbulent mixing with air at the upper flow boundary and promote density stratification so that upper parts of the current become less concentrated and, if hot, may loft, as in experimental models (Woods & Bursik 1994); and (2) they may stimulate localized deposition, particularly of larger or denser clasts, because of depletive velocity and consequent localized depletive current competence. This has been proposed to account for progradational lithic breccias in ignimbrites just downcurrent of a slope decrease (Freundt & Schmincke 1985; Macías *et al.* 1998). Deposit surfaces that dip and were accreted in an upcurrent direction, to produce regressive bed forms with upslope-dipping strata, have been interpreted by Schmincke *et al.* (1973) to record 'chute and pool' dynamics of a hydraulic jump.

In subcritical (tranquil) currents, waves can propagate upstream or downstream, whereas in supercritical currents the flow is too rapid for a wave to propagate upstream. Small stationary waves, which are unable to propagate against the flow, are a common feature of critical flow conditions. Internal waves can develop in stratified flows that lack sharp internal interfaces (Yih 1980), but they tend to be suppressed by buoyancy restoring forces. They exhibit a range of possible frequencies up to a maximum 'buoyancy frequency', $N^2 = -g/\rho \cdot d\rho/dz$, where g is acceleration due to gravity, z is the vertical oscillation and ρ is fluid density (Baines 1995). Lee waves, which form downstream of obstacles in

continuously stratified flows (Fig. 2.8C), are an example. Understanding of how internal waves may influence sedimentation and deposit lithofacies is improving for aqueous density currents (e.g. see review by Kneller & Buckee 2000), but direct translation of processes and scaling from such research to pyroclastic density currents is problematic.

In rapid cohesionless granular flows, granular jumps occur (Morrison & Richmond 1976; Savage 1979; Brennen *et al.* 1983) (Fig. 2.7C) and are analogous to hydraulic jumps in fluidal currents. It is possible that similar processes may occur in the lower parts of some high-concentration pyroclastic currents. Granular jumps occur either at a short fixed distance upcurrent of a slope decrease, or may propagate a substantial distance upcurrent from one (Brennen *et al.* 1983; Sadjadpour & Campbell 1999). A substantial and abrupt increase in thickness of the granular flow may occur at the jump (Savage 1979). On slopes less than the angle of repose, the subcritical flow downcurrent of the jump shears throughout its thickness and starts to deposit at the break of slope. This deposition may smooth out the break of slope (Type A in Fig. 2.7C). On slightly steeper slopes, deposition produces a wedge of sediment with a steep depositional surface that migrates upslope to an equilibrium location (Type B in Fig. 2.7C). On even steeper slopes, the accreting face of a depositing wedge continues to migrate upslope as long as flow is maintained (Type C in Fig. 2.7C). Drawing on this experimental work, it has been proposed that deposits registering granular jumps may have the form of either localized lenses that smooth out the topography or relatively long tabular sets of upcurrent-dipping cross-strata (Nemeč 1990). The deposits would be distinguishable from deposits formed by hydraulic jumps in having characteristics of granular

flow deposit, such as good sorting (see Fig. 3.4 and pp. 39 and 71). However, pyroclastic density currents that deposit ignimbrites are transitional in nature between granular flows and fluid-turbulence-dominated currents (see the next section on p. 20), and the nature and behaviour of jumps transitional between hydraulic (or pneumatic) and granular has not been explored. One might anticipate that they occur on slopes much less than the repose angle of pure grainflows (cf. Fig. 2.7C).

Thalwegs (flow axes) and lateral migration

Unconfined density currents may initially spread as 'sheet flows' that are moderately uniform laterally. However, with sustained flow they commonly become distinctly non-uniform. In flowing across plains they tend to develop main flow axes, called *thalwegs*, where the velocity, concentration and/or competence of the current may be significantly higher than in adjacent streamlines. Even where the terrain is quite flat, *thalwegs* form readily and shift laterally. Any pre-existing topography, or even microtopography, may help initially to determine and then constrain the position of *thalwegs* (see Allen 1985, p. 86), but fluid instabilities and consequent strong non-uniformity, for example near the current leading edge, may also form substrate irregularities that have similar effects, by differential erosion and/or deposition. Any small substrate irregularity will cause streamlines to become non-parallel, following which the current may further modify its substrate (including the deposit). Where the flow thickness is locally modified at a substrate irregularity, the shear stress acting on the bed and the shear gradient near the flow boundary will differ from nearby, and in this way contrasting depositional or non-depositional behaviour becomes accentuated. Numerical modelling of channel inception on submarine turbidite fans (Imran *et al.* 1998) indicates that channel-levée systems spontaneously develop from sustained spreading flows, because the tendency to erode (a function of the bed shear stress) decreases more rapidly in the transverse-to-current direction than does the rate of deposition (a function of the depletive flow). Development of *thalwegs* is self-sustaining, because any flow lines diverging from the *thalweg* tend to be depletive, favouring deposition adjacent to the axis of rapid flow, whereas flow lines converging into a *thalweg* are accumulative, favouring erosive channelling.

Thalwegs tend to migrate and braid because asymmetrical differential erosion (channelling) and/or deposition (e.g. ignimbrite bars or levees) may modify the substrate topography sufficiently to divert the flow lines, as in a braided river during flood. Local flow into *thalwegs* (convergence) or out of them (divergence or splaying), meandering and corkscrew vorticity in *thalweg* bends all may give rise to differing flow directions within different parts of a density current. The spatial pattern and migration history of *thalwegs* contributes to the facies architecture of an ignimbrite sheet or fan. However, evidence of *thalwegs* within large ignimbrite sheets may not be easy to discern, particularly where the ignimbrite is massive, and where a *thalweg* shifted progressively to construct a laterally extensive sheet (see p. 111). Well-developed *thalwegs* would increase the runout distance of a current, as is found to be the case for channelled versus spreading flow (Bursik & Woods 1996).

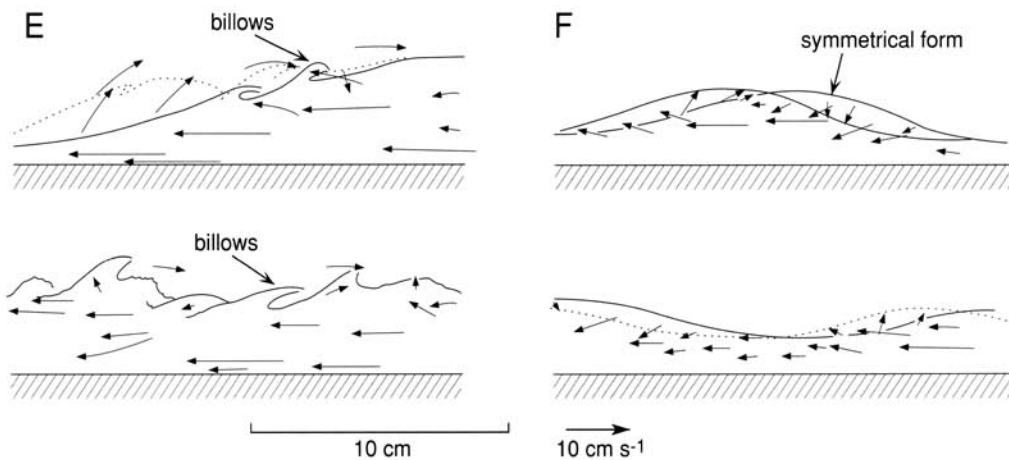
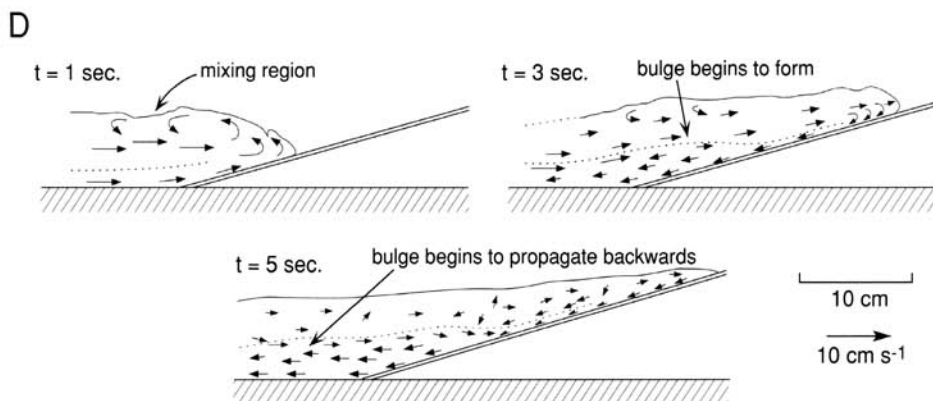
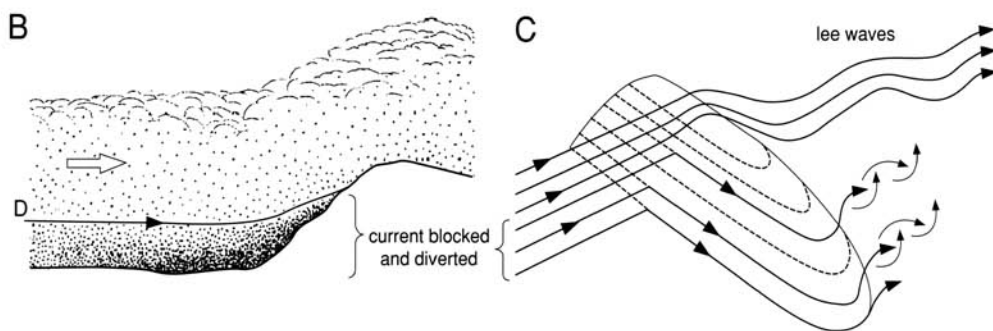
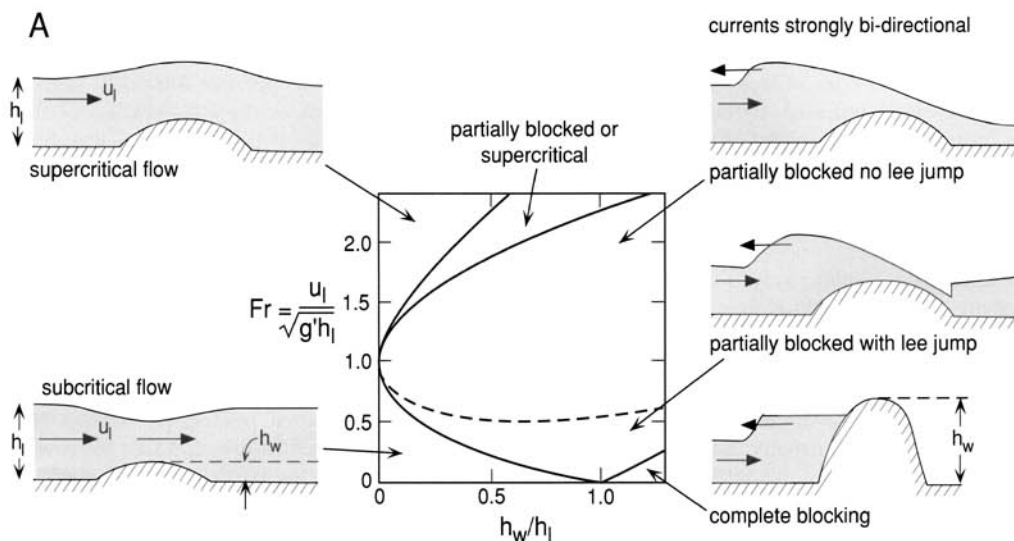
Effects of topography

Five ways in which a homogeneous steady current with a distinct

free surface may interact with an obstacle in its path are shown in Fig. 2.8A. The five scenarios are closely matched in the experiments of Woods *et al.* (1998), which used particle-laden saline currents to simulate turbulent pyroclastic density currents with low solids concentrations (c. $1\text{--}10\text{ kg m}^{-3}$), and which produced sedimentation patterns clearly related to the topography. For example, deposits were thicker on the upcurrent side of obstacles that caused particle blocking and upstream propagation of bores. In the case of a stratified current (e.g. Fig. 2.8B and C) only fluid above a critical level, known as the dividing streamline, D, has sufficient kinetic energy to counteract the buoyancy forces and surmount the obstacle. Denser levels of the current are blocked by the obstacle and become ponded or reflected, or are diverted through passes (saddles) and valleys (Baines 1995; Woods *et al.* 1998). The higher, less dense levels of the current are less constrained by topography and may travel further (Fig. 2.8B and C), unless mixing of air is promoted and causes the current to loft. Topographic separation of the upper levels of a current in this way is known as 'flow-stripping' for turbidity currents (Piper & Normark 1983) or 'decoupling' for pyroclastic currents (Fisher 1990a). The term *flow-stripping* may be preferable, because it does not suggest that the current originally comprised distinct but coupled parts prior to the separation. Currents with relatively steep density gradients (and/or low velocities) can be efficiently blocked and deflected horizontally because their buoyancy-related restoring forces are greater than those of currents that have less marked density gradients. Evidence for topographic blocking in the 18 May 1980 Mount St Helens blast has been described (Hoblitt & Miller 1984; Fisher 1990a), and it was the stripped upper parts of pyroclastic density currents that caused most devastation and fatalities in 1902 at St Pierre, Martinique (Fisher & Heiken 1982). Similarly, flow-stripping led to the fatalities at Unzen volcano in Japan, on 3 June 1991 (Yamamoto *et al.* 1993), and the fatalities at Montserrat on 25 June 1997 (Loughlin *et al.* 2002a, b).

Pyroclastic density currents have overwhelmed topographic barriers $\leq 1\text{ km}$ high: for example, 800 m determined from the Ata ignimbrite (Aramaki & Ui 1966), 500 m determined from the Fisher ignimbrite (Miller & Smith 1977), 600 m determined from the Xáltipan ignimbrite (Ferriz & Mahood 1984), 1000 m determined from the Taupo ignimbrite (Wilson 1985) and 685–1000 m from the Campanian ignimbrite (Fisher *et al.* 1993). Analogous marine turbidity currents similarly ascend slopes to heights over 1 km (e.g. Dolan *et al.* 1989). Muck & Underwood (1990) calculated that the thickness of a subcritical (aqueous) density current must be greater than about 65% of the height of a topographic barrier in order for part of it to surmount that barrier, although their calculation ignores the likely effects of density stratification and sedimentation. Modelling by Woods *et al.* (1998) indicates that low-concentration, steady density currents with mass fluxes $> 10^8\text{--}10^9\text{ kg s}^{-1}$ can in part extend across barriers as high as 1 km, tens of kilometres from source, and that the height of the lowest ridge capable of completely blocking a current increases with increasing mass flux at source. It was also found that for a radially spreading (depletive) low-concentration current, the height of the lowest ridge that can cause total blocking initially decreases with downcurrent distance from source as the current thins, but that further downstream this minimum height increases as the current becomes less concentrated through deposition and fluid entrainment. Based on momentum dissipation, Legros & Kelfoun (2000) show that, for a given mass flux, dense currents slow down with distance faster than do low-concentration currents.

Fig. 2.8. Responses of supercritical, subcritical and strongly stratified flows to topographic obstacles. (A) Five ways in which a dense layer of fluid can interact with a two-dimensional obstacle (after Rottman *et al.* 1985). (B–C) Flow-stripping due to partial blocking of a density-stratified current by a topographic barrier. In a continuously stratified flow only fluid above a critical dividing streamline, D, has the kinetic energy to surmount the obstacle. Waves and eddies form in the lee of the obstacle. (D)–(F) Experimental observations of topographic reflections of density currents (after Edwards *et al.* 1994). Initial current flowed to the right. Arrows indicate particle paths. (D) Generation of a bore at the foot of a ramp. (E) A strong bore developed at a ramp (to the right) resembles the head of a normal density current. (F) A weak bore developed at a ramp (to the right) resembles a solitary wave.



The influence of topography on the flow direction of lower parts of pyroclastic density currents has been interpreted from deposits in several ways. For example, the orientations of trees felled by the 18 May 1980 Mount St Helens blast-initiated pyroclastic current indicate topographically induced deflections and channelling, also with lee-side boundary layer eddying and flow separation (Kieffer 1981; Sisson 1995). Furthermore, the facies variations of the deposit across irregular ground indicate a strong topographic influence on the flow direction of lower, concentrated levels of the current during deposition (Fisher 1990a). Variations of particle fabrics in the Ata ignimbrite, Japan (Suzuki-Kamata & Ui 1982), indicate topographic deflections during deposition, and similar features in the Campanian ignimbrite, Italy, have been interpreted as recording backwards 'reflection' caused by local topography (Fisher *et al.* 1993). However, such reversed flow might have affected only the lowermost levels of the density current and thus may only record an increment of downslope settling (e.g. Fig. 2.4C). Turbidites similarly show that density currents are reflected by topography (Kneller *et al.* 1991; Pickering *et al.* 1992; Kneller & McCaffrey 1999; Kneller & Buckee 2000).

Edwards *et al.* (1994) showed that as a single-surge density current starts to ascend a slope a bulge develops at the base of the slope (Fig. 2.8D) and then collapses to generate a bore (a moving hydraulic ramp that transports mass), which propagates backwards at velocities approaching that of the original (oncoming) current (Fig. 2.8D). Strong bores (Fig. 2.8E) formed in this way are similar to the original current, in all but direction, and they may transport clasts and generate deposits like those formed by the original current. Where relatively weak bores form (Fig. 2.8F) the backwards-propagating disturbance forms a series of solitary waves that produce pulsations in velocity and might produce a layered and/or rippled deposit (Edwards *et al.* 1994; Kneller *et al.* 1997). Radially spreading density currents that impinge on linear ramps generate straight-crested solitary waves that propagate normal to the ramp, curved obstacles generate curvilinear waves and vertical obstacles (e.g. cliffs) produce an undercutting reverse flow (Edwards *et al.* 1994). Experiments with more sustained low-concentration currents (Woods *et al.* 1998) indicate that an upcurrent-propagating bore, originating from a ridge that initially blocks the current, thickens the current gradually until it surmounts the ridge. Currents initially blocked in this way produce thicker deposits upcurrent of the ridge. Models scaled for realistic clast-size populations are required to predict the responses to topography of sustained density-stratified pyroclastic density currents, and to learn about topographically induced deposition and current lofting (see Alexander & Morris 1994; Woods *et al.* 1998). Responses of currents in which clast interactions are important remain particularly poorly known.

A new twofold classification of pyroclastic density currents

Considerable progress has been made in understanding both the behaviour of low-concentration (dilute) currents in which clast support is by fluid turbulence and clast interactions are negligible, and the behaviour of high-concentration granular flows in which the effects of interstitial fluid are of secondary importance. However, pyroclastic density currents that deposit ignimbrites are transitional between these types. They constitute a spectrum of hyperconcentrated currents in which both clast interactions and interstitial fluid are important.

Previously, two distinct types of pyroclastic density currents, 'pyroclastic surges' and 'pyroclastic flows', have been conceived. Mindful that there is a continuous spectrum of currents and that a single current can deposit both stratified and massive lithofacies (see Chapter 6), we propose a new two-fold classification of pyroclastic density currents (Fig. 2.9). All gradations exist between the two types of current we define below.

- *Fully dilute pyroclastic density currents* are those in which collisional momentum transfer between moving pyroclasts has little effect upon particle support, segregation and current rheology, *throughout the full thickness* of the current (Fig. 2.9A and B). The currents can be density stratified, but, even down to the base, interactions between moving clasts are unimportant. Particle transport and support are dominated by effects of turbulence of the fluid phase (dusty gas) at all levels in the current, and commonly also involve traction and saltation. Deposits of fully dilute currents are typically parallel stratified and cross stratified. They occur within many ignimbrite sheets (where they are usually subordinate) and also within the bedded successions previously termed 'pyroclastic surge' deposits (where they commonly dominate).
- *Granular fluid-based pyroclastic density currents* are those in which clast concentrations towards the lower flow boundary are sufficiently high for particle support there to be dominated by collisional momentum transfer between moving grains and/or fluid escape. The currents may be density-stratified, and in some cases support by fluid turbulence may dominate at some level above the flow-boundary zone (Fig. 2.9 C–G). However, near the lower flow boundary turbulence is typically dampened and traction is reduced (Branney & Kokelaar 1997). Deposits are massive, diffuse-bedded or bedded, with various grading patterns (see Chapter 5).

This twofold classification is based upon processes and conditions that dominate around the lower flow boundary of the current, as reflected in the characteristics of the deposit. The distinction is not by absolute particle concentration because this can rarely be measured, and because the extent to which grain interactions dominate in the flow-boundary zone depends also on parameters such as grain-size distribution and current velocity, which vary. (Grain interactions may start to dominate at concentrations greater than about 8 vol. %; see the section on 'Granular temperature and dispersive pressure', p. 29). As both types of current can be density stratified, overall differences between the two types can be quite small in some cases (compare Fig. 2.9B and C), and changes from fully dilute to granular fluid-based currents do not require 'body transformations' of the entire current (see p. 92). Moreover, at any one time, an individual pyroclastic density current may be of different types in different reaches, and/or may vary laterally from one type to the other. We emphasise that 'granular fluid-based current' is not synonymous with either 'pyroclastic flow' or the 'giant fluidized bed' model (see p. 1 and Fig. 2.2A), in that it is defined according to conditions only around the lower flow boundary, rather than according to the overall mechanism of transport. However, a pyroclastic density current in which the entire thickness comprises a granular fluid (e.g. a modified grain flow) would, if it exists, be a variety of granular fluid-based current (Fig. 2.9G).

Tuff rings are composed of bedded successions with intercalated massive, stratified and cross-stratified layers. Previously all of these layers have been referred to as 'pyroclastic-surge' deposits. We consider some of them (e.g. the stratified layers) to be deposited from fully dilute pyroclastic density currents and others (e.g. massive layers) to be deposited from granular fluid-based currents. The bedded successions record phreatomagmatic eruptions that are typically of low mass flux and pulsatory, and give rise to short-lived, rapidly depletive currents with frequent alternations between fully dilute and granular fluid-based types.

In order to link ignimbrite characteristics to current properties, it will be necessary to understand deposition from stratified hyperconcentrated currents. This will require quantitative information on flow-boundary zone conditions and processes during deposition, as well as improved understanding of the ways in which density stratification is affected by changes in topography, clast diversity, waves, gas compressibility and air ingestion.

Fully dilute currents: dilute and turbulent throughout

Granular fluid-based currents: basal parts sufficiently concentrated for grain interactions and/or fluid-escape to dominate, irrespective of the nature of the rest of the current

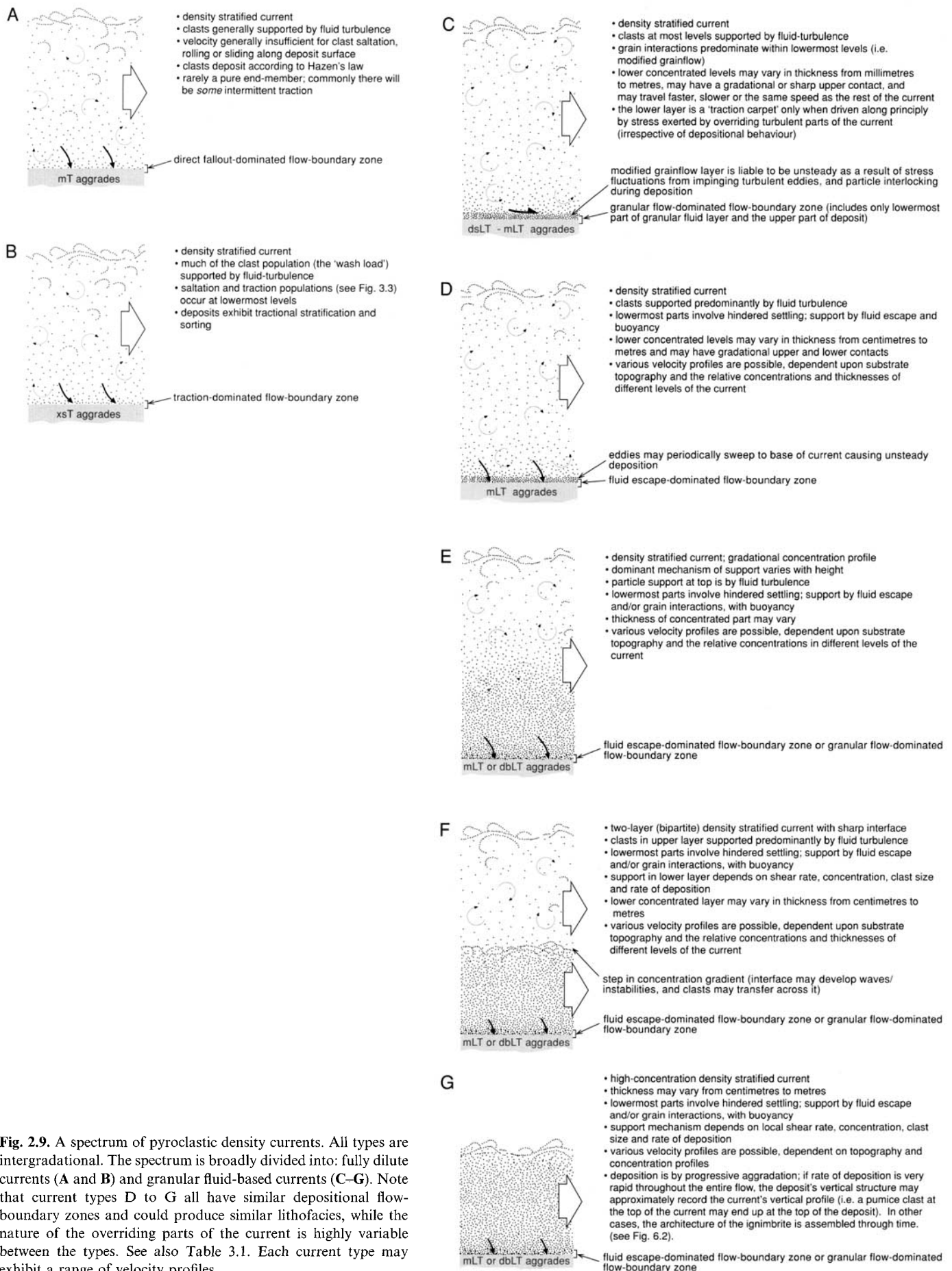


Fig. 2.9. A spectrum of pyroclastic density currents. All types are intergradational. The spectrum is broadly divided into: fully dilute currents (A and B) and granular fluid-based currents (C–G). Note that current types D to G all have similar depositional flow-boundary zones and could produce similar lithofacies, while the nature of the overriding parts of the current is highly variable between the types. See also Table 3.1. Each current type may exhibit a range of velocity profiles.

This page intentionally left blank

Chapter 3

Mechanisms of particle support and segregation

In this chapter, we consider the various mechanisms of clast support, and the associated clast-segregation effects, that are relevant to pyroclastic density currents.

Significance of current heterogeneity and pyroclast diversity

Ignimbrite-forming pyroclastic density currents have been modelled as grainflows (Denlinger 1987; Dobran *et al.* 1993; Straub 1994), semi-fluidized beds (Sparks 1976; Wilson 1980, 1984), low-concentration turbulent suspensions (Valentine 1987; Dade & Huppert 1996) and laminar plug flows (Wright & Walker 1981; Battaglia 1993). However, although simplification is necessary in modelling, assumption of just one clast-support mechanism or of notional bulk current properties is not appropriate for the consideration of sedimentation from a pyroclastic density current. This is because pyroclastic density currents are inherently heterogeneous and involve a range of clast-support mechanisms (Table 3.1). The heterogeneity that significantly affects clast transport and sedimentation can result from: (1) source variability (e.g. fluctuations in velocity, concentration and rheology) with time and with location, according to the nature of any unsteady or inhomogeneous vent discharge; (2) segregation within the current (Fig. 3.1), for example due to development of density stratification and stratification of support mechanisms (e.g. see Fig. 3.3) or of clusters and concentrations with a different rheology to that of the surrounding current (e.g. pumice rafts); (3) contrasting behaviour and properties of upper and lower flow-boundary zones (e.g. involving sedimentation, elutriation, entrainment and turbulence); (4) unsteady and non-uniform air ingestion and expansion; (5) effects of topography; and (6) sedimentation and/or erosion-induced changes in properties of the current and substrate with

time or location.

Clasts in a current are supported by combinations of different mechanisms, and these combinations change as the clasts move through the current and experience different concentrations and shear intensities. The diversity of clast shapes, sizes and densities (e.g. vitric dust versus lithic blocks and pumice lapilli) in a pyroclastic density current is characteristically much greater than that in any siliciclastic turbidity current. Because different pyroclasts are supported in different ways they behave differently and can become segregated. The nature of this segregation varies from point to point, dependent upon the local conditions. Consequently, adjacent clasts in an ignimbrite may have had quite different transport histories, and the precise composition of any batch of the initial erupted dispersion is not to be found in any one part of the ignimbrite; particle mixing and fractionation characterize both transport and deposition.

The influences of current heterogeneity and clast diversity in a pyroclastic density current are best understood by considering the nature, controls and effects of the various clast-support mechanisms. The following account draws on published work on powders, granular flows, particulate flows in pipes, aqueous turbidity currents, flume experiments and computer simulations. For each mechanism, the associated *segregation* effects are described because segregation determines ignimbrite character (lithofacies). Segregation occurs: (1) within the pyroclastic density current (Fig. 3.1); (2) at the flow boundary (Fig. 3.1); and (3) within the compacting deposit, for example during loading and formation of elutriation pipes. The flow-boundary zone is particularly important for segregation as it spans all three sites. Segregation within the current may produce current stratification (e.g. pumice transported at a higher level than large lithic clasts) and this may not be fully

Table 3.1. *Some support mechanisms in pyroclastic density currents. All gradations exist between fully dilute and granular fluid-based currents. Most clasts are supported by a combination of mechanisms. The relative contribution from each support mechanism varies with clast type, with height in a current where the current is density stratified, with distance where the current is non-uniform and with time when the current is unsteady. Some support mechanisms within uppermost levels of loose aggrading deposits are shown on the right, for comparison*

Fully dilute currents	Granular fluid-based currents	Aggrading deposits (just below the flow boundary, and in levees and lobate deposit terminations)
Suspension by fluid turbulence (of the suspension population and, intermittently, the saltation population)	Suspension by fluid turbulence (important in upper levels of the current; turbulence may also affect more concentrated dispersions at lower levels in the current)	
Intermittent substrate support (e.g. saltation and temporary deposition followed by re-entrainment)	Intermittent substrate support (of larger clasts, e.g. undergoing saltation, and temporary deposition followed by re-entrainment)	
Traction (rolling or sliding along the substrate)	Traction (rolling and/or sliding of large/heavy clasts along the substrate)	Sustained support by the substrate
	Grain interactions (in some cases just in lower levels)	Possible contribution by granular temperature, 'conducted' from current
	Hindered settling (most marked within lower levels)	Hindered settling (in the uppermost compacting deposit of a fluid escape-dominated flow-boundary zone)
	Fluid escape and elutriation (smaller/lighter clasts)	Fluid escape and elutriation (smaller/lighter clasts)
	Excess pore fluid pressure (especially in lowermost parts)	Excess pore fluid pressure
	Clast buoyancy (e.g. pumice)	Clast buoyancy (e.g. pumice in 'quick' deposit)
		Yield strength (quasi-static clast contacts)

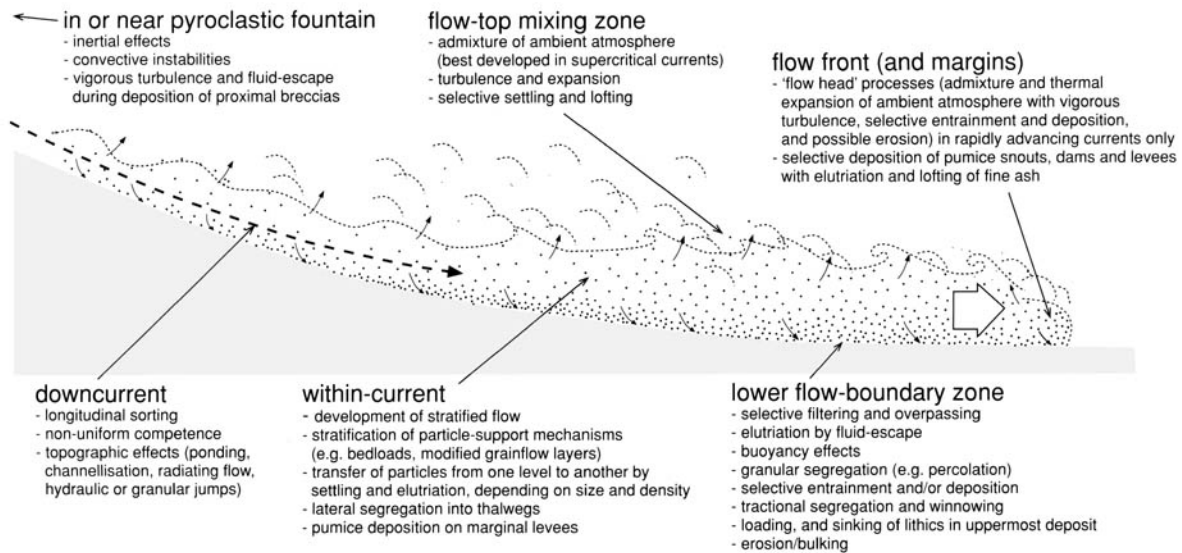


Fig. 3.1. Sites of particle segregation in a pyroclastic density current. Segregation may continue within the loose deposit (e.g. elutriation, loading).

recorded at any one site in the ignimbrite, which aggrades only from the base of the current. In Chapter 6 we consider the ways in which the varying segregation at the three sites can combine to determine the overall character of an ignimbrite.

Fluid turbulence

Support by fluid turbulence

Fluid turbulence acts as a support mechanism by exertion of fluid lift (Fig. 3.2) and drag on clasts with settling velocities less than, or comparable to, the upward component of the eddy velocity (Rouse 1939; Hunt 1969; Allen 1984; Ghosh *et al.* 1986). At concentrations below a few volume per cent (vol. %), clast interactions are

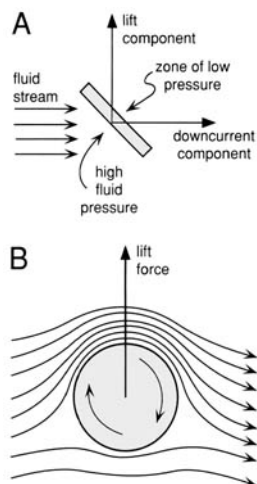


Fig. 3.2. Two aerodynamic lift effects: after Coulsen & Richardson (1990) and Tritton (1988). (A) The aerofoil effect is a lift component imparted to an inequid pyroclast when a horizontal fluid flow acts on its inclined surfaces. (B) The Magnus effect, or more correctly the Robins effect in the case of a non-cylindrical pyroclast, arises because saltating clasts tend to rotate around axes transverse to flow. Their upper surfaces move in the same direction as the enclosing fluid flow, which causes fluid acceleration above each clast, while their lower surfaces move in the opposite direction to the fluid, which retards the fluid beneath each clast and causes relatively high local pressure that exerts a lift force.

negligible and fluid turbulence is the dominant clast-support mechanism during transport. However, turbulence also contributes to clast support in those parts of currents in which clast interactions and dispersive pressure are important.

Vertical segregation of clasts in the current during turbulent transport

Clasts in a polydisperse fully dilute current tend to segregate vertically so that clasts with particular hydraulic/pneumatic properties tend to occupy three overlapping levels within the current according to their dominant mode of transport (Fig. 3.3) (Middleton & Southard 1984). Of the initial population, fluid turbulence tends to fully support only the smaller and/or less dense clasts (e.g. including fine ash), unless the current is especially energetic. These constitute the *suspension population* (wash load) and they travel at *all* levels within the current. Larger and/or denser clasts are only partially and/or intermittently supported by fluid turbulence, and spend most of their time in lower parts of the current (Fig. 3.3), where they constitute the *intermittent suspension population* (see 'Support on an interface', p. 25). The largest and densest clasts are transported along the deposit surface by fluid drag and are known as the *traction population*. This threefold division is a simplification because: (1) clasts change from one mode of transport to another as they travel downcurrent (where flow is non-uniform), and within the same reach of a current as it waxes or wanes (unsteady current); and (2) even in steady, uniform currents there is no sharp distinction between the populations (Allen 1984). Traction, saltation and suspension-population components may be distinguished granulometrically within some pyroclastic density current deposits (e.g. Frazzetta *et al.* 1989) (Fig. 3.3).

With increasing concentration in a turbulent current, the importance of clast collisions and buoyancy (see pp. 29 and 34) increases, especially within the basal part of the current where they may be more important than fluid turbulence as the principal support mechanism.

Segregation at the flow-boundary zone due to turbulence

In tractional transport, clasts frequently are deposited momentarily and then re-enter the current. Where there is no net aggradation, the proportion of clasts being deposited equals the proportion re-entering the current, whereas with net aggradation more clasts are

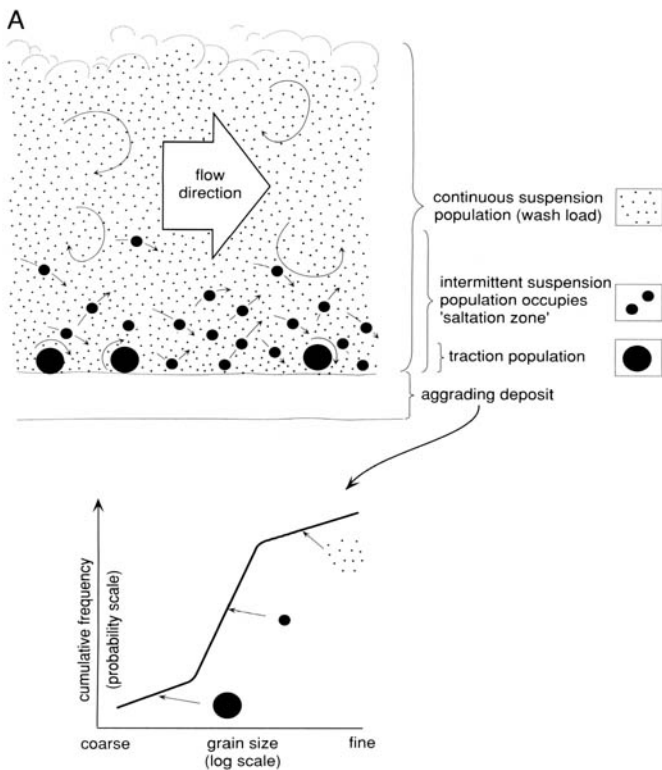


Fig. 3.3. Vertical segregation within turbulent polydisperse currents. **(A)** The clast population is segregated into three different, but overlapping, fractions according to their dominant mode of support. One fraction of the clast population, the 'wash load', is fully supported by fluid turbulence and is distributed throughout the current. Another fraction is only intermittently supported by fluid turbulence, with frequent returns to the substrate, and is concentrated within lower parts of the current. A third fraction moves by traction along the substrate surface. **(B)** A typical size distribution in a deposit derived from the current above (see **A**), with an interpretation shown in terms of the three overlapping fractions and hydraulic sorting during transport (after Middleton & Southard 1984). Clast interactions and fluid escape may become important additional support mechanisms in lowermost levels of currents that are of granular fluid-based type (pp. 20–21), in which case the deposits would tend to be less well sorted.

deposited than are re-entrained. In fully dilute currents the traction population moves more slowly than the other populations and has the greatest tendency to deposit, either temporarily or permanently. Where a turbulent eddy encroaches the lower flow boundary, it tends to *selectively entrain* clasts from the substrate according to their density, shape and size (Li & Komar 1992 and references therein). A heterogeneous clast population momentarily entrained just above the substrate by a turbulent eddy will segregate into: (1) relatively large/dense clasts that fall out to form a fines-poor lens; and (2) smaller or less dense clasts that remain entrained and which settle elsewhere when the turbulence has lessened sufficiently. Repeated passage of turbulent eddies may deposit stacked fines-poor layers or lenses (a type of lag) within a fines-rich ignimbrite (see also Hiscott 1994b). Lee-side lenses (Walker *et al.* 1980; Wilson 1985) are formed in a similar way, but where turbulent eddies are sustained downstream of obstacles. The degree of contrast in grain size between successive fines-poor lenses and the lens size may, respectively, reflect differences in the intensity and in the size of the turbulent eddies that encroach the deposit surface. Thus, mm- to cm-thick lenses or laminae with large grain-size contrasts are common in deposits of pyroclastic density currents in which lower flow-boundary zones have high turbulence intensities. Conversely, they are rarely well developed, and are more localized, in ignimbrites derived from currents in which the turbulence was less intense in lower flow-boundary zones due to lower velocities and/or higher concentrations (e.g. Walker & McBroom 1983). The restricted occurrence in some ignimbrites of lenses formed by turbulent segregation has been cited as evidence that turbulence was restricted in occurrence to large-scale eddies in the lee side of ground irregularities (Walker *et al.* 1980). This interpretation relates to only the lowermost part of the current, because more widespread turbulence higher in the current cannot be excluded.

Support on an interface

Sustained support: rolling and sliding

Drag exerted by the fluid causes particles to slide or roll along the

lower flow boundary of a current (traction; Middleton & Southard 1984). This is best known for fully dilute currents, but it also occurs in high-concentration parts of granular fluid-based currents in which, for example, large lithic blocks can roll along the base, where their transport is aided by clast interactions and buoyancy due to the surrounding finer grained dispersion. Such blocks may be found at any level within a massive deposit (e.g. ignimbrite) because the flow boundary along which they moved migrated upward during transport (progressive aggradation). Accordingly, their height records the compacted thickness of deposit that had aggraded at the time they were deposited. Some clasts may travel along an interface of contrasting rheologies within a current (e.g. Postma *et al.* 1988).

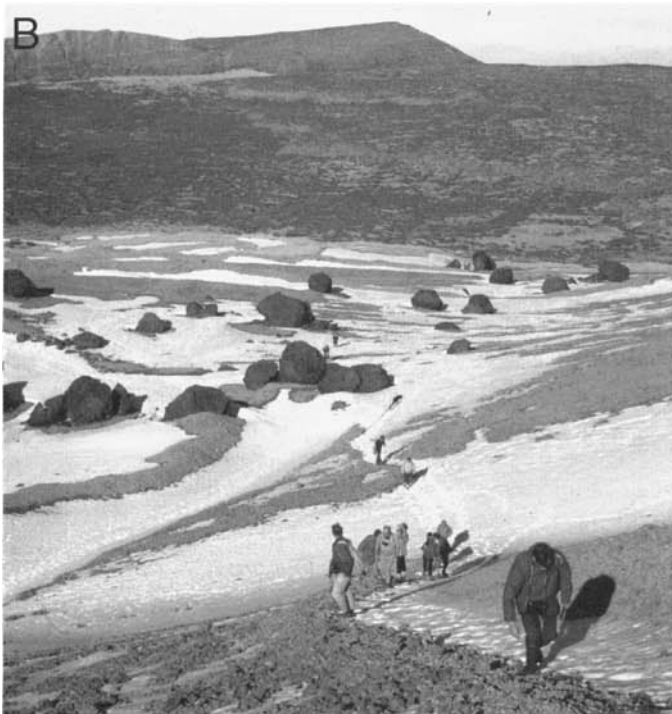
Intermittent support: saltation

In currents undergoing no net deposition, a significant fraction of the current load can comprise clasts that are deposited temporarily before being re-entrained by fluid lift and/or by the impact of other clasts. Once re-entrained, a clast may become suspended high in the current by fluid turbulence, or it may return rapidly to the basal flow boundary. 'Saltation' describes *any* leaping movement of clasts along an interface; the interface provides intermittent support. Saltation is particularly important in pneumatic systems. The lower part of a fully dilute current, where the saltation population is mostly transported, is termed the *saltation zone* (Fig. 3.3). However, its upper limit is not well defined because of velocity fluctuations and because different saltating clasts rise to different heights within the current. Experiments show that the mass flux of sand grains saltating in a gaseous current varies as a negative exponential function of the height above the flow boundary (Zingg 1953; Williams 1964). Saltation has been modelled as due to bouncing (Bagnold 1956, 1973; Murphy & Hooshari 1982) and as due to fluid lift and/or drag, coupled with intermittent suspension by fluid turbulence (Einstein & Chien 1955; Chepil 1961). Both processes are likely to contribute in pyroclastic density currents. Where the clast concentration is high, a saltating clast may receive additional support from collisional interactions and other support mechan-



Fig. 3.4. Effects of granular flow processes, segregation and overpassing.

(A) Longitudinal inverse size grading of blocks and lapilli on a talus cone, Pinatubo volcano, Philippines. Debris-fall blocks (p. 28) have outrun (overpassed) the ash and lapilli that were deposited by grain flows on the cone.



(B) Isolated debris-fall blocks that bounced and rolled down steep NE flanks of Teide (which is behind the viewer), Tenerife, and came to rest some distance beyond the break of slope.



(C) Isolated debris-fall blocks enclosed by finer grained ash and lapilli of grainflow origin, within block-and-ash flow deposits of Kaimondake volcano, Kyushu, Japan. Metre rule for scale.

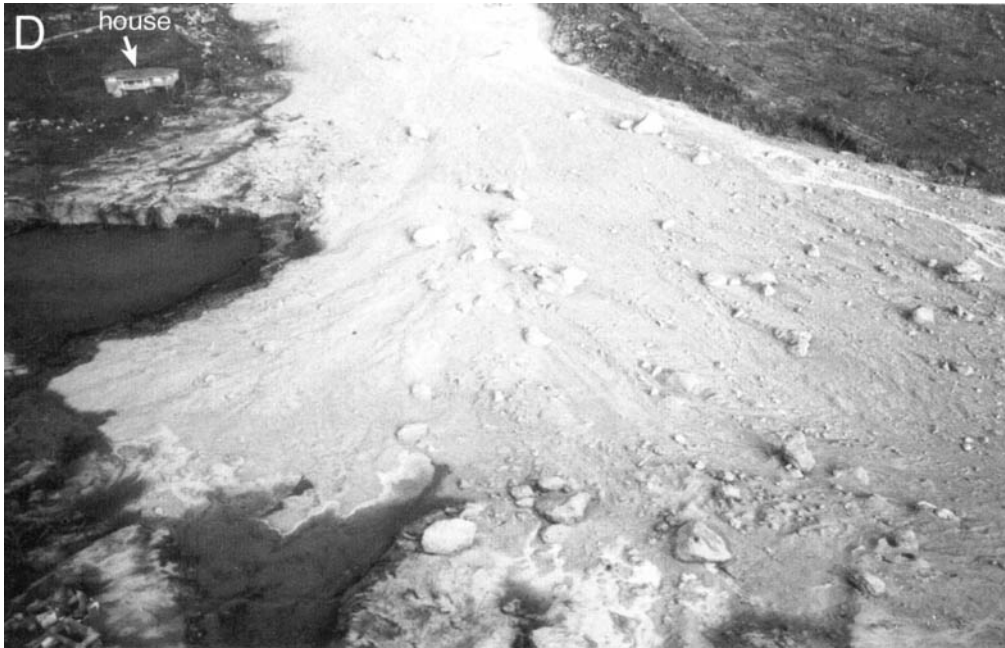
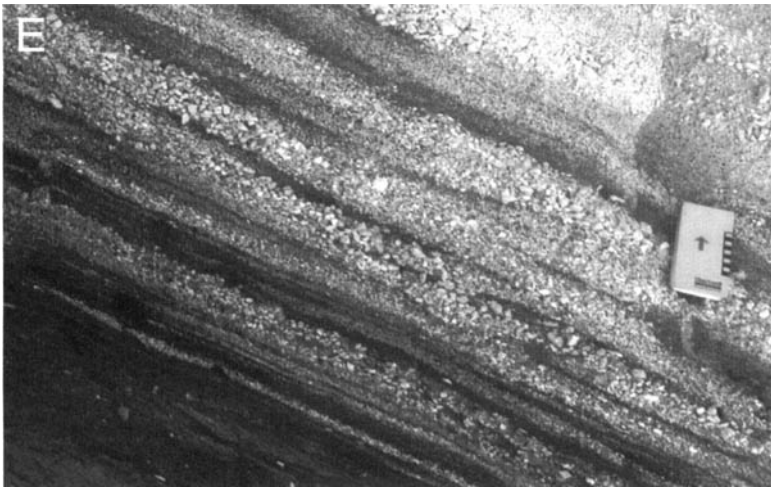


Fig. 3.4. (continued).

(D) Distal accumulation of large debris-fall blocks that bounced and rolled downslope primarily under their own momentum along with small pyroclastic density currents that deposited the pale block-and-ash flow lobe: Soufrière Hills Volcano, Montserrat. The house gives the scale. (Photograph: Tim Druitt).



(E) Products of granular segregation during unsteady, near repose-slope grainflow. Note inverse and normal grading, and lenticular, laterally impersistent bedding. Colour picks out grain-size variations: pale clasts are pumice lapilli and dark clasts are sand-grade obsidian fragments. Mud Springs Creek, eastern Idaho, USA.



(F) Products of granular segregation during unsteady, near repose-slope grainflow, in a Strombolian scoria cone, SE Tenerife. Note the well-sorted layers and lenses of scoria lapilli with inverse grading, pinch-and-swell bedding, downslope grading and lateral impersistence of bedding.

isms (see pp. 29, 33 and 34). Such additional support enables large, dense clasts within more concentrated dispersions to saltate in longer leaps and to higher levels in the current. At higher concentrations, a basal saltating layer may grade into a modified grainflow (Middleton & Southard 1984; see p. 29). Clasts may saltate along interfaces in the current other than the lower flow boundary. For example, Denlinger (1987), following Hanes & Bowen (1985), envisaged clasts in some granular fluid-based pyroclastic density currents saltating along the top of a lower granular-flow layer, so that the concentration of clasts decreased gradationally upwards from a basal granular flow into an overriding turbulent ash cloud via a saltation zone.

Debris fall (Nemec 1990; Sohn & Chough 1993) is a type of saltation in which each clast bounces downslope under its own momentum due to gravity, rather than being driven by fluid drag or lift, or by grain collisions (Fig. 3.4A–D). This is the kinetic or ‘streaming’ mode of granular flow (Campbell & Gong 1986; Campbell 1989). It differs from the ‘collision’ mode of granular flow (i.e. a grainflow), which is of higher concentration (> 8 vol. %) and in which momentum is transferred between clasts during frequent collisions (see later in this chapter). Debris fall requires slopes close to, or steeper than, the repose-angle, and it may dominate the transport of larger blocks in Merapi-type pyroclastic density currents (Francis 1993) derived from collapsing lava fronts or domes (e.g. Francis *et al.* 1974; Davies *et al.* 1978; Fujii & Nakada 1999; Miyabuchi 1999). Isolated blocks that rolled and bounced ahead of the leading edge of small pyroclastic density currents at Montserrat (video footage 1999), and blocks reported as being ‘occasionally ejected from the cloud at the head’ and ‘thrown ahead of the flow’ at Unzen (Yamamoto *et al.* 1993), were probably moving mainly by debris fall. Cataclastic textures and melt veneers on surfaces of large lava blocks in block-and-ash flow deposits at Montserrat confirm the high energy of block collisions, both with each other and with substrate (Grunewald *et al.* 2000). In pyroclastic density currents, debris-fall transport is generally modified by other clast-support mechanisms (e.g. involving gas and particle interactions). These facilitate debris fall on lower slopes than would be possible for individual blocks. At a decrease in slope, some debris falls partially or wholly transform into modified grainflows (Nemec 1990; Sohn & Chough 1993).

Overpassing: downcurrent segregation at an interface

Clasts transported with sustained or intermittent support on an interface (e.g. deposit surface) are subject to various segregation processes. For example, rolling clasts subject to shear by fully dilute currents sort themselves into impersistent, single-grain-thick moving sheets recorded in the deposit as subparallel tractional stratification (Arnott & Hand 1989). During tractional deposition, the rising interface may develop irregularities such as ripples or dunes (collectively ‘sandwaves’) that may be preserved in the deposit as various types of cross-stratification (Allen 1984) (see Figs 5.9 and 6.17B).

Segregation in which some clasts travel significantly further and/or faster than others is known as *overpassing* (Nemec 1990). In some instances, larger clasts outrun smaller clasts, because: (1) large clasts project from the flow boundary higher into the shearing fluid so that the drag exerted on them is greater; (2) in debris-fall transport, large clasts have greater momentum; and (3) large clasts rolling or sliding along the top of a layer of smaller clasts are less easily arrested by the surface roughness than are smaller clasts moving across a layer of larger clasts. Smaller clasts are more easily trapped between the clasts of the subjacent layer. This effect was invoked to explain the lack of pneumatic equivalence between lithic blocks and adjacent small pumice clasts in coarse lithic breccias of ignimbrites (Walker 1985) (Fig. 3.5); small pumice clasts were considered to have been trapped more easily than large pumice clasts in cavities between the lithic blocks in the aggrading deposit

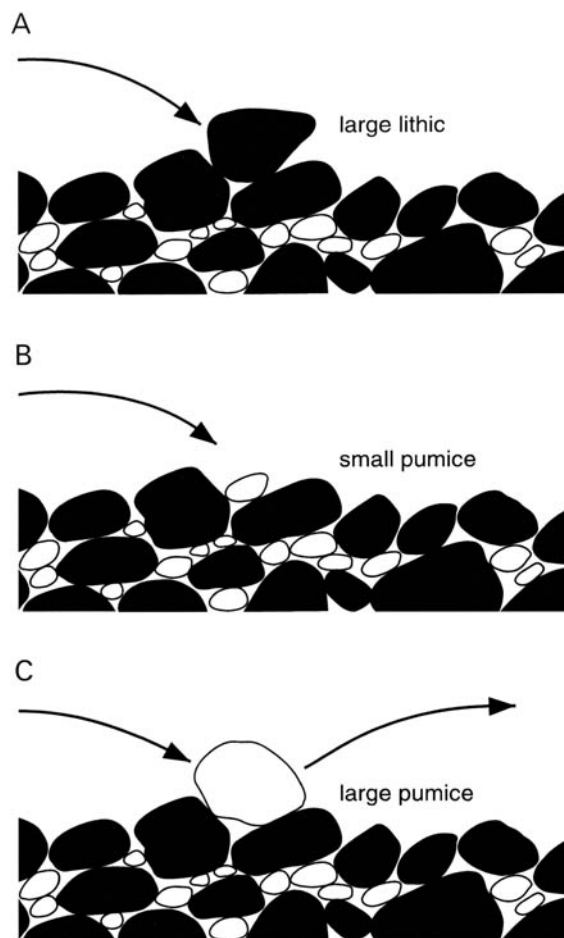


Fig. 3.5. Granular segregation by surface roughness. Large pumice clasts are less easily trapped in surface irregularities compared to small pumices or large lithics, and so tend to pass further downcurrent (overpassing). (A) Large saltating lithic block halts when trapped by a surface irregularity. (B) A small pumice clast is similarly arrested in a pocket in the irregular deposit surface. (C) A large pumice clast is less easily trapped and overpasses downcurrent. The aggrading grain mass exhibits pneumatic inequivalence, for example between large blocks and small pumices in a lithic breccia (modified after Walker 1985). For a thought experiment, consider what would happen in each case if the grain mass were diluted due to an elevated granular temperature, facilitating percolation.

surface. Experiments show that in these types of segregation, clast size is more important than density, and clast shape is of negligible importance unless highly non-spherical (Drahn & Bridgewater 1983).

Pyroclastic deposits recording segregation during debris fall accumulate where the steep flanks of a volcano pass into more gentle slopes (Fig. 3.4A–D). Distally the deposits are characterized by the presence of isolated large blocks (Fig. 3.4A–D), which in some instances may lie beyond the furthest limit of smaller clasts (Fig. 3.4A); that is, the lithics coarsen in a downcurrent direction (e.g. 12 June 1980, pyroclastic density current deposits between Mount St Helens and Spirit Lake; Rowley *et al.* 1981). Successive debris-fall events produce progradational deposits in which large isolated blocks are buried in subsequently deposited finer grained matrix (e.g. Sohn & Chough 1993) (Fig. 3.4C). Such characteristics have been described in some Merapi-type block-and-ash flow deposits (Francis *et al.* 1974; Davies *et al.* 1978; Fujii & Nakada 1999; Miyabuchi 1999) and in breccias emplaced by pyroclastic density currents at El Chichón, Mexico (Macías *et al.* 1998).

Granular temperature and dispersive pressure

Clast interactions and current mobility

Granular flow theory (see review by Campbell 1990) is important in understanding pyroclastic density currents. In a rapidly shearing mass of clasts, frequent clast collisions force the clasts apart so that they move quasi-randomly about the average motion vector of the shearing mass (Bagnold 1954; Savage 1979; Campbell & Brennen 1983). The clast vibrations are analogous to the thermal motion of molecules in the kinetic theory of gases, and so are termed *granular temperature* (Ogawa 1978; Campbell & Brennen 1983; Haff 1983; Savage 1983, 1984). Like thermodynamic temperature, granular temperature generates pressure and governs the internal rates of mass and momentum transfer. However, granular temperature cannot self-sustain, because clast collisions are inelastic and mechanical energy is dissipated as thermodynamic heat, so it must be maintained by shearing. Granular temperature varies approximately as the square of the local velocity gradient (shear rate) within the grain mass (Campbell & Brennen 1985). Steep gradients in granular temperature cause the conduction of kinetic energy from high- to low-granular-temperature parts of a shearing grain mass, just as in the thermodynamic counterpart. For example, the top of a deposit beneath a 'hot' shearing grain mass may acquire a granular temperature by conduction, and thus expand, loose strength and viscosity, and become more susceptible to re-entrainment (erosion), even though it undergoes no shear (Campbell 1990). In this non-shearing dilated dispersion, buoyancy and percolation may cause clast segregation. The pressure associated with granular temperature is *dispersive pressure* (Bagnold 1954), which forces particles apart causing bulk dilation. At high granular temperatures, dispersive pressure can maintain a grain mass in a liquefied state and it is thought to be an important clast-support mechanism in most moderate- to high-concentration currents (Bagnold 1954; Lowe 1976; Walton 1983). Dispersive pressures are highest where shear rates are highest (e.g. Lowe 1982; Campbell 1990). Currents dominated by granular temperature are termed *cohesionless debris flows* (Postma 1986). They are divided into (1) *true grainflows*, in which interstitial fluid is unimportant, and (2) *modified grainflows* (Lowe 1982), which occur in basal parts of some density-stratified currents, and in which the flow properties and behaviour are modified by the effects of intergranular fluid and/or the overlying part of the current (e.g. Hanes & Bowen 1985; Jiang 1995; Iverson & Vallance 2001). The spectrum of pyroclastic density currents may include both types of granular flow, but modified grainflows are prevalent because of the ubiquitous occurrence of interstitial dusty gas and because upper parts of the currents are turbulent and less concentrated.

Clast concentrations in grainflows may be as low as 8–10 vol. % (Bagnold 1955; Sohn 1995). For *well-sorted* natural sediments, frequent clast collisions occur when the separation distance, s , between clasts is about the same as or less than the grain diameter, D , so that the linear grain concentration, λ , is ≥ 1 , when $\lambda = D/s$, and the volume concentration is $\geq 8\%$ (Hanes & Bowen 1985; Sohn 1995). In pyroclastic density currents the concentration above which granular flow dominates will vary, for example with shear rate and with sorting.

Quantitative application of granular flow theory to natural density currents is fraught with complication, not least because granular temperatures, grain concentrations and fluid pressures all change spatially and temporally during transport and deposition (e.g. see Iverson & Vallance 2001). Nevertheless, simplified aspects of the theory have been used in computer simulations of pyroclastic density currents (e.g. Dobran *et al.* 1993), in interpretations of pyroclastic deposits on tuff cones (Sohn & Chough 1993) and in considerations of the mobility of small pyroclastic density currents (Hayashi & Self 1992; Straub 1996). The need for experimental verification of the parameters used has been stressed (Campbell 1990; Sohn 1995). Many granular-flow models assume monodis-

perse or bidisperse populations of infinitely elastic clasts with perfectly spherical shapes (or disc shapes in two-dimensional models), whereas pyroclastic density currents are polydisperse with a wide range of clast densities, and with pyroclasts that are neither infinitely elastic nor spherical. Clast abrasion and comminution are characteristic in the natural systems. Most models also do not account for segregation in a shearing dispersion or the development of orientated clast fabrics, which affect the granular fluid rheology and shear profiles (Campbell 1986; Pouliquen & Vallance 1999). They also do not rigorously consider the effects of admixed dusty gas (see Fink & Kieffer 1993), turbulence, buoyancy or the effects of fluid escape during hindered settling. Recent kinetic modelling of the effects of interstitial-gas content on granular flows down chutes (Zhang & Reese 2000, and references therein) indicates that gas may be significant in modifying the flow-velocity profile and energy dissipation characteristics of fully developed flows, largely by dampening the energy flux involved in maintaining granular temperature. This occurs from drag effects of the gas and mostly influences the behaviour of smaller particles (≤ 5 mm). Most granular flow models adopt invariant smoothness parameters for grains (Campbell 1990), which may be inappropriate for pyroclastic dispersions because of the breakage and abrasion of pumice that occur during transport and contribute much to the abundant fines and abraded pumice lapilli that characterize ignimbrites and cognimbrite plumes (Sparks & Walker 1977). These shortcomings are critical; the characteristic features of ignimbrites (e.g. their poor sorting, bedding, deposit dimensions; see page 51) show that they are not deposits of end-member grainflows (granular segregation in grainflows is highly effective and gives rise to well-sorted, framework-supported deposits). Recent innovative experiments by Pouliquen & Vallance (1999) have established significant effects of clast size and angularity on granular flow, elegantly demonstrating their influence in the initiation and growth of pumice-rich lobate terminations of pyroclastic deposits (see p. 47). Finally, although experimental and computer simulations of granular flows have started to consider boundary conditions and the transitional quasi-static zones that occur between granular flows and static substrates (see p. 35; Jenkins & Askari 1991; Zhang & Campbell 1992), these are proving difficult to model (e.g. see Kruyt & Verèl 1992; Zhang & Reese 2000) and such simulations are yet to be meaningfully applied in analysing the behaviour of pyroclastic density currents. Much more work using clast populations that are representative of those in pyroclastic density currents is required to understand flow boundary conditions *during deposition*.

Segregation in granular flows

Clasts in granular flows segregate according to size, density and/or shape (see reviews by Williams 1976; Dolgunin *et al.* 1998), although the relative effects of these parameters are sensitive to drag by interstitial fluid and the style of any granular-convective motions (Möbius *et al.* 2001). Inverse-graded layers of ignimbrites (see Figs 5.2F, 5.6 and 6.14A and B) have frequently been attributed to dispersive forces within shearing basal parts of semi-fluidized 'pyroclastic flows', which are a type of granular fluid-based pyroclastic density current. Bagnold (1954) suggested that in currents dominated by grain collisions (his 'grain-inertia' regime) a shear-rate gradient produces a gradient in dispersive forces that causes larger clasts to migrate preferentially to levels of minimum shear strain (such as the upper free surface of a grain flow). However, although it was understood that the dispersive forces are a function of the grain size of the shearing mass, Bagnold did not produce inverse grading experimentally. Furthermore, his interpretation of inverse grading in terms of dispersive forces has been challenged (Middleton 1970) on the basis that the dispersive-forces concept has only statistical validity and cannot be applied to the individual elements of a continuum, such as in the behaviour of an individual clast within a polydisperse flow. It also does not explain

the inverse grading that develops within non-shearing parts of granular dispersions (Ridgeway & Rupp 1971; Allen 1984).

Inverse grading (Figs 3.4E and F) can result from *percolation* (sometimes called *kinematic sieving*) in which smaller clasts percolate down between larger clasts in a granular flow (Scott & Bridgewater 1975; Bridgewater *et al.* 1985; Savage & Lun 1988), particularly where the flowing granular mass is dilated by elevated granular temperatures (Williams 1976). In addition, larger clasts tend to roll over the smaller clasts more easily than smaller clasts can roll over larger ones (*surface-roughness effect*; see p. 28). Occurrences of inverse grading in ignimbrites perpendicular to vertical or subvertical surfaces (Fig. 6.14E and F) (Sparks 1975; Druitt & Sparks 1982), and at fine-grained margins of clastic dykes, suggest that a type of segregation might result from forces other than gravity, and the surface-roughness segregation effect on sliding and rolling (p. 28) may be involved in these cases. Williams (1976) described experiments in which a single large dense clast rises through a non-shearing, vibrating mass of finer, less-dense particles. He considered that this resulted from the ability of the small vibrating particles to get underneath the large clast, whereupon they became locked into position by the weight of the large clast. Savage & Lun (1988) described two other possible segregation mechanisms in shearing grain masses. One, termed the *random fluctuating sieve*, is gravity induced and is based on the probability that a small particle will more frequently find a void into which it can fall within the granular flow than will a larger clast. The small clasts thus preferentially migrate downwards through the shearing mass. The second mechanism, termed *squeeze expulsion*, is not driven by gravity and results from unequal contact forces 'squeezing' individual clasts from one region to another within a shearing granular dispersion (Savage & Lun 1988; Sohn & Chough 1993). In contrast to Bagnold's idea that dispersive pressure drives large clasts to zones of low shear strain, experiments by Stevens & Bridgewater (1978) suggest that large clasts within a shearing mass of smaller grains migrate *towards* the zone of maximum shear rate because this is where available adjacent spaces in a shearing grain mass occur more frequently (Foo & Bridgewater 1983).

Existing granular-segregation models, including the percolation model, remain inadequate to predict the directions in which natural particles move to segregate, for example in a population of particles whose sizes and densities both differ. Vertical segregation of diverse particles has recently been ascribed to convective motions within a stationary vibrating grain mass (Knight *et al.* 1993) and it is likely that interstitial air played a role (Möbius *et al.* 2001). Forterre & Pouliquen (2001) showed that rapid granular flows can develop longitudinal vortices that register convective overturn according to dispersion density, which in turn reflects variations in shear intensity (i.e. dilation as a result of increased granular temperature). If this happens in natural polydisperse flows, relatively buoyant clasts carried upwards by such circulation cells may preferentially resist being circulated back down and so become segregated at high levels within the granular fluid. This constitutes yet another (theoretical) mechanism by which to produce inverse grading. Recent models of granular segregation in rapid granular flow invoke an interplay between convective, diffusive and segregation processes (Dolgunin & Ukolov 1995; Dolgunin *et al.* 1998). However, there is clearly a need for more experimental and theoretical work, particularly involving a fluid phase (dusty gas), boundary effects and polydisperse shearing dispersions.

The relationship between inverse grading within the bases of currents and the inverse grading seen in deposits is not simple. Consider inverse grading in a shearing layer at the base of a steady current (Fig. 3.6). At time t_1 the large clasts near the top of this shearing layer are not being deposited because they are not in contact with the flow boundary. Only the smaller clasts adjacent to the flow boundary can deposit at time t_1 . If the current is steady, other *small* clasts that have percolated down to the base of the shearing layer (during transport from upcurrent) will continuously

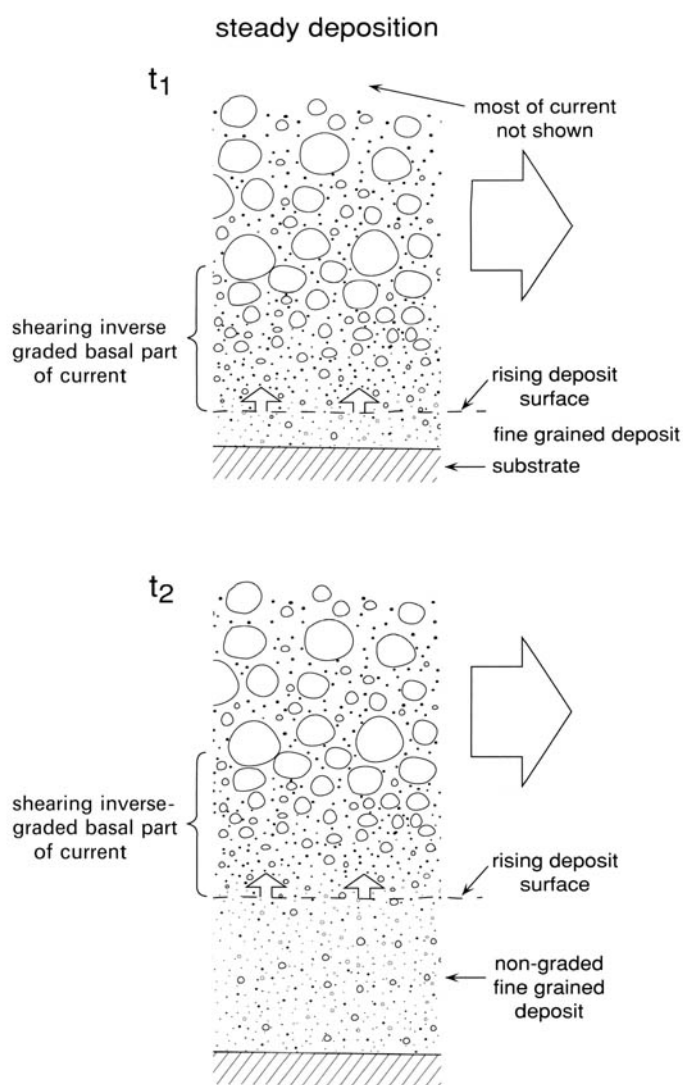


Fig. 3.6. Steady deposition from a granular fluid-based current in which granular segregation (e.g. due to percolation and dispersive forces) causes development of inverse grading within the lower part of the current. Only clasts at the base of the current can deposit at any one time, and at time t_1 only small clasts deposit. This continues (t_2) if the current remains steady, so that a fine-grained massive deposit forms and is better sorted and finer grained than the overriding current. Larger clasts overpass because granular interaction prevents them from reaching the deposit surface (selective filtering). In practice, unsteadiness is likely resulting in the development of thin layering, conceivably with inverse grading in the layers (cf. Fig. 3.7).

replace those deposited and so maintain the grading of the *current* base (t_2 on Fig. 3.6). Steady deposition from the base of such a current will thus produce a thick, non-graded fine-grained deposit, the grain size of which is not representative of the overall current. Formation of a graded deposit requires flow-boundary unsteadiness, for example due to waxing or waning flow (e.g. Fig. 3.7), or turbulent 'sweeping' (see discussion in Hiscott 1994b; see also Fig. 4.5). It is conceivable that segregation, loading and/or fabric development in the flow-boundary zone could cause a change in the rheology of the lowermost part of the current, and hence sudden frictional interlocking so that the flow boundary effectively jumps upwards (stepwise aggradation *sensu* Branney & Kokelaar 1992), thereby preserving the current's inverse-graded layer in the deposit.

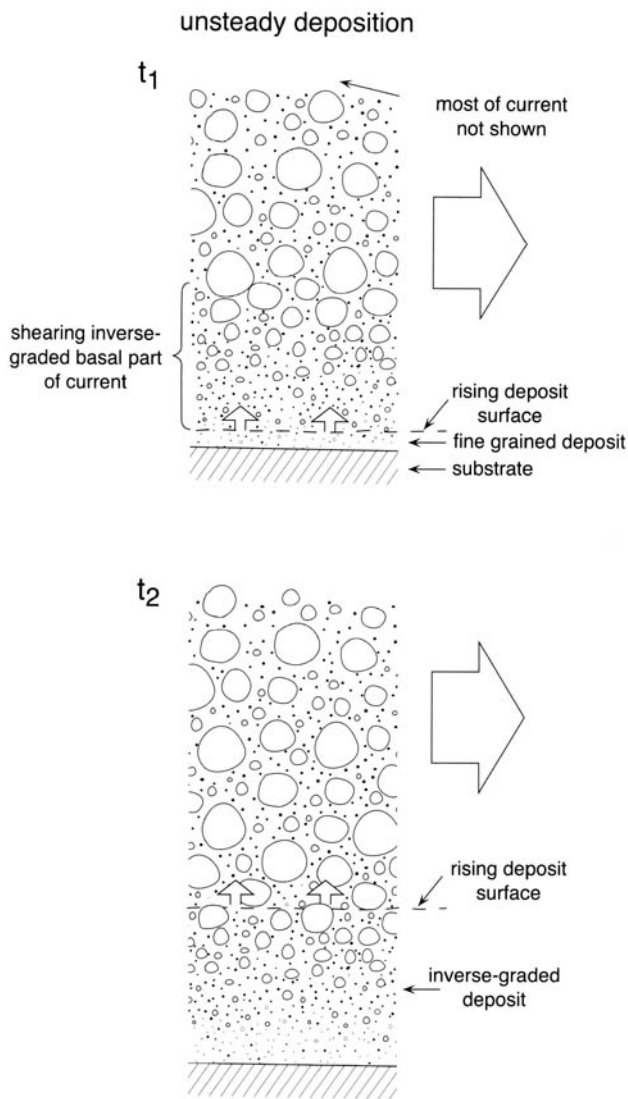


Fig. 3.7. Development of deposit grading by unsteady deposition from a granular fluid-based pyroclastic density current. Initially (time t_1) larger clasts are prevented from descending to the base of the shearing granular mass as a result of grain interactions (and possible additional effects of fluid escape and pumice buoyancy), so that the basal part of the current acquires inverse grading (as in Fig. 3.6). The larger clasts selectively filtered from the depositing population pass downcurrent (overpassing) whereas smaller clasts that can reach the base of the current (e.g. by percolation) may deposit, so that a fine-grained deposit layer aggrades. Current unsteadiness (such as decreasing shear rate) alters the selective filtering properties of the flow-boundary zone so that, for example, larger clasts are increasingly able to reach the flow-boundary and deposit (time t_2), and an inverse-graded deposit layer aggrades. The deposit surface may variously rise gradually or abruptly. With fluctuating unsteady flow, various stacking patterns of normal and inverse grading may develop.

Fluidization

Fluidization and transport

Gas-fluidization has long been held to account for the mobility of pyroclastic density currents, and for the grading, sorting, elutriation pipes and fines-depleted pods seen in ignimbrites (McTaggart 1960; Sparks 1976, 1978; Wilson 1980, 1984; Carey 1991; Francis 1993). In a gas-fluidized dispersion, an upward flow of gas exerts a drag force that partially supports the clasts so that the dispersion behaves like a fluid (Wilson 1980; see review by Kunii & Levenspiel 1991). The broad grain-size distribution of ignimbrites indicates that pyroclastic density currents can be only *semi-fluidized* (Sparks

1976; Wilson 1980), with only the smaller clasts fully supported by fluidization. This is because a gas flux strong enough to fluidize the large clasts (lithic lapilli and blocks) would elutriate the fines away almost completely. Hence, the large clasts must be supported by other means. Gas may permeate a dispersion uniformly, producing a homogeneous fluidized dispersion (this is *particulate fluidization*), or irregularly as bubbles or channels, forming an inhomogeneous dispersion sometimes with the formation of particle clusters and/or dense slugs (*aggregative fluidization*; Fig. 3.8A) (see Kwauk *et al.* 2000). Fluidization is affected both by the viscosity of the fluid phase and by the density contrast between the particles and that fluid. For example, stationary fluidization of sand by air tends to be more aggregative than is fluidization by water, although this difference may be diminished in pyroclastic density currents because shear suppresses aggregative behaviour, and because the density and effective viscosity of the fluid phase (dusty gas) may be significantly greater than air due to the abundant fine ash. With increasing gas flux a fluidized suspension expands and grades into *lean-phase fluidization* (Kunii & Levenspiel 1991), which occurs where there is explosive expansion, as in eruption conduits, lateral blasts, and places where hot pyroclastic density currents or their hot deposits admix with surface water or snow.

There are six types of fluidization (Fig. 3.8), and volcanologists have rarely been specific as to which type they invoke as a transport mechanism for a pyroclastic density current. In *flow fluidization* (Fig. 3.8B) gas moves from the substrate upwards into the current at a rate that supports the clasts. Such currents have been created experimentally (Botterill & Halim 1978; Ishida & Hatano 1983), but no natural examples are known (Allen 1984). Surface water, snow, ice, vegetation or degassing ash substrate might locally supply gas to an overriding current, but it is unlikely that a sufficient flux from the substrate could be maintained over the area covered by a large pyroclastic density current (as much as 10^3 or 10^4 km²) for its duration (several hours for large ignimbrites) to be the primary cause of current mobility.

In *bulk self-fluidization* (Fig. 3.8C) clasts are supported by the upward escape of air that has been engulfed beneath the front of the density current. This mechanism has been invoked for rockfalls (Kent 1966) and pyroclastic density currents (Walker *et al.* 1980; Wilson & Walker 1982). It is most effective in high-concentration currents (Allen 1984) and, because the air derives from flow-front advance, for currents of short length (head to 'tail'). It is least effective in sustained currents, which form thick massive ignimbrites, particularly during phases when the leading edge of the current is stationary or only slowly advancing. In ignimbrites, bulk self-fluidization may be most likely to register in the basal parts of some flow-units, as these can record processes within the advancing front (or 'head') of the current. In contrast, higher parts of thick ignimbrite flow-units are mostly deposited so far behind the leading edge of the current that the mechanism is ineffective, especially when the front of the current has stopped. The effectiveness of bulk self-fluidization is diminished by development of lobes and clefts (Rayleigh–Taylor instability) and by corkscrew vorticity along the base of the density current, involving the wedge of air being overridden, because these disrupt or localize the upward gas flow. Air drawn laterally towards the current by thermal convection (e.g. Huppert *et al.* 1986) would have to penetrate the density current deeply toward its flow axis to fluidize enough of the current to be a major factor in mobility. Allen (1984) calculated that bulk self-fluidization by air cannot occur in density currents in which the load is coarser than fine ash, even allowing for air expansion by heating from hot pyroclasts.

Grain self-fluidization (Fig. 3.8D) is envisaged to be due to gas exsolved from hot juvenile glass shards and pumice (Sparks 1978), or from steam generated from entrained ice and snow, or from expanding gases derived from the burning of entrained wood fragments. The fluidization effect would decrease towards the base of a current as the gas flux diminishes downward (Sparks 1978). Gas exsolution from juvenile glass, however, cannot be a general

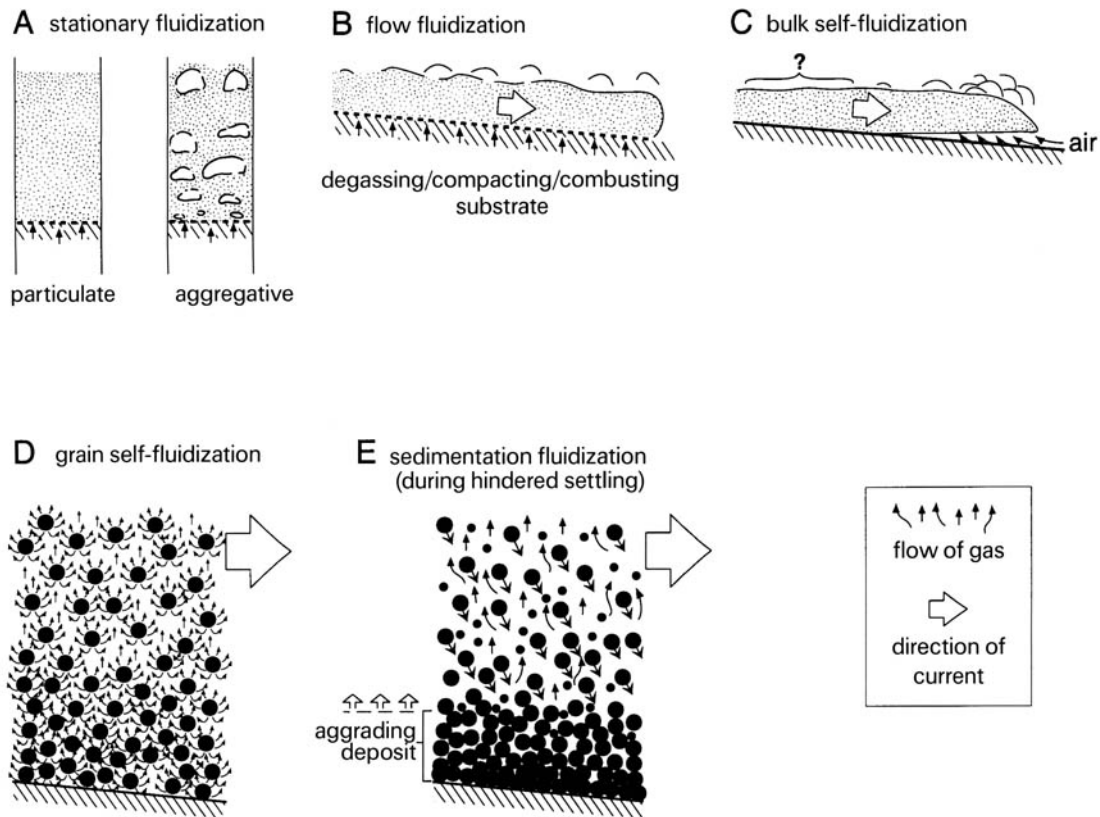


Fig. 3.8. Contrasting types of fluidization (modified from Allen 1984). See text for discussion.

explanation for pyroclastic density current mobility because similar pyroclastic density currents can originate by the collapse of gully walls eroded into un lithified ignimbrite several months to years after the ignimbrite was first emplaced (see p. 49; Torres *et al.* 1996). These deposit-derived pyroclastic density currents (Fig. 2.1F) had similar mobilities to the first-generation currents, and they deposited similar ignimbrite, even though they occurred long after the cessation of any vigorous exsolution of gas from juvenile pyroclasts.

Sedimentation fluidization (Fig. 3.8E) is driven by escaping interstitial fluid during hindered settling, and is considered fully on p. 33. Finally, proximal currents may undergo transient *decompression fluidization*, in which gas fluxes are produced by rapid decompression of gas, either at the base of a tall collapsing pyroclastic fountain (see Druitt & Sparks 1982) or in lateral blasts (Fig. 2.1D).

The above types of fluidization all involve laterally flowing particulate dispersions (*translatory fluidization* of Allen 1984) and cannot be simply related to the experiments from which most of our understanding of fluidization derives (references in Kunii & Levenspiel 1991). In most experiments gas is forced upward through a mass of particles that *does not flow laterally* (Fig. 3.8A) (*stationary fluidization* of Allen 1984). Thus, these fluidization experiments (e.g. Wilson 1980, 1984) are more pertinent to fluidization in just-formed *deposits*, and less pertinent to fluidization in the currents that deposited them. This is true irrespective of whether or not the experiments can reproduce grading and segregation styles similar to those seen in ignimbrites. Relating the experimental results directly to pyroclastic density currents is difficult, because clast support and segregation mechanisms differ significantly due to the effects of shear. Bubbling and channelling become suppressed at high shear rates (McGuigan & Pugh 1976; Botterill & Halim 1979; Ishida & Hatano 1983). Turbulence,

granular temperature, percolation, saltation, selective filtering and overpassing, all of which are shear-induced, occur in pyroclastic density currents and not in the stationary fluidization experiments. Furthermore, unlike the *in situ* collapsed dispersion formed in the stationary fluidization experiments, an ignimbrite is a deposit assembled through time (see pp. 87–91), during which segregation (e.g. selective filtering and selective entrainment) causes the deposit population to differ from that of the parent current (see p. 41). Finally, the flow-boundary zone of a current, which so fundamentally affects deposit character (Chapters 4 and 5), has no analogue in the stationary experiments. Consequently, it is important to maintain a clear distinction between the deposit and the current or 'flow'; neither ignimbrites nor ash in stationary fluidization rigs should be referred to as 'flows' (see Kokelaar & Branney 1996).

Hayashi & Self (1992) inferred, on the basis of similar ratios of vertical height dropped to horizontal distance travelled, that small-volume ignimbrites are emplaced with similar mobility to debris avalanches, and hence they concluded that fluidization was not necessary to explain the mobility of small-volume, high-concentration pyroclastic density currents. However, it is possible that fluidization caused by fluid escape during hindered settling (Fig. 3.8E) (see the next page) is involved in debris-avalanche emplacement. Present methods of estimating and comparing transport mobilities from ignimbrites are to an extent compromised for the following reasons. (1) There are few data on the maximum runout distances of medium to large pyroclastic density currents, because distal deposits are poorly preserved. (2) There are few data on the corresponding heights of parts of the eruption columns (potential energy) from which the density currents were derived. (3) The method of inferring current 'mobility' does not account for the sheet-like proximal to distal *distribution* of ignimbrite, and it assumes that all sedimentation postdates rather than accompanies transport. The method utilizes measures of the displacement of the

'centre of gravity' of an ignimbrite with respect to an imaginary pre-emplacement centre of gravity, as if it were a sliding rigid block (Mohr–Coulomb model reviewed in Druitt 1998), which has little relation to the dynamics of a sustained, depositing pyroclastic density current with an attendant plume. (4) The method assumes that the pyroclastic density current stopped moving at the distal limit of the deposit, whereas this location may merely mark where a moving current became sufficiently buoyant to loft entirely. If pyroclastic density currents are similar to cold debris avalanches, it would suggest that volatile exsolution and thermal-expansion effects are not as important as mass flux, granular temperature and fluid escape during hindered settling.

Segregation by fluidization

Most available information on segregation derives from non-shearing systems that may not be closely analogous to pyroclastic currents; the effects of shear are poorly known (see the previous section). Stationary fluidization may occur in deposits. In stationary-fluidization experiments, clasts segregate vertically mainly according to their relative density and, to a lesser extent, size. Less dense and smaller clasts tend to float within a fluidized bed ('flotsam'; Kunii & Levenspiel 1991), whereas dense large clasts ('lagan') sink to the base. The upward gas-flow velocity determines the segregation patterns (Wilson 1980; Hoffmann & Romp 1991); at low gas velocities, a polydisperse sand with a continuous size distribution segregates into two layers separated by a sharp interface (Hoffmann and Romp 1991). If a density current segregated in this way it would become stratified, and clasts in the lower, lagan-enriched levels would be deposited first, closer to source. With increasing gas flux in the static experiment, the thickness of the lower layer decreases and the concentration of lagan in it increases until, at high fluidization velocities, the lower layer disappears and the dispersion becomes well mixed throughout.

Stationary fluidization of ignimbrite *samples* produces distinctive segregation patterns (Fig. 3.9) (Wilson 1980). With a low gas flux, particle interlocking prevents segregation and elutriation (Type 1 segregation of Wilson 1980), but with a moderate gas flux the fine fraction is fluidized and the entire bed expands sufficiently to allow coarse-tail grading of pumice and lithic lapilli, but with limited elutriation (Type 2). A high gas flux causes bubbling and channelling, strong elutriation of fine ash, efficient segregation of pumice lapilli, and the formation of fines-poor lithic-rich segrega-

tion pipes, pods, lenses and layers (Type 3). These results were influential in the development of the giant fluidized flow model of pyroclastic density currents (p. 1), but segregation patterns in pyroclastic density currents (as opposed to in deposits) are, for the reasons explained above, probably not analogous. The experiments may be relevant for stationary degassing in non-compacted deposits, as in the formation of fines-depleted elutriation pipes in massive ignimbrite. The subvertical orientation of the pipes (Fig. 5.5) indicates that they formed after transport (shear) had ceased. Gas sources, such as burnt wood, are occasionally found at the bottom of such pipes in ignimbrite.

Segregation due to fluidization is very sensitive to humidity; if humidity is low, electrostatic effects between clasts affect segregation, whereas if it is high, adhesion of moist clasts occurs (see Hoffmann & Romp 1991). Humidity and electrostatic effects can be especially pronounced during large ignimbrite-forming eruptions, so there is likelihood that they influence segregation.

Hindered settling, fluid escape and sedimentation-fluidization

At its simplest, hindered settling is the net decrease in the rate at which clasts settle within a stationary two-phase particulate dispersion, owing to: (1) collisions between clasts; (2) interactions between settling clasts and their fluid wakes; and (3) the upward-flow of fluid (including entrained fines) displaced by the settling clasts (Selim *et al.* 1983). Even at concentrations as low as 1 vol. %, hindered settling causes average clast-settling velocities to be reduced relative to the settling velocities of clasts in an infinitely dilute suspension (Davis & Acrivos 1985), and the reduction increases with increasing particle concentration. In a polydisperse gaseous system, the settling of dense and/or large clasts may cause an upward flux of dusty gas (see point (3), above) sufficient to fluidize smaller and/or less dense clasts (Zimmels 1983; Druitt 1995; Doheim *et al.* 1997) (see Fig. 3.8E). We use the term *sedimentation fluidization* to refer to this type of partial fluidization driven by fluid escape.

Stationary hindered settling has been modelled by Kynch (1952) and Bürger *et al.* (2000). It is dynamically identical to stationary fluidization if the settling is steady (Richardson and Zaki 1954). Both are characterized by relative vertical motion between the clasts and interstitial fluid. However, hindered settling differs in that: (1) it is driven by sedimentation and thus only occurs when there is a downward flux of clasts relative to the substrate; and (2) it

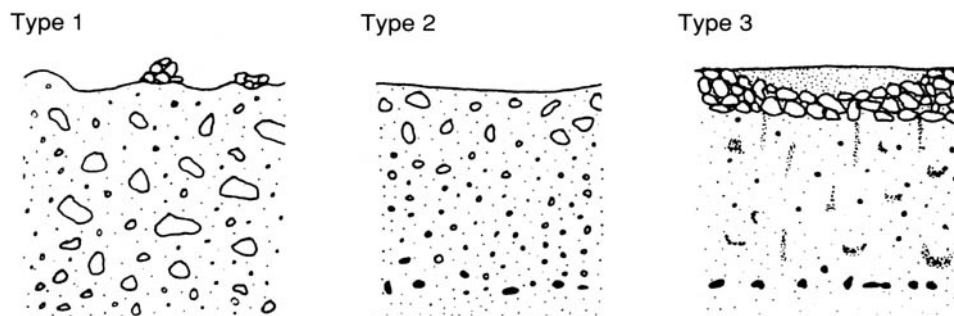


Fig. 3.9. 'Threefold classification of pyroclastic flows' proposed by Wilson (1980). The three illustrations are of types of deposits and the classification is based upon features developed experimentally in ignimbrite samples subjected to varying states of stationary fluidization. Type 1, inferred to have been least fluidized, is non-graded. Type 2, inferred to have been moderately fluidized, is coarse-tail graded, with an inverse-graded base and a concave top surface. Type 3, inferred to have been most vigorously fluidized, is strongly coarse-tail graded with lower lithic and upper pumice concentrations, and vertical elutriation pipes. These interpretations take the structures and vertical organization of deposits to reflect those of the moving flows. This treatment of pyroclastic density currents as though they were fluidized *in situ*, as in the stationary fluidization experiment (Fig. 3.8A), ignores effects of shear-induced segregation during transport (e.g. due to tractional and granular-flow processes) and any variations in the supply and mode of deposition of clasts with time.

does not require any additional supply of fluid (such as gas exsolution), although this is not excluded. In a stratified density current some clasts may be affected by hindered settling only as they enter lower, more concentrated parts of the current during sedimentation, which may be for only a short period relative to their transport history. Fluid escape and attendant hindered settling may occur both above and beneath the lower flow boundary of a pyroclastic density current (i.e. also in the compacting deposit); the processes do not of necessity involve shear.

Hindered settling also occurs in shearing systems (e.g. a concentrated density current), where the shear will affect grain collisions, wake interactions and fluid escape. For example, within a particle system of high concentration, the frequency of clast collisions increases with shear rate until the dispersion becomes a modified grainflow dominated by granular temperature. The effects of shear on hindered settling require investigation, and data on hindered settling of pyroclasts in air and dusty gas are required. In hot pyroclastic density currents, effects of fluid escape during hindered settling may be enhanced by thermal expansion of the interstitial air.

Hindered settling and current mobility

Fluid escape may be a significant clast-support mechanism in granular fluid-based pyroclastic density currents. Partial expulsion of fluid in the flow-boundary zone is necessary for deposition from high-concentration dispersions. At its simplest, it delays the rate at which clasts settle out of a current, so that the current has time to transport the clasts further and the runout distance increases. Sedimentation fluidization is likely to be a major process in currents that contain a broad range of particle sizes and densities, and it is likely to be more effective than are the types of fluidization that have previously been invoked to enhance the mobility of high-concentration parts of pyroclastic density currents. It involves particle support and effects on current rheology similar to the other types of fluidization, and it removes the need for an extensive, sustained external gas source, which has long been problematic in giant fluidized flow models (p. 1). There is close similarity between granular fluid-based pyroclastic density currents dominated by hindered settling, high-density turbidity currents and liquefied flows (Lowe 1976, 1979; Middleton & Southard 1984), all of which deposit by progressive aggradation (Carter 1975; Lowe 1979; Branney & Kokelaar 1992), as do hindered settling dispersions in stationary experiments (Druitt 1995). In some currents particles may be supplied to the flow-boundary zone at a rate greater than that at which they can settle to form deposit (see p. 92), so that fluid escape becomes a rate-limiting factor for deposition and the attendant hindered settling can thus considerably affect runout distance.

Segregation by fluid escape and hindered settling

Segregation during hindered settling involves elutriation of fine ash by sedimentation fluidization and buoyancy-driven segregation into flotsam (e.g. pumice lapilli) and lagan (dense lithics) (see p. 33). Understanding of these processes, which are similar to those caused by partial fluidization, has been derived from non-shearing dispersions (see Bürger *et al.* 2000). Nevertheless, because all massive ignimbrites form by sedimentation from granular fluid-based pyroclastic density currents, fluid escape and hindered settling must influence ignimbrite grain size, sorting and bed-form character. During stationary hindered settling, certain large and/or dense clasts may settle, whereas smaller and/or less dense ones are flushed upwards (Zimmels 1983; Bürger *et al.* 2000) so that layering is produced (e.g. Druitt 1995). The nature of any segregation depends on the particle concentration, and the size, shape, density and relative proportions of clasts. At very high concentrations (e.g. > 30 vol. %) segregation becomes increasingly suppressed. This suppression has been ascribed to 'hydrodynamic coupling' between

clasts and fluid (Locket & Al-Habbooby 1974) and due to interlocking of the clasts (Davies & Kaye 1971). The concentration above which segregation is suppressed in these ways varies between 30 and 65 vol. %, and is generally lower for clasts with irregular shapes and higher for suspensions with a broad range of sizes or densities (Selim *et al.* 1983; Druitt 1995). As with aggregative fluidization, stationary hindered settling with fluid escape can produce various segregation pipes, sheets and pods due to heterogeneous sedimentation, convection and streaming (Weiland *et al.* 1984; Batchelor & van Rensburg 1986; Allen & Uhlherr 1989; Druitt 1995). Segregation pipes, pods and sheets found in ignimbrites and associated breccias (e.g. Cas & Wright 1987; Buesch 1992) probably record heterogeneous hindered settling and fluid escape near and just below the current lower flow boundary in the uppermost forming deposit. Here, gas is partially entrapped by poorly sorted and rapidly aggrading ash, and, as the loose deposit starts to compact, the escaping gas produces the segregation structures. Thermal expansion of gases may enhance this process, although similar segregation structures are common in massive deposits of cold, aqueous high-concentration density currents (Laird 1970; Best 1989, 1992; Kneller & Branney 1995), so thermal expansion effects are not crucial. If segregation pipes started to form within the current they would be sheared out even as they developed, and so could not be preserved intact.

Clast buoyancy

Buoyancy and transport

The rate of settling or buoyant ascent of a clast immersed in a stationary *fluidal* dispersion is a function of the density contrast between the clast and its surroundings. The effective weight of an immersed clast declines with increasing particle concentration of the enclosing dispersion, so buoyancy effects are most significant in dispersions of moderate to high concentration; they increase towards the base of a density-stratified current.

Segregation by buoyancy

Buoyancy can cause pumice clasts to rise towards the top of stationary fluidized dispersions (experiments of Wilson 1980). It has been widely invoked to account for inverse grading of pumice in ignimbrites, where the pumice clasts are thought to have floated to the top of semi-fluidized pyroclastic density currents during laminar to plug flow (Sparks 1976). This interpretation cannot account for the assembly of an ignimbrite flow-unit through time by progressive aggradation (see pp. 87–91) or where the current was not entirely highly concentrated (density stratified; see p. 14). We propose the following modification of the idea. For many cases, significant thicknesses of a current may have an effective density less than that of the pumice clasts, so that these are transported near their own level of neutral buoyancy *within* the stratified current (as 'flotsam'; see Fig. 6.9, inset). Initially, the density of the dispersion towards the lower flow boundary of the current prevents deposition of most of the larger pumices due to their buoyancy (Fig. 4.3). If, for example during waning flow, the density of the lower part of the current at a fixed location decreases with time, successively larger pumices subside towards the flow boundary, where they are eventually deposited so that inverse grading arises in the aggrading ignimbrite (see Fig. 4.6 and pp. 66–71). In addition to the effects of buoyancy, such pumice segregation in the lower flow-boundary zone is likely also to involve granular segregation processes, including effects of surface roughness (Fig. 3.5), percolation and dispersive forces (see Fig. 3.7 and pp. 29–31). A combination of fluid escape-modified buoyancy and the kinetic effects of granular interactions determines the level in the current at which a particular pumice clast mostly resides during transport. The contributions made by these various effects will vary with rates of shear, rates of deposition and with concentrations around the flow boundary.

Acoustic mobilization

Acoustic mobilization and transport

'Acoustic fluidization' is a mechanism proposed to account for a perceived excessive mobility of rock avalanches on low-angle slopes (Melosh 1979, 1987). It was renamed *acoustic mobilization* by Middleton & Southard (1984) because, unlike fluidization, it does not involve an upward flow of interstitial fluid. In acoustic mobilization, elastic waves transmit directly through the framework of clasts that seldom lose contact within a densely packed grain mass. This is in contrast to the energy transfer in granular flows, which is by collisions between individually vibrating clasts. The elastic waves cause pressure to oscillate to above and below the static overburden pressure within a body of the debris that has dimensions less than the acoustic wavelength but larger than a clast. During moments of low pressure, small volumes of debris can slide under a shear stress much less than would be possible under static overburden pressure. Frequent failure events of this type result in creep-like motion of the entire mass in response to relatively small shear stresses. Some dilation occurs through intermittent opening of microcracks. The model assumes that acoustic energy that was originally transmitted to the debris by some initial catastrophic event is lost at a rate low enough to permit significant transport (Melosh 1987). The process may intergrade with granular temperature and it may occur in sector, dome or lava-front collapses. It may enhance debris-avalanche mobility and the fracturing of large blocks, but it is difficult to envisage any relevance for pyroclastic density currents derived from eruption columns.

Segregation by acoustic mobilization

Interlocking inhibits segregation during acoustic mobilization (see the last section in this chapter), although the grain-size population may change through attrition.

Support by strength

Strength is the property of some materials to resist deformation on application of a finite amount of stress. In particulate materials it may arise from (1) friction between neighbouring particles in the *quasi-static* regime of non-cohesive granular flow (Savage 1979), and (2) by cohesion. The strength of natural flowing dispersions varies with concentration and shear rate (shear-thickening and shear-thinning suspensions), temporally and spatially.

Quasi-static grain contacts

At very low rates of shear clast concentrations over about 35–58 vol. % can form a supporting framework of clasts in contact with each other (Davies & Kaye 1971; Rodine & Johnson 1976; Mróz 1980; Pierson 1981; Spencer 1981) in which strength derives from frictional resistance to motion between the clasts. Yield strengths of pyroclastic currents have not been measured, but are probably lower than those of little-compacted ignimbrites (between 300 and 2000 N m⁻² at Mount St Helens; Wilson & Head 1981). With increasing shear rate, granular temperature increases, dominates and ultimately replaces the quasi-static grain contacts (this is the

rapid flow regime of granular flow, p. 29). However, dependent on the shear profile of a current, quasi-static grain contacts may continue to provide strength and clast support in parts of a rapidly moving current, such as within a layer undergoing little shear or within the substrate (deposit) at the base of the current. Cohesionless solid-gas systems exhibit a yield strength only at concentrations close to full packing (Schügerl 1971; Wilson 1984).

Cohesion

Cohesion between moist clay particles imparts a yield strength that, unlike that due to friction at quasi-static grain contacts, can persist at high shear rates. Ignimbrite grading and sorting have been interpreted in terms of current segregation controlled by current yield strengths of similar magnitude to those of cohesive debris flows (Wright & Walker 1981; Freundt and Schmincke 1986; Carey 1991). However, hot (> 100°C) pyroclastic density currents are unlikely to contain moist clay particles, and, although yield strength may have a role in some low-temperature pyroclastic currents of phreatomagmatic origin due to the presence of water, rapidly shearing pyroclastic density currents in general may be regarded as lacking strength (Postma 1986), as with aqueous turbidity currents and cohesionless debris flows. In some extremely hot pyroclastic density currents that produce high-grade (agglutinated or coalesced) welded ignimbrites (see p. 83), fluidal, low-viscosity pyroclasts may cause cohesion and agglutination, and hence possibly a yield strength. This may be the case particularly where clast concentrations are high and the shear rate is low, such as in the lower flow-boundary zone of a density-stratified current (Branney & Kokelaar 1992; Freundt 1998).

Segregation associated with strength

Segregation tends to be inhibited by cohesivity, and segregation is hindered by particle interlocking in the case of non-cohesive currents that are sufficiently concentrated to acquire strength through frictional particle interactions. Fine ash may be generated by abrasion at shearing quasi-static grain contacts, and it may be lost by elutriation from a degassing deposit in which strength is provided by a framework of coarser clasts.

Particle interlocking

A clast in a concentrated dispersion may be lifted, entrained or deposited simply because it is trapped between neighbouring clasts. Conversely, a particle may be prevented from being entrained in a current simply because it is interlocked with surrounding grains. Interlocking generally acts to prevent segregation (Davies & Kaye 1971) and so preserves poor sorting. It has been invoked to account for the fine ash between spatter rags in coarse spatter-rich pyroclastic density current deposits (Triglia & Walker 1986), and may account for the deposition of pumice clasts with adjacent dense clasts of markedly contrasting pneumatic properties. Interlocking is an important mechanism by which fine ash is deposited from pyroclastic density currents, and hence is implicated in the widespread occurrence of poor sorting in ignimbrites. It is most likely to occur in flow-boundary zones of granular fluid-based pyroclastic density currents during the style of deposit aggradation sometimes described as 'freezing up from the base' (see p. 39).

This page intentionally left blank

Chapter 4

Conceptualizing deposition: a flow-boundary zone approach

In this chapter we present ways of conceptualizing ignimbrite deposition. We explore possible types of deposition and what processes may influence them.

Deposition from steady currents

We have explained earlier (Chapter 1) that unsteady (e.g. waning flow) conditions are not prerequisite for deposition as has sometimes been assumed, but that deposition (e.g. of massive ignimbrite) can occur during waning, quasi-steady and even waxing flow conditions. In order to explore the processes of deposition it is useful first to consider the simplest case, that of deposition during steady conditions, before considering possible consequences of waxing and waning flow.

Deposition during steady flow proceeds at a constant rate, so that the surface of the deposit rises steadily with time (Fig. 4.1A). We call this type of aggradation 'gradual' to distinguish it from 'stepwise' aggradation, which proceeds in a series of abrupt jumps (Branney & Kokelaar 1992). Note that this use of gradual does not imply a slow rate. Gradual aggradation was first invoked to describe the formation of massive sediment-gravity flow deposits by Carter (1975): 'a surface separating stationary from moving particles moves rapidly up ... deposition is therefore not simultaneous throughout the bed. If the depositional surface migrates up gradually, a comparatively homogenous bed might be expected'.

Any clast depositing from a pyroclastic density current must cross the lower flow boundary of the current. All flow-boundary zones must exhibit gradients in velocity and concentration (see p. 4), so any pyroclast undergoing deposition must descend through successive levels of different shear intensity and concentration as it encroaches the deposit. As it descends, the pyroclast must respond at each level to the successive prevailing combinations of support and segregation effects (Chapter 3), according to its density, shape and size. It follows that the depositional mechanism and thus the lithofacies type formed are highly influenced by the profiles of shear, concentration and rheology across the flow-boundary zone (Fig. 4.1). We now consider four intergradational types of flow-boundary zone, each characterized by a dominant mechanism of deposition (Fig. 4.1): (1) flow-boundary zone dominated by direct fallout; (2) flow-boundary zone dominated by traction; (3) flow-boundary zone dominated by granular flow; and (4) flow-boundary zone dominated by fluid escape. Each is now described as it operates under steady conditions.

Direct fallout-dominated flow-boundary zone

Direct fallout from a pyroclastic density current occurs when clasts deposit directly, with negligible rolling, sliding or saltation, negligible clast interactions and negligible fluid-escape effects (Fig. 4.1B). It differs from the 'direct suspension sedimentation' of Lowe (1982) in which grain interactions and/or hindered settling may be important (see discussion in Kneller & Branney 1995). Direct fallout occurs when the lowermost part of the current is sufficiently dilute for grain interactions and fluid escape (see below) to be unimportant and where velocities are too low to cause significant traction or saltation (see p. 25). Velocities too low for traction may occur, for example, at the base of slow-moving clouds of fine-grained ash that roll gently across the landscape (e.g. Talbot *et al.* 1994), analogous to subaqueous nepheloid flows (Pickering *et al.* 1989) and some distal turbidity currents that comprise clouds of

fine sediment and deposit structureless fine-grained layers referred to as 'hemiturbidites' (Stow & Wetzel 1990). Low-concentration pyroclastic currents of this type commonly loft due to thermally induced buoyancy, but cooler ones (e.g. of phreatomagmatic origin) may maintain contact with the ground for significant distances.

A flow-boundary zone dominated by direct fallout must have a sharp rheological and clast-concentration interface at the deposit surface, and no more than a minor step in the velocity profile (see Fig. 4.1B). Weak directional grain fabrics may form where fluid velocity is sufficient to orientate the settling clasts. Because there is no mechanism of segregation at the flow boundary, any deposit that aggrades during steady flow will tend to be non-stratified and sedimentation of all particle sizes will occur according to individual clast-settling velocities, giving a population distribution in accord with Hazen's law (Hazen 1904; Woods & Bursik 1994). Significantly, the other types of flow-boundary zone do not produce deposits with particle populations that accord to Hazen's law. In practice, some weak stratification is likely to arise because perfectly steady fallout directly from turbulent suspension is unlikely.

There are two other situations in which direct fallout might occur. Both require the base of the current to be sufficiently dilute to render grain interactions and fluid escape unimportant. The first is when the pyroclasts are sticky, for example by being moist or molten, so that they immediately adhere to the substrate on contact and traction is inhibited. The second is where deposition is so rapid that each clast becomes buried almost immediately it touches the deposit surface, before it has any time to bounce or roll. This mechanism has been proposed by Arnott & Hand (1989) to account for experimental observations that traction is inhibited at high rates of deposition. However, their recorded observations do not seem to preclude the possibility that grain interactions and/or fluid escape occurred in the flow-boundary zone. In nature, conditions analogous to those in Arnott & Hand's experiments (i.e. very high rates of deposition) might occur locally where a fully dilute pyroclastic current is markedly depletive, such as at a topographic barrier, or where it suddenly spreads (diverges), or where lofting arrests downslope advance and promotes fallout of the non-lofted material. However, such currents may alternatively develop high basal particle-concentrations at such locations (see p. 93), so that direct fallout does not occur.

Traction-dominated flow-boundary zone

Pyroclastic density currents with a traction-dominated flow-boundary zone have a sharp lower flow boundary, with a marked step in velocity and rheology gradients between the lower part of the current and the substrate (Fig. 4.1C), such that fluid turbulence commonly extends to within a clast-diameter of the flow boundary and is the major transport mechanism (p. 24; Middleton & Southard 1984). Shear at the flow boundary causes individual clasts there to be subjected to lift and/or drag by fluid so that they slide, roll or saltate along the substrate surface before they are finally deposited (see p. 25). Low clast concentrations mean that interactions between the moving clasts are minimal, right down to the base of the current (a fully dilute pyroclastic density current). Interactions between the current and the substrate cause localized non-uniformity, typically leading to development of various bed forms (e.g. dunes). Impingement of turbulent eddies accompanied by tractional sorting of the bedload causes selective entrainment and hence segregation (pp. 24 and 28). These processes produce stratified and cross-stratified deposits that tend to be moderately

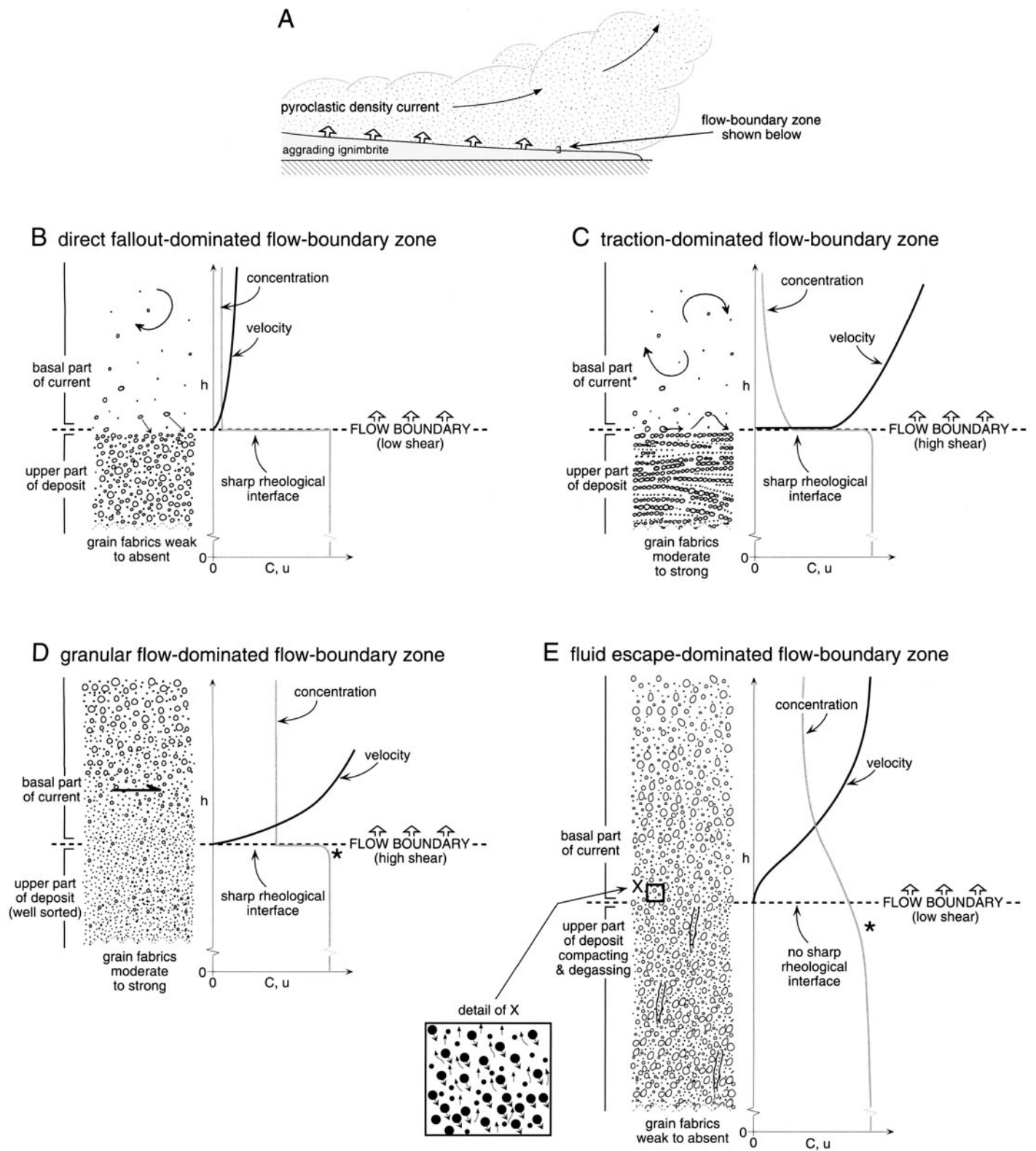


Fig. 4.1. Four types of flow-boundary zone during steady conditions, with schematic concentration and velocity profiles. (A) Scale and location of the flow-boundary zone, emphasizing that the depicted zones (B–E) include only the basal part of the current and uppermost part of the deposit. (B) Direct fallout-dominated flow-boundary zone; (C) traction-dominated flow-boundary zone; (D) granular flow-dominated flow-boundary zone (half-arrow indicates sense of shear); (E) fluid escape-dominated flow-boundary zone. Most currents have flow-boundary zones that are intergradational between these types. In (E) the uppermost part of the deposit is extremely poorly compacted and ‘quick’, similar to the lowermost part of the current. In (D) small-scale unsteadiness is likely to be recorded as diffuse stratification (see text).

sorted to well sorted (p. 74; Figs 6.10C–E and 6.17B). Deposits formed by a traction-dominated flow-boundary zone include stratified facies of so-called 'pyroclastic surge deposits' (e.g. Cas & Wright 1987) and also of ignimbrites.

Granular flow-dominated flow-boundary zone

In a granular flow-dominated flow-boundary zone (see Fig. 4.1D), clast concentration and shear intensity are sufficient for grain interactions to dominate clast support (p. 29). This is irrespective of the nature of the current away from the flow-boundary zone. Granular temperature dilates the dispersion within in lowermost parts of the current, which move by *modified* grainflow (Lowe 1982) rather than by true grainflow, because of the presence of interstitial dusty gas (the fluid phase), buoyancy effects and because they are subjected to drag (shear stress) exerted by overriding levels of the current, which commonly are less concentrated (see pp. 21 and 42).

During deposition the flow boundary may coincide approximately with the interface between the rapid (collisional) and the quasi-static regimes of granular flow (pp. 29 and 35; Savage 1979). The granular temperature within lowermost parts of the current may conduct down across the flow boundary and cause some dilation within the uppermost part of the deposit (see p. 29), making the rheological transition across the flow boundary somewhat diffuse (asterisk in Fig. 4.1D). In *steady* deposition, frictional interlocking with the substrate causes successive lowermost slow-moving clasts within the modified grainflow to come to a halt, so that a massive deposit aggrades gradually from the base up (see Hein 1982; Hiscott 1994b). The clasts do not deposit individually, but interlock and halt together with adjacent clasts. The interlocking hinders segregation of contrasting (and pneumatically non-equivalent) types of clasts at the flow boundary. At levels slightly above the flow boundary, however, segregation typical of well-developed rapid-regime granular flow is likely (e.g. percolation and overpassing; pp. 28–31) (see Fig. 3.6). Such segregation, which commonly favours deposition of the relatively small grains, means that any deposit layer at a particular location is not representative of the population of any batch of the current (Fig. 3.6). Grain fabrics, such as cluster patterns, clast alignments and/or imbrication, develop by granular shear in the flow-boundary zone and typically are preserved in the deposit.

Aggradation at this type of flow-boundary zone, which involves frictional interlocking of clasts, has sometimes been referred to as 'frictional freezing up from the base' (also see p. 40) and 'en masse deposition at an upward-migrating surface' (e.g. Carter 1975). However, we avoid using these expressions as they may cause confusion with the more common usage of 'freezing' and 'en masse' deposition for the simultaneous coming to rest of an entire current, or a substantial thickness of one, such that the flow boundary abruptly jumps a substantial distance upwards (see p. 45).

The granular flow-dominated type of flow-boundary zone is poorly understood because of a paucity of theoretical and experimental analysis of granular flow at flow boundaries (Zhang & Campbell 1992), and because most extant granular-flow models do not consider the important effects of buoyancy, interstitial fluid, poor sorting, clast shape and fabric development (see pp. 29–31).

A granular flow-dominated flow-boundary zone can occur at the base of pyroclastic density currents with diverse concentration profiles (see Fig. 2.9C–G). The current might be generally dominated by fluid turbulence, but have a thin modified grainflow at its base (Fig. 2.9C and p. 42), or it might be more generally dominated by clast interactions (i.e. a type of cohesionless debris flow; Fig. 2.9G), or it might be intergradational between these types (Fig. 2.9D–F). Because the lower flow boundaries and mechanisms of deposition are similar in each case, it may be difficult to distinguish the general character of the overriding current from the deposits.

Fluid escape-dominated flow-boundary zone

In a flow-boundary zone dominated by fluid escape, clast support is predominantly a result of fluid expelled upwards as a consequence of deposition (Fig. 4.1E). It requires high clast concentrations to limit the permeability of the sedimenting dispersion, and low rates of shear to minimize granular temperature effects within the basal part of the current. It is maintained by deposition, which creates the upward flux of fluid (dusty gas). Within the flow-boundary zone, clast concentration, effective viscosity and yield strength increase downward from lowermost levels of the current into the upper levels of the forming deposit, and shear-strain rate within the current decreases gradually down to zero at the lower flow boundary (Fig. 4.1E). These profiles arise as a result of: (1) a downwards decrease in the upward flow of escaping fluid and the clast support it provides (see p. 33); (2) a downwards decrease in dilation due to dispersive pressures (granular temperature is mostly zero in the non-shearing deposit); and (3) density stratification of any polydisperse bed-load population that occurs. Mobility within the lowermost part of the current is maintained primarily because the upward expulsion of fluid that is displaced to allow packing prevents the dispersion acquiring yield strength through quasi-static frictional interlocking. This type of flow-boundary zone has recently been produced experimentally (Vrolijk & Southard 1998) and is analogous to the lowermost part of a layer dominated by hindered settling that was produced experimentally by Middleton (1967). Deposits that accumulate rapidly from high-concentration suspensions are among the most loosely packed of natural sediments (Kolbuszewski 1950; Allen 1972). As a result of fluid escape and the loose packing (asterisk in Fig. 4.1E), the uppermost part of such an aggrading deposit is 'quick', with a rheology closely similar to the lowermost level of the current from which it was deposited only moments before. Static frictional clast contacts within it are only just sufficient to prevent shear. In this scenario, there is no sharp discontinuity with respect to velocity or concentration at the deposit surface (Fig. 4.1E; note that the deposit surface is defined as the highest level in the sediment mass where downcurrent velocity is zero, see p. 4). With distance beneath the flow boundary, concentration increases into the forming deposit (asterisk in Fig. 4.1E) as the rate of compaction and upward expulsion of interstitial fluid decrease. Where the rate of fluid escape is high, the escaping fluid may become channelled, with clast segregation forming fines-depleted elutriation pipes (see p. 61; Fig. 5.5). Only those parts of pipes that were formed beneath the flow boundary can be preserved intact; any parts that extended above the boundary must show shear deformation or be obliterated.

Whether or not overlying parts of the current are turbulent, any turbulence that penetrates a fluid escape-dominated flow-boundary zone tends to be suppressed by the combined effects of high effective viscosity arising from high clast concentrations and the stabilizing effects of density gradients. Because of this, and because the rheology of the basal part of the current is gradational down into that of the deposit (Fig. 4.1E), flow immediately above the flow boundary is laminar irrespective of turbulence intensity higher in the current (e.g. Kneller & Branney 1995). The thickness of the laminar part of the current may vary considerably, for example with current velocity, concentration, grain size and rate of deposition.

As clasts in a current encroach a rising fluid escape-dominated flow-boundary zone, they decelerate gradually to a standstill as the flow boundary passes up across them (Fig. 4.1E). Their deposition is partly due to interlocking and frictional coupling with the substrate, there being just insufficient escaping fluid at that level to maintain a flowing dispersion. The grains immediately above then find themselves resting on the (cryptic) deposit surface, and in this way the deposit surface rises; a massive deposit will continue to aggrade for as long as a steady flow is maintained (e.g. Vrolijk & Southard 1998).

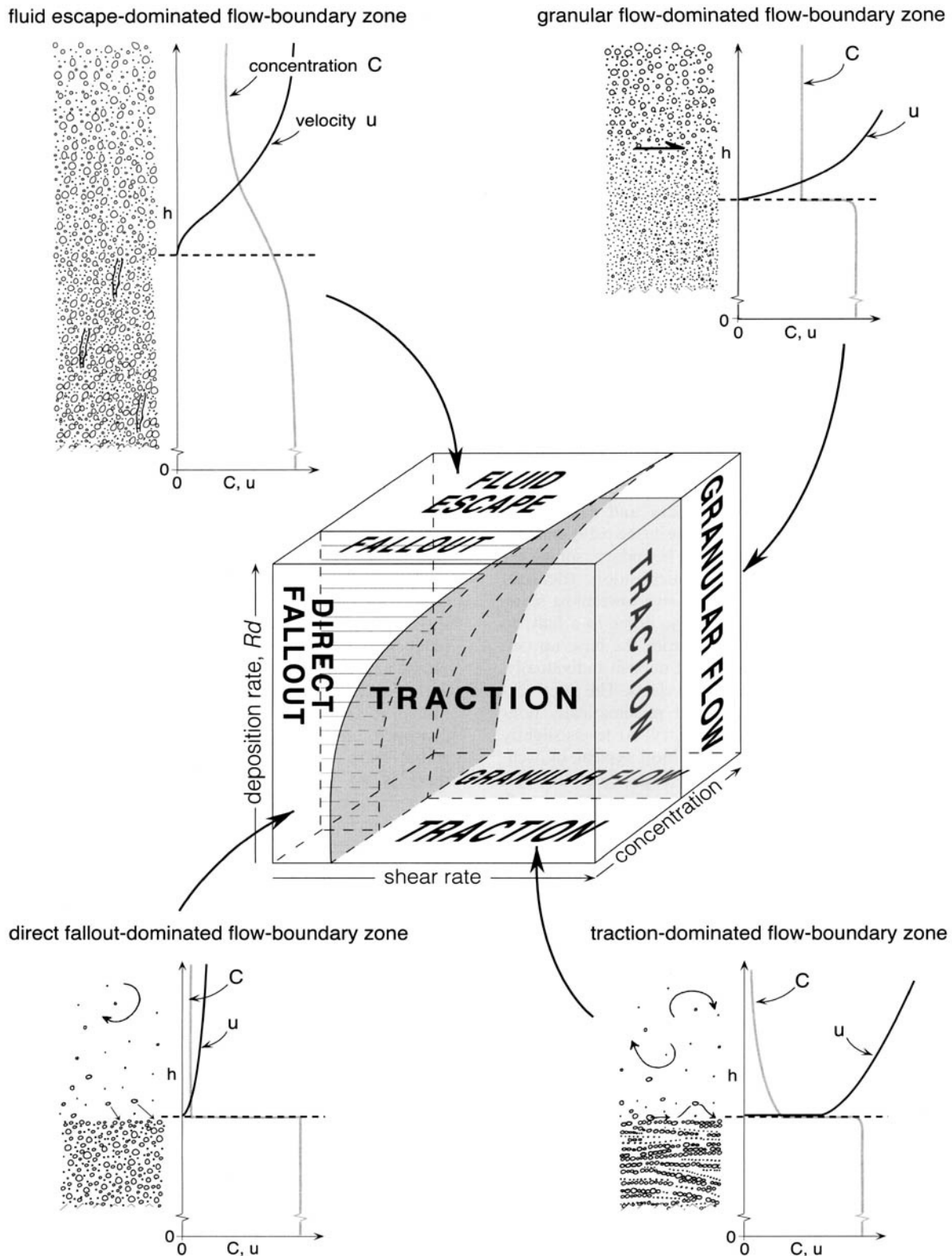


Fig. 4.2. Conceptualization of the relative fields of the four types of flow-boundary zone in steady currents. Complete gradations occur between the flow-boundary zone types. Note that the parameters represented by the three axes of the cube are for the flow-boundary zone only, not for the current as a whole (conditions at higher levels in a current may differ). Rate of deposition, R_d , is the mass-flux of pyroclasts into the deposit per unit area of the flow boundary.

Some workers have referred to this mechanism of deposition (as well as deposition from a granular flow-dominated flow-boundary) as 'freezing upwards from the base' and 'direct suspension sedimentation' (e.g. Lowe 1982). Here we emphasize the importance of the interaction of the escaping displaced fluid with the clasts, and note that a poorly sorted clast population that is rich in

finer particles cannot deposit instantaneously, or nearly so, because the interstitial fluid requires time to escape up through the dispersion before deposition can be completed. Sustained rather than near-instantaneous deposition is indicated by the general sheet-like morphology of most (non-ponded) massive ignimbrites; ignimbrites would tend to develop more in the form of piles or heaps if

aggradation was virtually instantaneous. Experiments using hot pyroclasts and using dusty gas as the continuous phase in sustained depositing currents are required to investigate this type of flow-boundary zone and the rates of deposition possible there.

Gradational types of flow-boundary zone

The four types of flow-boundary zone described above are transitional into each other (Fig. 4.2). For example, a direct fallout-dominated flow-boundary zone must, with increasing current velocity, grade into a traction-dominated flow-boundary zone as the (fully dilute) current can increasingly transport traction and saltation populations. Such an intergradation may exist, for example, during a phreatomagmatic eruption in which there is true ashfall, direct-fallout deposition from gently rolling ground-hugging ash clouds and tractional sedimentation from slightly higher velocity density currents. The transitional types of flow-boundary zone are recorded by hybrid deposits with variously developed stratification (e.g. Branney 1991; Talbot *et al.* 1994; Valentine & Giannetti 1995; Wilson & Hildreth 1998). Similarly, because clast-settling behaviour depends on the concentration of clasts in a dispersion, a direct fallout-dominated flow-boundary zone must grade, with increasing particle concentration, into a fluid escape-dominated flow-boundary zone.

As granular temperature is a function of shear rate, a fluid escape-dominated flow-boundary zone must, with increasing rates of shear (i.e. increasing current velocity), become increasingly affected by grain collisions until it transforms into a granular flow-dominated flow-boundary zone. Conversely, a granular flow-dominated flow-boundary zone must ultimately become transitional into a fluid escape-dominated flow-boundary zone as the mass flux of clasts into the deposit increases and the zone becomes increasingly modified by the effects of escaping fluid. The intensity of grain fabric in a massive deposit may indicate whether the flow-boundary zone was dominated more by granular flow (stronger fabrics; Fig. 4.1D) or fluid escape (weaker fabrics; Fig. 4.1E). A traction-dominated flow-boundary zone can become transitional into one dominated by granular flow via an increase in bed-load concentration. There is some experimental evidence that a traction-dominated flow-boundary zone may become transitional into a direct fallout-dominated flow-boundary zone with increasing rates of deposition if clasts are buried by other clasts before they have chance roll or bounce (Arnott & Hand 1989). However, it is difficult to discount the possibility that hindered settling played some role in these experiments.

There is field evidence that rates of deposition from fluid escape-dominated flow-boundary zones are higher than those from contemporary adjacent granular flow-dominated and traction-dominated flow-boundary zones (see p. 109). This is in the form of 'splay-and-fade' stratification (see Fig. 6.16), in which a substantial thickness of massive ignimbrite (inferred to be deposited by a fluid escape-dominated flow-boundary zone; 'Massive lapillituff lithofacies' in Chapter 5), traces laterally over a few decimetres into a much thinner layer of diffuse-bedded, and then stratified, ignimbrite (inferred to be deposited, respectively, from granular flow-dominated and traction-dominated flow-boundary zones; see Chapter 5). Both the thick and the thin divisions must have been deposited during exactly the same period (see p. 110).

The three conditions we have described for the four types of flow-boundary zone, that is, clast concentration, shear rate and rate of deposition, are conceptually summarized in Fig. 4.2. Only qualitative relationships can be expressed. No single value could adequately represent the concentration of clasts in a particular type of flow-boundary zone, because most (except that dominated by direct fallout) are density stratified. Shear rates also vary with height within each type of flow-boundary zone (see profiles), and the effect of shear rate may vary with different grain populations and with the development of grain fabrics or segregation structures

in the shearing mass. Similarly, the effects of clast concentration on grain interactions and on fluid escape are influenced by the grain-size distribution of the shearing (polydisperse) dispersion, and the grain-size distribution will commonly vary with height across the flow-boundary zone. The different types of flow-boundary zone are intergradational, so that the conceptual fields do not have sharp boundaries (despite being drawn in this way for clarity on Fig. 4.2), and much of the internal volume of the cube conceptually represents transitional types of flow-boundary zone. Field evidence for this is in the common occurrence of all intergradations between the various types of ignimbrite lithofacies (see Chapter 5).

Figure 4.2 uses the rate of deposition, R_d (the mass-flux of pyroclasts into the deposit per unit area of the flow boundary), rather than 'suspended-load fallout rate' (Lowe 1988; Druitt 1998), because the latter concept, strictly, is only valid for currents with fallout-dominated flow-boundary zones. This is because in stratified granular fluid-based currents it is not meaningful to quantify a 'suspended-load fallout rate'; the downward flux (fallout) of clasts differs with height in the current as a result of the different mechanisms of clast support. For example, at higher, less-concentrated levels of a current the downward flux of clasts may be controlled by depletive current velocity, while the downward flux (actual deposition) at the base of such a current may be influenced by fluid escape, which is a function of the concentrations (permeabilities) in the flow-boundary zone (see p. 33; Fig. 6.8, inset). In this way, the downward flux of particles ('suspended-load fallout rate') at one level in the current can differ from, and be partly independent of, the downward flux of particles at another level in the same current at the same location.

The overall controls that determine what type of flow-boundary zone develops in a current require further investigation, in particular to determine how the stratification of support mechanisms in a granular fluid-based current readjusts (i.e. how mass is transferred between the different levels in the density-stratified current) in response to deposition and to changes in topography, capacity and competence.

Selective filtering: flow-boundary zone segregation and overpassing during deposition

Certain clast types deposit at a flow boundary more readily than others. For example, at a granular flow-dominated flow-boundary zone, clast percolation enables smaller clasts to descend through the shearing granular mass toward the flow boundary more readily than larger clasts of the same density (p. 29; see Fig. 3.6). Thus, the smaller clasts preferentially enter the deposit, whereas larger clasts have a greater tendency to remain in the current and are consequently transported further ('overpassing' of Nemeč 1990). This type of flow-boundary zone forms a deposit that is depleted in larger clasts relative to the current that deposited it (Fig. 3.6). The flow-boundary zone, therefore, acts as a dynamic *selective filter* to certain sizes of clast. In this case, during steady conditions, sustained selective filtering and overpassing will mean that larger clasts are persistently transported to a more distal location (where different flow-boundary conditions enable them to deposit; the flow is non-uniform).

At a fluid escape-dominated flow-boundary zone, clast density is important in selective filtering (see p. 34). Large pumice clasts ('flotsam') that are buoyant with respect to the partially fluidized layer in the flow-boundary zone are unable to sink through the flow boundary (Fig. 4.3). They 'float' due to a combination of buoyancy and granular segregation effects within the shearing mass near their level of neutral buoyancy within this zone (see Fig. 6.9, inset), and will overpass for as long as this level lies above the flow boundary. In contrast, dense lithic clasts ('lagan') preferentially sink through the flow-boundary zone and enter the deposit (Fig. 4.3), through which some may then sink further. The resultant ignimbrite at that

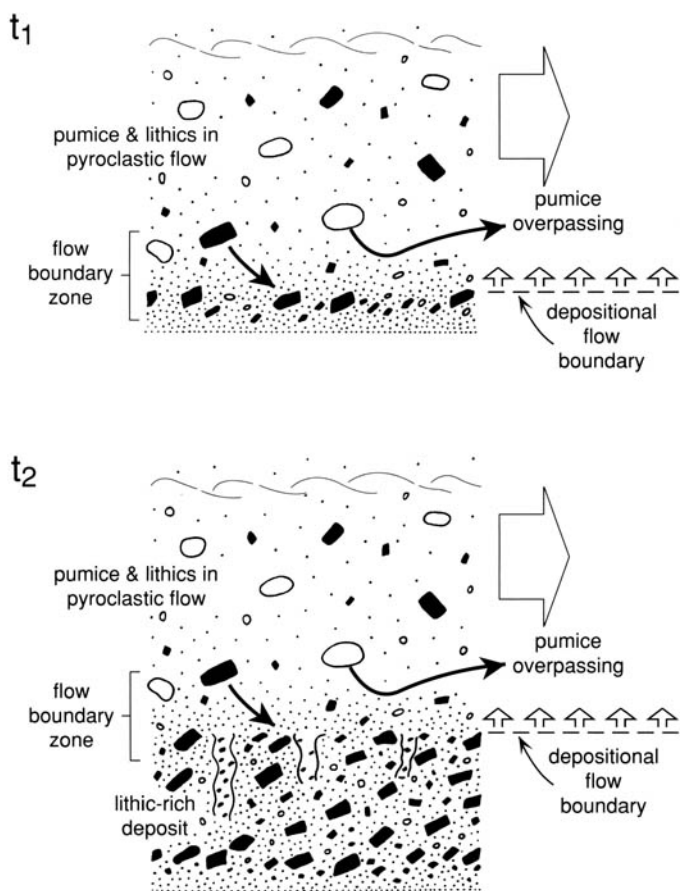


Fig. 4.3. Selective filtering and overpassing of large pumice clasts in a steady, depositing pyroclastic density current with a fluid escape-dominated flow-boundary zone. Dense lithics sink through the flow-boundary zone more readily than do large pumice clasts, whose buoyancy prevents their reaching the deposit surface. The deposit is consequently enriched in lithic clasts relative to the composition of the current that produced it (t_1). After a short period of time (t_2), a greater thickness of massive, lithic-rich lapilli-tuff has aggraded. Large pumices still cannot sink to the rising deposit surface and are carried downcurrent (overpassing).

location is enriched in lithic clasts relative to the current that passed there (Fig. 4.3). Such selective filtering and overpassing of pumice in the flow-boundary zone of pyroclastic density currents cause formation of distal accumulations of large pumice clasts (Fig. 4.4), which are commonly reported from ignimbrites (p. 76; Fig. 4.7B). Also in a fluid escape-dominated flow-boundary zone, the escaping fluid (see p. 33) is likely to elutriate fine ash upwards into overriding parts of the current. Thus, even a fines-rich deposit may actually be depleted in fines relative to the current that deposited it. It is a major consequence of selective filtering that the particle population of the deposit at any one location differs from that of the density current that produced it (Fig. 4.3). This is true for most types of flow-boundary zone (least so in the case of a direct fallout-dominated flow-boundary zone), although the extent and nature of this difference varies with flow-boundary type, because segregation processes, including selective filtering, vary with varying flow-boundary zone conditions.

Traction carpets

The concept of a 'traction carpet' derives from marine and fluvial sedimentologists, and until recently it has received little consideration by volcanologists. A traction carpet is a bed load that is

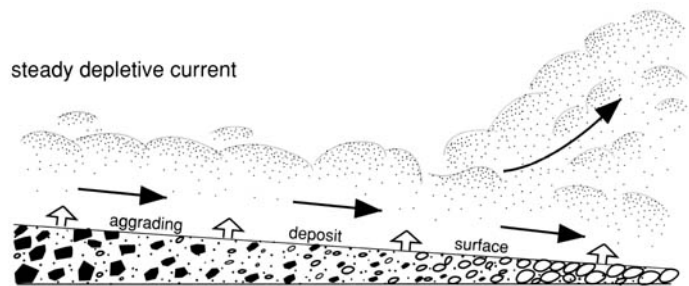


Fig. 4.4. Longitudinal segregation of pumice and lithic clasts due to selective filtering and overpassing of pumice (see Fig. 4.3) in a steady, depletive current. Owing to the combined effects of granular segregation and buoyancy, large pumice clasts are less able to enter the deposit proximally than are lithic clasts. Larger pumice clasts preferentially overpass proximal areas and travel downcurrent to be deposited distally, where the flow-boundary conditions differ (e.g. lower shear rate, lower concentration). The resultant proximal ignimbrite contains more lithics and less large pumice clasts than the original current at this location. Note the normal downcurrent grading of lithics and inverse downcurrent grading of pumice, towards a pumiceous snout. (Vertical scale and clast size exaggerated).

sufficiently concentrated for turbulence to be largely suppressed. It is a thin, modified grainflow driven along principally by tangential shear stress exerted by overriding, less concentrated and more turbulent parts of the same current (as may occur in the scenario of Fig. 2.4B; Dzulynski & Sanders 1962; Middleton 1970; Hiscott & Middleton 1979; Todd 1989; Sohn 1997).

The traction carpet concept arose from an observation that groove-marked substrates (scoured by dragged clasts) preserved at the bases of turbidites are characterized by an absence of flute marks, which form by scour from turbulent eddies. This led to the inference that some turbidity currents exerted sufficient shear stress towards their base to transport a thin, high-concentration, high-viscosity laminar flowing basal sheet (Hsü 1959), referred to as a 'traction carpet' by Dzulynski & Sanders (1962). Subsequent workers invoked this traction carpet concept to account for thin bedding in deposits ('spaced stratification' of Hiscott & Middleton 1979; Lowe 1982; Todd 1989; see below). However, the concept and its application have not been universally accepted (see Carter 1975; Postma 1986; Best 1992), mainly due to a lack of experimental corroboration. For example, experimental high-concentration turbidity currents of Middleton (1967), did not form traction carpets, but this was probably because the currents were of single-surge type, waned too rapidly and exerted insufficient shear on the substrate. Rather, the currents segregated a basal concentrated layer ('quick bed' of Middleton 1967) dominated by hindered settling (see p. 33) after flow had virtually ceased. The traction carpet concept does, however, find support from limited observations of rivers in spate (see Todd 1989), from interpretations of deposits (e.g. Dzulynski & Sanders 1962; Chun & Chough 1992; Sohn 1995) and in the transport behaviour of heterogeneous two-phase suspensions in horizontal hydraulic and pneumatic pipeline conveying systems (Coulsen & Richardson 1990; Laouar & Molodtsov 1998).

Hiscott (1994b) argued that typical density currents are only capable of moving carpets a few grain diameters thick, but this assessment was based on the shear stress required to move an initially stationary bed to create a plug-like carpet of very high clast concentration (55 vol. %). Significantly, traction carpets probably: (1) are of lower concentration than this (e.g. 10 vol. %); (2) form from clasts already moving in the current rather than form by shearing an initially static substrate, which requires higher shear stress than does maintaining motion; and (3) shear throughout their thickness (Sohn 1995). Hiscott's calculation also treated traction carpets as grainflows, whereas they are modified grainflows in that their behaviour may be variously affected by interstitial fluid, fluid

lift, clast buoyancy and fluid escape. Also, in contrast to Hiscott's scenario, the overriding part of the current that exerts shear stress on a traction carpet need not be entirely an end-member low-concentration type; it may be significantly density stratified and the top of the traction carpet may be gradational rather than a sharp interface, with turbulence intensity diminishing with depth gradually rather than abruptly (Middleton & Southard 1984, p. 230). Traction carpets are perhaps best thought of as laterally variable and impersistent, with the form of a low-profile shifting bedform (cf. 'migrating dunes' of Wen & Simons 1959). Some may be disrupted by periodic large-scale eddies (Jackson 1976; Hiscott 1994b). Their dominant clast-support mechanism is likely to vary with height in the carpet, with differing grain-size populations, clast concentrations, shear rates and rates of deposition (see Chapter 3). Gradations into less-concentrated tractional bed loads are likely (Dzulynski & Sanders 1962), as are gradations into other types of granular fluid-based density currents (Fig. 2.9C–G). Experimental work is needed to define the hydrodynamic controls and possible stability fields for traction carpet formation. Although unsteadiness has been invoked to cause their formation (Lowe 1982), there is no reason why this should be a prerequisite; traction carpets have been maintained by steady flow in pipes (Coulsen & Richardson 1990; Laouar & Molodtsov 1998).

The possible relationships between deposit characteristics (e.g. layering) and mechanisms of deposition from traction carpets are not resolved. Near-horizontal, 3–5 cm thick sandstone layers with basal scours, inverse grading and grain imbrication have been interpreted as each representing a traction carpet that attained some critical thickness whereupon it entirely collapsed and deposited by frictional 'freezing', so that each deposit layer represents an *in situ* former traction carpet (Hiscott & Middleton 1979). Similarly, 0.4–3 m thick fluvial gravel beds have been inferred to represent the thickness of former traction carpets (Todd 1989). Sand layers, 0.5–5 cm thick, with basal shear laminations, inverse-graded centres and massive tops also have been interpreted as representing plug-like traction carpets that 'collapsed and froze en masse', after having been thickened by a supply of clasts from above (Lowe 1982). However, each of these interpretations assumed that no deposition occurs from a traction carpet prior to its complete and instantaneous collapse. Evidence for plug flow and 'en masse freezing' behaviour of traction carpets is lacking, and in a steady depositing current a traction carpet may maintain its thickness while depositing incrementally from its base as sediment is added to it from above. This seems likely, as shear is applied to the top of the carpet and friction is greatest at its basal contact with the substrate. This type of incremental deposition was invoked for the formation of 2 m-thick massive turbidite divisions that lack vertical variations in fabric, by Hein (1982), who proposed that they aggraded progressively from a basal modified grainflow layer that was much thinner than the massive divisions, but continuously replenished from overriding parts of the current (also see Sohn 1997). In this scenario, the thickness of the modified grainflow layer is not registered in the deposit. In a thin traction carpet it is also possible that shear-induced fabric development and granular segregation may cause inherent localized unsteadiness, such as abrupt 'locking up' of grain layers, causing stepwise aggradation (see 'Fluctuating deposition' below).

We conclude that the term 'traction carpet' is useful to describe a thin (and possibly discontinuous) laminar modified grainflow component of a stratified current, where the motion of the layer predominantly derives from shear stress exerted from overriding, more turbulent parts of the current. The term, however, should not be used either for a particular mode of deposition (see Hiscott 1994b) or for a particular type of stratification within a deposit. As with other granular fluid-based currents, the exact mechanism of deposition and the character of the resultant deposit will depend upon the nature and behaviour of the current flow-boundary zone, which may be dominated by granular flow or fluid escape (see p. 39), and/or may be interrupted by periodic impingement of eddies

('Fluctuating deposition' below). The formation of thin discontinuous layering with inverse grading, which is commonly attributed to traction carpets, is considered in the next section and in Chapter 5 (pp. 71–74). Gradations probably exist between traction carpets and other types of granular fluid-based currents (see Fig. 2.9C–G), and with fully dilute currents that have moderately developed bed loads.

Deposition during unsteadiness

Unsteadiness (p. 2) affects flow-boundary deposition on all scales. On a small scale, repeated waves or momentary encroachment of turbulent eddies onto the flow boundary may give rise to thin layering, whereas larger scale waxing or waning flow may cause the flow-boundary zone to evolve with time and be recorded as vertical grading and/or a vertical succession of contrasting lithofacies.

Fluctuating deposition

Spontaneously forming vortices and eddies are typical of turbulent currents, and they may affect the different types of flow boundary in various ways. In a traction-dominated flow-boundary zone they give rise to stratification (pp. 74–76). Passing energetic eddies may produce small scours, and the waning velocity in their wakes may deposit a downcurrent-fining, normal-graded lens. In the case of a current with a granular flow-dominated flow boundary (e.g. a current with a traction carpet, see previous section), passage of particularly energetic eddies may momentarily sweep aside the entire modified grainflow layer so that any aggrading deposits record alternations between granular flow-dominated and fallout- or traction-dominated flow-boundary zones (Fig. 4.5A) (see Hiscott 1994b). In a current that has a relatively thick basal laminar zone dominated by grain interactions, turbulent eddies from the overriding levels are less able to impact directly as far down as the flow boundary, because of the high clast concentrations there. Such eddies may, however, cause momentary fluctuations, or surging, of the shear stress at this type of flow boundary (Fig. 4.5B). Where this happens so that the shear stress momentarily drops to allow an increase in yield strength to develop in the lowermost part of the shearing granular mass this part may lock-up suddenly, so that the deposit surface jumps rapidly upwards (this is the 'stepwise aggradation' of Branney & Kokelaar 1992). The lowermost part of the former current, and any grading developed within it, may then be preserved intact in the deposit as a thin layer (see Fig. 3.7). Repeated passage of such eddies high within the current may give rise to stacked laterally impersistent thin layers of this type. Where granular segregation in the flow-boundary zone caused development of inverse grading, the inverse grading will be preserved in each thin layer of the stack (Fig. 4.5B). This is a common lithofacies in ignimbrites (see 'Diffuse-stratified and thin-bedded lithofacies', p. 71; e.g. Fierstein & Hildreth 1992). With increasing dominance of fluid escape in the flow-boundary zone (Fig. 4.5C), the passage of overriding eddies is less likely to be recorded in the deposit, because of less efficient downward transmission of stress fluctuations through a thick and fluidal flow-boundary zone. Hence, massive ignimbrite may aggrade under quasi-steady conditions, irrespective of any turbulent fluctuations at higher levels in the current, because with proximity to the flow boundary most minor fluctuations are progressively dampened out (Fig. 4.5C).

Sustained gradual changes

Gradual changes in deposition rate, or in concentration and shear profiles across the flow-boundary zone, will affect any selective filtering gradually, and thereby may cause the grain size, sorting

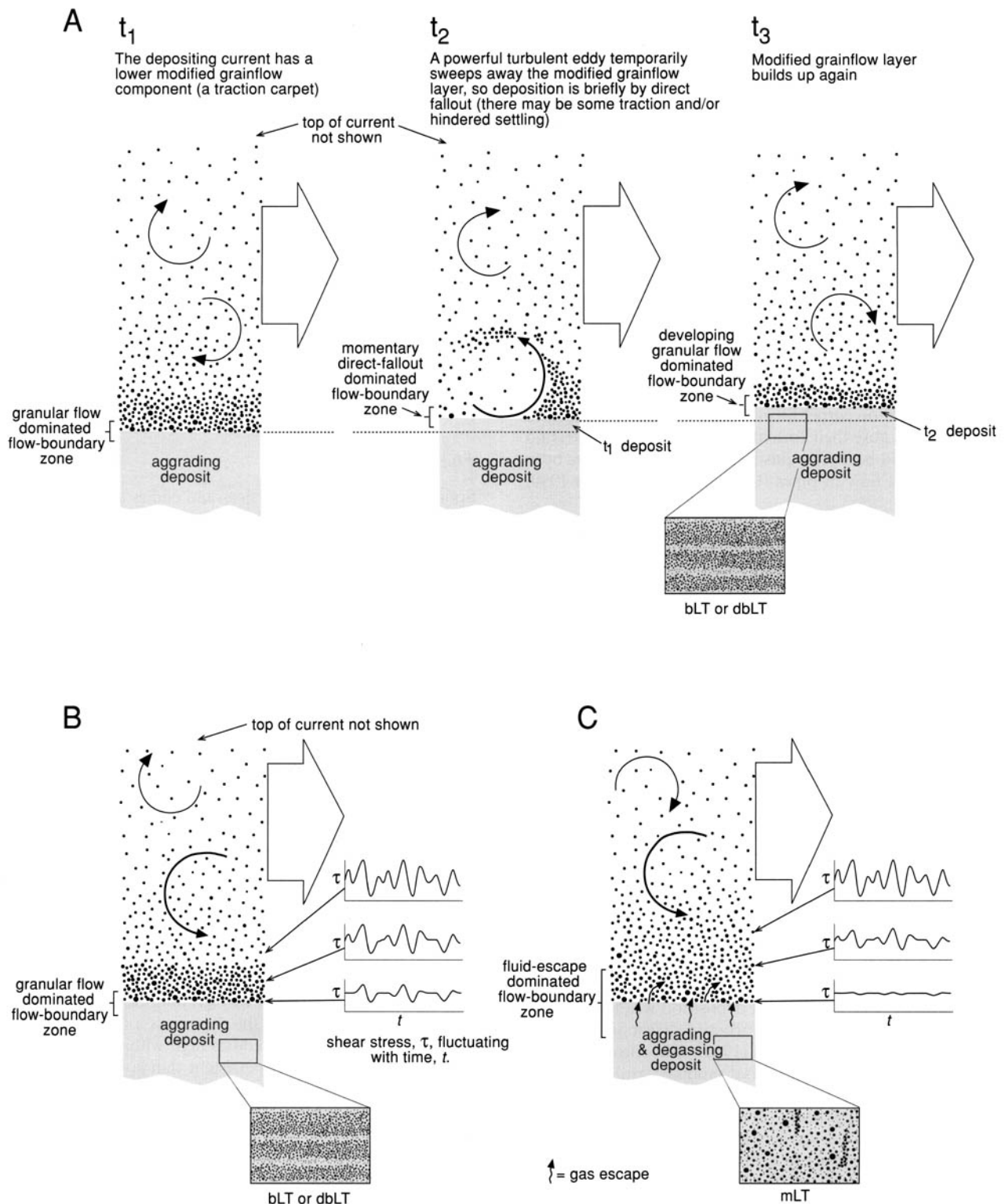


Fig. 4.5. Deposition during small-scale unsteadiness (see ‘Fluctuating deposition’ in this chapter). (A) Thin-bedded (bLT) or diffuse thin-bedded tuff (dbLT) deposited by short-lived traction carpets periodically swept away by the impingement of turbulent eddies from higher in the current (see Hiscott 1994b), so that the flow-boundary type fluctuates between granular flow-dominated and other types (direct fallout-, traction-, or fluid escape-dominated). (B) In this scenario, turbulent eddies are unable to penetrate down as far as the flow boundary, but exert fluctuating shear stresses, τ , on the lower modified-grain-flow part of the current, which then deposits unsteadily (‘stepwise aggradation’, by frequent locking-up), producing thin, impersistent and variably diffuse bedding. (C) Turbulent eddies again are unable to penetrate down as far as the flow boundary, but in this case the fluctuating shear stresses they produce are not transmitted down to the flow boundary at all, because they are damped by a relatively thick high-concentration fluidal layer dominated by fluid escape. Deposit aggradation is thus fairly steady, despite overriding perturbations, and massive lapilli tuff (mLT) is formed.

and componentry of a deposit to vary gradually with height (grading; see p. 66). For example, consider a location (e.g. point x on Fig. 4.6A) where most large pumice clasts overpass and where lithic clasts are preferentially deposited. With waning flow, the

selective filtering properties of the flow-boundary zone change so that pumice clasts of a size that previously overpassed to more distal reaches are now able to deposit at location x . As waning flow continues, the depositional limit of these pumice clasts recedes

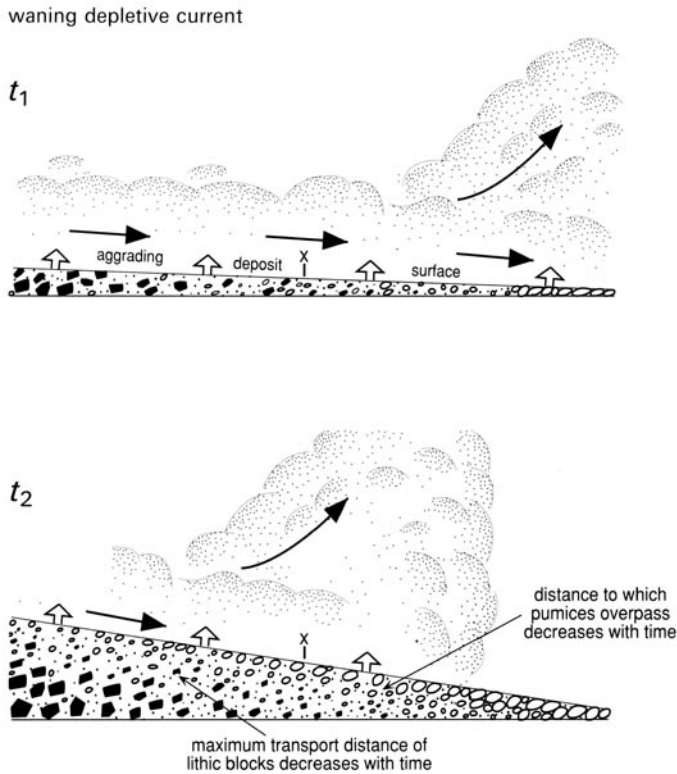


Fig. 4.6. Effects of waning flow on ignimbrite grading. Waning flow causes changes in the selective filtering properties of the lower flow-boundary zone at all locations. At time t_1 , flow-boundary segregation processes prevent proximal deposition of many large pumice clasts (see Fig. 4.3), which overpass to beyond location x , where, as a result of different selective filtering properties (due to depletive flow), they are able to enter the deposit. At time t_2 the current has waned, and changes in selective filtering properties of the flow-boundary zone along the length of the current have decreased the overpassing distance for large pumice clasts, enabling them to deposit upstream of location x . At time t_1 the current had sufficient competence at location x to transport lithic blocks of a certain size, but as current competence wanes, by time t_2 , the current at location x is no longer able to support lithic blocks of this size and so these are deposited more proximally. Note how the resultant ignimbrite has developed normal coarse-tail grading of lithics and inverse coarse-tail grading of pumice. Not to scale (vertical scale and clast-sizes are exaggerated).

sourcewards so that the aggrading ignimbrite develops inverse pumice grading (t_2 on Fig. 4.6; Fig. 3.7). Similarly, the current that once had sufficient competence to transport a lithic clast of a particular size as far as location x (t_1 on Fig. 4.6) can no longer transport lithic clasts of this size as far as x . As the deposit aggrades it thus develops normal grading of lithic clasts (t_2 on Fig. 4.6). As a pyroclastic density current gradually waxes and wanes, all manner of grading patterns (Figs 5.6 and 5.8) may be produced as selective filtering in the granular flow- or fluid escape-dominated flow-boundary zone changes with time (this is explored further on pp. 66–71). Substantial changes in the current can ultimately cause the flow-boundary zone to change from one type to another, so that an entirely different lithofacies is deposited on top of the former lithofacies (Fig. 6.10). There also may be periods during which deposition declines to zero (non-deposition) or is replaced by erosion.

Rapid deposition

Progressive aggradation may occur extremely rapidly and the entire thickness of an ignimbrite may represent only a few moments of

deposition. A short, single-surge current may travel down the side of a volcano and then deposit rapidly (e.g. where the slope decreases) so that the current over its entire length dies out rather abruptly. Material is not replenished from upcurrent as occurs with more sustained deposition. If such a current were dominantly laminar (e.g. a laminar modified grainflow) the resultant deposit may resemble a sheared-out version of the current and preserve its vertical structure. This is similar to, but not the same as (see next section), the Sparks *et al.* (1973) paradigm of en masse deposition of a giant semi-fluidized flow, in that large flotsam pumices travelling near the top of the current may be preserved towards the top of the deposit layer, whereas clasts travelling near the base of the current become buried within the lowest part of the deposit. To create this very simple geometrical similarity between the current and the deposit layer by rapid deposition, all parts along the length of the current must start and stop depositing at virtually the same time as do the trailing parts, irrespective of the local substrate slope. This special circumstance may occur, but other scenarios are more likely. For example, deposition may begin in leading parts of a current as they cross onto shallower slopes before it begins in trailing parts that have not yet reached the shallower slopes. The trailing parts of the current may then variously deposit upslope of, directly on top of, or even downslope of the deposits of the leading parts of the current. Alternatively, rapid deposition may begin from trailing parts of the current, which, for example, may be less energetic. In this case, the reach in which deposition occurs extends forward rapidly to catch up with the current leading edge moments later. In these different scenarios, the relationship between the vertical structure of the deposit layer and that of the former current differs markedly. Therefore, an understanding of the diachroneity of a deposit (e.g. the time-line architecture; see pp. 87–92) is required to reconstruct the vertical nature of the current.

It is important to note that rapid deposition is a flow-boundary process, however rapidly an ignimbrite aggrades and however brief the duration of aggradation is. Thus, the nature of the deposit (e.g. lithofacies character) must be influenced by flow-boundary zone processes and conditions.

En masse deposition

The most extreme form of unsteady sedimentation is in the concept of en masse deposition. This is when the entire current, or a substantial thickness of one, stops virtually instantaneously to form a deposit. It does not involve progressive aggradation and is not a flow-boundary process; the structure of the deposit directly preserves the structure of the current. It is difficult to envisage gradations, in terms of processes, between en masse deposition and rapid progressive aggradation. En masse deposition has been invoked in various sedimentological contexts, for example for cohesive debris flows (Johnson 1970), high-density turbidity currents (Lowe 1982), hyperconcentrated flood flows (Smith 1986) and ignimbrites (Sparks 1976; Wright & Walker 1981; Carey 1991), usually to account for the formation of poorly sorted, non-stratified deposits. However, en masse deposition is not a unique explanation for the origin of such deposits, and how it might be achieved in terms of processes is not always made clear. Interpretations of en masse deposition generally invoke one of four main mechanisms. We evaluate these here for their possible relevance to ignimbrites.

- (1) Clasts in a current in which support is dominantly by fluid turbulence are dumped suddenly when there is an abrupt decrease of turbulence, for example due to topographically induced deceleration. This, however, would cause rapid progressive aggradation rather than en masse deposition. If it occurred in a sustained current, it would cause aggradation of a localized thick deposit at the site where turbulence

dropped. The mechanism is difficult to justify for uniform sheet-like ignimbrites as it would entail the abrupt cessation of turbulence simultaneously over the entire area of a current.

- (2) Relatively minor, deceleration-induced deposition from a current in which support is dominantly by clast interactions triggers en masse 'collapse' of the entire coarse-clast population (e.g. Lowe 1982). In this scenario, initial deposition decreases the overall clast concentration, which, in turn, reduces the support of remaining clasts, which then also deposit. In this way, deposition rapidly quickens into collapse of the entire coarse-particle dispersion, leaving only suspended fines to pass downcurrent (Dzulynski & Sanders 1962; Middleton 1970; Lowe 1982). This cannot apply for sustained currents that replenish clasts in the depositing reach of the current so as to sustain a concentrated clast dispersion, in which case deposition would be by progressive aggradation. The scenario also ignores the effects of the fluid phase within the dispersion. Hindered settling experiments show that, when a concentrated dispersion with a fluid phase is not constantly replenished, the dispersion rapidly becomes density stratified, and, in the absence of particle support by grain collisions, it deposits by progressive aggradation. The *thickness* of the concentrated layer decreases during deposition, rather than there being a wholesale drop in concentration to some critical point after which 'collapse' occurs (e.g. Selim *et al.* 1983; Bürger *et al.* 2000; see p. 33).
- (3) Water that is aiding mobility of a concentrated non-cohesive flow of water-plus-solids drains into a porous dry substrate causing development of a high yield strength in the current and hence a plug zone to develop within its upper part. This may then halt en masse to form a lobate deposit ('sieve deposit' of Collinson 1986). This mechanism is unlikely to occur with pyroclastic currents where the interstitial phase is gaseous, although the localized winnowing of fine ash from pumiceous levees by powerful draughts of air (see the front cover, and photographs in Guarinos & Guarinos 1993) may be somewhat analogous in effect.
- (4) Flowing high-concentration dispersions of cohesive materials develop high yield strengths and form plug flows that tend to halt en masse when the basal shearing layer thins to zero (see p.13). Emplacement of massive ignimbrite has been envisaged to involve a giant semi-fluidized flow undergoing laminar shear while gradually deflating wholesale until it forms a decelerating plug that eventually halts en masse (Fig. 2.2A) (Wright 1981; Wright & Walker 1981; Freundt & Schmincke 1986; Carey 1991; Battaglia 1993). Branney & Kokelaar (1992, 1994a), however, proposed that plug flow generally plays only a minor role in ignimbrite emplacement. Problems with plug flows as a general mechanism for ignimbrite emplacement are discussed below. First, we outline alternative explanations for ignimbrite features previously invoked to indicate plug flow and en masse emplacement.

Five features of ignimbrites have been used to infer en masse emplacement of plug flows. We list them here and then suggest possible alternative interpretations: (1) massive ignimbrite overlying a thin inverse-graded layer was considered to be a 'frozen' record of a high yield-strength plug that moved on a basal laminar shear zone; (2) matrix-supported lithic blocks and lapilli within massive ignimbrite were inferred to indicate that the current had a yield strength sufficiently high to cause plug flow; (3) correlations between maximum lithic size and deposit thickness were inferred to indicate that both current competence and current thickness were determined by yield strength in a plug; (4) steep ignimbrite lobes and levees that were interpreted, respectively, as plug-flow fronts and lateral dead zones accreted from decelerating plugs; and (5) even layer-parallel compositional zoning in ignimbrites was inferred to indicate an absence of turbulent mixing during flow and to be consistent with plug-flow emplacement (Wright & Walker 1981).

Possible alternative explanations for each feature are as follows.

- (1) Massive ignimbrite is deposited progressively from granular

flow-dominated to fluid escape-dominated flow-boundary zones (see pp. 51–57). Inverse graded layers may form during unsteady flow-boundary deposition by several mechanisms involving waxing flow and/or granular segregation (see pp. 66–71 and 101). (2) Lithic blocks and lapilli may roll or saltate along a rising flow boundary during progressive aggradation, and are supported by the yield strength of the underlying newly formed *deposit*, not any yield strength of the current. (3) Deposit thickness relates to the rate and duration of deposition, not to current thickness (see p. 117), so any correlations between ignimbrite thicknesses and maximum clast size simply reflect a generally tendency for large-magnitude currents to be both more sustained and more competent to move large clasts as bed load than smaller magnitude currents. Other problems in interpreting such correlations in terms of current yield strength are discussed by Nemeč (1990). (4) Deposit lobes and levees record depositional non-uniformity and the yield strengths of pumice-rich lobe and levee *deposits*, which differ rheologically from pyroclastic currents. The currents may have been density stratified, partly turbulent, partly channelled and partly dammed by the levees (see pp. 47–49). Ignimbrite lobes and levees are most likely to aggrade as depicted in Figure 6.6E (p. 90). However, distal pumice dams and levees may move as plug flows for small distances (see below). (5) Vertical chemical zonation within massive ignimbrite (Fig. 6.1) is difficult to reconcile with plug flow, because plug flows should record compositional changes during an eruption *longitudinally* through deposits, from distal limits towards source, rather than vertically. Realizing this, Wright & Walker (1981) proposed that the vertical chemical zonation in their plug model was formed within a proximal laminar reach of the current, sourceward of where plug flow developed (see Fig. 2.2A). This is geometrically implausible (Branney & Kokelaar 1992, 1994a); for example the instantaneous flow lines depicted on Figure 2.2A are incompatible with the velocity profiles. Palladino & Valentine (1995) address this by reducing the thickness of their plug zone to a pumice raft (part of the ignimbrite that shows no vertical zonation), so that 90% of the thickness of their ignimbrite was deposited by progressive aggradation ('from the bottom lamina up', Palladino & Valentine 1995, p. 362).

The extensive sheet-like form of ignimbrites is best reconciled with deposition generally occurring during transport, rather than as a discrete depositional phase following a transport phase (see the final section on p. 49). An extensive plug flow cannot halt instantaneously across its length and breadth, because of flow non-uniformity and topographic irregularities. If leading parts of a plug zone halt first they will be overridden by following parts (depletive current), and if trailing parts halt first then the leading parts will detach (in an accumulative current). As seen in lavas, in cohesive debris-flow deposits and in densely welded ignimbrite that undergoes hot-state sliding (Jahns 1949; Voight 1978; Keefer & Johnson 1983; Prior *et al.* 1984; Kastens & Shor 1985; Nemeč 1990; Kokelaar & Königer 2000; Sumner & Branney 2002), internal stresses in a plug flow commonly lead to development of compressional structures (ogives, buckles, ridges, ramps, shear zones, sheet imbrication) and attenuation structures. Yield strength would ensure the preservation of such structures if they formed, but they are not documented from upper surfaces of ignimbrite sheets, which are typically rather planar. Similarly, exposed cross-sections through ignimbrite sheets show that internal textural layers and compositional zonation generally are not internally disturbed. Coarse-tail grading patterns that are seen in ignimbrites also are inconsistent with plug flow because strengths sufficiently high to support plugs of thicknesses similar to many massive ignimbrite layers (tens of metres) would preclude buoyant rising and sinking, respectively, of pumice and lithic lapilli through the flowing plug.

Plug flow may be important locally when terminal pumice dams are shoved forward or shouldered aside, and where pumice levees are shifted sideways (see next section). Such movement may commonly be a form of remobilization in that the pumice dam initially formed as a deposit before being moved forward by the

accumulating fluidal ('quick') dispersion behind. In such cases the distal parts of some ignimbrites may shift several tens of metres. Plug flow of such pumice dams and levees may occur because strength derives from quasi-static grain contacts, and escaping dusty gas provides negligible support as it can escape readily through the highly porous open framework of the coarse deposit. Increased shear rates, however, would lead to increased granular temperature and dilation, with consequent loss of strength and a return to fully laminar, and possibly even turbulent, conditions.

Non-uniform deposition

All pyroclastic density currents are non-uniform, and their spatial variability must change through the course of ignimbrite emplacement. Some large volume ignimbrites can be remarkably monotonous over vast areas. However, even in large currents, the flow-boundary zones may change their character longitudinally or transversely as a result of depletive (e.g. diverging) or accumulative (e.g. converging) flow, and as a result of changes in topographic slope. Marked non-uniform conditions are characteristic, for example, near breaks-of-slope and near the margins of the current. Such changes give rise to lateral facies variations, for example from massive to stratified. Many small-volume ignimbrites show relatively pronounced lateral and longitudinal variability, which is a reflection of the greater non-uniformity of smaller currents. Chapter 6 explores how spatial changes in deposition may contribute to the diverse lithofacies architectures of ignimbrites.

Interpreting ignimbrite lobes and levees

Although the position(s) of former current thalwegs may not be obvious with extensive ignimbrite sheets, they are recorded in distal parts of pristine small-volume ignimbrites by ribbon-shaped strips and lobate terminations (Fig. 4.7; Rowley *et al.* 1981; Wilson & Head 1981). Most lobes that have been described are less than 2 m thick, with convex-up relief, steep sides and fronts, and relatively flat tops. Some have a central channel between two lateral levees, and many are bifurcated and have distal terminations with lobe-and-cleft (cat's paw) morphologies. The levees and lobe fronts are pumice-rich (see p. 76), mostly comprising a framework of large rounded pumice clasts with less fine ash than is in the ignimbrite elsewhere (Fig. 4.7B) (Kuno 1941; Rowley *et al.* 1981; Wilson & Head 1981; Sparks *et al.* 1997b; Calder *et al.* 2000). In contrast, the deposit that occupies the channels between the levees is of more typical matrix-supported ignimbrite (see p. 51), commonly gas-rich and 'quick' prior to compaction. The outer slopes of the levees and lobe fronts are at, or slightly less than, the angle or repose for loose pumice clasts. Wilson & Head (1981) reported inverse grading of pumice in some levees.

Previously, the shape and thickness of ignimbrite lobes have been used as evidence that pyroclastic density currents move as high yield-strength plug flows (see the previous page and pp. 13–14) (Wilson & Head 1981; Battaglia 1993; cf. Kokelaar & Branney 1996). The pumice clasts at the top of the lobes were thought to have floated to the top of the current. The clast densities are only slightly less than the density of the ignimbrite matrix (Wilson & Head 1981), and the presumed floatation was taken to indicate that the current density, and thus its clast concentration and rheology were similar to those of the ignimbrite lobe prior to compaction.

We interpret ignimbrite lobes and levees in a different way. We propose that their morphology is the product of non-uniform deposition and not just a consequence of current rheology, and we propose that there is no simple relationship between the thickness of the ignimbrite and the current that deposited it. Critical to our interpretation is that the levees and the steep snouts of the lobes comprise framework-supported pumice lapilli and blocks, different to the nature of the ignimbrite in the centre of the lobe (which is of

matrix-supported massive lapilli-tuff). Thus, a homogenous rheology cannot be assumed. We invoke deposition of the massive lapilli-tuff at a fluid escape- to granular flow-dominated flow-boundary zone (see pp. 56–57), where large pumice clasts are mostly prevented from descending to the base of the current (selective filtering, pp. 41–42) due to the combined effects of buoyancy, fluid escape, dispersive forces and granular segregation processes (see earlier sections in this chapter). Most larger pumice clasts thus overpass, each travelling downcurrent within the stratified current at a level where buoyancy and dispersive forces acting on it are equal to the gravitational force (Fig. 6.9). The pumice clasts eventually approach the distal (or lateral) limit of the current in contact with the ground, where flow-boundary conditions are markedly non-uniform. Here, the velocity and concentration of the lowermost part of the current decrease so that pumices are no longer supported by buoyancy and dispersive forces as before. Any support derived from fluid escape related to hindered settling (see p. 39) also declines to zero at this limit (although inrush and expansion of ambient air may confer some lift). Many pumices, therefore, deposit near the distal limit of the current on the ground. Most of the fine-grained material remaining in the current at this location lofts. During quasi-steady flow, successive pumice clasts arrive at the distal limit of the current and rapidly accumulate there as a framework-supported mound or 'snout'. Levees form in a similar way, as flow streamlines locally carry pumice flotsam towards the lateral edges of the current. The levees may then help to channel the thalweg of the current, and can produce slow secondary flow circulation within the rough-walled channels (see Savage 1979, fig. 5b).

Gas-rich, 'quick' massive lapilli-tuff rapidly aggrades behind the pumice dam and exerts increasing stress on it. The thickening steep-sided deposit may rapidly become unstable, and may remobilize (Fig. 4.7B) either by being shoved forwards or by being breached and shouldered aside to form levees. This displacement of levees and pumice dams may involve laminar or plug flow. The dam has a yield strength due to the static frictional contacts between pumice clasts, and whilst being shoved forward it may retain strength via quasi-static grain interactions (see p. 35). Where the front slope is oversteepened, pumice clasts will roll and bounce down (individually, by debris fall or as grainflows). Rapid shearing of any levee or frontal dam will cause its granular temperature to rise so that material will transfer from the quasi-static to the rapid granular flow regime (Savage 1979). Complex multilobate edges to ribbon-like ignimbrite lobes (Fig. 4.7A) are probably formed by the breaching of pumice levees. Pouliquen & Vallance (1999) have succeeded in simulating a similar lobe and levee structure in the laboratory, wherein relatively large and angular clasts that overpass to the flow front accumulate there, while (hot) liquefied poorly sorted clastic material pushes from behind. This configuration, with the behaviour of levees and dams dominated by Coulomb friction and the behaviour of the flows behind being more fluidal, becomes unstable with the liquefied material eventually breaking through the coarse barrier to form finger-like lobes with marginal levees. It was found that granular segregation was essential for the instability to develop and it seems that the spacing of the deposit lobes and intervening clefts may be a characteristic function of the contrasting material rheologies. In nature, however, the spacing of lobate breakouts from former levees, or of the lobes in cat's paw terminations (Fig. 4.7A), may be more to do with substrate irregularity, unsteady flow conditions and the currents internal distribution of thalwegs (i.e. non-uniformity).

Quick, fines-rich matrix from the channel-filling massive lapilli-tuff may infiltrate the framework-supported pumice dam and levees. However, percolation during any granular shear should maintain the pumice framework and may produce inverse grading (pp. 29–31), while fine ash on the outer slopes of the lobe may be winnowed away by air currents that stream inwards towards the hot pyroclastic density current as a consequence of vigorous convective ascent of the associated plume (e.g. see the front cover;

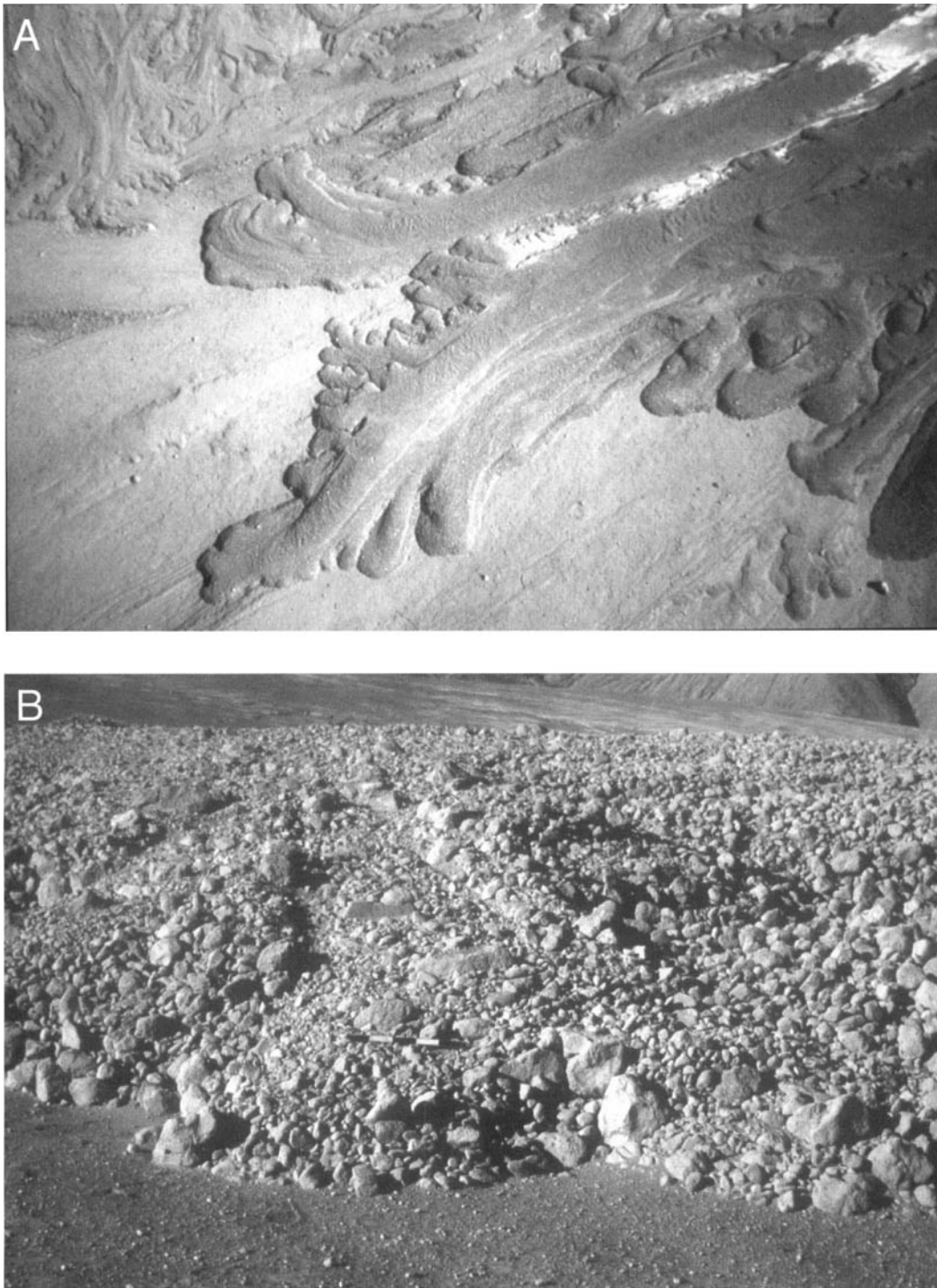


Fig. 4.7. Pumiceous lobes and levees. **(A)** Aerial view of 7 August 1980 pumice-rich lobes and levees on the Mount St Helens ignimbrite fan (see Rowley *et al.* 1981). The ignimbrites are small-volume and ribbon shaped, with cat's-paw terminations caused by localized breaching of levees and terminal pumice dams. (Photograph: U.S. Geological Survey). The lobe in the centre of the photograph is 150 m wide and ≤ 7 m thick. **(B)** Detail of distal pumice-rich snout of an ignimbrite lobe of 22 July 1980 at Mount St Helens. The convex shape is due to the strength of the deposit not the rheology of the current. Note the large size, framework-support, and good sorting of the pumice lapilli and blocks which travelled to the termination because their proximal deposition was prevented by selective filtering. The lobe shows development of a small subsidiary lobe (centre, foreground) formed by minor remobilization of a pumice dam. The scale interval is 10 cm. (Photograph: Stephen Self). Also see back cover.

Guarinos & Guarinos 1993, figs 4, 6 and 7; also fig. 9a in Calder *et al.* 2000).

Lobe and levee morphology thus records thalweg geometries and the changing rates and durations of aggradation. Lobe thickness relates to the rate and duration of pumice accumulation, and the steepness of lobe margins relates to the friction at quasi-static grain contacts of the pumiceous levee *deposits*, not any overall rheology

of the pyroclastic currents that deposited them. High yield strengths in the current probably occur only in the unstable pumice dams being shoved forward and shouldered aside. The density current as a whole would travel more rapidly, be density stratified, transport clasts by varying combinations of fluid turbulence, buoyancy, rapid grain interactions and fluid escape, and deposit mainly massive ignimbrite characterized by poor sorting (see p. 51).

Our interpretation is similar to the observed development of shifting dams and levees in subaerial cohesionless debris flows (e.g. Sharp 1942; Pierson 1981; Johnson & Rodine 1984), in which overpassing lithic blocks move more rapidly than the advance of the frontal coarse-grained dam, so that they accumulate there (conveyor-belt mechanism of Allen 1984; Pierson 1986; Nemeč 1990). In a similar way, overpassing pumices in a pyroclastic current travel faster than the coarse pumice dam, where they then accumulate. In the pyroclastic density current case, buoyancy is likely to be particularly important in the overpassing of pumice and, also, the current may not have a discrete upper surface, but may pass up into low-concentration, turbulent clouds.

In summary, steep sides and snouts of ignimbrites are coarser grained, better sorted and contain less fine-grained ash than in more typical, matrix-supported massive ignimbrite. Their shape and physical properties do not reflect the overall rheology of a pyroclastic density current, but reflect non-uniform deposition and friction at quasi-static grain contacts within frontal and lateral high-concentration pumice accumulations. These are either static deposits or slowly shifting distal accumulations undergoing low rates of shear with respect to the rest of the current. The velocity and rheology of these distal elements are likely to be vastly different from those of the majority of the current.

As a sustained current waxes and wanes, the position of distally formed pumice accumulations can shift back and forth, so that pumice-rich lenses become interstratified with other ignimbrite lithofacies (see pp. 76 and 77). Thus, the lobes and levees seen at distal tips of ignimbrite sheets record only the moments of maximum runout.

Postdepositional remobilization

Recently deposited poorly sorted massive ignimbrite has very little strength and is highly susceptible to remobilization. This may result from loading by and/or shear from an overriding current (see p. 108), or by retrogressive collapse of unstable accumulations, such as where retaining pumice dams are breached or where loose deposit surfaces are oversteepened by stream erosion (Fig. 2.1F; see back cover). Remobilization of loose ignimbrite at Mount St Helens in 1980 produced small collapse scars and deposit-derived pyroclastic density currents (Rowley *et al.* 1981). Following the 1991 eruption of Mount Pinatubo, large, hot, deposit-derived pyroclastic density currents, which travelled as far as 10 km, occurred as long as 3 years after the original ignimbrite emplacement (Torres *et al.* 1996) and smaller ones occurred some time after this, usually when undercutting by streams increased due to heavy rainfall. The lithofacies and granulometry of the ignimbrites formed by the deposit-derived currents are similar to those of the parent ignimbrite, which suggests similar mechanisms of transport and deposition. Because just-formed massive ignimbrite has such low strength, it seems likely that remobilization of just-formed ignimbrite is a common process even *during* the sustained aggradation of large ignimbrite sheets, in which case considerable volumes of pyroclasts in medial and distal parts of

ignimbrites could have been previously deposited more proximally before entering the current again to be transported further (see Fig. 6.12I). In long-duration sustained currents, a significant volume of ignimbrite may be shifted downcurrent in this way in a series of steps. Temporary residence times in the deposit may vary from seconds to hours. Compositional mixed zones and localized compositional reversals in some ignimbrite sheets (e.g. in the Acatlán ignimbrite, Mexico; authors' unpublished data) may record such syn-eruptive remobilization.

Effects of deposition on current behaviour

The sheet-like geometry and sheet-parallel persistence of internal architectural elements of extensive ignimbrites suggest that deposition generally accompanies transport in large pyroclastic density currents. This is in contrast to deposition occurring only during a discrete, post-transport 'depositional phase', which would tend to produce less laterally uniform accumulations. This constrains models of pyroclastic density currents to include significant decoupling of clasts from fluid during transport.

Because deposition accompanies transport, transport may be affected by deposition. The runout distance of an unconfined current must be influenced by deposition (and any elutriation and lofting). For example, deposition from a fully dilute density current may cause it to become less dense with distance so that its distal limit (runout distance), where the current leaves the ground, is a function of the deposition (see Druitt 1992; Bursik & Woods 1996). Deposition from a granular fluid-based current may similarly influence the current runout distance, but at a rate dissimilar to that of a fully dilute current, with the effect that the runout will be different. Whereas in a fully dilute current the rate of deposition is a function of decreasing current velocity and hence decaying turbulence intensity, in a granular fluid-based current the rate of deposition may be limited by the rate of fluid escape (see p. 33) in the flow-boundary zone. This is a function of the properties (e.g. clast concentration and grain-size distribution) of the flow-boundary zone rather than of any properties (e.g. velocity) of the current as a whole. Clasts whose deposition is hindered as a result of escaping fluid remain in the current for longer than they would otherwise. This prolongs the existence of the fluidal dispersion (i.e. the current), which, where topography permits, will continue spreading due to gravity until all clasts in the granular fluid have finally deposited. Such a current thus flows further than it would have done in the absence of hindered settling. In addition to this prolonging effect, the escaping fluid may also act to partly fluidize lower parts of the granular fluid-based current, lowering its internal friction and hence its effective viscosity. Thus, deposition affects runout distance of a granular fluid-based current in different ways to that in which it affects the runout distance of a fully dilute current. It follows that in hazards analyses, models of pyroclastic density currents should incorporate realistic mechanisms of deposition in order to anticipate runout distances. This would involve consideration of the nature of the flow-boundary zone.

This page intentionally left blank

Chapter 5

Interpreting ignimbrite lithofacies

This chapter presents an approach for ignimbrite description and interpretation. It draws on field, granulometric and fabric data from published descriptions of ignimbrites. To describe ignimbrites, we adopt a non-genetic lithofacies scheme (Table 5.1). This avoids possible connotations of 'ideal' sequences or of specific emplacement models (as in the previous schemes of 'Layers 1, 2a, 2b', 'ignimbrite types 1–3', 'ground layer' and 'basal layer'). We describe some of the more common lithofacies in ignimbrites. Our list is not intended to be prescriptive, and it is to be expected that workers will in the future modify or subdivide our groupings. We then show how the lithofacies might be interpreted in terms of flow-boundary zone processes. Understanding is far from complete, and in some cases we give possible alternative interpretations that require testing (also see summary on Table 7.1, p. 120). Consideration of lithofacies that record sedimentary reworking (e.g. by wind or water) is beyond the scope of this work.

A lithofacies scheme for ignimbrites

A *lithofacies* refers to the character of a deposit, or part of a deposit, that is distinct according to some combination of stratification, grain size, grain shape, sorting, fabric and composition. It is non-genetic and non-stratigraphic. Some common ignimbrite lithofacies are listed in Table 5.1, with convenient abbreviations. Primary lithological descriptors include tuff (T), lapilli-tuff (LT), lapillistone (L) and breccia (Br), subdivided into lithofacies according to stratification type, sorting, composition and fabrics, for example massive lapilli-tuff (mLT) or stratified lapilli-tuff (sLT). The list can be extended and further subdivisions made as desired. Sorting is described in terms of graphical standard deviation ($\sigma_\phi = \phi_{84} - \phi_{16}$), after Inman (1952) and Walker (1971). The lithofacies are not defined on the basis of granulometry alone, because each lithofacies exhibits a range of grain-size and sorting characteristics, and because these overlap with those of other lithofacies. It is therefore best to use a combination of features (e.g. including bedding and grain fabrics) to define a lithofacies. This approach has the additional advantage of applicability to indurated ignimbrites that cannot be sieved. A single lithofacies may be preserved variously in a non-lithified or lithified state (e.g. ash versus tuff) as a result of differing postdepositional histories. For simplicity, we use a common lithofacies grouping when the primary objective is to interpret sedimentary processes (e.g. LT for both lapilli-tuff and lapilli-ash; see Table 5.1). Welding, which can be important in terms of emplacement, may be incorporated using terms such as eutaxitic, rheomorphic and/or vitrophyre, as appropriate (Table 5.1). For some lithofacies or groups of lithofacies the mechanism of deposition may be readily inferred, but others may not have a unique origin. In the latter case interpretation may be aided by characterizing the *lithofacies association* in which they occur. However, experimental work is needed to constrain the flow-boundary zone conditions that control the development of certain lithofacies.

Massive lapilli-tuff lithofacies (e.g. mLT; mLTi; mLTf)

Description

Massive lapilli-tuff (mLT) is the most common ignimbrite lithofacies (e.g. Marshall 1935; Murai 1961; Ross & Smith 1961; Sparks 1976; Wilson & Walker 1982; Branney & Kokelaar 1997). It is commonly poorly to very poorly sorted (σ_ϕ 2–5; Walker 1971) with a median grain size within the ash range, and with grain-size distributions that vary between Gaussian and polymodal (Murai 1961; Sheridan 1971; Walker 1971). The lithofacies lack internal

Table 5.1. Non-genetic lithofacies terms and abbreviations. For example, $mLT_{(i)}-mLT_{(nl, ip)}$ is massive lapilli-tuff with inverse grading overlain by massive lapilli-tuff with normal-graded lithic clasts and inverse-graded pumice clasts.

Symbol	Lithofacies
mLT	massive lapilli-tuff (or lapilli-ash)
$mLT_{(nl, ip)}$	massive lapilli-tuff/ash with normal-graded lithics and inverse-graded pumices
mLTf	massive lapilli-tuff with directional grain fabric
sLT	stratified lapilli-tuff/lapilli-ash
dsLT	diffuse-stratified lapilli-tuff/lapilli-ash
bLT	thin-bedded lapilli-tuff/ash (beds centimetres-thick)
sT	stratified tuff/ash
//sT	parallel-stratified tuff/ash
xsT	cross-stratified tuff/ash
//bpL	parallel-bedded pumice lapilli
lenspL	lens of pumice lapilli
lenspC	lens of pumice cobbles
lenslBr	lens of lithic-rich breccia
fpoorT	finest-poor tuff/ash
mLTpip	massive lapilli-tuff/ash, with finest-poor pipes
mIBr	massive lithic breccia
mScAg	massive scoria agglomerate

Recommended abbreviations	
T	tuff/ash
LT	lapilli-tuff/lapilli-ash
L	lapilli
Br	breccia
Ag	agglomerate
Co	cobbles (i.e. rounded blocks)
m	massive
(n)	normal-graded
(nl)	normal-graded lithics
(i)	inverse-graded
(ip)	inverse-graded pumices
(n)-(i)	normal-to-inverse graded
s	stratified (e.g. tractional)
xs	cross-stratified (e.g. tractional)
//s	parallel-stratified (laminated)
//b	parallel-bedded (thin beds)
p	pumice-rich
l	lithic-rich
sc	scoria-rich
o	obsidian-rich
cr	crystal-rich
fpoor	finest-poor
frich	finest-rich
f	directional grain fabric
i	isotropic; no directional grain fabric – may have a compaction fabric.
acc	accretionary lapilli-bearing
ves	vesicular
lens	lens(es)
e	eutaxitic
vap	vapour-phase altered (e.g. sillar)
lava-like	lava-like
v	vitrophyre (welded and glassy)
rheo	rheomorphic (e.g. with elongation lineations and folds)

stratification and comprise various proportions of pumice and subordinate lithic lapilli supported in a matrix of vitric ash with or without crystal fragments (Fig. 5.1). They form layers from a few centimetres to hundreds of metres thick (Fig. 5.1C–E). Pumice lapilli commonly show rounding caused by abrasion; lithic lapilli show this to a much lesser extent (Fig. 5.1A and B). Massive lapilli-tuff lithofacies vary from isotropic (mLTi; i.e. lacking grain fabrics)

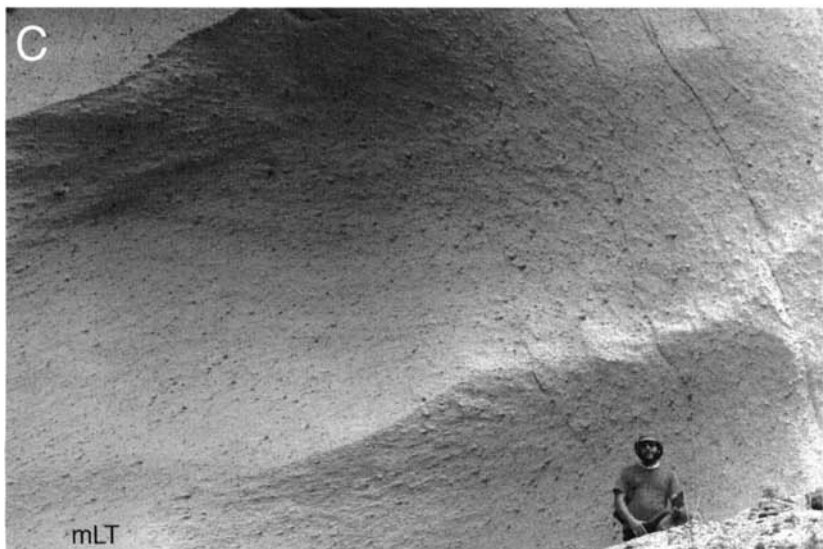


Fig. 5.1. Massive lapilli-tuff lithofacies (mLT).

(A) Detail of mLT with inequant rounded pumice lapilli (pale) and subordinate angular lithic lapilli (dark) supported in a sand-grade ash matrix. Xáltipan Ignimbrite, Puebla, Mexico. The coin is 1.5 cm.



(B) Detail of mLT with pumice (pale) and lithic lapilli (dark) supported in a poorly sorted fines-rich ash matrix. Lower Bandelier Tuff ignimbrite, White Rock, New Mexico, USA. The lens cap is 6 cm.



(C) Exposure of mLT showing total absence of stratification. Upper Bandelier Tuff ignimbrite, Pueblo Mesa, New Mexico, USA.



Fig. 5.1. (continued).



(D) Ignimbrite of the La Caleta Formation, SE coast of Tenerife (Brown *et al.* 2003). Although this is essentially massive, very subtle impersistent diffuse layering can just be discerned from a distance, and suggests that there was slight unsteadiness at the flow-boundary zone while the lapilli-tuff progressively aggraded. The lithofacies is transitional between mLT and dsLT.

(E) Thick mLT exposed in quarry face over 70 m high. Ito ignimbrite, Kyushu, Japan. The geologist on the ledge in the foreground gives the scale.

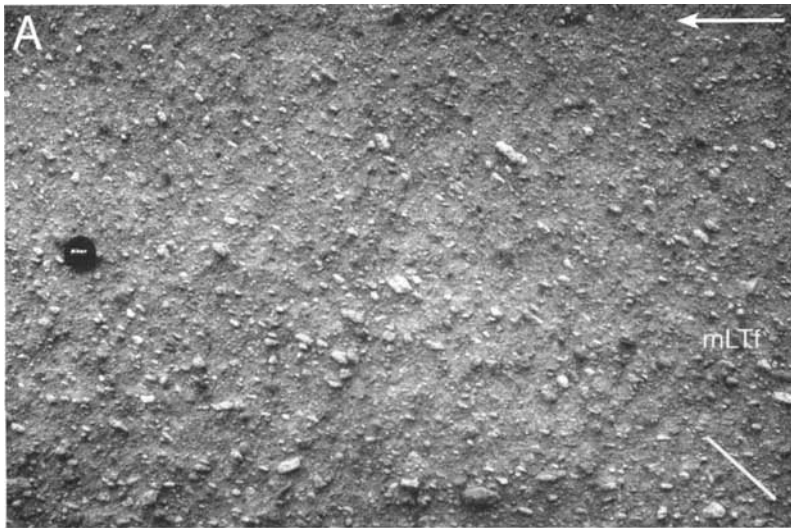
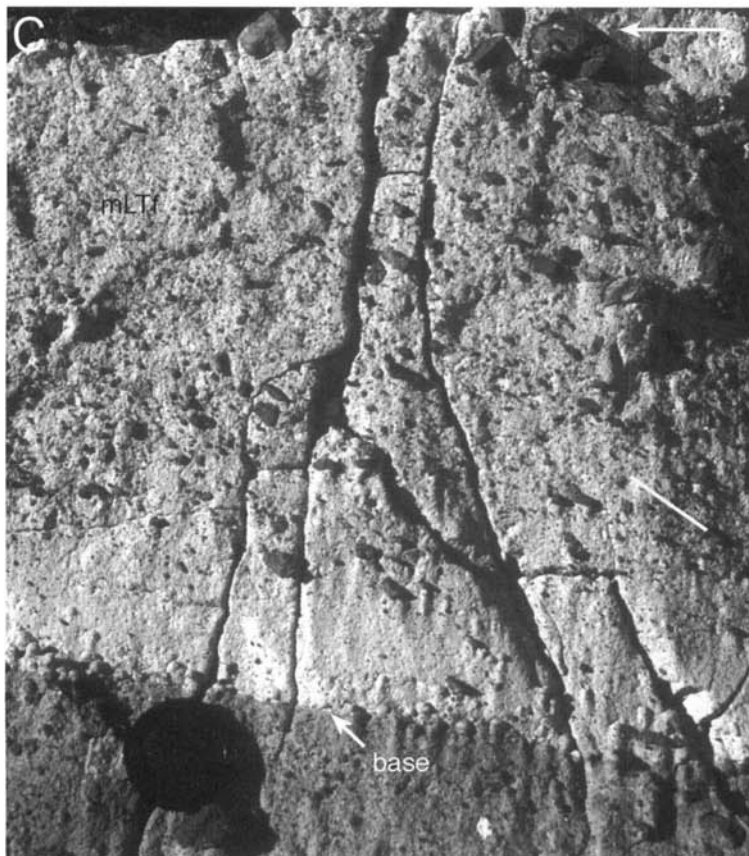


Fig. 5.2. Massive lapilli-tuff with grain fabrics (mLTf). The orientation of rulers and white lines indicates the orientation of the inclined fabric. Note that imbrication angle is the angle between the fabric and the inferred aggradation surface (e.g. bedding). Arrows indicate the inferred apparent flow direction.



(A) Pervasive steep imbrication of inequant pumice lapilli in non-indurated massive lapilli-tuff. Upper Bandelier Tuff ignimbrite, Pueblo Mesa, New Mexico, USA. The lens cap is 6 cm.

(B) Imbrication (parallel to the arm) in this mLTf is best discerned where it affects lithic lapilli, which are concentrated within a diffuse lithic-rich layer. Poris ignimbrite, Guimar, Tenerife.



(C) Well-developed imbrication in the Peach Springs Tuff ignimbrite, Cane Wash, SE California. Imbrication is pervasive throughout, including within the lower, finer grained layer, which is not distinctly inverse-graded. The lens cap is 6 cm.

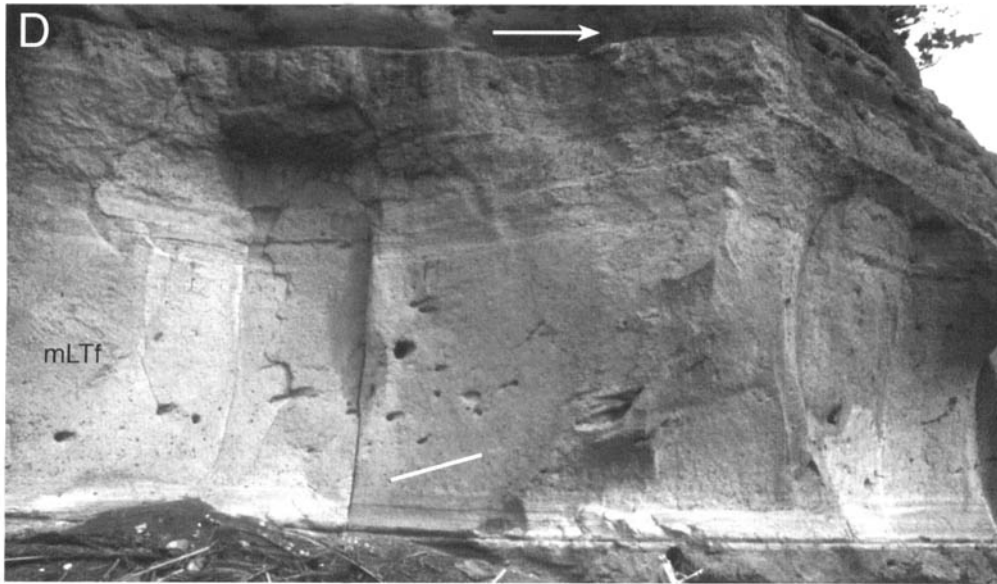
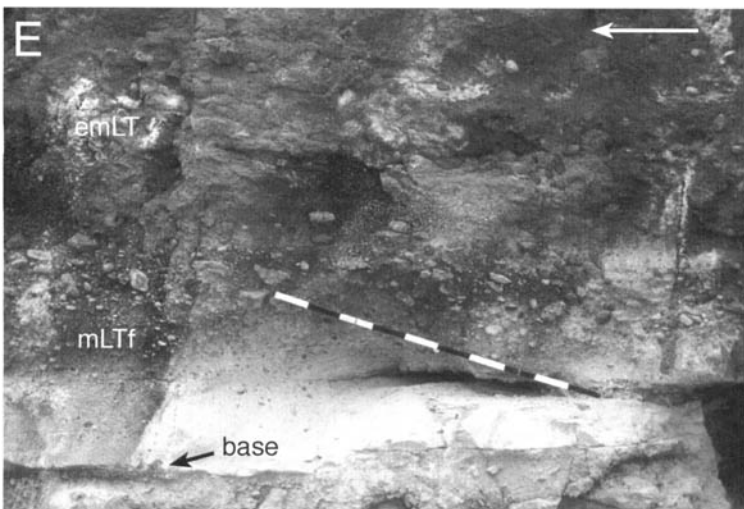
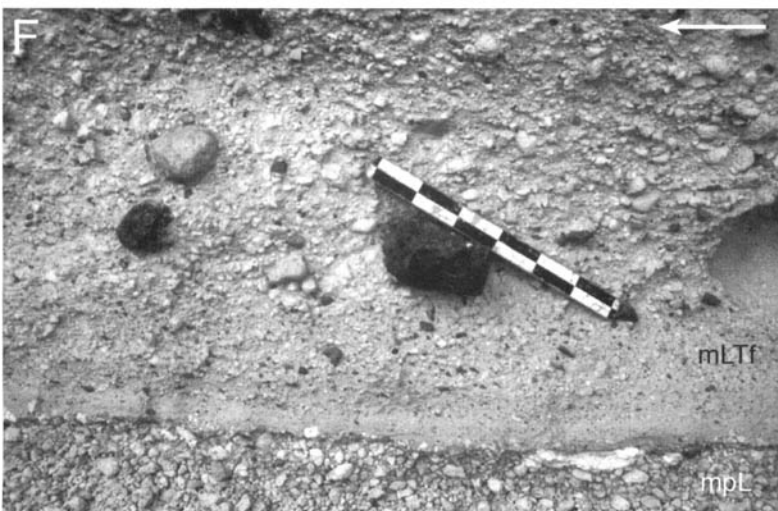


Fig. 5.2. (continued).

(D) Imbrication of transported trees preserved as moulds within central massive layer of the Poris Formation ignimbrite at Guimar, Tenerife. The base and top of the ignimbrite show diffuse bedding.



(E) Imbrication within the base of the Arico ignimbrite at Arico, Tenerife. Imbrication extends from the lower non-welded zone (white) through into an oblique eutaxitic fabric within the welded zone (darker, top-half of the photograph). Clast composition changes gradually with height indicating a changing supply during the progressive aggradation. Metre rule for scale.



(F) Imbrication within inverse coarse-tail graded ignimbrite ($mLT_{(f)}$) that overlies a Plinian pumice fall deposit (mpL). Granadilla Formation, southern Tenerife. The scale interval is 5 cm.

to those with variously developed fabrics (mLTf) defined by planar or linear preferred orientations or arrangements of lapilli, crystals and/or matrix particles (Fig. 5.2) (Elston & Smith 1970; Kamata & Mimura 1983; Potter & Oberthal 1987; Ui *et al.* 1989). Grain fabrics may register as an anisotropy of magnetic susceptibility (Ellwood 1982; Knight *et al.* 1986; Fisher *et al.* 1993; Capaccioni & Sarocchi 1996; Baer *et al.* 1997), even where they are not visually discernible. The fabrics vary from bedding-parallel to inclined by as much as 45° to the depositional surface (imbricated; Fig. 5.2A). The nature, intensity and azimuth orientation of directional fabrics can vary with height through thick layers of mLTf (MacDonald & Palmer 1990; Hillhouse & Wells 1991; Hughes & Druitt 1998; Capaccioni *et al.* 2001). For example, some layers have pronounced fabrics in lowermost parts that become weakly developed to absent in middle to upper parts (Mimura 1984; Hughes & Druitt 1998).

Massive lapilli-tuff lithofacies can be non-graded or can display several styles of grading (see p. 66). Common variants include lithic-rich (lmLT) and eutaxitic (emLT) massive lapilli-tuff, and massive lapilli-tuff with fines-poor pipes (mLTpip; see p. 64). There is a complete intergradation between mLT and diffuse-stratified lapilli-tuff (dsLT; see p. 71).

Interpretation

The poor sorting and absence of stratification indicate a fluid escape-dominated flow-boundary zone in which turbulent shear-induced tractional segregation is suppressed (pp. 39–41). The lithofacies yields no information on clast concentrations or turbulence intensities at higher levels in the current. The matrix of mLT commonly contains a greater proportion of crystals than the proportion of crystals in individual pumice clasts (e.g. Sparks & Walker 1977), indicating a depletion in (crystal-poor) fine ash that can amount to as much as 50% or more of the original dispersion. We interpret this as partly resulting from the elutriation of fine ash in the fluid escape-dominated flow-boundary zone. However, the abundance of fine ash in mLT indicates that, although fluid escape may have characterized the flow-boundary zone and involved elutriation of fine ash, the process was not sufficiently developed to elutriate all of the fine ash. Particle interlocking, electrostatic agglomeration (when >100°C) or moist agglomeration (≤100°C; see Simons 1996; Schaafsma *et al.* 1998) each may counteract the effects of elutriation by fluid escape to some extent, and aid the deposition of fine ash. Some fine ash is probably produced locally in the flow-boundary zone by shear-induced clast abrasion and breakage (Potapov & Campbell 1997). Crystal fragments may record breakage caused by expansion of melt inclusions during eruptive decompression (Best & Christiansen 1997) or may be related to the tendency for gas bubbles to nucleate on crystal surfaces (Hurwitz & Navon 1994). Contrasting adjacent clasts within mLT may have had quite different transport histories, having travelled at different levels within the current and probably having experienced different combinations of support (see p. 24) before being deposited together.

Evidence that mLT in general is deposited by progressive aggradation is provided: (1) by lateral gradations into stratified lithofacies (see pp. 71 and 109) that clearly aggraded gradually; (2) by gradational variations with height in mLT of grain size and sorting, chemical composition (Fig. 6.1; commonly of regional extent), and in the strength and azimuth orientations of lineated and imbricated grain fabrics (see below); (3) by occurrences of complex grading and sorting profiles (Branney & Kokelaar 1992, 1997; Bryan *et al.* 1998b; Hughes & Druitt 1998; Figs 5.6 and 5.8A–C); and (4) by onlap relationships between compositionally zoned mLT and topography (Branney & Kokelaar 1997). The variations with height in mLT can readily be ascribed to unsteadiness during sustained deposition, whereas mLT that lacks any vertical variations indicates that steady conditions prevailed during sustained deposition; no fundamentally different mechanism of deposition (e.g. *en masse*) is required. Aggradation rates of mLT

are unknown, but ‘splay-and-fade’ stratification (see p. 109) indicates that mLT commonly aggrades more rapidly than adjacent stratified lithofacies. Aggradation rates have been estimated as ≥2.5 mm s⁻¹ for the Bishop Tuff (Wilson & Hildreth 1997), and averaged ≥12.3 mm s⁻¹ for the climactic 15 June 1991 Pinatubo ignimbrite (Scott *et al.* 1996; 200 m of mLT aggraded during *c.* 4.5 h). These are minima, in that the estimated durations of emplacement may have included periods of reduced deposition, non-deposition and/or erosion.

We interpret massive lapilli-tuff that *lacks* directional fabrics (mLTi) to record deposition from a near-end-member-type fluid escape-dominated flow-boundary zone, in which grains experience minimal granular shear as they finally approach the flow boundary and come to rest (Fig. 4.1E). Temporary blocking by slight topographic irregularities on the substrate or on the top of the forming deposit (e.g. between growing ignimbrite lobes, low-angle bed forms or confined behind growing pumice dams and marginal levees) may be sufficient to render conditions at the flow boundary close to stationary hindered settling (see p. 33), so that directional fabrics are not produced. Nevertheless, similar conditions, also producing isotropic mLTi, may occur more generally on low slopes and valley bottoms, whenever flow-boundary zones have low shear intensities.

Origin of fabrics in massive lapilli-tuff lithofacies (mLTf)

We interpret massive lapilli-tuff with a directional fabric (mLTf; Fig. 5.2) to record deposition from a flow-boundary zone dominated by fluid escape, but with significant shear close to the flow boundary and hence a component of granular flow (transitional between D and E on Fig. 4.1). (Such a flow boundary lies a short distance to the right of the rear-left vertical edge of the cubic plot of deposition rate vs. shear rate vs. concentration, Fig. 4.2). As clasts approach the flow boundary, they are organized and orientated by the shear. Trends of lineation and inclined grain fabrics (e.g. imbricated pumices) record the shear sense *within the flow-boundary zone* at that location. They record only the last increments of shear undergone by clasts as they deposit (e.g. see Fig. 2.4), so that the fabrics may not directly record the overall behaviour, conditions, or shear directions of the pyroclastic density current at that location.

The strength (Kjær & Kruger 1998) of directional fabrics in massive lapilli-tuff is a product of: (1) the shear intensity at the flow boundary (see velocity profiles in Fig. 4.1D and E); (2) the residence time of clasts within this shearing zone as they sediment through it, which is related to deposition and aggradation rates (Fig. 4.2); and (3) clast shapes and sizes. However, disruption caused by fluid escape within the compacting deposit (i.e. just below the flow boundary) can diminish or obliterate a fabric (see below). The *nature* of the directional fabrics, for example prolate versus oblate, inclined (imbricated) versus bedding-parallel and whether long-axis azimuths are parallel or transverse to shear direction, also records flow-boundary zone conditions and processes. Clasts orientated with their longest axes transverse to current direction are commonly interpreted to have rolled into their final position (e.g. Bertran *et al.* 1997; Jo *et al.* 1997), whereas clasts orientated with long axes parallel to the inferred shear direction are thought to have aligned within a shearing high-concentration dispersion without rolling (Rees 1966; Postma *et al.* 1988). It is conceivable that contrasting grain-size subpopulations (e.g. blocks versus ash) within an ignimbrite may exhibit contrasting preferred orientations owing to their contrasting modes of transport immediately prior to deposition. This occurs in some deposits of hyperconcentrated lahars (Smith 1986), which contain long-axis-transverse boulders together with long-axis-parallel gravel. Similarly, large blocks emplaced by debris fall (see p. 28) low on talus slopes tend to have long axes transverse to transport direction while grainflow-dominated upper parts of talus slopes have long-axis-parallel fabrics (Francou 1991). The most commonly reported preferred

orientation of lineations in ignimbrites is long-axis parallel to the inferred shear direction (Hughes & Druitt 1998 and references therein). We infer that they develop in flow-boundary zones dominated by granular flow and/or by fluid escape. Experiments are needed to understand the mechanisms and controls: for example, to investigate how, at what rate and at what level fabrics develop during deposition at flow boundaries of polydisperse modified grainflows.

Directional fabrics can be modified, destroyed or overprinted in the forming deposit just beneath the flow boundary, soon after deposition by: (1) degassing, with or without segregation or convective overturning of 'quick' deposit; (2) burial compaction, which rotates inclined particles toward the horizontal and tends to produce fabrics that are near horizontal to slope-parallel oblate, or constitute a 'girdle'; and (3) welding compaction and/or rheomorphism. Directional fabrics may be less well preserved around some elutriation pipes (mLTpip; Fig. 5.5) than elsewhere in the deposit, because of modification during degassing.

Variations in fabric azimuth with height through individual mLTf layers (e.g. MacDonald & Palmer 1990; Hillhouse & Wells 1991; Capaccioni & Sarocchi 1996; Hughes & Druitt 1998) record temporal changes in flow-boundary zone shear direction during the sustained passage of a current (Branney & Kokelaar 1992). Such changes in shear direction are to be expected due to: (1) lateral shifts and twisting of current thalwegs, and temporal changes in the shape and position of irregularities on the deposit surface, such as lobes, bars and levees (Branney & Kokelaar 1992); (2) passage of large eddies or waves; and (3) changes in channelling, reflection and drainback caused by changing topography as a result of deposition and/or erosion by the current, or due to caldera subsidence.

Massive to stratified lithic breccia lithofacies (e.g. mlBr; dslBr)

Description

Massive lithic breccias (mlBr; Fig. 5.3) are a common proximal lithofacies of ignimbrites and also occur in medial parts (Bacon 1983; Druitt 1985; Druitt & Bacon 1986; Druitt *et al.* 1989; Walker 1985; Walker *et al.* 1981a; Freundt & Schminke 1985; Marsella *et al.* 1987; Suzuki-Kamata & Kamata 1990; Buesch 1992; Branney *et al.* 1992; Cole *et al.* 1993; Allen & Cas 1998; Bryan *et al.* 1998a; Macías *et al.* 1998; Giannetti & De Casa 2000). They can occur at the base (Wilson & Walker 1982), in the middle (Self *et al.* 1986) or towards the top of an ignimbrite sheet (Scott *et al.* 1996), and may locally constitute the entire sheet thickness (Druitt & Sparks 1982). Their development is commonly topographically controlled, being thickest in valleys, and they may occur interstratified with mLT as one or more discrete layers, as lenses or as irregular-shaped pods (e.g. Fig. 5.3A; Druitt & Sparks 1982). Contacts between mlBr and other lithofacies (e.g. mLT) may be gradational (Fig. 5.6F), sharp (Fig. 6.10B) or erosive, or with bulbous load structures (Figs 5.3C and 6.13E; Cole *et al.* 1993; Giannetti & De Casa 2000).

Sorting values of mlBr commonly lie within the range σ_{ϕ} 1.5–4.5 (Druitt & Sparks 1982; Walker 1985; Druitt & Bacon 1986; Scott *et al.* 1996) but some lie outside this range (Walker 1985; Roobol *et al.* 1987). They allow arbitrary subdivision of the breccias into: (1) matrix-supported; (2) clast-supported fines-rich; and (3) clast-supported fines-poor types, although all intergradations occur between these. Matrix can be ubiquitous or only patchily present (Fig. 5.3A), and may vary from fines-rich and pumiceous (like mLT) to fines-poor (e.g. Scott *et al.* 1996). Variations in grain size and sorting within a breccia may define vertical pipe-like to highly irregular-shaped segregation structures (Fig. 5.3A) (Druitt 1985; Walker 1985). Typical mlBr contain blocks several centimetres to decimetres in size, although some blocks can exceed 1 m. Exceptionally coarse breccias within calderas include megablocks as large as hundreds of metres in size (megablocks of Lipman 1976).

Most mlBr are heterolithic, and the composition of the blocks

may vary vertically and laterally in the deposit. The clasts may be cognate (e.g. scoria or spatter), accessory (e.g. intrusive or hydrothermally altered volcanic rocks ejected from the vent) and/or accidental (e.g. substrate-derived rocks), and typically include both fresh and hydrothermally altered lithologies. The blocks generally are angular to subrounded. Some have delicately preserved remnant exfoliation rinds (Fig. 5.3E) that easily detach so that original angular corners and edges fall away revealing a subrounded core, commonly with curvilinear facets. Complementary *rock flakes* with curvilinear sides and sharp edges (Fig. 5.3D) commonly occur haphazardly enclosed within the matrix of mlBr. These features suggest that thermal spalling (i.e. by stresses caused by rapid thermal expansion and/or contraction of block margins) during ignimbrite emplacement was partly responsible for the rounded shapes of the blocks. Fine matrix penetrates pervasively into the joints and curvilinear cracks of some lithic blocks, and suggests that in some cases the spalling occurred when the block was already enclosed by fine ash. The intact preservation of some highly friable blocks and the angularity and thin shapes of the rock flakes indicate that breakage and abrasion by collisions during emplacement were limited.

Imbrication in mlBr is common (Fig. 5.3B), but is not obvious everywhere. All gradations exist from mlBr into massive lapilli-tuff (mLT), into massive block-rich or lithic-rich lapilli-tuff (lmLT), and into diffuse-stratified and cross-stratified lithic breccias (dslBr and xslBr), as occurs in the 'Lower Pumice 1' deposit on Santorini (Druitt *et al.* 1989). Lithic blocks also occur as massive or stratified dune-like lenses (Druitt & Bacon 1986; Bryan *et al.* 1998a; Calder *et al.* 2000), or as layers, irregular pods or trains within mLT (figs 12 and 13 of Moore & Kokelaar 1998; Allen & Cas 1998; Bryan *et al.* 1998a). Most lack abundant large pumices.

Interpretation

We interpret massive lithic breccias (mlBr) as a coarse facies of ignimbrite, deposited through the lower flow boundary of a pyroclastic density current in essentially the same way as are other ignimbrite lithofacies (e.g. mLT), albeit more energetically. Blocks in mlBr can be derived from one or more of: (1) erosion or collapse of the eruption conduit and/or vent walls; (2) avalanches into the pyroclastic current; and (3) erosion of substrate by the density current. Hybrid derivations are likely in calderas where a fissure vent occurs at a developing fault scarp (e.g. at Scafell and Glencoe calderas; see Branney & Kokelaar 1994b; Moore & Kokelaar 1998). The hydrothermal alteration shown by many accessory lithic blocks is consistent with derivation from metasomatized zones around the eruption conduit and/or magma chamber, particularly where the chamber roof fails mechanically and disintegrates during caldera collapse. All gradations exist between end-member rock-fall avalanche mesobreccias, interbedded with and sometimes loaded into ignimbrites, and true pyroclastic breccias formed of clasts that were transported and deposited by pyroclastic density currents (Branney & Kokelaar 1994b; Moore & Kokelaar 1998).

Variations in the character of the breccias, such as clast versus matrix support and the degree of development of fabrics and stratification, are largely a product of flow-boundary zone conditions, dominated variously by direct fallout, traction, granular flow or fluid escape (see pp. 37–41). For example, lithic breccias exhibiting cross-stratification (xslBr) are deposited from a traction-dominated flow-boundary zone, whereas parallel-bedded lithic breccia (//blBr) lacking fabrics and with lithic impact structures may involve a larger component of direct fallout. Most mlBr, however, have thickness variations that correspond to underlying topography, and are inferred to derive from granular flow- and/or fluid escape-dominated flow boundaries of pyroclastic density currents. They are essentially a coarser equivalent of mLT, into which they commonly grade (e.g. Druitt & Sparks 1982; Branney & Kokelaar 1997; Moore & Kokelaar 1998). As with mLT, the strength of fabrics may reflect the effect of flow-boundary

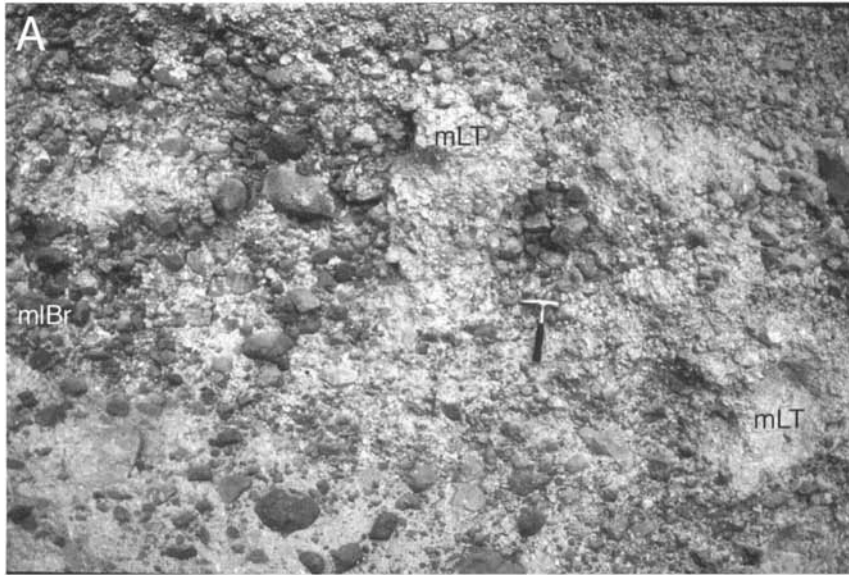
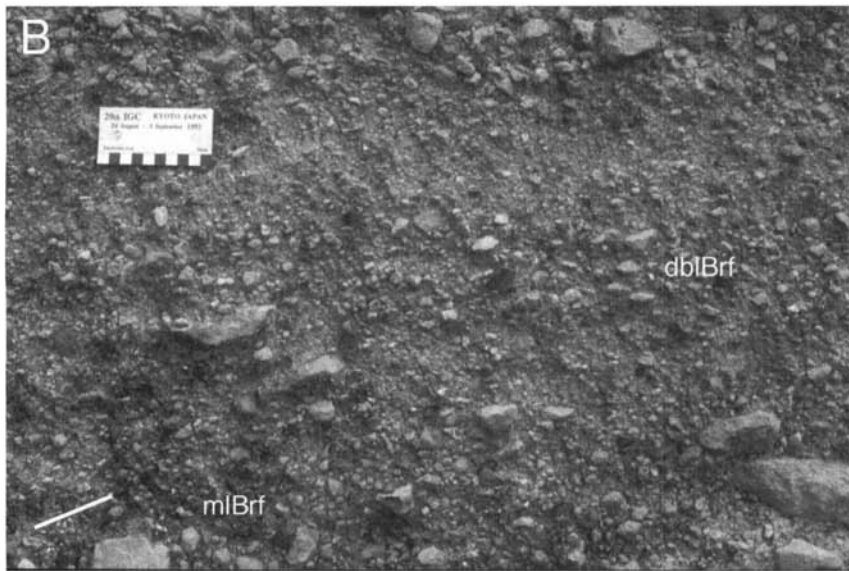
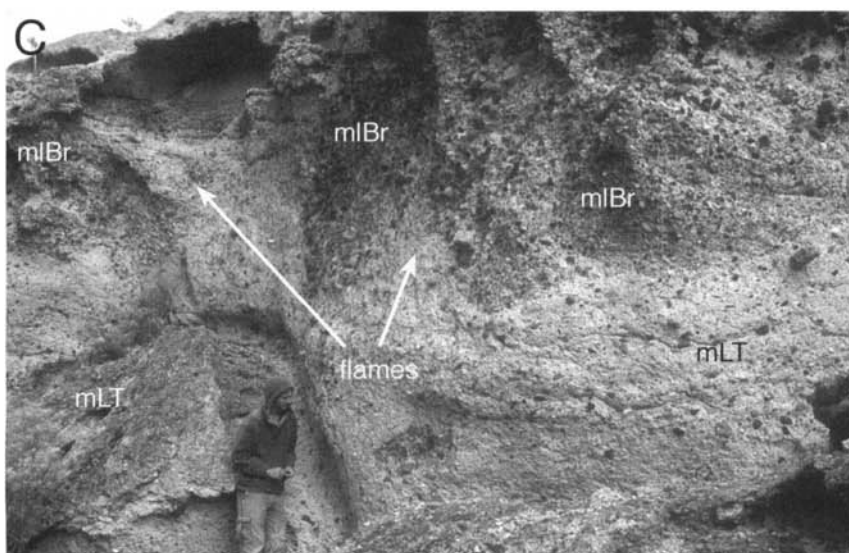


Fig. 5.3. Massive lithic breccia lithofacies (mlBr).



(B) Lithic breccia with diffuse thin bedding (db) and grain fabrics (f). Breccia is framework supported and varies from massive (mlBrf) to diffuse bedded (dblBrf) with normal and reverse size grading. Blocks show subtle imbrication (many dip left relative to bedding), indicating apparent flow direction from left to right. Proximal Aso 4 ignimbrite, NW rim of Aso caldera, Kyushu. Scale is 10 cm.



(C) Load structures of massive lithic breccia (mlBr), with flames of underlying massive lapilli-tuff (mLT). Poris Formation ignimbrite, southern Tenerife.

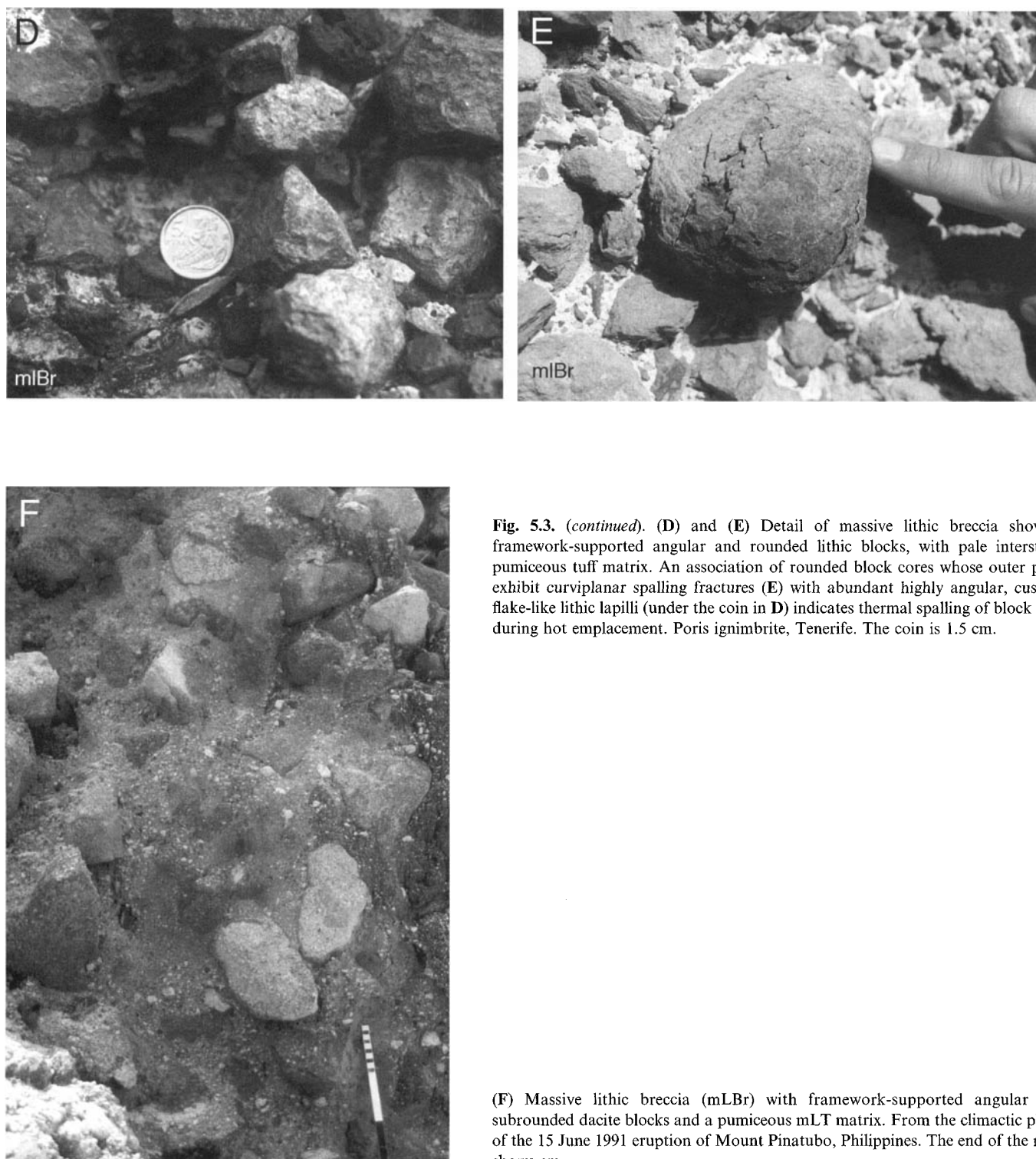


Fig. 5.3. (continued). (D) and (E) Detail of massive lithic breccia showing framework-supported angular and rounded lithic blocks, with pale interstitial pumiceous tuff matrix. An association of rounded block cores whose outer parts exhibit curvilinear spalling fractures (E) with abundant highly angular, cusped flake-like lithic lapilli (under the coin in D) indicates thermal spalling of block rims during hot emplacement. Poris ignimbrite, Tenerife. The coin is 1.5 cm.

(F) Massive lithic breccia (mLBr) with framework-supported angular and subrounded dacite blocks and a pumiceous mLT matrix. From the climactic phase of the 15 June 1991 eruption of Mount Pinatubo, Philippines. The end of the ruler shows cm.

shear during deposition (see p. 56). Downcurrent transitions from proximal mLBr into pumiceous mLT (i.e. downcurrent grading, such as is commonly used to infer ignimbrite vent positions) record depletive currents that only in proximal regions were sufficiently competent to transport the lithic blocks (Fig. 4.4). More distal and localized occurrences of mLBr in lower parts of ignimbrite sheets commonly comprise substrate-derived blocks; these indicate erosion and redeposition of local substrate by the pyroclastic density current (Buesch 1992) prior to its complete burial by aggrading ignimbrite. Localized occurrences of breccias record localized current non-uniformity, such as depletive competence due to a break of slope (e.g. Macías *et al.* 1998).

The pipe-like and irregular-shaped segregation structures that

occur in proximal mLBr (e.g. proximal Acatlán ignimbrite; Branney & Kokelaar 1997) (Fig. 5.3A) are most simply reconciled with heterogeneous or localized vigorous elutriation and/or loading during rapid deposition. The elutriation may be enhanced by thermal expansion of trapped air or hydrothermal fluids.

Although some mLBr have low contents of ash and pumice, four lines of evidence suggest that the blocks in mLBr were transported by currents containing considerable proportions of finer grained constituents, and that during transport and deposition block interactions were cushioned by the former presence of a high-concentration pumice and ash-rich interstitial fluid. (1) Downcurrent transitions from proximal mLBr to medial and distal pumiceous mLT (e.g. Walker 1985) are common and, on a smaller

scale, mlBr is commonly intimately related with typical ash-rich mLT with both gradational and complex (e.g. podiform) contacts (Fig 5.3A and C) (Druitt & Sparks 1982). (2) Lenses of mlBr locally occur within ignimbrites where local topographic effects caused deposition of blocks (e.g. Freundt & Schmincke 1985; Buesch 1992; Bryan *et al.* 1998a). (3) The widespread distributions, massive nature, lack of typical granular-segregation structures and evidence for minimal abrasion (the intact preservation of delicate clasts and evidence that much of the rounding of blocks was by thermal spalling) are difficult to reconcile with transport simply by very coarse grainflow (see p. 29). (4) Ash-rich matrix is locally preserved on tops of large slab-like blocks, in contrast to open-framework, matrix-poor breccia that otherwise surrounds and underlies the same large blocks (as in Fig. 5.4B). These 'life-raft structures' (new term) are inferred to represent remnant pockets of ash that remained protected from vigorous upwards-elutriation in shadow zones above the large blocks as they were rapidly deposited at a fluid escape-dominated flow-boundary zone. The low content of fines elsewhere is attributed to elutriation. Closely similar life-raft structures also occur in proximal open-work breccias deposited rapidly from marine fines-rich blocky sediment gravity flows (e.g. Scheck breccia; Zalasiewicz *et al.* 1997), and a similar origin is inferred.

Abundant ash and pumice in the current would aid support and transport of lithic blocks: (1) by providing some buoyant support through increasing the effective density of the fluid; (2) by increasing the effective viscosity of the fluid (dusty gas), and hence hindering the settling of blocks at a fluid escape-dominated flow boundary; and (3) by increasing the overall mass of the density current, and thus its gravitational impetus, velocity and competence. However the current would not need to support all the blocks fully; many would receive at least intermittent support from the substrate surface (see p. 25).

Segregation of blocks from pumice and ash

Changing proportions of lithic blocks within an ignimbrite may record changes in the proportion of lithics in the erupting pyroclastic dispersion. However, we infer that the low contents of ash and pumice in some mlBr records efficient segregation of the blocks from the rest during transport and deposition. The mechanism by which this occurs can be conceptualized in four ways, although in reality these overlap. (1) Depletive current competence (e.g. due to depletive velocity) can cause downcurrent segregation in that it limits the distance to which the current is able to transport large blocks; lapilli and ash may be carried further (overpassing p. 42). (2) Selective filtering, in which rapid deposition of lithic blocks at a fluid escape-dominated flow-boundary zone causes updraughts of dusty gas (pp. 33 and 34) powerful enough to elutriate not only fine ash but also pumice and small lithic clasts. These smaller constituents are flushed up from the flow-boundary zone, back into overriding parts of the current. (3) The very broad grain-size population distribution in the proximal current may give rise to marked current stratification (p. 14), in which whole-current turbulent mixing is suppressed by steep density gradients. Proximal deposition occurs from the lower levels of the current, which contain most of the lithic blocks (as traction and saltation populations; pp. 24 and 25) together with fine ash and pumice (wash load). Proximal areas are bypassed by higher levels in the current, which comprise mostly ash and pumice with few larger clasts. Similar bypassing due to development of marked density stratification was inferred for the pyroclastic density current that originated explosively at Montserrat on 26 December 1997 (Ritchie *et al.* 2002; Woods *et al.* 2002). (4) The large size of lithic blocks helps them decouple from a proximal vigorously turbulent current. The decoupled blocks either enter a lower layer of dense granular fluid in which turbulence is suppressed and whose rheology differs significantly from overriding turbulent levels of the current, or they

may just deposit proximally at direct fallout-dominated or traction-dominated flow-boundary zones. In some cases, localized segregation and accumulation of lithic blocks may be enhanced by a hydraulic jump (Freundt & Schmincke 1985; Macías *et al.* 1998).

Interpretation of stratified breccias and breccia lenses

Lithic blocks in ignimbrites can form dunes, bars, levees and lee-side lenses, with variously developed imbrication and stratification (e.g. xslBr and dslBr; Fig. 5.3B) analogous to gravel bars in rivers and hyperconcentrated floods. Stratified breccias with *b*-axis imbrication deposit at traction-dominated flow-boundary zones, with rolling and saltating blocks. Where lithic lenses lack internal stratification (mlBrLens) they may record bar formation from flow-boundary zones in which turbulence and traction were largely suppressed. Large lithic lapilli may roll along over, rather than percolate down through, some granular flow-dominated flow-boundary zones so that they overpass rather like large pumices (see pp. 76 and 77) to accumulate on distal block-rich dams or marginal levees where flow-boundary conditions are markedly non-uniform (see p. 93). Origins of layering of lithic blocks are considered on pages 66 to 71.

Classifications of ignimbrite breccias

Walker (1985) classified ignimbrite lithic breccias into five types, as follows: (1) debris inferred to have 'settled through' a pyroclastic flow; (2) debris that comprises blocks picked up from the ground by the pyroclastic flow; (3) 'ground breccias' inferred to be segregated from the fluidized head of a pyroclastic flow; (4) 'lag-breccias' inferred to be deposited from a 'proximal deflation zone' that also generated a pyroclastic flow; and (5) breccias derived from rock falls or avalanches. Although some of these processes and derivations are likely, the categories in this classification are not mutually exclusive, and they mix derivation, transport mechanism and depositional process. Moreover, it is a genetic classification, the applicability of which is dependent upon the validity of the embodied emplacement models.

We propose that ignimbrite breccias are best classified non-genetically in the first instance (e.g. mlBr, mlBrf, xslBr, dblBr, mlBrLens). We infer that the lithofacies characteristics of these breccias mainly reflect *depositional* mechanisms (e.g. fallout, traction, granular flow, hindered settling with fluid escape) rather than derivation and/or mode of transport. Thus, we treat all the breccias as a coarse ignimbrite lithofacies. The location of a breccia within an ignimbrite sheet (e.g. proximal, below, above or within mLT) and the sharp or gradational nature of contacts then are interpreted to reflect the spatial and temporal variations of the current(s) (see pp. 95–98). All blocks in ignimbrite breccias settled through some part of a pyroclastic density current (cf. Walker's first type, above), whether they were initially ejected from the vent, picked up during transport or supplied to the current by rock avalanches. Also, because segregation and overpassing of other material are involved in the deposition of all lithic breccias in ignimbrites (i.e. not just proximal ones), they all constitute 'lag' deposits (as indeed do most lithofacies), so the term 'proximal lithic breccia' is more appropriate than 'lag breccia' (*sensu* Walker 1985).

Evidence that proximal lithic breccias aggrade from a density current flowing across the ground, rather than from rapid fallout in a discrete 'proximal deflation zone' that lies ventward of the forming current (see p. 10 and Fig. 2.2A), is provided by clast alignment and imbrication, by topographic control of deposition, by the absence of impact structures and by the persistence of the breccias to as far as 14 km from source (Druitt 1985; Druitt & Bacon 1986). Deposition from high-concentration flow-boundary zones of pumiceous density currents is indicated by rapid gradations into normal pumiceous ignimbrite (mLT).

Massive agglomerate lithofacies (e.g. mAg; dbAg)

Description

Some ignimbrite sheets include coarse agglomerates (mAg) composed of large cognate scoria or spatter clasts, commonly of basic or intermediate composition, with or without mLT matrix (Fig. 5.4). Such lithofacies occur at Acatlán (Wright & Walker 1981; Branney & Kokelaar 1997), Taal caldera, Santorini caldera (Druitt *et al.* 1989; Mellors & Sparks 1991), Vulcini (Marsella *et al.* 1987; Branney & Kokelaar 1992), Campi Flegrei (Rosi *et al.* 1996), Scafell caldera (Branney & Kokelaar 1994b) and Vanuatu (Robin *et al.* 1994). Sorting ranges are similar to those of mlBr (e.g. σ_ϕ 1–3.3; Mellors & Sparks 1991) and the deposits range from matrix-supported to framework-supported, either openwork or with some interstitial pumiceous matrix. As in mlBr, the grain-size distributions of the matrix are similar to those of mLT. Ignimbrite agglomerates commonly grade laterally and/or vertically into lithic breccias (mlBr). The cognate clasts range from dense spatter to moderately vesicular scoria. Their shapes are subspherical, ellipsoidal, spindle, discoidal and fusiform to highly irregular (amoeboid; Fig. 5.4D and E), and commonly indicate formation whilst hot and fluidal. Many have thin chilled rinds surrounding more vesicular interiors. Some have cauliform shapes; others are slightly bread-crustured with chilled rinds patterned with close-spaced cooling-contraction cracks (Fig. 5.4F). Some clasts show ductile folding and some are draped or wrapped around other clasts (Fig. 5.4E), although many such clasts have one or more angular, faceted surface caused by brittle breakage. Scattered lithic blocks in mAg commonly have sizes similar to, or somewhat smaller than, the cognate clasts. A common distinctive feature is the presence of small, angular accidental lapilli contained within individual cognate scoria clasts and/or adhering to their edges. Agglomerates range from non-welded, which indicates significant cooling between initial fragmentation and deposition, through slightly welded spatter, to intensely welded eutaxitic agglomerate (Fig. 5.4D) and thick vitrophyres.

Massive agglomerate lithofacies locally grade into, or occur as layers, lenses or irregular pods within, massive lithic breccias (mlBr). As with mlBr, mAg commonly show vertical, lateral and downcurrent transitions into pumiceous ignimbrite (mLT). They tend to be most thickly developed proximally, such as near caldera rims, and show marked topographically controlled thickness variations. Also like mlBr, the agglomerates commonly are massive with poorly to well-developed imbrication (Figs 5.4A and C), and can show crudely developed gas-escape structures, grading and/or diffuse bedding (dbAg). Lapilli-tuff matrix in mAg varies from sparse to abundant, and from non-welded to welded, and all gradations occur into pumiceous mLT that contains just a few isolated scoria or spatter clasts.

Interpretation

Massive agglomerate lithofacies can superficially resemble thick proximal spatter fallout deposits. However, massive agglomerates deposited from pyroclastic density currents can be distinguished from fallout agglomerates (such as coarse Strombolian spatter) on the basis of a combination of characteristics, including: (1) clast imbrication; (2) field relations that show marked topographic control of thickness and geographic distribution; (3) the presence of locally variable amounts of pumiceous matrix; and (4) local intergradations with mLT and mlBr (Druitt *et al.* 1989; Mellors & Sparks 1991). In addition, the preservation of delicate clast edges, life-raft structures, patchy development of fines-rich lapilli-tuff matrix, crude segregation pipes, pumice lapilli and the downcurrent transitions into pumiceous ignimbrite (mLT) together indicate that mAg (as with mlBr) is deposited proximally from flow boundaries of currents that were rich in ash and pumice.

Sedimentologically, the denser cognate clasts behave in a similar way to the lithic blocks of proximal lithic breccias, and a similar emplacement mechanism is invoked, involving particle segregation during rapid deposition of cognate clasts, vigorous fluid escape, elutriation and overpassing of pumice and fines. The dense cognate clasts have similar hydrodynamic properties to lithic blocks, so that changes in the relative proportion of scoria clasts to lithic blocks with height in a deposit probably reflect differences in supply at source (e.g. see Rosi *et al.* 1996). Pumice lapilli in mAg may be of the same composition as the scoria or spatter clasts, but more finely vesicular, or they may be of a different composition indicating a heterogeneous magma supply (e.g. Druitt *et al.* 1989; Mellors & Sparks 1991; Branney & Kokelaar 1997). Field relations, such as common proximity to flooded calderas, and features of the cognate clasts that resemble those of cauliflower bombs at maar volcanoes (Fisher & Schmincke 1984) suggest that scoria agglomerates may be linked to eruptions that are phreatomagmatically enhanced. As with mlBr, some eruptions of mAg may occur when parts of a high-level hydrothermal system collapse into a depressurized magma chamber (Druitt *et al.* 1989), causing explosive expansion of hydrothermal fluids.

Lithofacies with fines-poor (elutriation) pipes, sheets or pods (e.g. mLTPip; mlBrpip)

Description

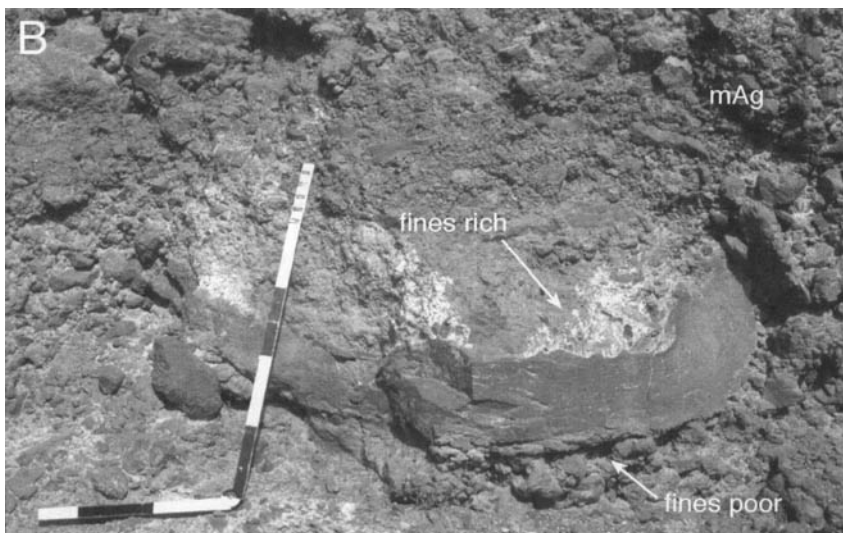
Vertical pipes (Fig. 5.5), sheets and pods composed of clast-supported crystal and lithic-rich, fines-poor coarse ash to lapilli (coarse-sand grade to gravel grade) are a common, although not ubiquitous, feature of massive ignimbrites (e.g. Yokoyama 1974; Wilson 1985; Sigurdsson & Carey 1989; Francis 1993). They are richer in crystals, lithic fragments and pumice lapilli than the enclosing massive lapilli-tuff, and they are better sorted (σ_ϕ 1–2.6; Walker 1971), poorer in fine ash and more porous (Walker 1972; Wilson 1985). Coarser grained pipes and pods occur in lithic breccias (mlBrpip; e.g. Duyverman & Roobol 1981; Wright 1981; Druitt 1985; Cas & Wright 1987) (Figs 5.3A and 5.5E). Fines-poor pipes vary from centimetres to several metres long, from millimetres to decimetres wide and from subtle to well-developed. They can be straight, sinuous, curvilinear or branching, with subcircular to irregular cross-sections. Shapes also range to sub-vertical planar sheets and irregular pods. Some show deformation by late-stage shear or burial compaction. They may be regularly spaced, mainly at particular levels within massive divisions, or they may be localized, in some cases rising from charcoal or wood-moulds (e.g. Carrasco-Núñez & Rose 1995) or from lithic blocks (Fig. 5.5B). They occur in welded lithofacies (see p. 83), for example in the Upper Bandelier Tuff (Self & Sykes 1996), but examples of this are few.

Elutriation pipes have been reported to occur above formerly wet substrate (Bond & Sparks 1976; Sparks *et al.* 1985; Cas & Wright 1987), but the substrate at the most commonly cited example (Bond & Sparks 1976), originally thought to have been a wet flash-flood conglomerate, has been reinterpreted as ignimbrite lithic breccia (Druitt *et al.* 1989). Elsewhere, ignimbrites emplaced onto wet substrates have produced flame or dyke-like intrusions of disaggregated fluidized substrate material (Fig. 6.13F and G) (Kokelaar 1982; Kokelaar *et al.* 1985; Nelson *et al.* 1989; Bailey & Carr 1994) rather than elutriation pipes. Coastal exposures of fines-poor ignimbrite (fpoormLT) have been inferred to record wholesale elutriation of ash finer than 200 μm by steam generated where pyroclastic density currents from Tabora volcano entered the sea (Sigurdsson & Carey 1989), although the pyroclastic density currents may still have been subaerial at the site of these coastal exposures (see discussion in Kokelaar & Königer 2000).

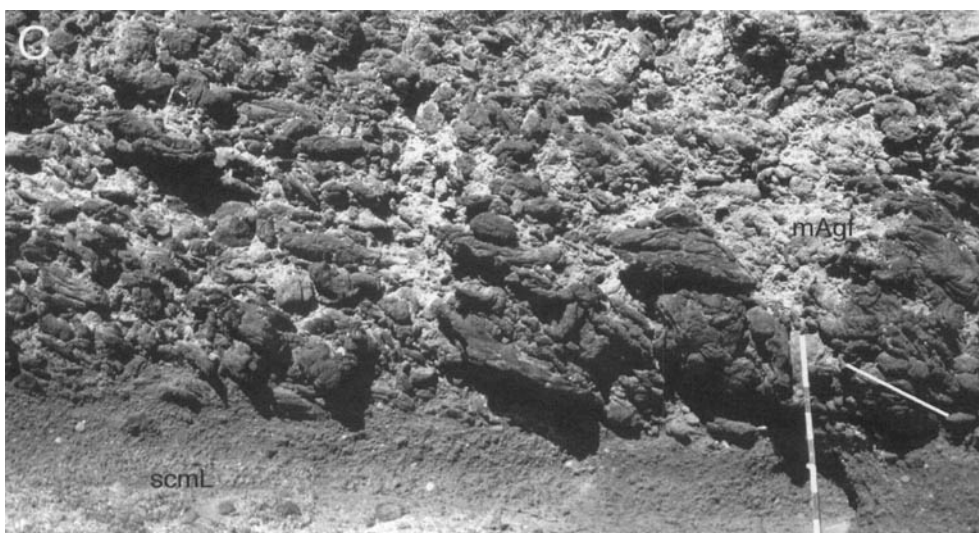
Some large elutriation pipes contain abundant sublimates and/or show effects of hydrothermal alteration and oxidation, indicating



Fig. 5.4. Massive agglomerates (mAg) in proximal parts of ignimbrites.



(B) 'Life-raft structure' in massive agglomerate, inferred to form by the elutriation of fines in a fluid escape-dominated flow-boundary zone during rapid deposition, with local preservation of fine ash in shadow zones above large spatter clasts (same unit as in A). The end of the ruler shows centimetres.



(C) Massive agglomerate with well-developed imbrication of spatter (mAgf). The inferred apparent current direction is right to left. The base of the photograph shows a fall deposit (scoria-rich massive lapilli lithofacies, scmL). Upper Scoria 1 Member near Akrotiri, Santorini (Druitt *et al.* 1989). The metre rule is for scale.



Fig. 5.4. *continued*).

(D) Massive agglomerate with a eutaxitic, welded lapilli-tuff matrix (emAg). Note fluidal amoeboid scoria clasts (bottom and right). Proximal Acatlán ignimbrite, central Mexico.



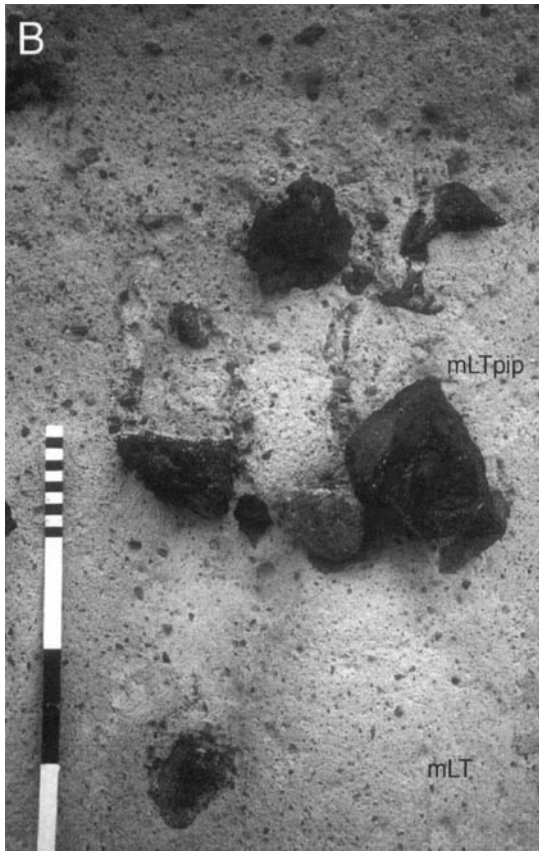
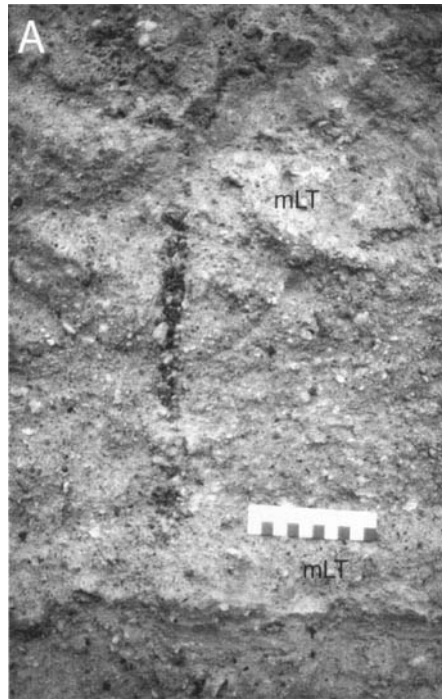
(E) Folded, swan's neck-shaped spatter rag in proximal massive agglomerate (mAg) indicates that clasts were hot and fluidal during emplacement. The deposit comprises non-welded, framework-supported spatter, scoria and subordinate lithic blocks and lapilli. Pavey Arc Breccia, Scafell caldera, England. The scale interval is 5 cm.



(F) Scoria clasts from a massive agglomerate showing fluidal shapes and prismatic jointed, quenched rims. The deposit has a pumiceous lapilli-tuff matrix (not shown). Caldera rim, Taal caldera, Luzon, Philippines. The lens cap is 6 cm in diameter.

Fig. 5.5. Fines-poor pipes formed by elutriation. The high concentration of lithic lapilli within the pipes, relative to enclosing mLT (e.g. in A) suggests that elutriation was accompanied by inward migration of 'quick' mLT. The vertical attitude indicates formation in the deposit rather than in the current.

(A) Small vertical elutriation pipe within massive lapilli-tuff. Acatlán ignimbrite, Jalisco, Mexico. Scale is 10 cm.



(B) Elutriation pipes rising from edges of isolated and clustered lithic blocks within massive lapilli-tuff (mLT). Upward gas flow was channelled by the blocks, and may have been enhanced by localized compaction beneath the blocks as they sank through gas-rich mLT, and/or enhanced by thermal expansion due to heating by the blocks. La Caleta ignimbrite, SE Tenerife. The end of the ruler shows centimetres.



(C) Clustered elutriation pipes within massive lapilli-tuff (mLT), Matahina ignimbrite, Bay of Plenty coast, New Zealand. The pipes contain framework-supported lithic lapilli and little ash. The end of the ruler shows centimetres.

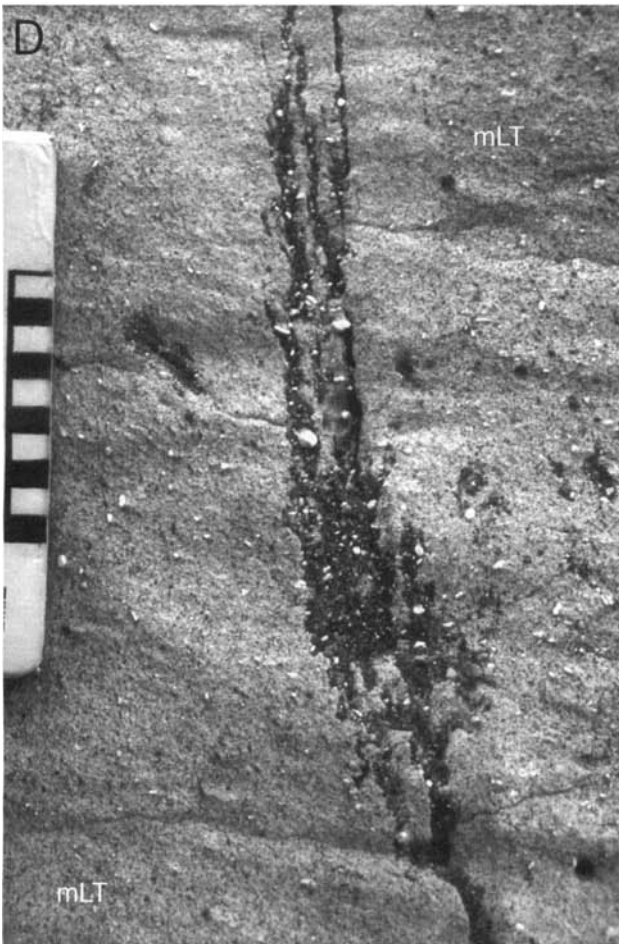
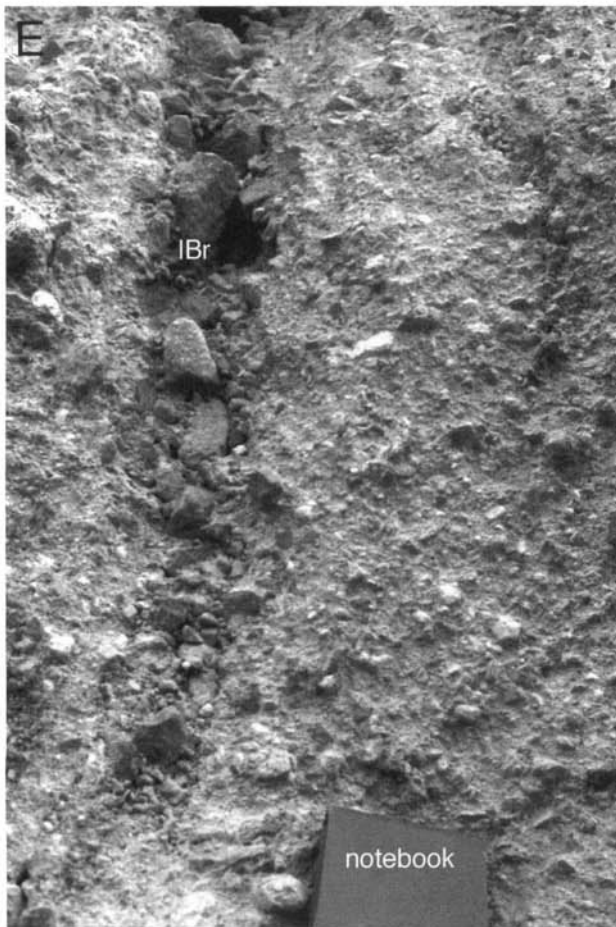


Fig. 5.5. (continued).

(D) Ramifying subvertical elutriation pipes containing framework-supported, coarse sand-grade obsidian ash (black). Similar obsidian clasts occur supported within the fine ash matrix of the enclosing massive lapilli-tuff (mLT). The pipes are highly irregular in plan-section. Ignimbrite of the Wolverine Creek Tuff, Ririe Reservoir, eastern Idaho. Scale in centimetres.



(E) Coarse-grained elutriation pipe of framework-supported lithic blocks and lapilli (lBr), enclosed within fine-grained massive lithic breccia that locally contains pumice lapilli and fine ash matrix. Cape Riva, Santorini.

that they were used as fumarolic pathways during cooling of the ignimbrite sheet. Not all fumarolic pipes, however, are sited on elutriation pipes that formed during deposition (e.g. Mahood 1980; Bacon 1983; Self & Sykes 1996).

Interpretation

The paucity of fine ash in the pipes, sheets and pods relative to the enclosing mLT suggests removal of the fines, presumably as a result of elutriation by gas escaping through the uncompacted or compacting deposit. Elutriation pipes in ignimbrites were originally interpreted to have formed in the moving flow by fluidization (Wilson 1980; Cas & Wright 1987; Francis 1993). Fluid-escape may cause segregation within a current (see pp. 33 and 34), but, despite observations that elutriation pipes resist mixing in stationary fluidization experiments (Wilson 1980), vertical pipes and sheets starting to form within either laminar or turbulent pyroclastic density currents will shear-out (become transposed), probably even as they form. Thus, pipes are not likely to be preserved during transport and then deposited intact as subvertical structures. The widespread occurrence of non-deformed vertical elutriation pipes and sheets in some massive ignimbrites is indicative of formation *in situ* within rapidly aggrading mLT deposits as a result of fluid escape (see pp. 33, 34 and 39). Formation within the deposit rather than in the current is confirmed by occurrences of elutriation pipes that cut bedding (e.g. Fisher 1979; Bailey & Carr 1994; Colella & Hiscott 1997).

Gas and fine ash are expelled upwards through a fluid escape-dominated flow-boundary zone primarily as a result of (hindered) settling, deposition and compaction. Under some conditions this type of rapid deposition causes aggregative-type segregation, or channelling, within an aggrading deposit (see pp. 31–33), and just below the flow boundary (e.g. Druitt 1995). The gas-volume flux upwards through the forming deposit may be enhanced by thermal expansion and, more locally, by wood combustion or by the production and expansion of steam from liquid water by heating. In some well-developed pipes a considerably greater abundance of lithics and crystals relative to the abundance in an equivalent volume of the surrounding mLT suggests that pipe formation involved localized lateral movement of loose deposit (mLT) inwards from enclosing, compacting and degassing 'quick' mLT. We envisage that as mLT encroaches the margin of the developing pipe its fines are elutriated upwards leaving the large or denser clasts trapped in the pipe, where they become concentrated. We anticipate that primary (depositional) directional fabrics are poorly preserved around well-developed elutriation pipes (mLT_{pip}; see p. 61), because of such advective movement within the degassing deposit.

Elutriation pipes are not restricted to deposits of hot pyroclastic density currents as was once thought (e.g. Walker 1971; Duyverman & Roobol 1981); they can form at low temperatures due to water escape in aqueous hindered settling experiments (e.g. Weiland *et al.* 1984; Batchelor & van Rensburg 1986; Druitt 1995) and in some massive turbidity current deposits and hyperconcentrated flood-flow deposits (e.g. Laird 1970; Lowe 1975; Best 1989).

Vertical grading patterns (e.g. mLT_(n); mLT_(i); mLT_(i-n); mLT_(ip,n))

Description

Massive lapilli-tuff can show normal (mLT_(n)), inverse (mLT_(i)) or more complex vertical grading patterns (e.g. mLT_(i-nl,ip)), defined by more or less gradual changes in grain size, grain density (e.g. pumice versus lithics) and/or sorting (Fig. 5.6) (see Sparks 1975, 1976; Wright 1981; Freundt & Schmincke 1986; Wilson 1986). Grading also occurs within other lithofacies (e.g. in sT, xsT, mBr). Vertical grading typically occurs across a few centimetres to several

metres. It can affect the entire grain-size population (distribution grading), but in mLT it is most common and obviously involves the larger pyroclasts (coarse-tail grading), with little or no grading of clasts smaller than 0.5–3 mm diameter (Sparks 1976; Freundt & Schmincke 1986). Coarse-tail grading (e.g. of pumice or lithic lapilli) may be in the form of size grading and/or abundance grading. The grading patterns of pumice clasts can variously be similar to, or the mirror image of, or independent of, the grading patterns of the lithic clasts (see Figs 5.6 and 5.8). Inverse-to-normal coarse-tail grading of pumice (mLT_(ip-np)) and normal to inverse-grading of pumice (mLT_(np-ip)) are common within some ignimbrites (e.g. Fierstein & Hildreth 1992) and can define diffuse decimetre-thick bedding (Fig. 5.6) or diffuse thin bedding (dBLT; see p. 71 and Fig. 5.8B and D).

Interpretation

Vertical grading records deposition changing with time. Table 5.2 summarizes various possible causes, which are not mutually exclusive. The changes in deposition may be widespread (e.g. generated by changes at source) or localized (e.g. due to migration of local thalwegs, bed forms, levees, dams and/or channels; see Chapter 2), and may arise due to: (1) temporal changes in the size of clasts incorporated upcurrent (e.g. Giannetti & De Casa 2000); (2) gradual changes in the competence of the current, which affect the maximum clast size that the current is able to transport (irrespective of what may be supplied at source); and/or (3) gradual changes in the selective filtering properties of a flow-boundary zone, in turn related to changing concentration (density) and shear gradients (see pp. 43–45). An example of the latter is where clasts of a size that at first could not pass down across a flow-boundary (e.g. due to buoyancy and/or granular segregation effects) and so overpassed, subsequently become able to sink and/or percolate down across the flow boundary and deposit (e.g. Figs 3.7 and 4.6) due to changing flow-boundary conditions. In addition, sinking of lithic clasts and floating of pumice clasts through 'quick' newly formed deposit just below the flow boundary may produce grading, or modify any just-formed grading patterns, within the compacting deposit (see Fig. 5.7). The wide variety of grading patterns evident in nature indicates that changes in current competence, supply and selective filtering in fluid escape-dominated flow boundaries are common, and reflect various, sometimes complicated, waxing–waning histories of sustained pyroclastic density currents.

Normal coarse-tail grading of lithic clasts in mLT is widespread and it is unlikely that all occurrences have the same origin (Table 5.2). It can result from waning flow competence (Fig. 1.1C), so that the maximum size of clasts that the current is able to transport to a particular location decreases with time. This may be accompanied by temporal decreases in maximum transport distances of each size of lithic clasts (Fig. 4.6). Some normal coarse-tail grading of lithic clasts may reflect decreasing erosional flux from the eruption conduit walls or proximal slopes, or progressive burial of substrate by ignimbrite, so that the potential lithic source area diminishes with time (Branney & Kokelaar 1997). Finally, of a mixed population of clasts deposited at the same instant, the larger and denser clasts may preferentially sink further down into the aggrading 'quick' deposit (in which yield strength may increase with depth as it degasses), causing normal coarse-tail grading to develop *within the deposit* (Fig. 5.7).

Inverse grading of lithic clasts is also common, and records a temporal increase in the size of clasts deposited. Again, it is unlikely that all examples have the same origin (Table 5.2); some may record deposition during waxing flow competence (area 1 of Fig. 1.1C), some may record increased availability and supply of large clasts, for example from vent-collapse events or proximal rock-fall avalanches, and some may derive from lateral migration of thalwegs or migration of lithic-rich bed forms. Inverse grading (mLT_(i)), particularly at the base of a flow-unit deposited from a

Table 5.2. Some possible interpretations of grading patterns in massive lapilli-tuff formed during sustained deposition. See text for fuller explanations.

Grading feature in mLT	Alternative interpretations
Normal grading of lithic clasts (nl)	<ol style="list-style-type: none"> 1. Waning current competence; maximum clast size the current can transport decreases with time overall or locally, e.g. due to lateral migration of thalweg 2. Decreasing availability of lithics due to: <ol style="list-style-type: none"> (a) progressive burial of landscape by aggrading ignimbrite; (b) a decrease in conduit and/or vent erosion; (c) a decrease in erosive capability of the current in proximal reaches; and/or <ol style="list-style-type: none"> (d) an initially sheet-like current increasingly becomes channelled, such that lithics are diverted into a thalweg away from the observed location, which increasingly becomes overbank 3. Segregation within a fluidal ('quick') forming deposit (large lithics sink further than smaller lithics) 4. Increasing rates of shear in the flow-boundary zone cause an increase in granular segregation, so that larger lithic lapilli are increasingly prevented from depositing (selective filtering). Probably associated with an upward increase in fabric strength
Inverse grading of lithic clasts (il)	<ol style="list-style-type: none"> 1. Waxing current competence; maximum clast size the current can transport increases with time overall or locally, e.g. due to lateral migration of thalweg or bed form 2. Lithics of increasing size become available, e.g. supplied to proximal current by rock-fall avalanches 3. Lithic clasts formerly selectively prevented from depositing due to granular segregation processes are increasingly able to deposit as a result of changing flow-boundary zone conditions, for example associated with decreasing rates of shear and/or increasing rates of deposition (see Fig. 3.7). Probably associated with an upward decrease in fabric strength
Inverse grading of pumice clasts (ip)	<ol style="list-style-type: none"> 1. Waxing current competence; maximum clast size the current can transport increases with time; may be accompanied by inverse grading of lithics 2. Increasing availability of pumice clasts 3. Selective filtering during waning flow overall (Fig. 4.6) or locally, e.g. due to lateral migration of the current's flow axis; may be accompanied by normal grading of lithics 4. Floatation of large pumice clasts in the 'quick' forming deposit
Various lithic and pumice grading patterns	<ol style="list-style-type: none"> 1. Deposition from laterally or downcurrent-migrating pumiceous and/or lithic-rich bed forms (e.g. bars, lobes, discontinuous traction carpets) 2. Changes in availability of pumice versus lithic clasts 3. Changes in the selective filtering properties of the flow-boundary zone (e.g. during unsteady flow)

polydisperse current, may also form as a result of slower transport, and hence later arrival, of larger clasts (e.g. which roll or saltate) relative to smaller ones (e.g. see Hand 1997).

Thin (millimetres–centimetres thick) $mLT_{(i)}$ divisions, in which inverse grading affects the coarse tail of both pumice and lithic clasts, may record segregation in a granular flow-dominated flow-boundary zone (see surface roughness effects on p. 28 and percolation on pp. 29–31). Larger clasts may initially be selectively prevented from depositing as a result of being unable to penetrate down through a rapidly shearing mass of grains, and thus may overpass while only smaller clasts are deposited. The amount of granular segregation that a depositing batch of clasts is subjected to depends upon the net granular shear (i.e. finite shear strain) it undergoes. This is a function of the shear rate within the flow-boundary zone and the length of time that the batch is subjected to this shear rate. The latter depends on the speed at which the flow-boundary zone rises through the system: that is, how fast the deposit aggrades. It follows that temporal changes in the rates of flow-boundary shear (i.e. due to changes in current velocity), and/or in rates of deposition, will cause a corresponding temporal change in selective filtering and hence a change in the amount of segregation undergone by successively depositing batches of clasts (see Fig. 3.7). This is an important cause of grading. For example, a decrease in flow-boundary shear rate and/or an increase in the rate of deposition will decrease the net granular segregation in the flow-boundary zone that affects successively depositing clasts. Thus, successively larger clasts can penetrate down to the flow boundary, so that the deposit forms with inverse grading. Conversely, an increase in flow-boundary shear rate and/or decrease in the rate of deposition can produce normal grading, by changing the selective filtering properties of the flow-boundary zone in the opposite sense.

The grading patterns exhibited by pumice clasts commonly differ from those shown by lithic clasts within the same part of an ignimbrite (Fig. 5.6). This is mainly because the lower density of

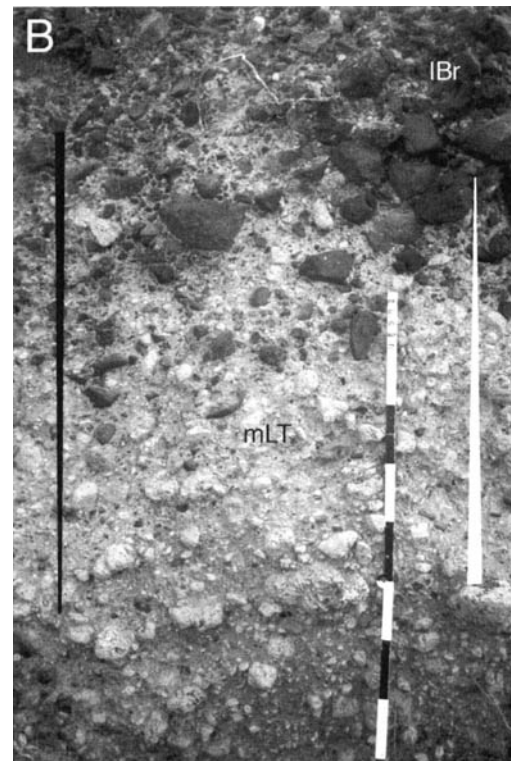
pumice causes its depositional behaviour at a fluid escape-dominated flow-boundary zone to differ significantly from that of the denser lithics (Fig. 4.3). For example, selective filtering due to a combination of granular segregation and relative clast-buoyancy effects may permit deposition of large lithic clasts while preventing deposition of large pumice clasts (p. 41; location x on Fig 4.6 at time t_1). With waning flow, however, the rate of granular shear and/or the clast concentration in the lowermost part of the current may decrease, so that the selective filtering gradually becomes less effective and successively larger pumice clasts are able to deposit with time (see pp. 43–45; Figs 3.7 and 4.6). In this way, the waning flow is recorded by an increase in size and/or abundance of large pumice clasts with height within a layer of massive lapilli-tuff ($mLT_{(ip)}$; point x on Fig. 4.6 at time t_2). This is a common feature in ignimbrites (e.g. Fig. 5.6A and E). The waning flow is likely to be associated with waning current competence that is recorded by normal grading of the larger lithic clasts. Thus the ignimbrite develops both normal coarse-tail grading of lithic clasts and inverse grading of pumice ($mLT_{(nl, ip)}$; e.g. Fig. 5.6A and E; note that this is 'Layer 2b' of Sparks *et al.* 1973). Conversely, deposition during waxing flow can result in normal coarse-tail grading of pumice clasts accompanied by inverse grading of lithics ($mLT_{(np, il)}$; e.g. Fig. 5.6B). A sustained current that undergoes successive waxing and waning phases (e.g. fluctuating flow conditions) may produce massive lapilli-tuff that exhibits a varied succession of normal and/or inverse coarse-tail-graded divisions, and in which the grading patterns of the lithic coarse tail are almost the converse of those exhibited by the pumice coarse tail (e.g. Figs 5.6C–E and 5.8A–C).

Inverse grading of pumice together with normal grading of lithics ($mLT_{(nl, ip)}$) commonly characterizes a greater proportion of the thickness of an ignimbrite sheet than does the reverse type of grading. This suggests that in pyroclastic density currents more deposition occurs during waning flow than during waxing flow.

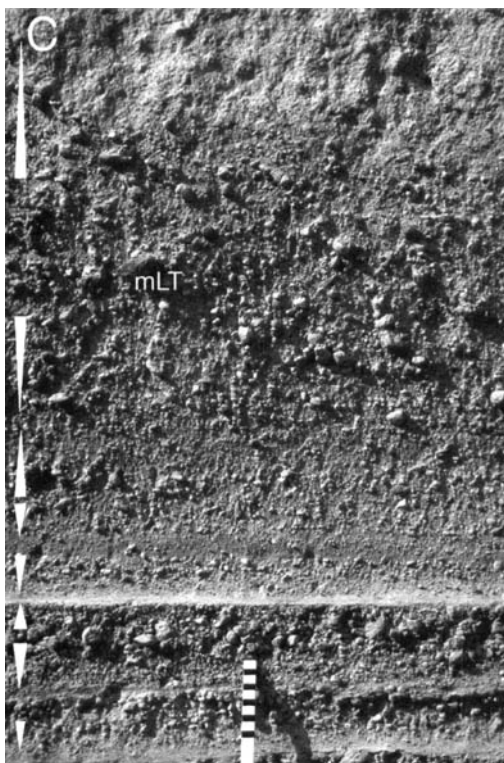


Fig. 5.6. Diverse grading patterns in lapilli-tuff. Black and white wedges indicate coarse-tail grading directions of lithic and pumice lapilli, respectively (wedges are absent in non-graded sections).

(A) Normal coarse-tail graded lithics with inverse graded pumices (compare with the left side of E) in massive lapilli-tuff (mLT) forming a possible flow-unit. Interpreted as mostly recording deposition during waning flow. Mayor Island, New Zealand.



(B) Inverse grading of lithic lapilli and normal grading of pumice lapilli in massive lapilli-tuff (mLT), interpreted as recording deposition during waxing flow. Phira Quarry, Santorini. The metre ruler is for scale.

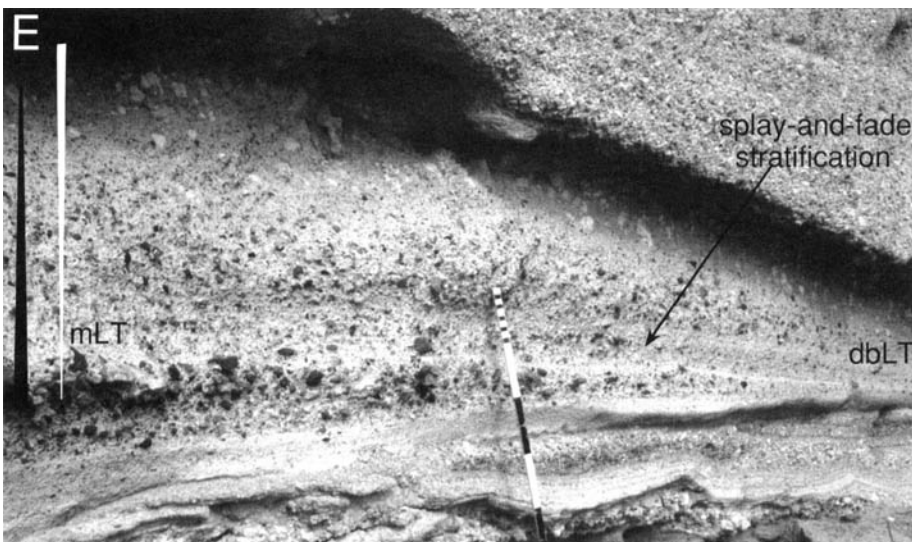


(C) Complex grading patterns, Rio Caliente ignimbrite, Mexico. Note grainsize changes range variously from subtle to marked, and from sharp to gradational, with abundant reversals in grading trend. Deposition from a highly unsteady current. The ruler shows centimetres.

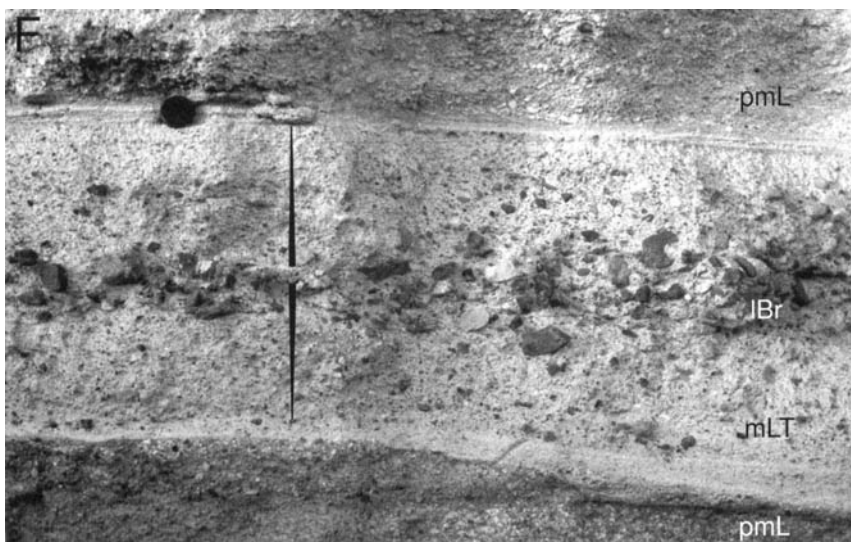


Fig. 5.6. (continued).

(D) Symmetrical (normal and inverse) vertical grading patterns picked out by pumice lapilli (some altered to cavities). Alternation between coarse and finer grained massive lapilli-tuff beds via normal and inverse grading. The sequence looks identical when inverted and lacks obvious flow-unit boundaries. Granadilla ignimbrite, Tenerife (Bryan *et al.* 1998b). The metre rule is for scale.



(E) Massive (mLT) division on the left exhibits normal grading of lithics and inverse grading of pumice with a thin inverse-graded base (mLT_{(i)-(nl, ip)}). This grading pattern is commonly regarded as 'standard ignimbrite' (see A). It shows a gradual lateral transition to diffuse bedded lapilli-tuff (dbLT) on the right. The diffuse bedding must have aggraded progressively, and the lateral transition suggests that the entire massive division also aggraded progressively. Elsewhere, the entire unit shows low-angle cross-stratification (not shown). Ignimbrite of the Fasnía Formation, Tenerife (Brown *et al.* 2003). The ruler shows centimetres.



(F) Single ignimbrite flow-unit with symmetrical inverse to normal coarse-tail grading (mirror grading) of lithic clasts: looks identical when inverted. Ignimbrite of the Fasnía Formation, southeastern Tenerife. The lens cap is 6 cm.

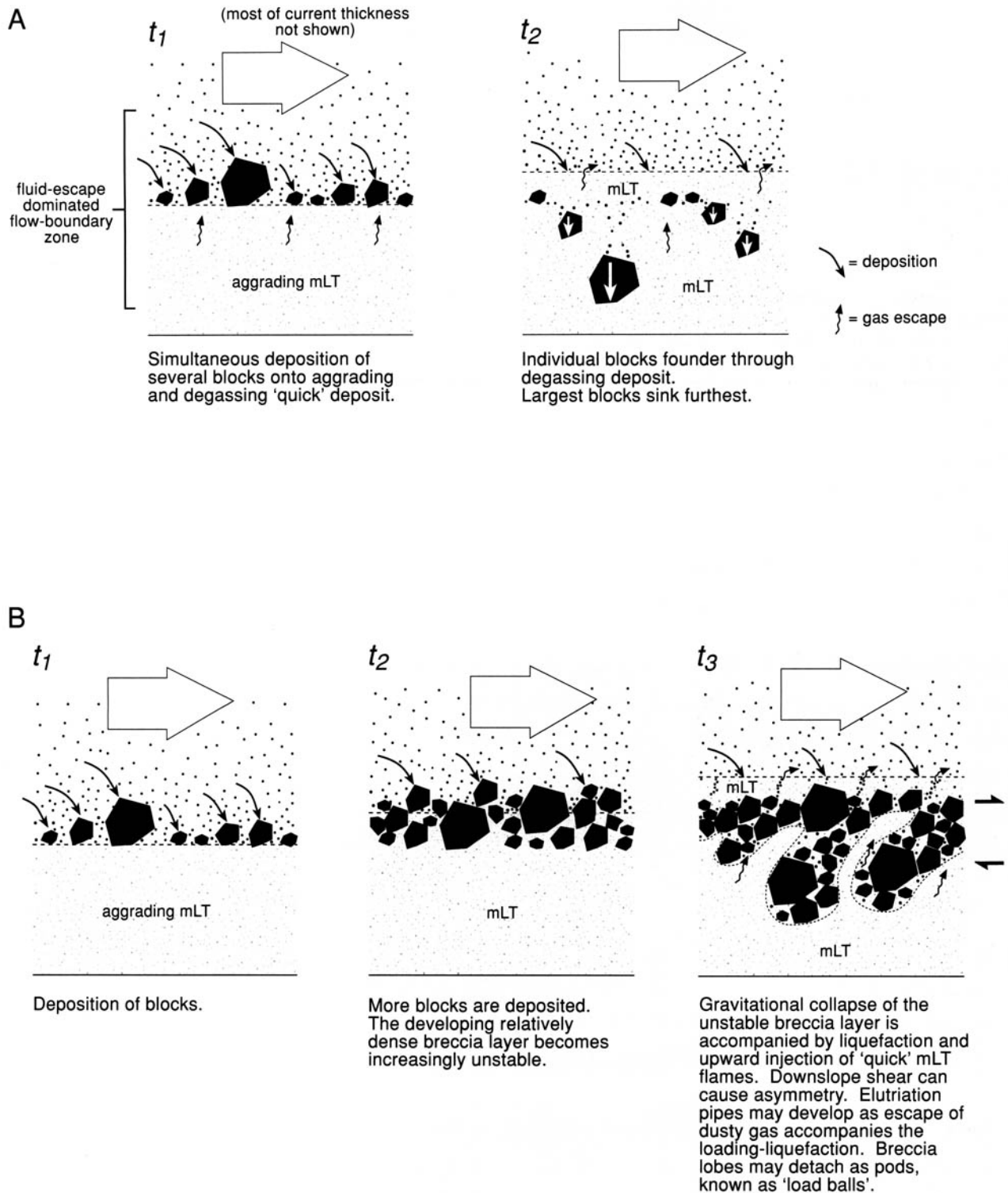


Fig. 5.7. Segregation of lithic clasts within the lower part of the flow-boundary zone. In example (A), of a lithic population deposited at one instant, larger lithics sink furthest through loose degassing uppermost deposit. This may produce normal vertical grading of lithics, isolated lithics in mLT or subvertical trains of lithics seen locally in mLT just below lithic breccia (mLBr) layers. With sustained deposition, sinking of lithic blocks may disguise the initial depositional organization. In (B) the deposit is able to support the lithics until the increasing load triggers a loading-liquefaction event. Processes A and B may occur together.

Part of the reason for this can be seen in the substantive acceleration equation (see p. 3). This shows that for a single-surge depletive current in which flow competence waxes and then wanes at the same rate, deposition and, hence, aggradation at any location during the waning phase is generally greater than that during the

waxing phase when deposition may be minimal, zero or even negative (erosion). As a result, more of the ignimbrite thickness will record waning flow (i.e. $mLT_{(nl, ip)}$) than waxing flow. Partly for this reason, waxing phases of pyroclastic density currents are relatively under-represented in terms of thickness within ignim-

brites. Vertical grading patterns that are similar to those caused by waxing followed by waning flow may also result from lateral migration of a thalweg in a sustained current (p. 111). As a thalweg migrates across a particular location, the location experiences an initial waxing phase followed by waning flow.

In the interpretation of lithic grading patterns, caution is needed when using maximum size of lithic blocks to infer current conditions (see p. 9). This is because downslope transport of lithic blocks is generally by intermittent rolling, sliding and/or saltation (see p. 25), in which the clasts are partly decoupled from the rest of the current. For example, blocks may move partly due to their own momentum (debris fall; p. 28), which on steep slopes may be faster than the rest of the current, or they may move as a result of tractional stress exerted by the current, in which case on low slopes they generally move slower than the rest of the current. Also, the abundance and size of lithic blocks at a particular horizon in an ignimbrite may reflect a momentary influx, for example from a rock avalanche upcurrent, rather than the local flow conditions.

Diffuse-stratified and thin-bedded lithofacies (e.g. dsLT, dbLT, bLT)

Description

Diffuse-stratified and thin-bedded lithofacies (Fig. 5.8) are common and under-reported subordinate lithofacies of most ignimbrites. They typically comprise lapilli-tuff with thin (millimetre- to decimetre-scale) variably diffuse layering defined by gradational and sometimes subtle grain-size variations, commonly of the pumice coarse tail and/or by varying abundances of pumice lapilli. Their sorting may range between values typical of mLT ($\sigma_\phi \leq 5$) and values exhibited by stratified lithofacies ($\sigma_\phi \geq 1$). For example, in the Taupo ignimbrite these lithofacies have sorting values of σ_ϕ 1.7–2.9 (Walker *et al.* 1981b). The diffuse stratification can be subparallel, but gradual thickening and thinning, and even spalling, are common (Figs 5.8F, 6.16 and 6.17C) together with lateral changes in grain size and sorting. Most individual layers within diffuse-stratified and thin-bedded lithofacies are laterally impersistent over decimetres or a few metres, and low-angle truncations may be abundant (Fig. 5.8D and F). They may show (asymmetric) inverse grading or normal grading, and commonly (more symmetric) normal-to-inverse grading or inverse-to-normal grading. Typically, a minor proportion of upper or lower boundaries of such internal layers are sharp, but commonly these become diffuse when traced laterally. Diffuse-stratified lithofacies commonly grade vertically and/or laterally into massive (mLT) and/or stratified (sLT; xsLT; sT) ignimbrite; diffuse-stratified and thin-bedded lapilli-tuffs can occur associated with pumice lenses (see topographic veneers, p. 111 and Fig. 5.10A).

Examples of various diffuse-stratified and thin-bedded lithofacies are documented by Kuno (1941), Fisher & Schmincke (1984, figs 8.17, 8.18, 8.31 and 9.23) and Busby-Spera (1986, figs 6A and 12), and occur in parts of the Minoan ignimbrite (fig. 16 of Sparks 1976; fig. 3 of Branney & Kokelaar 1992), in topography-draping parts of the Taupo ignimbrite (Walker *et al.* 1981b; Wilson 1985), in distal parts of the Valley of Ten Thousand Smokes ignimbrite (Fierstein & Hildreth 1992), and within ignimbrite packages of the Bishop Tuff (Wilson & Hildreth 1997).

Diffuse-stratified lithofacies commonly occur in the gradational transitions between stratified (sLT or sT) and massive (mLT) lithofacies. Examples include occurrences in the Upper Bandelier Tuff (Fig. 6.10E), occurrences in gradations from proximal sLT to medial mLT in the Mount St Helens 1980 ignimbrites (Rowley *et al.* 1985; see pp. 91 and 92), in gradations between valley-side or topography-draping sLT and valley-filling mLT lithofacies of the Taupo ignimbrite (Walker *et al.* 1981b; Wilson 1985; see pp. 111–114), in the climactic 1991 Pinatubo ignimbrite (Scott *et al.* 1996),

and in the Fasnía, Poris and Granadilla ignimbrites of Tenerife (figs 10.20 and 10.21 of Francis 1993; Bryan *et al.* 1998b; Brown *et al.* 2003).

Interpretation

Some diffuse-stratified and thin-bedded lithofacies may represent rapidly stacked and partially amalgamated flow-units (Kuno 1941), although this interpretation may be difficult to sustain when evidence for pauses between successive currents is lacking (pp. 95–98). Critical to the interpretation of diffuse-stratified lithofacies is that all gradations exist *laterally* between it and mLT, on the one hand (the latter with or without complex grading patterns), and with stratified tuff on the other. The gradations are commonly such that precise delimitation of each lithofacies can be difficult and somewhat arbitrary (see Fig. 5.1D). Locally, mLT, dsLT and sT grade continuously into each other across a few metres of deposit (Fig. 6.17C; see pp. 109–115). From this we infer that diffuse-stratified lithofacies are deposited when flow-boundary zone conditions (i.e. the particle concentration and shear gradients) are intermediate between those of fluid escape-dominated and traction-dominated flow-boundary zones, which deposit mLT and sLT, respectively (see p. 41). Some thin diffuse stratification in ignimbrites closely resembles thin stratification seen in sandy deposits of high-density turbidity currents, known as ‘stratification bands’ (Hiscott & Middleton 1979, 1980) or ‘S₂ divisions’ (Lowe 1982) and may have a similar origin.

We infer that diffuse stratification commonly records subtle unsteadiness within the flow-boundary zone of a sustained, depositing current. The unsteadiness likely arises from one or more of: (1) successive surges or waves in a fluctuating sustained current; (2) periodic impingement into the flow-boundary zone of turbulent eddies; and (3) intrinsic frictional effects within a thickening granular flow-dominated flow-boundary zone (see p. 43). We draw out these three possibilities as thought experiments in an attempt to unravel, at least partly, what may be concurrent intergradational processes.

- (1) The first mechanism arises when successive surges of the whole current cause fluctuations in clast populations supplied to, and hence in the selective filtering properties of, a granular flow-dominated to fluid escape-dominated flow-boundary zone. This causes successively deposited pumice or lithic populations to fluctuate with time (see pp. 43–45), and is similar to the underlying controls of formation of complex grading patterns in mLT (pp. 66–71). However, in this case the flow-boundary zone lies somewhat further from the fluid escape-dominated end-member (Fig. 4.2), as indicated by gradations into tractional lithofacies. Fluctuations in the relative dominance of flow-boundary granular flow versus fluid escape may be recorded in a deposit by variations in fabric strength with height across individual diffuse layers. Marked fluctuations may even cause momentary traction, non-deposition or erosion and hence lithofacies more akin to sT and xsT.
- (2) The second possible cause of unsteadiness, the periodic impingement of turbulence locally towards the flow boundary, is also invoked, because dsLT commonly occurs within lateral or vertical gradations between mLT and sT (Figs 6.10E, 6.16 and 6.17C; see Chapter 6). It is close to the first mechanism (above) except that the fluctuations in turbulence intensity arise spontaneously, without requiring whole-current unsteadiness. Because mLT indicates suppression of turbulence-induced traction in the flow-boundary zone (pp. 43 and 56) and sT indicates turbulence-induced traction (see the next section), diffuse-stratified lithofacies of transitional character are likely to record an intermediate condition. We envisage an intermediate condition in which turbulence does not constantly impinge directly on the flow boundary so as to cause traction, but in which turbulent fluctuations in overriding levels of a

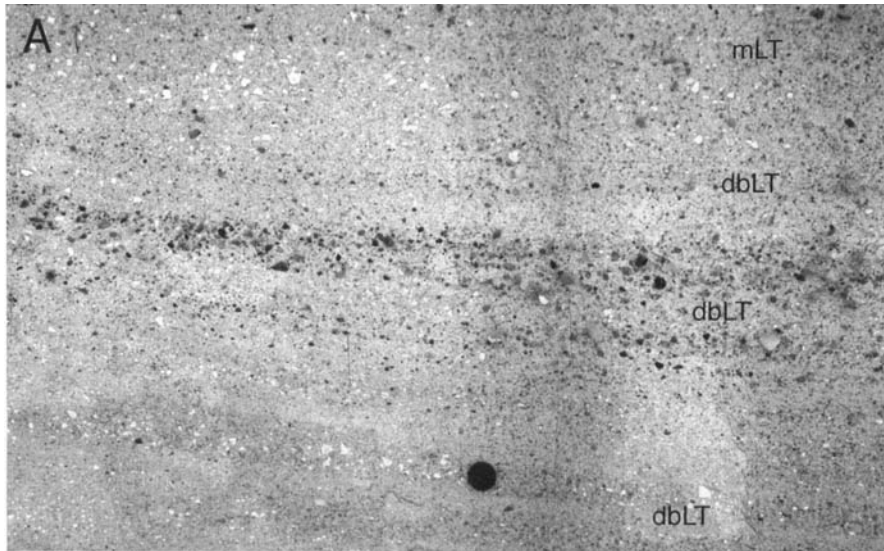
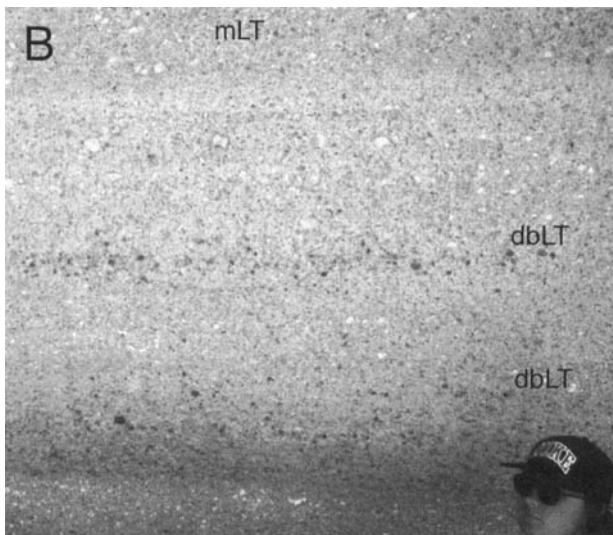


Fig. 5.8. Diffuse-stratified (dsLT) and thin-bedded (bLT) lithofacies.

(A) Diffuse bedding (dbLT) is marked by size and concentration grading of pumice and lithic lapilli, and ranges from trains of single clasts to units over 20 cm thick. There are no sharp bedding planes, and the lithofacies is locally transitional into massive lapilli-tuff (mLT). Note imperistence of some diffuse layers. La Caleta ignimbrite, Tenerife. The lens cap is 6 cm.



(B) Diffuse bedding (dbLT) defined by symmetric, normal-to-inverse grading patterns, from which way-up could not be determined. Parts are transitional into massive lapilli-tuff (compare with Fig. 5.1D). Some beds fade out beyond the view in the photograph. Granadilla ignimbrite, southern Tenerife.



(C) Mainly diffuse-bedded ignimbrite (dbLT) with some intervening sharply defined bedding planes. Note that these grading patterns show no systematic asymmetry from which the way-up could be determined. Minoan ignimbrite at Monolithos, Santorini. The end of the ruler shows centimetres.

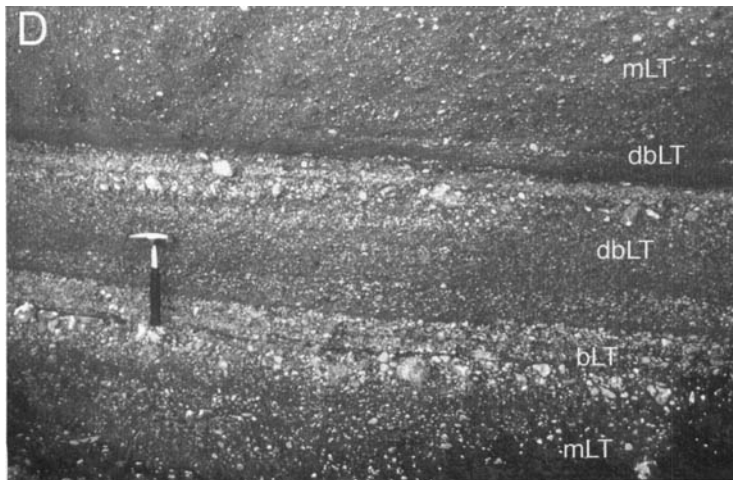
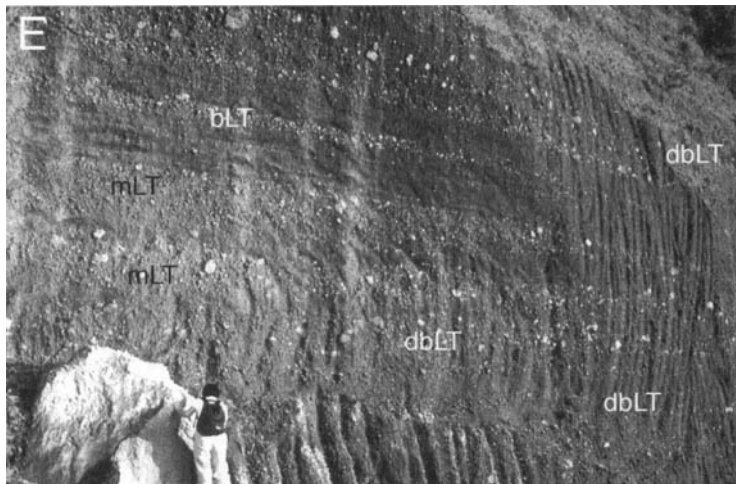


Fig. 5.8. (continued).

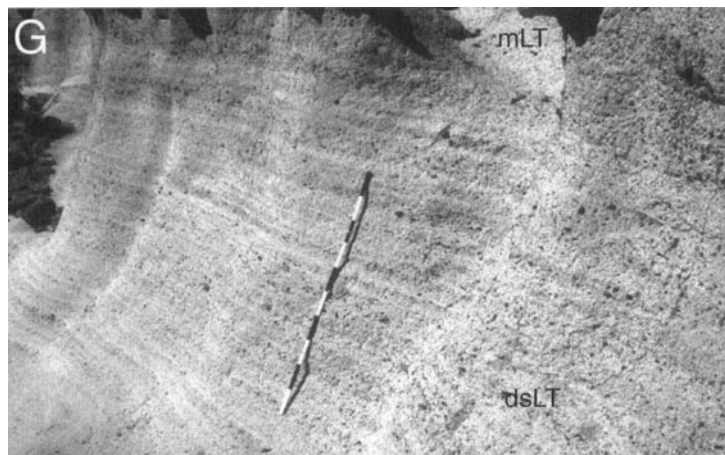
(D) More distinct, thin-bedded (bLT) and diffuse-bedded lapilli-tuff (dbLT). The section superficially resembles one of simple flow-units, but note the presence of all gradations between sharp, well-defined bedding planes and the subtle, diffuse and impersistent strata, which record varying degrees of current unsteadiness. Grades locally into massive lapilli-tuff (mLT). Rio Caliente ignimbrite, La Primavera caldera fill, Jalisco, Mexico.



(E) Part of a 40-m thick succession of thin-bedded (bLT) and diffuse-bedded lapilli-tuff (dbLT) of an intra-Plinian ignimbrite that elsewhere is massive. Thin and diffuse bedding is thought to record localized unsteadiness near flow margins (Ui *et al.* 1992). Some surfaces probably represent flow-unit boundaries, although all gradations between sharp, diffuse-bedded and variously graded massive lapilli-tuff (mLT) are represented, with common lateral impersistence and low-angle truncations. Pumices are imbricated (not visible on the photograph). The ignimbrite formed from an eruption at Aira caldera; the exposure is in Tarumizu Quarry, southern Kyushu, Japan.



(F) Thin-bedded lapilli-tuff showing lateral impersistence and thickness changes of beds. The bedding planes appear diffuse when viewed close up. Poris ignimbrite, SE Tenerife. Exposure height 1 m. (Photograph: Richard Brown).



(G) Diffuse-stratified lapilli-tuff, with very low-angle impersistent strata. The ignimbrite appears almost massive in the field when viewed close up. Poris ignimbrite, southern Tenerife. The metre rule is for scale. (Photograph: Richard Brown).

stratified current are sufficient to cause repeated unsteadiness within a generally non-turbulent, modified grainflow-like lower part of the current (see pp. 43 and 44 and Fig. 4.5B for a fuller explanation). Such unsteadiness will affect granular temperature and related phenomena, such as percolation and frictional interlocking, as well as affecting the rate and behaviour of fluid escape associated with hindered settling. However, the effects of stress fluctuations on depositional, high-concentration two-phase dispersions (modified grainflows) are yet to be thoroughly explored. In some stratified currents overriding turbulent eddies may be sufficiently energetic momentarily to sweep right down to the flow boundary (see Fig. 4.5A; Hiscott 1994b).

Small-scale unsteadiness caused by either of the two above extrinsic mechanisms is best recorded by a granular flow-dominated flow-boundary zone, because a substantial part of this type of flow-boundary zone may rapidly acquire a significant yield strength as soon as its granular temperature drops. Even small fluctuations in steadiness may cause shear stress to fall, and so cause rapid frictional 'locking-up' of the lowermost levels of shearing grains within the base of the current (unsteady or 'stepwise' aggradation of Branney & Kokelaar 1992) (Fig. 4.5B). Any grain-size stratigraphy developed (e.g. by granular segregation) in the lowermost part of the current may then be preserved (e.g. as inverse grading) in the abruptly deposited thin layer. Successive 'locking-up' of lowermost parts of the current in this way may cause thin bedding (stratification bands). This is in contrast to the behaviour of a more end-member type of fluid escape-dominated flow-boundary zone, where the behaviour is more fluidal (low yield strength), even when the local shear rate drops, because the escaping fluid prevents rapid 'locking-up' of grains (see Fig. 4.5C). Therefore, a fluid escape-dominated flow-boundary zone registers small fluctuations in current velocity less sensitively (see 'Deposition during unsteadiness' pp. 43 and 44) and hence it typically deposits more homogeneous massive lapilli-tuff. Depending on the relative importance of granular flow versus fluid escape, the flow-boundary zone may variously give rise to massive lapilli-tuff, diffuse banding, more sharply defined layering and even soft-state slide surfaces formed in the unconsolidated deposit. Because grain-fabric formation is favoured in granular flow-dominated flow boundaries (p. 39), diffuse stratification in ignimbrites is likely to be associated with development of well-defined directional fabrics, as it is in some turbidites (Hiscott & Middleton 1980).

- (3) It is likely that a flow-boundary zone of a steady current develops its own inherent unsteadiness, with effects similar to those of the second mechanism above. Shear and/or deposition within the flow-boundary zone may cause cyclic variations in the yield strength of the lowermost parts of the current and/or in uppermost parts of the deposit. For example, vibrations due to passage of the current may periodically decrease the strength of the uppermost part of the deposit by inducing liquefaction or raising the granular temperature. Also, lowermost shearing layers (millimetres-centimetres) of a current may periodically increase in yield strength as a result of shear-induced development of grain fabrics, and improved sorting and/or changes in grain size as a result of granular segregation processes (see pp. 29–31). As with the other mechanisms (above), this may cause successive lowermost shearing layers of grains to lock-up once a critical strength threshold is exceeded, to produce stacked thin and impersistent, inverse-graded or inverse- to normal-graded layers in the ignimbrite.

Stratified and cross-stratified tuffs (e.g. sT, xsT, sL)

Description

These lithofacies comprise fine tuff to lapillistone that exhibit well-developed submillimetre- to subcentimetre-scale stratification

defined by sharp to gradational changes in clast size, density and/or sorting (Figs 5.9, 6.10C–E and 6.17B). Sorting varies from well sorted to poorly sorted (mostly σ_ϕ 1–3), with less fine ash than mLT (Walker 1984). Pumice lapilli commonly show evidence of abrasion. The stratification is discontinuous in that individual laminae can rarely be traced over a few decimetres to metres. It varies from subparallel, through pinch-and-swell stratification with low-angle truncations, to cross-stratified tuff (xsT; Fig. 5.9). The latter can have low- to high-angle erosional truncations and constructional bedforms, with strata deposited as steep as 30–40°.

Stratified tuffs have been described both in ignimbrites, for example topography-draping parts of the Taupo ignimbrite (Walker 1985), proximal 1980 ignimbrites at Mount St Helens (Rowley *et al.* 1985), proximal Valley of Ten Thousand Smokes ignimbrite (Fierstein & Hildreth 1992), proximal and ridge-draping parts of the 1991 Pinatubo ignimbrite (Scott *et al.* 1996), the Neapolitan Yellow Tuff (Cole & Scarpati 1993) and the Toconquis Ignimbrite Formation (Sparks *et al.* 1985), and in deposits ascribed to 'pyroclastic surges' (Fig. 6.17B; Fisher & Waters 1970; Walker 1984; Sigurdsson *et al.* 1987; Sohn & Chough 1989; Colella & Hiscott 1997 and references therein).

All gradations exist between stratified (sT; xsT) and diffuse-stratified (dsLT) lithofacies on the one hand (e.g. Rowley *et al.* 1985; Fierstein & Hildreth 1992; Scott *et al.* 1996; Fig. 49E), and, in terms of bedding, sorting characteristics and deposit thickness variations across topography, between stratified lithofacies and well-sorted massive fallout tuff (mT) on the other hand (Talbot *et al.* 1994; Valentine & Giannetti 1995).

Steep, vertical and even overhanging stratification occurs in some fines-rich lithofacies, due to adhesion-enhanced aggradation (as in 'plastered base-surge' deposits; Waters & Fisher 1971; Delino *et al.* 1990) and/or due to postdepositional soft-state deformation (Crowe & Fisher 1973).

Interpretation

The subparallel stratification, cross-stratification, and good sorting (if present), indicate deposition from traction-dominated flow boundaries (as described on p. 37). The subparallel stratification differs from ash-fall lamination (/xT) in that individual laminae are discontinuous in detail and the lithofacies exhibit grain fabrics (including AMS fabrics, e.g. Cagnoli & Tarling 1997); it is analogous to 'transcurrent lamination' and 'horizontal discontinuous stratification' in sands deposited by unidirectional currents (Allen 1984). Most fine clasts were fully or intermittently supported by fluid turbulence, whereas denser/larger clasts saltated, slid or rolled along the substrate. Progressive, metre-scale bedforms with stoss-side scour and lee-side, near-repose-slope deposition are common (e.g. Allen 1984; Sigurdsson *et al.* 1987), consistent with bed-load transport and deposition. Inverse-graded laminae and lenses (e.g. on the near-repose slopes of dunes) probably indicate unsteady deposition and clast segregation at localized unsteady granular flow-dominated flow-boundary zones (see pp. 29–31 and p. 43). Low-angle bedforms in which the stratification indicates up-current or downcurrent migration, some with constructional stoss-side ('backset') layers, may record antidunes or chute-and-pools and hence upper flow-regime conditions, including hydraulic jumps (see pp. 16–19; Schmincke *et al.* 1973; Cole 1991), or, alternatively, adhesion-enhanced moist accretion (Allen 1984) (Table 5.3). Steeply climbing bedforms with both stoss and lee sets preserved indicate high rates of aggradation, and thick bed sets with simple internal architectures indicate quasi-steady aggrading conditions. Conversely, deposits predominantly composed of multiple, thin lenticular cross-sets with abundant internal scour surfaces suggest either that the currents had low net rates of aggradation (e.g. 'starved' dunes) or that the currents were too unsteady to construct well-developed sandwaves. Asymmetric block-impact structures



Fig. 5.9. Stratified (sLT) and cross-stratified (xsLT) lithofacies.

(A) Proximal cross-stratified lapilli-tuff. 18 May 1980 Mount St Helens ignimbrite. Flow direction was from right to left, obliquely out of the field of view toward the viewer. This deposit correlates with massive ignimbrite further away (Rowley *et al.* 1985).



(B) Cross-stratified lapilli-tuff in the 15 June 1991 climactic ignimbrite of Mount Pinatubo, Philippines. The deposit partly filled a small radial canyon, about 6 km from source, and passes up into mLT. Flow direction was away from the viewer. The metre ruler is for scale.



(C) Cross-stratified fines-rich lapilli-tuff, locally transitional into thin-bedded and diffuse-stratified lapilli-tuff (cf. Fig. 5.8F). Slightly welded. Cape Riva ignimbrite, near Oia, Santorini (Druitt 1985). Current direction was away from viewer.

Table 5.3. Characteristics of stratified tuff that indicate moist ($\leq 100^\circ\text{C}$) deposition versus dry ($> 100^\circ\text{C}$) deposition. Most differences are attributable to adhesive behaviour of moist ash (e.g. agglomeration) during and after deposition.

Deposits of cool, moist currents	Deposits of hot, dry currents
Vesicles common in ash/tuff matrix	Matrix vesicles absent
Pellets and/or armoured lapilli common	Pellets and armoured lapilli usually absent
Accretionary lapilli common	Accretionary lapilli present in some cases
Oversteepened foresets and/or backsets common	Oversteepening of bedding is rare
Steep to overhanging surfaces commonly plastered	Deposition on slopes $> 35^\circ$ is rare
Load structures and/or convolutions common	Load structures and convolutions are rare
Lapilli-impact structures commonly preserved	Lithics sink through ash with little record of plastic deformation
Rain impact marks and/or adhesion ripples may be preserved on some bedding planes	No rain impact marks or adhesion ripples
Nearly always have abundant fines	Fine ash may be abundant or scarce
Poor sorting common	Typically moderately well sorted
May harden rapidly	May remain loose and dusty

indicate either influxes of ballistic ejecta, or block transport by current-modified debris fall (saltation; see 'Support on an interface' on p. 25).

Stratified lithofacies can be divided, according to a range of characteristics, into two categories inferred to indicate: (1) moist deposition ($\leq 100^\circ\text{C}$) and (2) dry/hot deposition ($> 100^\circ\text{C}$) (see Table 5.3). For example, bedding steeper than typical repose angles, soft-state deformation structures, vesicular tuffs and pellets indicate accretion or plastering by sticky, moist ash at $\leq 100^\circ\text{C}$ (e.g. Waters & Fisher 1971). Vesicles commonly are shaped according to the host material, viz. rounded within fine ash and interstitial within coarse-ash- to lapilli-grade deposits. They may indicate rainfall during or just after deposition (Rosi 1992).

As with mLT, vertical-grading patterns in stratified tuff may indicate current waxing and waning (e.g. Sigurdsson *et al.* 1987) or they may record lateral or longitudinal migration of thalwegs and/or bedforms. In stratified deposits, distinguishing between the record of a fluctuating sustained current and that of several successive currents may be difficult (fully dilute currents may variably erode and/or deposit), although in some instances pauses between successive currents (see pp. 95–98) are recorded by thin intercalated (millimetre- to centimetre-scale) non-stratified fallout layers (mT; Walker 1984). Intercalated ashfall layers are probably more common in deposits of cool, moist pyroclastic density currents because: (1) suspended ash is better able to settle on deposits that are cool and do not generate a vigorous thermal plume; (2) ash fallout is enhanced by moist clumping and pellet formation; and (3) moist and sticky deposits are less readily whisked away by subsequent currents than are dry and loose ash deposits.

Lithofacies intergradational between stratified (sLT) and diffuse stratified (dsLT) indicate that the parent currents had flow-boundary zones intermediate between tractional and granular flow-dominated, whereas lithofacies that range between stratified (sLT) and laterally continuous, well-sorted layers (e.g. mT, mL) indicate that the currents had flow-boundary zones gradational between tractional and direct fallout-dominated end-member types (Fig. 4.2).

Pumice-rich layers, lenses and pods (e.g. pmLT, plensL, mpCo, plensCo)

Description

Many ignimbrites exhibit subordinate lithofacies that are particularly rich in large rounded pumice lapilli and/or cobbles (and/or pumice blocks) (Fig. 5.10) (Kuno 1941; Walker *et al.* 1981b; Wright 1981; Wright & Walker 1981; Wilson & Walker 1982; Sparks *et al.*

1985; Freundt & Schmincke 1985; Bryan *et al.* 1998b; Giannetti & de Casa 2000). Sorting ranges from very well sorted ($\sigma_\phi < 1$, e.g. Walker *et al.* 1981b; Wilson 1985) through to poorly and very poorly sorted ($\sigma_\phi > 4$), and all gradations occur from framework supported pumice lapilli (pL, pCo) with or without a matrix of ash (e.g. Wilson & Head 1981) through to pumice-rich massive lapilli-tuff (pmLT; sometimes referred to as pumice 'concentration zones' or pumice 'swarms') and typical mLT. Pumice-rich lithofacies commonly have bimodal (pumice lapilli and matrix) or negatively skewed grain-size distributions (e.g. Sparks 1976; Sparks *et al.* 1997b) relative to mLT.

Most pumice-rich layers and lenses lack large lithic clasts. They range from massive to stratified and cross-stratified (e.g. Walker *et al.* 1981b), and they can show lateral grading, or vertical normal, inverse, symmetrical or complex grading. They can comprise discrete layers, lenses, dune-shaped or irregular-shaped bodies, or subtle concentrations with diffuse margins that grade continuously into enclosing mLT (Fig. 5.10). They vary from centimetres to several metres thick, and from decimetres to many tens of metres laterally, and they can lie variously at the base of, within or at the top of massive ignimbrite (mLT) layers, or at distal or lateral margins (Fig. 4.7B). Pumice-rich lithofacies that appear to be continuous layers (sheets) at the scale of individual exposures may prove to have stringer or bar-shaped, lenticular morphologies. Exposure limitations commonly make resolution of three-dimensional geometries practically impossible, although geophysical techniques like ground-penetrating radar may help overcome this problem.

Interpretation

Pumice-rich lithofacies record deposition either from currents that were particularly pumice-rich, or from currents in which pumice segregation occurred during transport and deposition. The considerable variety of shape and character of lithic- and pumice-rich layers and lenses in ignimbrites suggests that they form in several ways. However, there are three requirements in common: (1) unsteady deposition; (2) flow boundaries that temporarily favour deposition of coarse pumice; and (3) non-uniform deposition, indicated by the discontinuous nature of the lenses.

Pumice is interesting sedimentologically, because it can segregate in two ways. First, it may segregate as 'flotsam' (see p. 33) within a current as a result of its buoyancy and/or inability to percolate down between the vibrating particles of a granular flow-dominated or fluid escape-dominated flow-boundary zone. Secondly, it may segregate out of a current as 'lagan' where it is denser than low-concentration lowermost parts of the current and/or where it is able to percolate down to the base of the current.

Pumice flotsam preferentially travels downcurrent (overpassing)

as a result of selective filtering (p. 41). Overpassing pumice clasts are unlikely to float along the true top of a density-stratified current, but rather at the level where the buoyancy forces (fluid escape-dominated flow-boundary zone) and/or percolation with dispersive-pressure effects (granular flow-dominated flow-boundary zone) counteract settling within the current. This will vary with pumice size (Fig. 6.9B, inset). They may overpass at these neutral levels individually or as pumice rafts. If flow-boundary zone conditions remain unfavourable for deposition of these pumices they may continue to overpass at these levels until they reach the distal termination or lateral margin of the current, where depletion and lofting have sufficiently modified the flow-boundary conditions (concentrations and shear rates) to enable the pumice flotsam to deposit; that is, the neutral levels have descended across the lower flow boundary. This is the primary mechanism by which lateral pumice levees and distal pumice dams form (see p. 95). During waning flow the distal locations of pumice deposition retreat sourcewards (Fig. 4.6) and individual pumice clasts or pumice rafts may become stranded as pumice-rich layers or as irregularly shaped accumulations at or near the top of the deposit (Fig. 5.10E). However, if the current waxes, the distal limit of the current should advance (Fig. 6.7B) so that it may breach, override, erode and remobilize earlier formed pumice accumulations. Deposited pumices may float off if overridden during a subsequent current pulse, or they may be buried under mLT (see Fig. 6.7B). In this way, pumice accumulations that were originally at the distal margin of the ignimbrite end up as pumice lenses beneath mLT, either at the base of, or within, the ignimbrite sheet (Figs 5.10C–G).

All gradations exist between ignimbrites with sharply defined upper pumice layers and mLT with inverse coarse-tail pumice grading (mLT_(ip)). We interpret this as recording whether the current waned abruptly or more gradually (see p. 66), and whether overpassing pumice flotsam travelled and stopped as isolated clasts or in rafts. Where pumice flotsam encroaches the lateral margins of the current it may dock against the marginal pumice levee (thus adding to the levee) or adjacent to the valley sides in the case of a valley-confined current (e.g. lateral pumice-rich lithofacies described in Freundt & Schmincke 1986). The downcurrent transport of other pumice flotsam may remain unimpeded until it reaches a terminal pumice dam. With lateral migration of thalwegs, successive pumices are added to one marginal levee so that it accretes laterally, whilst pumices on the inside of the opposite levee either float off or are buried under mLT. If this process continues, the lateral migration may give rise to a stack of two pumice-rich layers separated by mLT within the resultant ignimbrite sheet. Such processes clearly can give rise to a range of shapes of pumice-rich bodies.

Lagan pumice can form pumice bars and/or dunes. The known range of deposits, from cross-stratified pumice dunes to massive pumice lenses, suggests that all gradations exist between true tractional pumice-gravel dunes to fully shearing low-angle 'hogs-back' shoals or bars that shift downcurrent as a moving 'quick bed', analogous to the slug-flow regime of pneumatic transport (references in Coulsen & Richardson 1990). The latter are part of the current (e.g. a lenticular pumice-rich traction carpet) rather than true deposit bedforms. Their deposits will lack well-developed tractional stratification, but may exhibit diffuse discontinuous layering and/or imbrication. The pumices of the moving 'quick bed' behave in a way intermediate between flotsam and lagan, in that their stable level of transport (e.g. level of neutral buoyancy) is at or close to the lower flow boundary. Parts of such pumiceous 'slugs' are prone to stopping (depositing) temporarily, or floating off as within-current rafts. Similar shearing 'quick' bars of near-neutrally buoyant pumice gravel migrate rapidly within basal parts of hyperconcentrated lahars and produce similar, poorly stratified lenticular bedforms (e.g. 1991 lahars of Hudson volcano, Chile; MJB unpublished data). As with pumice levees, pumice bars in sustained currents may give rise to sheet-like pumice-rich layers by downcurrent accretion or by lateral accretion accompanying

thalweg migration.

Pumice lenses preserved on the downcurrent side of topographic obstacles (e.g. lee-side lenses of Walker *et al.* 1981b; Wilson 1985) (Fig. 5.10A) may form as bars by localized turbulent segregation and deposition in the lee of the obstacles (pp. 24–25). They do not require the 'tail' of a current to have locally parted company with the ground, as has previously been proposed (Walker *et al.* 1981b). They may also form as overridden temporary levees or pumice rafts that were protected from reworking by the current in the lee of the obstacle during progressive aggradation. In both cases (buried bars and buried remnant levees) the common paucity of fine ash in the lenses is the result of granular (e.g. percolation) and turbulent (winnowing) segregation, and the well-rounded nature of the pumice lapilli or cobbles is due to abrasion.

Some pumice-rich layers or lenses (mpL, plens) are remnants of eroded Plinian pumice fallout layers (see the next section) that aggraded between ignimbrite flow-units (Fig. 6.10A). They may contain fine ash infiltrated from any overlying fines-rich layer (e.g. mLT) and may have been modified by the succeeding current. Unless substantially reworked, lenses of this origin can be recognized by the high angularity of the pumice clasts.

Pumice lenses at bases of ignimbrites are considered further on page 101.

Massive and parallel-bedded lapilli deposits (e.g. pmL, p//bL)

Description

Lithofacies of this group comprise very well sorted (σ_ϕ 0–1) to moderately well sorted (σ_ϕ c. 2) layers, predominantly of angular pumice lapilli with subordinate lithic lapilli and ash (e.g. Walker 1971) (Fig. 5.11A–C). The layers range in thickness from that of a single clast to a few metres thick. They are internally massive and variously graded or non-graded, or they exhibit diffuse to sharp, laterally continuous parallel bedding (Figs 5.10F and 6.10E). They are framework-supported, typically open-work (Fig. 5.11A) and lack tractional stratification, segregation pipes or lenses. They may occur at any level within ignimbrite sheets (Chapter 6) and are common at the base. Tops and bases of the lithofacies typically are sharp, and upper surfaces may show evidence of erosional scour. Basal contacts may exhibit lapilli-impact structures (Fig. 5.11B).

In some massive or parallel-bedded lapilli deposits, the pumice and lithic lapilli are highly angular with little or no evidence of abrasion (Fig. 5.11A), and larger pumice clasts commonly have some straight or curved fracture faces. Typically, some of the pumice lapilli are cracked or broken, with component pieces almost *in situ*. In such layers, dense lithic lapilli are typically smaller than the largest pumice lapilli at the same horizon, and the layers uniformly drape topographic slopes less than about 33°, with little outcrop-scale variation in thickness except where the upper contact has been scoured. Such layers may, if not extensively scoured, be traced for tens of kilometres, and grain sizes and layer thicknesses show systematic regional variations that are independent of topography (Walker 1971; Fisher & Schmincke 1984).

Interpretation

The better-sorted lithofacies in this group (e.g. σ 0–2) are best interpreted as deposited by fallout from eruption plumes, for example Plinian or sub-Plinian pumice fall layers. This may be confirmed by identifying systematic regional variations in grain size and bed thickness that are independent of local topography, commonly via the construction of isopach and isopleth maps (see Walker 1971). Laterally continuous parallel layering suggests unsteady, but near-uniform, deposition. Vertical grading patterns, particularly of lithics, may record changes in eruption column

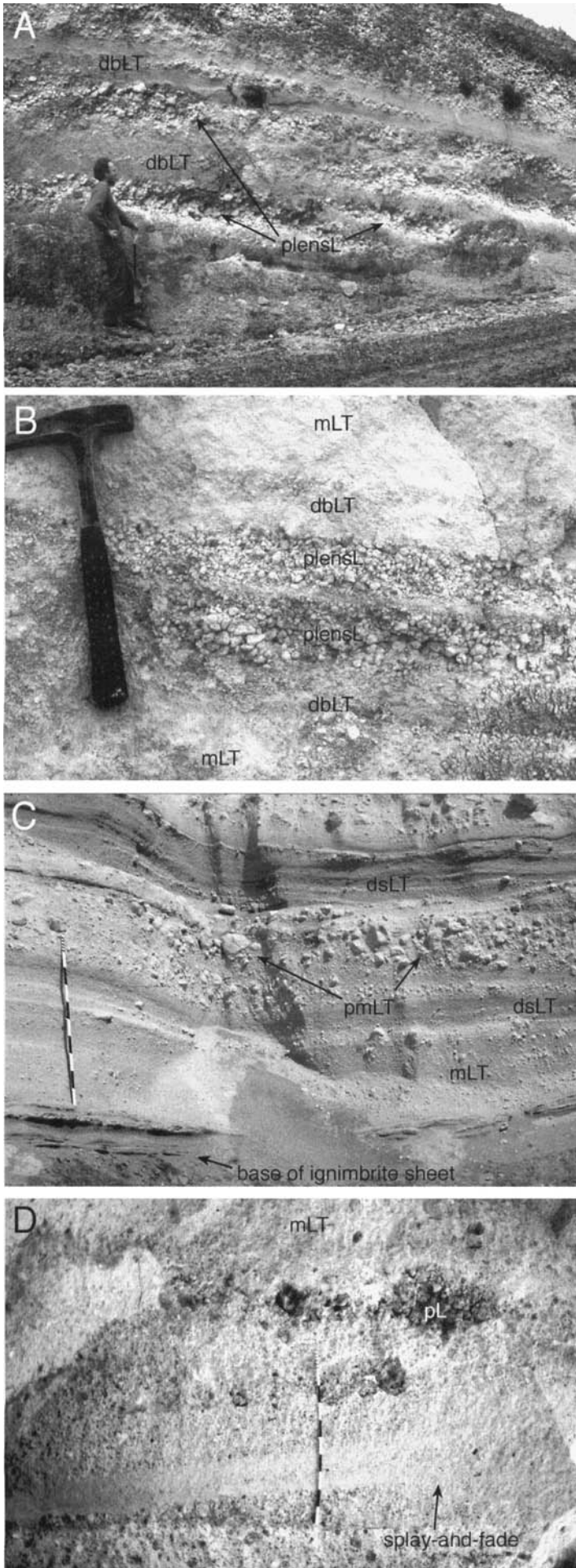


Fig. 5.10. Pumice-rich lithofacies.

(A) Framework-supported pumice lapilli and cobbles in lee-side pumice lenses (plensL) intercalated with diffuse-bedded lapilli-tuff (dbLT). Current direction was left to right. Taupo ignimbrite, lee side of a topographic obstacle, 18 km SE of inferred vent, New Zealand.

(B) Small lenses of pumice lapilli (plensL) in massive (mLT) and diffuse-bedded lapilli-tuff. Framework-supported pumice lapilli are subtly imbricated (bottom left to top right). The White Trachytic Tuff of Roccamonfina volcano, Italy (Giordano 1998).

(C) Pumice-rich massive lapilli-tuff (pmLT) intercalated with diffuse-stratified to massive lapilli-tuff. Climactic 15 June 1991 ignimbrite of Mount Pinatubo, Philippines. Note the gradational nature and lateral impersistence of the layering. Metre rule for scale.

(D) Small lenses of framework-supported pumice lapilli in massive lapilli-tuff (mLT). Note the splay-and-fade stratification (see the section on this in Chapter 6 for an explanation). Granadilla ignimbrite, Tenerife. (Brown *et al.* 2003). Metre rule for scale.

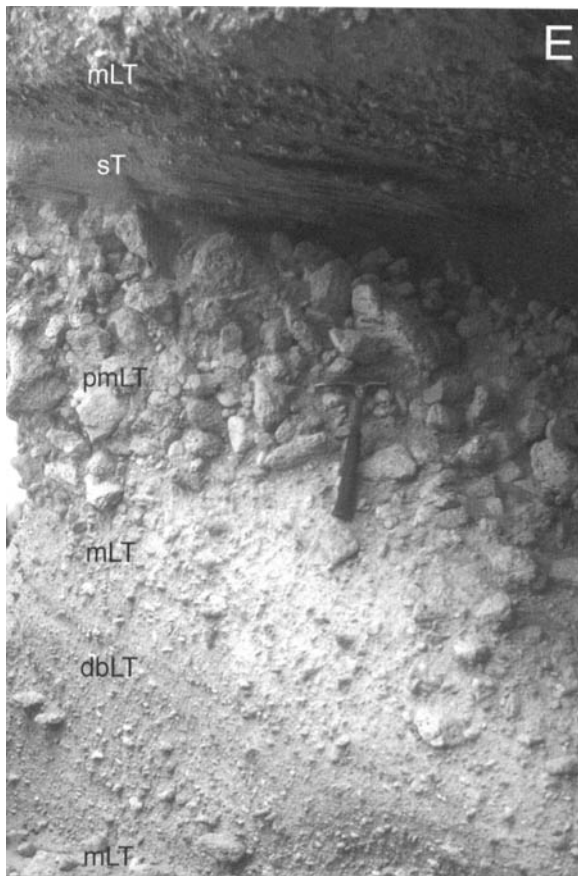
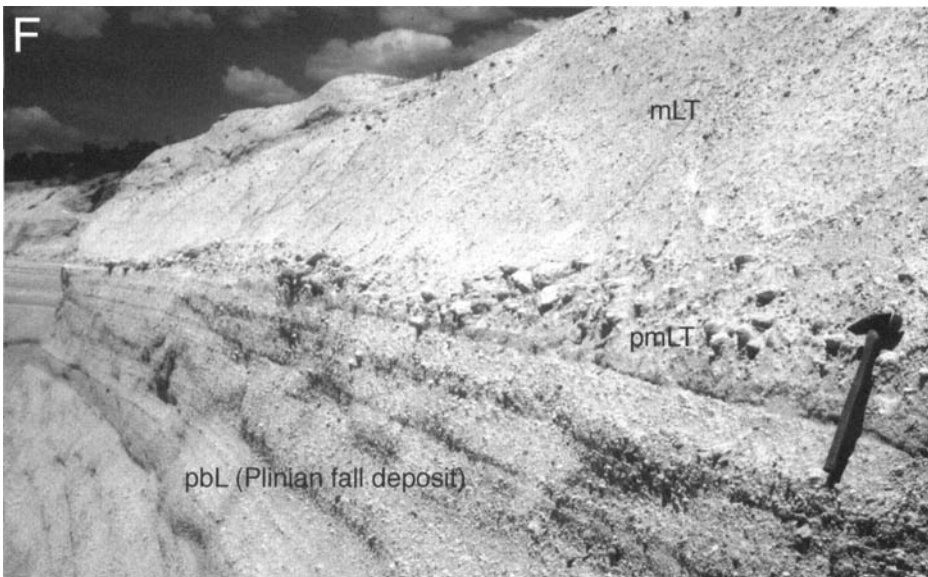
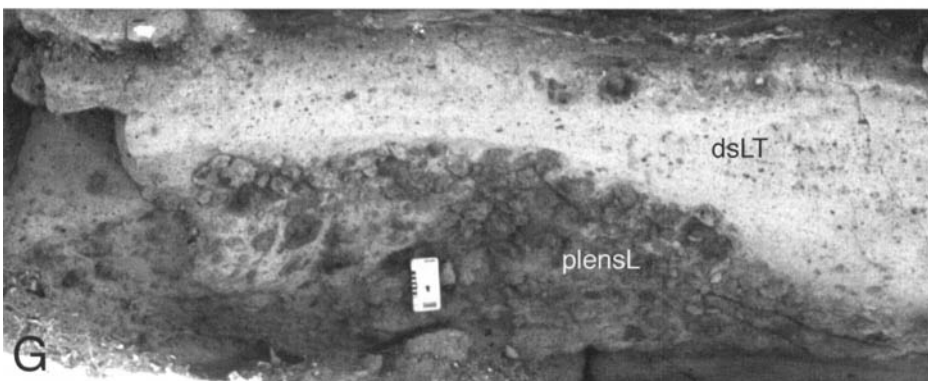


Fig. 5.10. (continued).

(E) Inverse coarse-tail graded pumice concentration within the Upper Bandelier Tuff ignimbrite, Jemez Mountains, New Mexico.



(F) Lens of framework- to matrix-supported pumice lapilli (pmLT) at the base of, and locally gradational into, massive lapilli-tuff (mLT). Note the well-sorted Plinian pumice fall deposit (pL). Lower Bandelier Tuff, Copar Pumice Quarry, Los Alamos, New Mexico (Self & Sykes 1996).

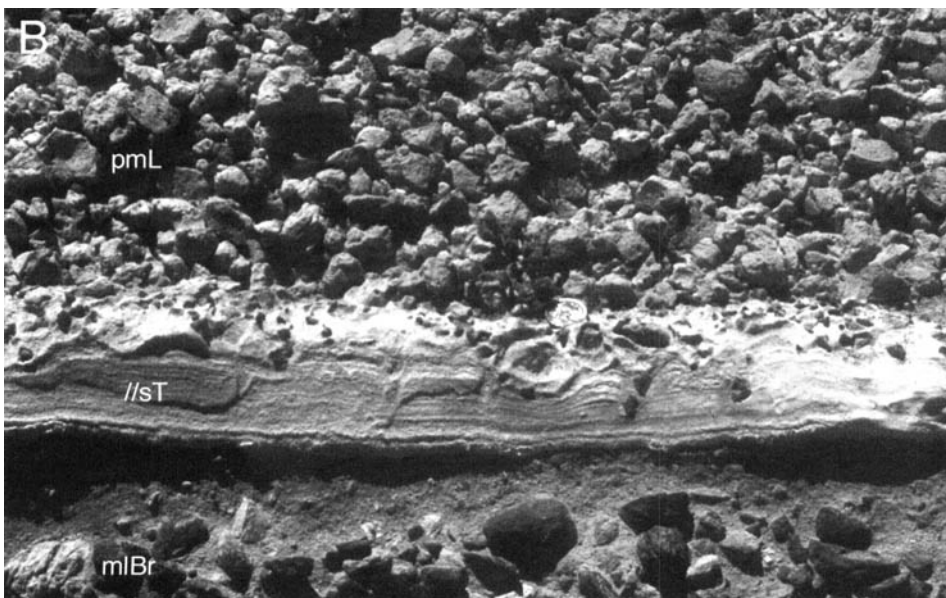


(G) Convex-up pumice lens, mostly clast supported, within the upper non-welded part of the Arico ignimbrite, SE Tenerife (base of the ignimbrite is not shown). The lens is overlain by splaying diffuse-stratified lapilli-tuff, which grades up into mLT (not shown).



Fig. 5.11. Massive and bedded lapilli lithofacies (pmL, p//bL), and parallel-stratified and parallel-bedded tuff lithofacies (//sT; //bT) (also see Figs 5.10F and 6.10E; see pp. 77 and 83).

(A) Pumice-rich massive lapilli lithofacies (pmL) with angular, open-work, framework-supported pumice lapilli, and subordinate angular lithic lapilli. Note the prismatic jointing in the pumice block caused by *in situ* cooling contraction, whereas breakage along cooling-contraction joints during fallout and deposition is indicated by the faceted shapes of several of the pumice lapilli. Pumice fall deposit, Laacher See, Germany. Lens cap is 6 cm.



(B) Pumice-rich massive lapilli deposit (pmL) division overlies a 6-cm thick, parallel-laminated tuff division (//sT) (see p. 83). A fallout origin of the pmL is indicated by good sorting, angular pumices, impact structures of some of the basal lapilli (right of centre) and draping of the division over topography (see C). The //bT is interpreted as an ashfall deposit, but closely similar lithofacies may be deposited from a fallout-dominated flow-boundary zone of a dilute, low-velocity rolling ash cloud (see p. 37). La Caleta Formation of southern Tenerife (Brown *et al.* 2003). The coin (right of centre) is 1.5 cm.

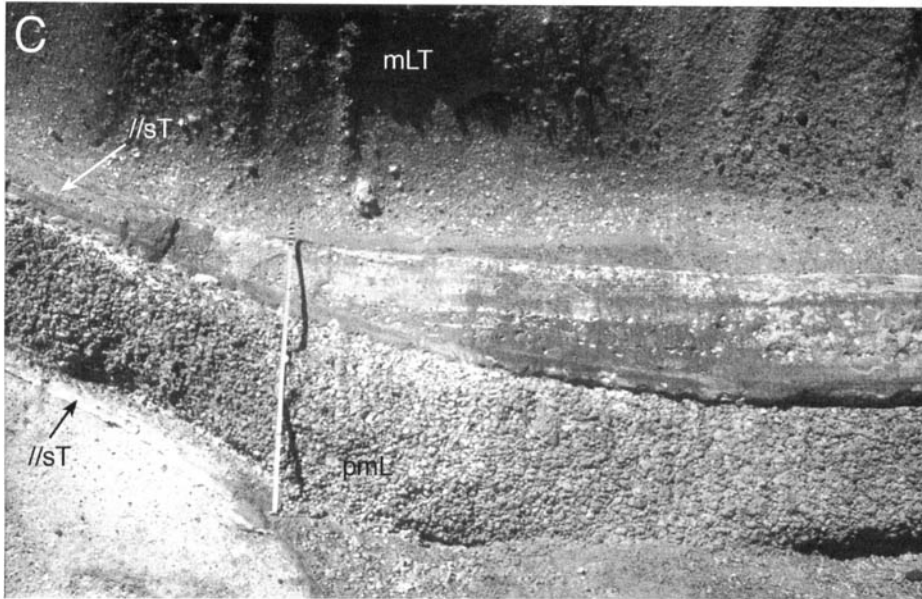
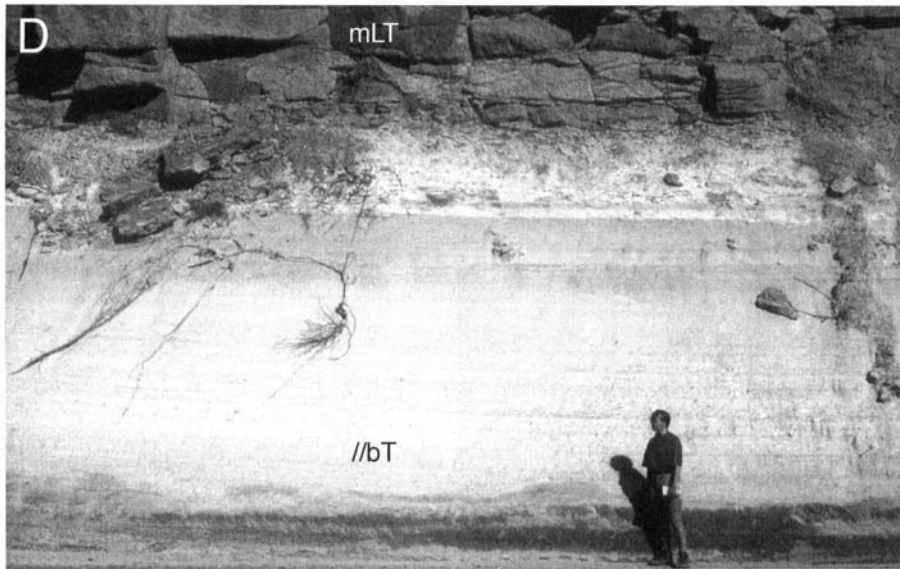
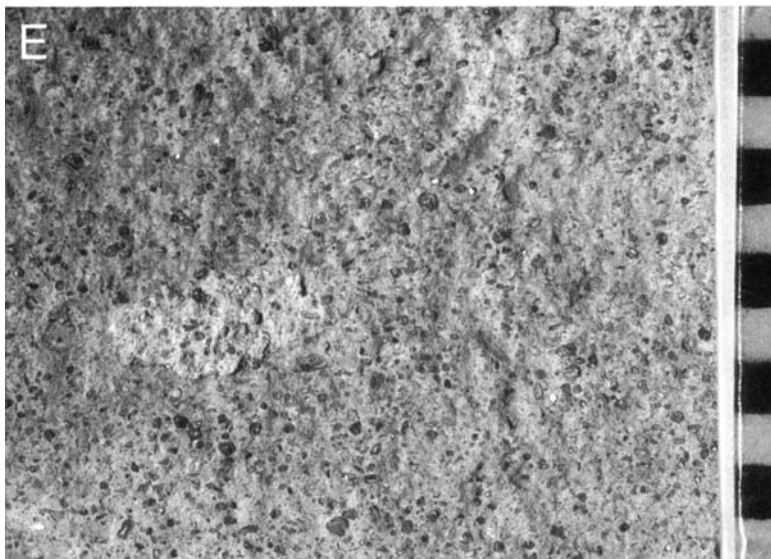


Fig. 5.11. (continued).

(C) Pumice-fall origin of pmL is indicated by draping of topography. Overlying //sT layers include layers deposited by fallout (these drape the pumice-fall layer with no change in thickness) and overlying layers deposited by pyroclastic density currents (these thicken and coarsen into valley). La Caleta Formation, southern Tenerife. The metre rule is for scale.



(D) Thick layer of parallel-bedded ash (//bT) mostly of ashfall origin underlies ignimbrite (mLT). Mesa Falls Tuff, near Mesa Falls, eastern Idaho.



(E) Detail of //bT in D, showing absence of tractional stratification and abundant crystal fragments supported in a fine ash matrix. The scale is in centimetres.

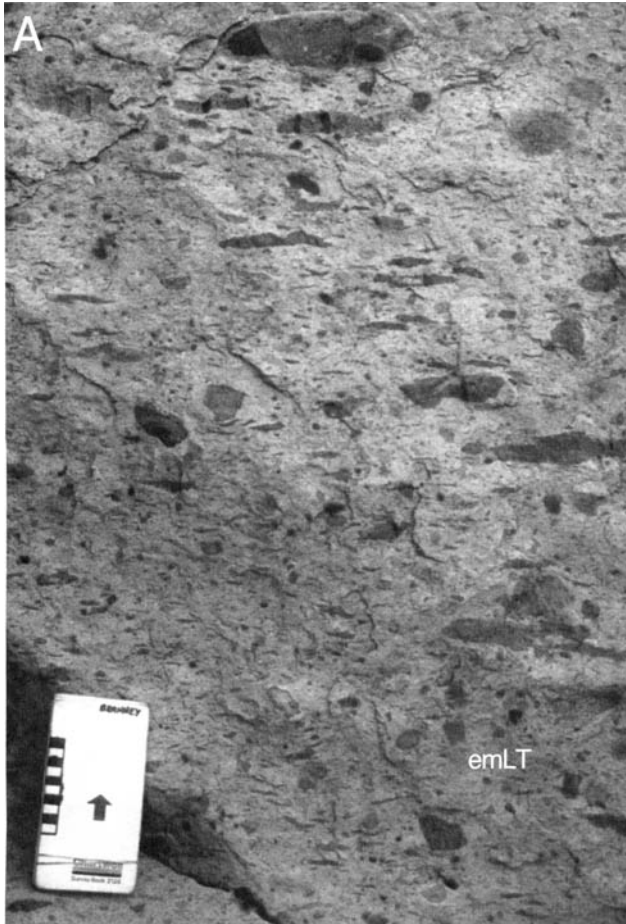
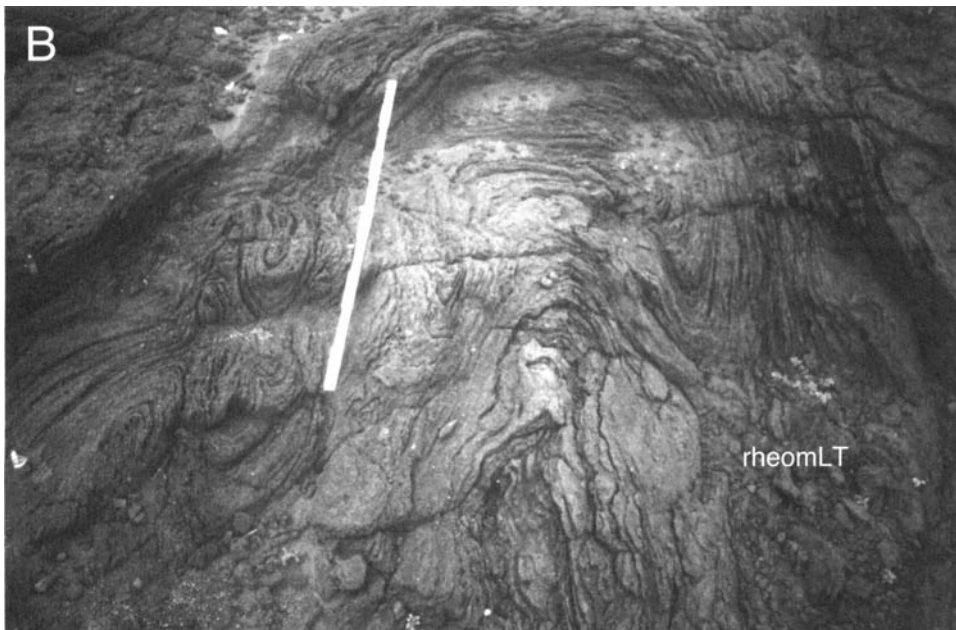


Fig. 5.12. Eutaxitic and rheomorphic lapilli-tuff lithofacies.

(A) Eutaxitic massive lapilli-tuff (emLT) showing flattened fiamme and equant lithic lapilli supported in a welded tuff matrix. Arico ignimbrite, SE Tenerife.



(B) Refolded folds in eutaxitic massive lapilli-tuff (rheomLT). The rheomorphic Green Tuff ignimbrite, Pantelleria (Mahood & Hildreth 1986). The metre rule is for scale.

height, which is a function of the eruptive mass flux, or changes in wind direction (Sparks *et al.* 1997a). Remnant fallout layers that are discontinuous or that pinch and swell as a result of scour by subsequent pyroclastic density currents may be distinguished from pumice lenses (plensL) deposited from pyroclastic currents by the angularity of the pumice lapilli and by the recognition of correlatable fall stratigraphy that shows systematic regional variations.

The less well sorted lithofacies within this group may include proximal pumice fallout deposits from an eruption plume, which

are typically less well sorted (e.g. Sparks *et al.* 1997a), or Plinian or sub-Plinian pumice fallout that was accompanied by rain flushing of fine ash (Walker 1981), and/or simultaneous ashfall from co-ignimbrite or phreatomagmatic ash plumes (see the next section). Where pumice fall was followed by fine-ash deposition, the uppermost few centimetres of a pumice fall layer may acquire an ash matrix by percolation from above.

The presence of pumice fall layers within a sheet of mLT or xsT records temporary cessations of flow *at that location* (see pp. 91 and 95).

Parallel-bedded and parallel-laminated tuffs (e.g. //bT, //sT)

Description

Lithofacies of this group range from fine to coarse ash (Fig. 5.11B–E). The fine-ash lithofacies typically comprise predominantly vitric shards with subordinate crystal and lithic particles, whereas coarser grained ash typically comprises predominantly granule- to sand-grade fragments of pumice, obsidian and/or crystal fragments with subordinate lithic particles and vitric shards. The lithofacies form layers from millimetres to decimetres thick, and in rare cases can reach as much as a few metres thick. Some layers are internally massive and typically show subtle or marked vertical grading patterns, whereas others exhibit diffuse to sharp, laterally continuous parallel bedding (//bT) or lamination (//sT) picked out by subtle or marked grain-size changes (Fig. 5.11B–D). The lithofacies lack tractional stratification, cross-stratification, segregation pipes or lenses. They may occur at any level within an ignimbrite sheet (Chapter 6), and tops and bases of layers may be diffuse or sharp, with or without evidence of erosional scour or loading. The lithofacies range from very well sorted (σ_ϕ 0–1) to moderately sorted (σ_ϕ c. 2) and poorly sorted (σ_ϕ 2–4; e.g. Walker 1971). Beds and laminations may uniformly drape topographic slopes less than 33° with little outcrop-scale variation in thickness, except where there has been subsequent scouring. Such layers may, if not extensively scoured, be traced for tens of kilometres, and show systematic regional variations in thickness and grain size that are independent of topography (Walker 1971; Fisher & Schmincke 1984). Other layers thicken in topographic lows (Fig. 5.11C) and thin over topographic highs; they may grade vertically or laterally into stratified, cross-stratified tuffs and/or massive lapilli-tuffs (sT; xsT; mLT). They may occur plastered against steep to vertical slopes, and may contain accretionary lapilli (e.g. //bTacc), pellets (e.g. //bTpel; //sTpel) and/or ellipsoidal or irregular-shaped vesicles (e.g. //bTvcs; //sTvcs).

Interpretation

These lithofacies include fall deposits from eruption plumes and deposits from ash-rich pyroclastic density currents. It can be difficult to distinguish between these origins at a single exposure. Four criteria for discrimination may be considered. (1) Individual beds and laminations may be traced tens of metres in order to determine whether they maintain constant thicknesses and grain sizes, as in ashfall deposits from an eruption plume, or whether they thicken and/or coarsen into topographic lows and thin over topographic highs and/or show asymmetric draping relationships, as would be the case if they were deposits of pyroclastic density currents (Fig. 5.11C). (2) By correlating individual beds and laminations between exposures, it may be determined whether they show systematic regional thickness and grain-size variations (especially of the coarse tail) consistent with an origin by ashfall from an eruption plume. (3) They may be traced to determine whether they show lateral gradations into tractionally stratified and cross-stratified tuffs (sT; xsT) or into lapilli-tuffs (dbLT; mLT), which would be consistent with an origin from a pyroclastic density current. (4) Pumice clasts within them may show evidence of rounding, indicative of abrasion during transport in a pyroclastic density current. Ashfall deposits may be from vent-derived magmatic or phreatomagmatic eruption plumes or from co-ignimbrite or phoenix plumes (Fig. 2.2).

Some lithofacies in this group may record ash fall enhanced by rain-flushing (Walker 1981; Talbot *et al.* 1994) or by electrostatic or moist agglomeration (clustering) of fine ash (Schumacher & Schmincke 1995; Sparks *et al.* 1997a). The latter is sometimes indicated by fines-rich lithofacies that contain vesicles and/or pellets and/or accretionary lapilli (Table 5.3). Rain-flushing may be indicated by poor sorting, raindrop impact structures (Walker 1981), vesicles (Lorenz 1974; Rosi 1992) and/or isopach distribu-

tions that indicate localized showers. An origin involving water can also be indicated by evidence for syneruption rill erosion (Branney 1991) and slurry flows (Lorenz 1974). Rain or moisture within an ash plume may be due to a phreatomagmatic eruption, or may result from precipitation of meteoric moisture, in some cases enhanced by convective perturbation of the atmosphere caused by the explosive eruption.

Parallel-bedded or laminated, moderately sorted ash layers may be deposited from a direct fallout-dominated flow-boundary zone of a fully dilute pyroclastic density current (see p. 37). This type of flow-boundary zone occurs where current velocities are too low for traction to occur, and where the lowermost part of the current is too low in concentration for significant grain interactions or hindered settling effects. In rare cases it may also occur in currents of higher velocities, where the rates of deposition are sufficiently high to suppress traction (Arnott & Hand 1989; see p. 37). Laterally continuous parallel layering suggests unsteady but virtually uniform deposition. Gradations into other lithofacies (e.g. mLT; xsT) reflect intermediate flow-boundary types.

The presence of ashfall layers within a sheet of mLT or xsT records temporary cessations of flow *at that location* (see pp. 91 and 95; Fig. 6.10A). Conversely, the presence of localized tractional (sT, xsT) layers enclosed within fallout layers (//bT; //sT) may record momentary gusts of wind during sustained pyroclastic fall, or momentary passage of turbulent eddies within a density current otherwise undergoing direct fallout-dominated deposition.

Eutaxitic, rheomorphic and lava-like lithofacies (e.g. emLT; edbLT; rheomLT; lava-likeT)

Description

Some massive and bedded lithofacies of ignimbrites possess a eutaxitic fabric of deformed juvenile pyroclasts, for example fiamme and flattened shards (Fig. 5.12) (Ross & Smith 1961). Eutaxitic fabrics most commonly record hot welding deformation of pyroclasts, but can also form by depositional alignments of discoidal pyroclasts, by cold burial-compaction associated with diagenesis (Branney & Sparks 1990), by hot deformation of lava autobreccias, or by tectonic deformation.

Welding varies from 'incipient', with barely detectable pyroclast deformation, through to 'intense', with good eutaxitic fabrics (emLT), and to 'coalescence', wherein pyroclast outlines are completely obliterated so that the lithology resembles lava ('lava-like' of Branney *et al.* 1992; Freundt & Schmincke 1995). 'Grade' in ignimbrites refers to both the proportion and the intensity of welding development relative to the sheet thickness; for example, extremely high-grade ignimbrites are intensely welded even close to the sheet margins (Walker 1983; Branney & Kokelaar 1992). Bulk rock density and fiamme length-to-thickness ratios generally increase with increasing welding intensity, although they can start to decrease again in some extremely high-grade ignimbrites as a result of inflation of the hot tuff caused by *in situ* vesiculation during or after welding (Schmincke 1974). Development of pronounced elongation lineations, folds, kinematic indicators, boudins and thrust repetitions in intensely welded lapilli-tuff (rheomLT) indicate syn- and/or postwelding hot-state ductile shear deformation, known as rheomorphism (Fig. 5.12B) (Schmincke & Swanson 1967; Chapin & Lowell 1979; Wolff & Wright 1981; Branney & Kokelaar 1992; Leat & Schmincke 1993; Kokelaar & Königer 2000; Sumner & Branney 2002).

Interpretation

Welding in ignimbrites traditionally has been interpreted in terms of loading-compaction and cooling of a gas-permeable, initially

isothermal, sheet (a 'cooling unit') or succession of rapidly stacked isothermal sheets (a 'compound cooling unit') (Ross & Smith 1961; Riehle 1973; Riehle *et al.* 1995). However, vertical variations in welding intensity through an ignimbrite sheet also may, in part, reflect variations in the rheological properties of successive pyroclast populations supplied to a current's depositional flow boundary during progressive aggradation (Branney & Kokelaar 1992). This is manifestly the case where the intensity of welding in chemically zoned ignimbrites clearly correlates with the compositional layering (Leat & Schmincke 1993; Freundt & Schmincke 1995; Branney & Kokelaar 1997; Sumner & Branney 2002), rather than just with depth of burial or proximity to sheet margins. Elsewhere, the former differences (e.g. in temperature or volatile content) between successively deposited pyroclast populations may be less apparent. Factors that may affect the welding behaviour of successive batches of pyroclasts at the site of deposition include temporal changes in the compositions, volatile contents, temperatures, grain-size populations and lithic contents of the pyroclast populations. These, in turn, probably reflect changes in the eruptive mixture at source, and/or modifications during transport and deposition (e.g. mass flux, cooling, degassing, air ingestion, overpassing, elutriation and erosional incorporation). Evidence of welding-intensity variations independent of ignimbrite thickness (e.g. Branney & Kokelaar 1992; De Silva 1989; Streck & Grunder 1995; Schumacher & MuesSchumacher 1996) suggest that in some ignimbrites lithostatic load in welding was less important than were contrasting rheologies of the hot pyroclasts in determining welding variations.

In some cases welding evidently starts *during* deposition and it can, in a sense, initiate within the base of the current. Such rapid welding is termed 'agglutination', and is inferred from field evidence, such as inclined linedated welding fabrics (Branney & Kokelaar 1992; Sumner & Branney 2002), from internal erosional truncation of welding fabrics (Chapin & Lowell 1979; Kokelaar & Königer 2000), from textural evidence (Branney *et al.* 1992; Freundt & Schmincke 1995) and from analogue modelling (Freundt 1998). Touching pyroclasts agglutinate by developing a connecting 'sinter neck', which involves a very localized flow of hot glass (Seville *et al.* 1998). Thus, agglutination is dependent on the viscosity of the pyroclasts, the duration of the contact and the force applied. Stationary fluidization experiments show that when hot clasts start to agglutinate, agglomeration causes abrupt deposition with or without formation of vertical pipes (Gluckman *et al.* 1976; Freundt 1998; Seville *et al.* 1998). This observation has been used to infer that pyroclastic density currents must primarily be low-concentration, turbulent suspensions with few grain interactions (Fisher 1989; Freundt 1998). However, in contrast with stationary fluidization experiments, high granular temperatures within rapidly shearing pyroclastic density currents may reduce the tendency for agglutination, and consequently the tendency for the concentrated dispersion to collapse. This is because short-duration high-velocity impacts do not favour neck formation, and because sinter necks are very fragile in their early stages of formation (see Seville *et al.* 1998) and are easily broken by shear and attrition.

Flow-boundary processes are unaffected by postdepositional welding ('load welding' of Freundt 1999), but they may be significantly affected by agglutination. In a density-stratified current, agglutination is most likely to occur close to the lower flow boundary where clast concentrations are high and the granular temperature is low. Here, clast interactions are more frequent, more sustained and have lower velocity impacts. It may be that agglomeration caused by agglutination higher in the current increases the rate of settling from a turbulent suspension (Freundt 1998).

It is interesting that welding is more commonly observed in massive ignimbrite than it is in tractionally stratified lithofacies. Viewed simplistically, this may be taken to suggest either that fully dilute currents tend to be colder and so rarely produce welded deposits (but modelling suggests that cooling in low-concentration

currents may be minimal; Freundt 1999), or that evidence for hot, low-concentration transport is missing because agglutination widely prevents traction. The presence of fines-poor elutriation pipes in some moderately welded ignimbrites (e.g. Upper Bandelier Tuff at Los Alamos; Self & Sykes 1996) suggests that welding at these locations began in the deposit below the level where the elutriation pipes developed (see pp. 61–66), because welding would prevent the elutriation of fine ash.

Ignimbrite permeability (which in non-welded ignimbrite is a function of sorting) can influence welding intensity. Soluble gases, such as water vapour, trapped within a hot aggrading ignimbrite may be resorbed into hot pyroclasts and lower their viscosity, thus enhancing welding. However, if gases can escape, water vapour is not so readily resorbed and welding is inhibited (Sparks *et al.* 1999). Abundant postwelding vesicles in some extremely high-grade ignimbrites indicate entrapment of exsolved gases caused by agglutination during deposition (Schmincke 1974; Branney & Kokelaar 1992). Zones of spherulitic lithophysae indicate the presence of dissolved water within vitrophyric parts of some densely welded ignimbrites (Ross & Smith 1961). Dissolved gases, such as water vapour or halogens, high alkali contents (as in strongly peralkaline ignimbrites; Mahood 1984) and high emplacement temperatures can serve to maintain a low viscosity of an agglutinate and facilitate rheomorphism.

Clearly, there is much more to learn about the exsolution and resorption behaviour of pyroclasts and agglutinate during emplacement and welding of ignimbrites: for example concerning the different exsolution rates and effects on pyroclast rheology of different volatile species. Vesicularity in rheomorphic ignimbrites is commonly heterogeneous and may occur preferentially in either flammé or matrix, and the variety of vesicle and pyroclast shapes indicates that vesiculation occurs before deposition, during rheomorphism and after rheomorphism.

Origin of poor sorting in ignimbrites

The major parts of ignimbrites are characteristically very poorly sorted (σ_ϕ 2–5), rich in fine ash and have matrix-supported lapilli and/or blocks ('diamicts' *sensu* Harland *et al.* 1966). Six factors contribute to this poor sorting. (1) The erupted grain-size population is very poorly sorted with abundant fine ash. This is due to explosive fragmentation processes (e.g. rapid shear, decompression and vesicle rupture) and to turbulent mixing with limited segregation in the eruptive fountain. (2) Fine ash is produced by attrition of friable microvesicular pumice clasts during hyperconcentrated flow in lower parts of density currents. Attrition involves both breakage, to form relatively large particles, and abrasion, to form fine ash (Stein *et al.* 1988; Kalman 1999), the evidence for which is in the ubiquitous rounding of pumice lapilli in ignimbrites relative to those in Plinian fall deposits. Breakage during transport produces fragments with fragile and easily abraded sharp edges. It results from high-velocity impacts with the substrate and with other large clasts, and is enhanced by stresses within clasts due to rapid changes in temperature and pressure. (3) Particle agglomeration and clustering of fine-ash particles (e.g. due to electrostatic forces) causes deposition at settling velocities far greater than those of the individual constituent particles. Fine ash also deposits by adhering to larger clasts (e.g. lapilli). Particle agglomeration is a well-known cause of aggregative fluidization behaviour in gas-fluidized systems, in which powders can be rapidly dumped (deposited) at gas flow rates that would be sufficient to elutriate or fluidize them were they more homogeneously dispersed (e.g. Kwauk *et al.* 2000). Well-formed agglomerations (pellets and accretionary lapilli) are found in ignimbrites, but the majority of deposited loose-particle clusters are unlikely to survive so as to be recognizable following compaction and changes in moisture. (4) Poor sorting is enhanced by particle interlocking (see p. 35) in the flow-boundary zone of granular fluid-based pyroclastic density currents, where particle concentrations are high. Unlike typical

siliciclastic grains, pyroclasts (other than pumice lapilli) normally have highly irregular and/or inequant forms that tend to prevent them rolling or sliding past one another. (5) Poor sorting results partly from the simultaneous existence of multiple transport mechanisms in density-stratified pyroclastic density currents. Pyroclasts of diverse size and density deposit together when depletive flow causes simultaneous deposition of clasts moving by different transport mechanisms. For example, large lithic blocks rolling along relatively slowly may deposit at the same time and location as small pumice lapilli and ash particles that were erupted later than the blocks but which were transported more rapidly by different mechanisms. (6) Poor sorting arises due to the rapidity of

emplacement. Compared to most other sedimentary systems, ignimbrites are exceptionally immature in that there may only be seconds to minutes between the formation of the clasts (fragmentation, rock fall, erosion) and their deposition. Although many segregation processes do occur (reviewed in Chapter 3), they may have little time in which to operate. Also, even as fine ash is segregated by elutriation, more is produced by attrition, possibly at rates similar to those at which it is lost (e.g. Stein *et al.* 1988). As described in earlier sections, some ignimbrite lithofacies are relatively well sorted (e.g. some pumice lenses, lithic breccias, scoria-agglomerates and some cross-stratified tuff), indicating that particle segregation is efficient locally.

This page intentionally left blank

Chapter 6

Ignimbrite architecture: constraints on current dynamics

This chapter explores how ignimbrite architectures and lithofacies associations can be used to infer how flow-boundary zones of pyroclastic density currents vary with time, downcurrent, laterally and with topography. The approach hopefully will be developed further so deposits can be used more precisely to constrain the dynamics of pyroclastic density currents.

The initial analysis of a complex ignimbrite sheet should be purely descriptive. An ignimbrite sheet may be divided into 'divisions'. A division is a basic architectural unit, and may comprise a layer, lens or any specified part of the deposit that has some common characteristics and/or bounding surface(s). A division may be characterized by a lithofacies or a group of lithofacies.

Conceptualizing architecture in a time-geometry framework

To determine how a pyroclastic density current evolved in time and space requires correlation of the internal lithofacies and divisions of an ignimbrite within a time-geometry framework. The deposition of layers, lithofacies and compositional zones in ignimbrites (Fig. 6.1) may be diachronous (see below). It is useful, therefore, notionally to subdivide an ignimbrite sheet with time surfaces, which form time-lines in cross-section. One type of time-surface is a depositional isochron, or *depochron* (new term), which joins pyroclasts deposited at the same instant in time (Fig. 6.2). A depochron represents an instantaneous aggradation surface. Ignimbrite lithofacies along a depochron record the depositional processes at the flow boundary of an entire pyroclastic density

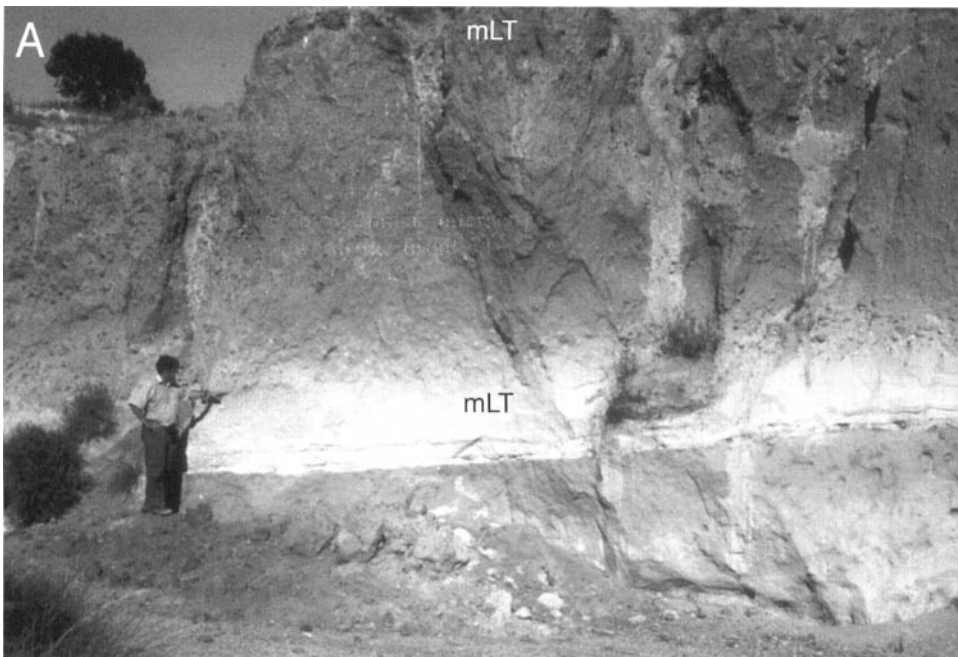


Fig. 6.1. Compositionally zoned ignimbrites.

(A) Gradational chemical zonation within massive lapilli-tuff (mLT). The gradual colour variation with height reflects a gradually increasing abundance of dark andesite pumice clasts, reflecting temporal changes in the clast population supplied to the site of deposition from a sustained pyroclastic density current. The geologist points to the first appearance of andesite pumice. This horizon, or 'entrachron' (see next page), may be correlated widely within the sheet. Zaragoza ignimbrite, Pueblo, central Mexico.



(B) Gradational vertical chemical zoning in the Mazama ignimbrite, outflow sheet of Crater Lake caldera, Oregon, USA (Bacon 1983). The ignimbrite comprises massive and locally diffuse-bedded lapilli-tuff, inferred to be deposited from a sustained pyroclastic density current.

current at a single instant in time. Variations in lithofacies along a depochron indicate depositional non-uniformity, whereas variations between successive depochrons indicate how deposition changed with time. Depochron spacing is proportional to rate of aggradation (Fig. 6.2); convergent depochrons indicate spatially decreasing aggradation rates, and merging or cross-cutting depochrons record a depositional hiatus or erosional event.

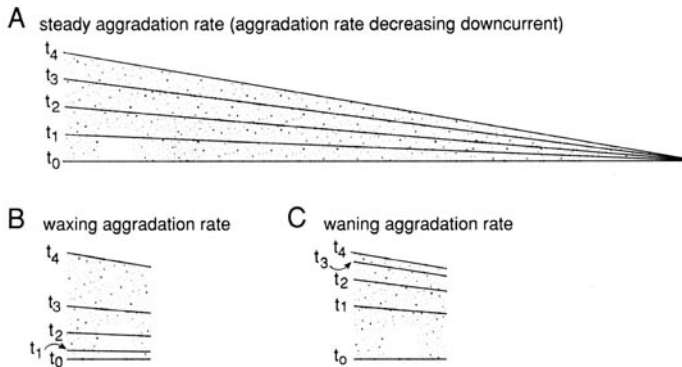


Fig. 6.2. (A) A schematic longitudinal section through an ignimbrite wedge deposited by a steady pyroclastic density current, showing depositional isochrons, or *depochrons*, for times t_0 – t_4 . Depochron spacing is proportional to rate of deposition. (B) and (C) Depochrons from unsteady currents.

Depochrons can have the form of subhorizontal to gently sloping cryptic surfaces (Fig. 6.2). Some may practically coincide with layers and bedding surfaces on the scale of individual exposures. However, on the scale of an entire ignimbrite sheet, depochrons can be oblique to layering or bedding, which typically marks the progress of an eruptive surge, or lull between surges, advancing downcurrent current with time. Because the proximal and distal limits of deposition of pyroclastic currents advance and/or retreat with time, the top and bottom surfaces of ignimbrite sheets commonly are diachronous (Fig. 6.4). In practice, depochrons are difficult to distinguish and trace within an ignimbrite sheet, because they tend to be cryptic. They are, for example, invisible within massive lapilli-tuff (mLT). However, depochrons are useful conceptually to envisage how deposition may proceed.

Another sort of time line through an ignimbrite sheet joins pyroclasts that entered the pyroclastic density current together at the same time and place (at source, for example), and is here termed an entrainment isochron, or *entrachron* (new term). Because diverse pyroclasts that entered the current at the same instant may end up scattered through some considerable part of the thickness of an ignimbrite sheet as a result of their differing transport speeds, an entrachron is taken as the line or surface that joins their *first*

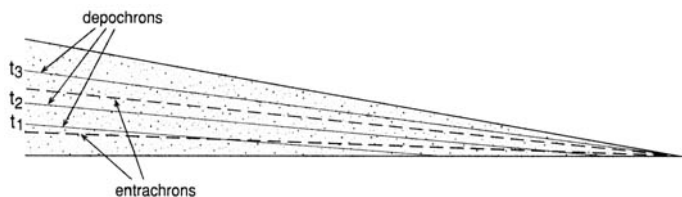


Fig. 6.3. Two types of time-lines depicted within a longitudinal section through an ignimbrite. Depochrons (depositional isochrons) represent instantaneous aggradation surfaces, and entrachrons (entrainment isochrons) connect first appearances of pyroclasts that entered the current instantaneously as a batch. Entrachrons may be picked out by compositional zoning (Fig. 6.1). Each entrachron is slightly diachronous because of the time taken for the batch of pyroclasts to reach the depositional limit. The two types of time-line are oblique to each other, but appear virtually parallel on the scale of an individual field exposure.

appearances as located upwards from the base of the ignimbrite. Entrachrons can be traced both laterally and longitudinally from one ignimbrite lithofacies into another in the field by following compositional changes (zoning; Fig. 6.1) (e.g. Wright & Walker 1981; Druitt & Bacon 1986; Branney & Kokelaar 1997). For example, an entrachron may be marked by the first appearance of a new type of pumice, crystal or lithic clast. Entrachrons can show how flow-boundary conditions along the length of a current related to variations in the supply at source: for example, to changing mass flux, composition or vent dimensions. Entrachrons can be parallel to bedding. In longitudinal sections through an ignimbrite sheet they lie slightly oblique to depochrons, and typically transgress gradually upwards across them with distance from source (Fig. 6.3). However, on the scale of an individual field exposure the two types of time lines practically coincide.

Consideration of time lines helps one explore how the architecture of an ignimbrite was constructed. A longitudinal section through an ignimbrite that progressively aggraded from a steady depletive current is shown in Fig. 6.2A. The depochrons converge at the distal tip of the ignimbrite wedge, which marks the stationary runout limit of the current. Their spacings show that the rate of deposition decreased with distance from source, but remained constant at each location. Such steadiness is rare, and depochron spacing commonly varies with height (e.g. Fig. 6.2B and C).

The runout distance of a pyroclastic density current normally varies with time: for example, the initial waxing phase is typically accompanied by leading-edge advance. Deposition during this phase may be progradational (Fig. 6.4A). In other cases the advancing front part of the current may not deposit until it has passed proximal steep slopes and then, with sustained aggradation, deposition may onset progressively nearer source (retrogradational

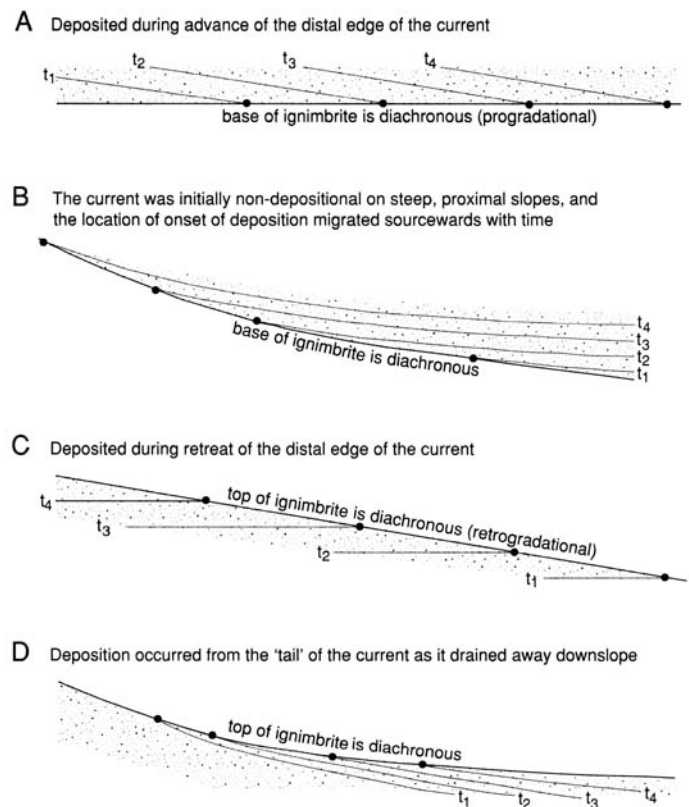


Fig. 6.4. Diachronous tops and bases of ignimbrite sheets (stippled) in longitudinal section. These schematic architectures relate to variations in current non-uniformity with time. Time-lines t_1 – t_4 are depochrons, which depict instantaneous aggradation surfaces.

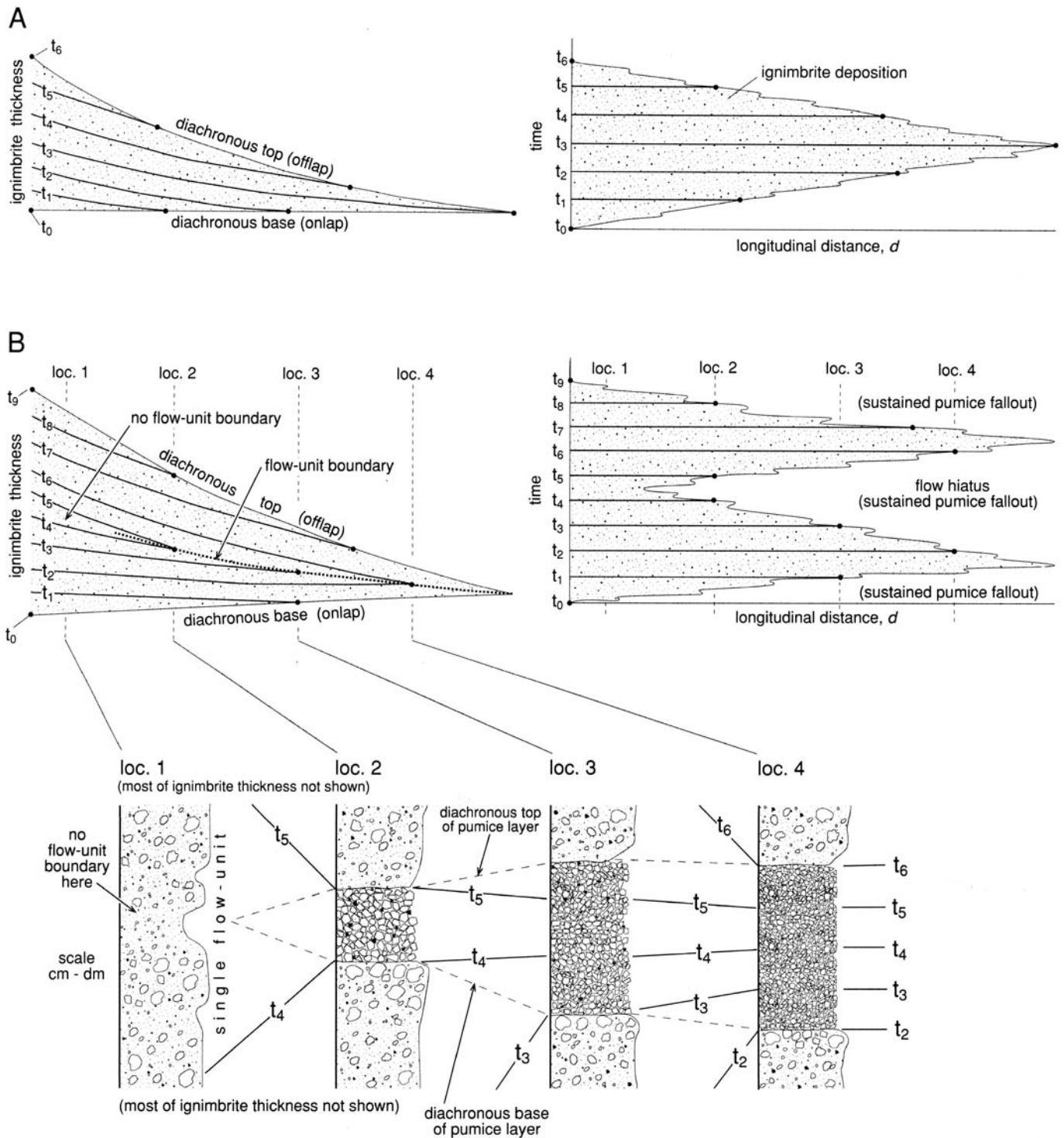


Fig. 6.5. Longitudinal architectures of ignimbrites, shown both as vertical cross-sections (left) and plotted against time (right). (A) Ignimbrite deposited from a sustained depletive current that first waxed, then waned. The time-lines (depochnons) t_1 – t_5 are not generally marked by bedding surfaces and much of the ignimbrite sheet could be massive. (B) Ignimbrite deposited from a sustained depletive current that waxed and waned twice during continuous Plinian pumice fallout. At locality (loc.) 1 the ignimbrite comprises one flow-unit, whereas at localities 2–4 it comprises two flow-units separated by a flow-unit boundary that represents a hiatus in flow (see left). As the pyroclastic density current was accompanied by pumice-fallout, a pumice fall layer occurs intercalated within the ignimbrite sheet (inset, below). The base and top contact of the intercalated pumice fall layer are diachronous and the layer thickens distally, even though it becomes finer grained with distance from source. Beyond the ignimbrite the layer merges with the pumice-fall layer that underlies the ignimbrite (not shown).

onset of deposition; Fig. 6.4B). During the final, waning phase of a sustained current the distal edge of the current may retreat sourceward, causing retrogradational cessation of deposition (Fig. 6.4C). Alternatively, the location of proximal onset of deposition may migrate away from the volcano as the tail of a current drains away downslope (Fig. 6.4D). Various combinations of these

scenarios produce quite different time–space architectures. Resolution of these architectures would be necessary, for example, to reconstruct fully the compositional zonation of a magma body from a zoned ignimbrite sheet. Some ignimbrite sheets may have cryptic internal progradational or retrogradational architectures (e.g. Brown 2001).

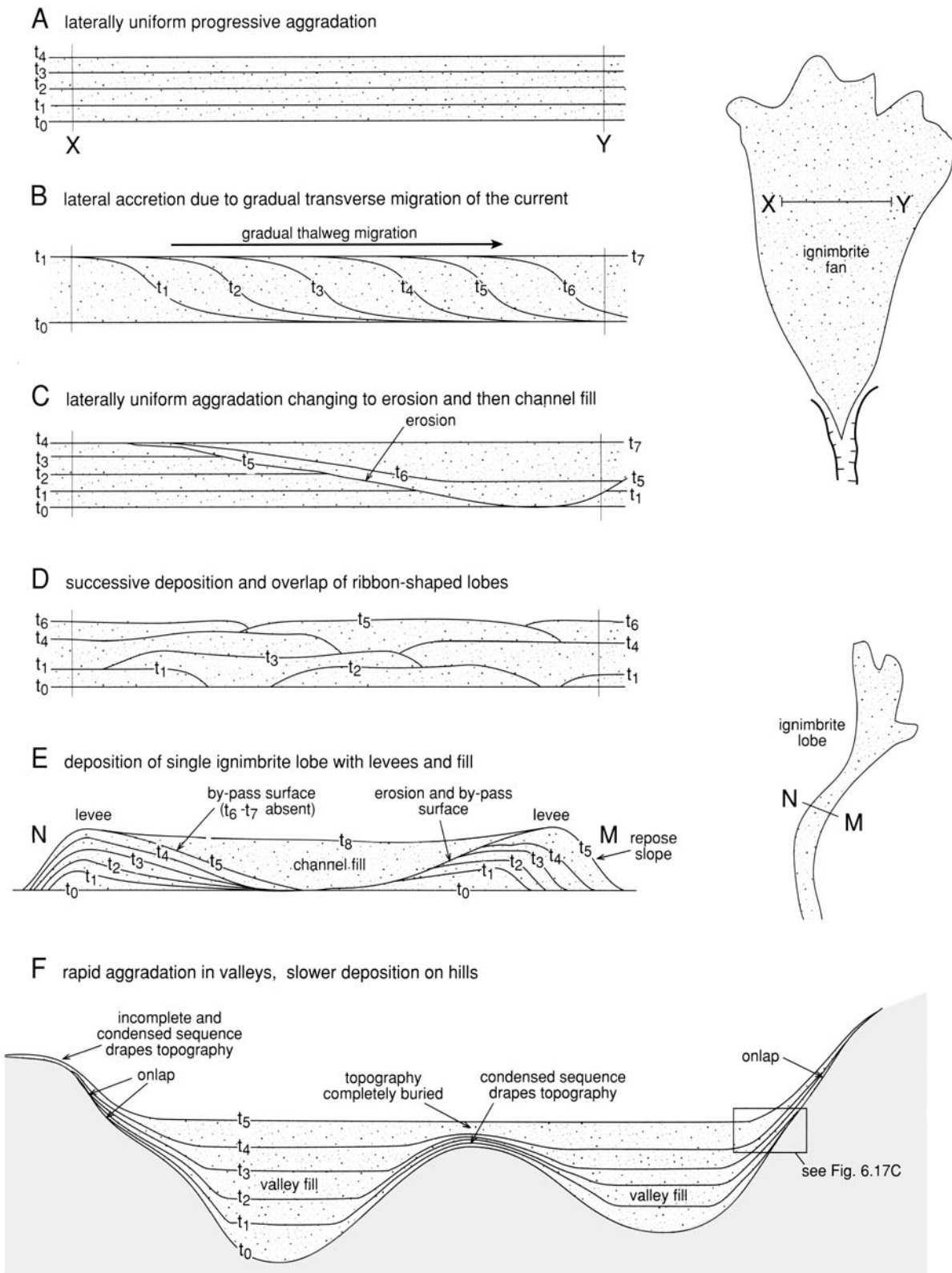


Fig. 6.6. Transverse architectures of ignimbrites showing various possible deepochron stacking patterns in vertical sections. See text for discussion. The uppermost three ignimbrite sections shown (A–C) could resemble each other in overall appearance because the deepochrons are cryptic: the ignimbrites may be massive. However, the underlying section (D), which shows deposition and overlap of ribbon-shaped lobes, may exhibit internal flow-unit boundaries even if the current was sustained at source.

Longitudinal architectures

A hypothetical longitudinal architecture for an ignimbrite sheet formed by a sustained current that gradually waxed and then waned is shown in Fig. 6.5A. The longitudinal variations are plotted first against thickness (on the left) and then also against

time (on the right). An explosive eruption that is sustained for several minutes or hours may generate a pyroclastic current that waxes and wanes more than once so that its distal limit migrates back and forth two or more times. This can produce an ignimbrite sheet that comprises a thick, massive proximal flow-unit that splits distally into two, or more, stacked units (e.g. Fig. 6.5B). Several

ignimbrite sheets have architectures with such characteristics: for example the main 1991 ignimbrite of Mount Pinatubo (M. J. Branney unpublished data), parts of the Bishop Tuff (Wilson & Hildreth 1997) and parts of the Ata ignimbrite (Aramaki & Ui 1966). Distal hiatuses are recorded as flow-unit boundaries within the distal parts of the sheet, but in proximal areas (locality 1 on Fig. 6.5B) deposition was sustained without a hiatus and the ignimbrite there comprises a single flow-unit (see 'Bedding and flow-unit boundaries' on p. 95).

In contrast, a pause in pyroclastic fountaining will produce a widespread, albeit short, cessation of the current, recorded as a flow-unit boundary that can be traced right back to source.

It is useful to consider what happens if steady fallout of pumice accompanied the emplacement of an ignimbrite. This happened, for example, during emplacement of the Valley of Ten Thousand Smokes ignimbrite (Fierstein & Hildreth 1992) and the Bishop Tuff (Wilson & Hildreth 1997). Where pumices fall directly into the current they do not produce a fallout layer. Thus, the thickness of a pumice-fallout layer at a particular location (e.g. Fig. 6.10A) is determined partly by the duration of the hiatus(es) in flow at that location (Fig. 6.5B). Note that thickness variations of such a fallout layer then do not relate simply to dispersal, even at locations where there has been no erosion. Beyond the distal limit of the ignimbrite some levels within the pumice-fall layer are lateral time-equivalents of parts of the ignimbrite. If the average accumulation rate of the pumice-fallout layer can be estimated, the thicknesses of intercalated pumice fallout layers could be used to constrain the aggradation rates of the correlative parts of the ignimbrite (see e.g. Wilson & Hildreth 1997; also Fig. 6.19B). A consequence of the diachronous tops and bases of ignimbrites (e.g. Figs 6.4 and 6.5) is that the upper and lower contacts of apparently horizontal intercalated pumice-fall layers also can be diachronous. The basal part of a pumice-fallout layer that rests on ignimbrite at one location was deposited at a time slightly different to that when the basal part of the same fallout layer at another location was deposited, so that the base marks different time-slices of the same Plinian phase of the eruption (lower part of Fig. 6.5B). This is important, because traceable concordant (non-erosive) contacts between ignimbrite and fallout layers (including co-ignimbrite ash-fall layers) are commonly assumed to represent instantaneous event horizons, but they can be diachronous on time-scales that are significant in terms of the eruption duration (minutes to hours).

Transverse architectures

Depochrons may also be used to subdivide transverse sections through ignimbrites (see Fig. 6.6). Laterally uniform deposition produces stacked horizontal depochrons (Fig. 6.6A). In cases where currents flowed radially from a central vent, such depochrons may trace circumferentially around the volcano with constant vertical spacing. However, markedly less regular circumferential depochron stacking patterns may be the norm, even for apparently symmetrical radial ignimbrite distributions. It seems likely that most pyroclastic currents deposit different radial lobes or fans at different times, and that these may merge to form a continuous radial apron of ignimbrite as current directions changed during a sustained eruption (see Fig. 6.6B and pp. 115–117).

Depochrons converge where rates of deposition were lower, for example towards the locations of former lateral margins of a current, and over topographic highs (Fig. 6.6C, E and F). Convergent and cross-cutting depochrons (Fig. 6.6C–F), respectively, characterize sites of non-deposition and erosion, such as sites of former erosional thalwegs and channel margins. Lateral migration of current thalwegs may produce more complex, asymmetric stacking patterns (Fig. 6.6B, D and E). Thus, apparently horizontal tops and bases of some ignimbrite layers can be diachronous in transverse sections, just as in longitudinal sections.

Interpreting longitudinal (proximal to distal) lithofacies variations

We now consider how arrangements of lithofacies may relate to time–distance reference frames within large ignimbrite sheets. Proximal to distal changes in lithofacies along a depochron record downcurrent changes in flow-boundary conditions. These reflect current non-uniformity, such as depletive or accumulative velocity, concentration, or capacity (see p. 2), changes between subcritical and supercritical flow (pp. 16–19) and/or changes in turbulence intensity (pp. 11–12). Most pyroclastic density currents have extensive reaches that are depletive as a result of flow divergence (fanning out), flow onto slopes of lower gradient, and/or loss of gravitational impetus due to deposition, air resistance, air incorporation and lofting. Some reaches, however, are accumulative and erosive (see p. 2), such as where the topography causes flow lines to converge (e.g. become channelled) or where the slope locally increases downcurrent (e.g. a convex downslope profile).

Longitudinal coarse-tail grading

A decrease in the maximum size of lithic clasts from proximal mBr to distal mLT (Fig. 6.7A) is a common type of longitudinal variation (e.g. Walker 1985; Druitt & Bacon 1986). It probably records depletive competence, for example in a quasi-steady current. Such grading may be accompanied by longitudinal reverse grading of pumice clasts (Fig. 6.7A), because the low density of pumice lapilli can selectively hinder their deposition proximally (Figs 4.3 and 4.4) so that some overpass and deposit as distal pumice concentrations (see pp. 47 and 76). The longitudinal lithofacies succession along each depochron therefore can comprise mBr proximally, mLT medially and pmLT distally (Fig. 6.7A; note that depochrons cut across the lithofacies contacts). Although depochrons have yet to be traced throughout large ignimbrite sheets, aspects of this general type of facies architecture, such as proximal breccias passing into distal mLT, have been demonstrated, effectively using compositional zoning to define entra-chrons, for example at Acatlán (Wright & Walker 1981; Branney & Kokelaar 1997) and at Crater Lake (Druitt & Bacon 1986) (Figs 2.2B and 6.1B).

With waxing flow the locations of longitudinal lithofacies changes shift away from source with time, and hence with height in the ignimbrite (progradation), so that a vertical succession is formed with pmLT at the base overlain by mLT, in turn overlain by mBr (see Fig. 6.7B). With waning flow the locations of the longitudinal changes between the lithofacies migrate sourceward with height in the ignimbrite (retrogradation), resulting in vertical sections with lithic-rich bases and pumice-rich tops (Fig. 6.7C). Many ignimbrite flow-units have this type of architecture (e.g. 'standard' ignimbrite flow-unit of Sparks *et al.* 1973) and there are similarities with deposits from waning high-density turbidity currents (Lowe 1982). Architectures formed by currents with more complex waxing–waning flow histories are explored in the section on 'Complex longitudinal architectures' (p. 98).

Downcurrent lithofacies changes from stratified to massive

Several ignimbrite sheets exhibit longitudinal transitions from relatively thin stratified lithofacies (sT, xsT, xsLT) on steep proximal slopes, to thicker, massive medial and distal facies (mLT) on lower slopes (Rowley *et al.* 1985; Scott *et al.* 1996). Some smaller deposits also show transitions from proximal xsT to medial mLT (Wohletz & Sheridan 1979). Such downcurrent changes could be interpreted by invoking a *flow transformation* from a current that is turbulent to one that is laminar (Fisher 1979). Interpreting lithofacies changes in terms of a flow transformation, however, can be oversimplistic, because the lithofacies record

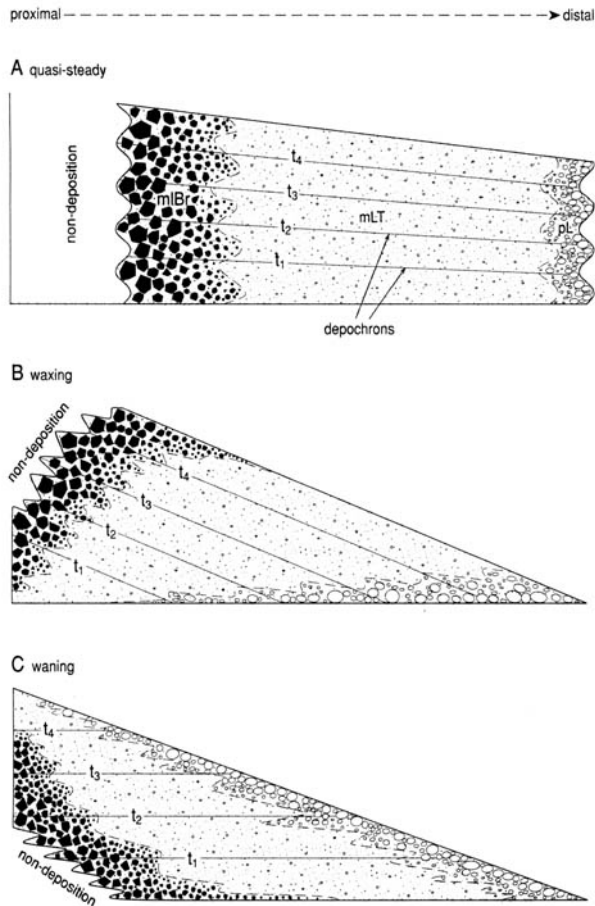


Fig. 6.7. Simple longitudinal ignimbrite lithofacies architectures from depletive currents (shown with considerable vertical exaggeration). (A) Lithofacies architecture of a steady current with depletive competence, in which some pumices overpass medial regions to be deposited at distal pumice accumulations. The ignimbrite is longitudinally normal-graded with respect to lithic blocks, and longitudinally inverse-graded with respect to pumice lapilli. (B) As (A) but with waxing flow. Vertical sections through the ignimbrite have abundant pumices at the base and lithics towards the top (e.g. Fig. 5.6B). (C) As (A) but with waning flow. Vertical sections of the ignimbrite have abundant lithics near the base and abundant pumice near the top (e.g. see Fig. 5.6A and E).

mainly the flow-boundary zone conditions and not the overall nature of the density current at that location (Chapter 1), and because currents, particularly those exhibiting some form of density stratification, can exhibit varying degrees of turbulence rather than abrupt wholesale transformations from one end-member flow state to the other (see p. 13).

We propose that longitudinal changes from proximal stratified ignimbrite to more distal massive ignimbrite *along a depochnon* record downcurrent changes in flow-boundary zone conditions, from traction-dominated to fluid escape-dominated (Fig. 4.1). These changes may or may not correspond with an overall flow transformation; some may represent only a minor difference in the overall fluid dynamic behaviour of the current (see Fig. 4.2). We therefore prefer to use the (new) term *flow-boundary zone transformation*. Consider, for example, a current that is depletive as a result of flowing onto lower slopes, or losing gravitational impetus through deposition or lofting. The depletive flow may cause: (1) a downcurrent decrease in flow-boundary shear rate; (2) an increase in depositional flux, as typically is indicated by a greater

thickness of massive ignimbrite on the lower slopes compared with the lesser thickness of stratified lithofacies on steeper proximal slopes; and/or (3) a downcurrent increase in concentration of the lowermost parts of the current, for example development of a concentrated bedload or traction carpet (see pp. 42–43), that is, a change from a fully dilute current to granular fluid-based current (see p. 20). Any of these may cause a downcurrent change from stratified to massive ignimbrite as a result of differing flow-boundary zone conditions.

The mechanisms and controls of development of high basal concentrations from a proximal fully dilute current require further research. Experiments show that rapid sedimentation of mono-disperse particles from low-concentration suspensions onto a topographic slope can lead to the formation of a high-concentration flowing granular layer (Nir & Acrivos 1990). This is because grains that have settled to the substrate surface continue to move downslope. In polydisperse currents, high concentrations in lowermost parts also develop as a result of the tendency for larger clasts that require intermittent substrate support to reside mostly in lowermost parts of the current as a bed load (see Fig. 3.3 and pp. 14–15). Pyroclasts settling rapidly onto a slope from a fully dilute pyroclast density current may continue to flow downslope in the form of a thin basal concentrated dispersion (e.g. modified grainflow), either before they properly come to rest, or by remobilization of a loose, momentarily deposited layer (see p. 49). Either way, once a thin high-concentration shearing layer is produced, tractional segregation within it is suppressed and the current's flow-boundary zone has changed from tractional to fluid escape-dominated or granular flow-dominated. There will be a resultant change in ignimbrite lithofacies from stratified to massive (Fig. 6.8A). This may have occurred in the 18 May 1980 blast-generated pyroclastic density current at Mount St Helens (Fisher 1990a) and in some small pyroclastic density currents at Montserrat (Druitt *et al.* 2002). Even where there is little or no topographic slope, a process similar to that in the experiments of Nir & Acrivos (1990) may occur, but in which the basal high-concentration dispersion is driven along the ground by shear exerted from the overriding part of the current as a traction carpet (pp. 42–43), rather than simply by draining downslope.

Once the traction-dominated flow-boundary zone has changed to fluid escape-dominated, the density current downstream may evolve rapidly. This is because the depositional flux from the current (Rd on Fig. 6.8, inset) is now limited by the rate of fluid escape in the flow-boundary zone, which in turn is a function of the voidage (clast concentration and grain-size distribution) of the lowermost part of the current (see p. 33). In contrast, the flux of pyroclasts supplied by the current to the basal, high-concentration part of the current (Rs on Fig. 6.8) is a function of depletive capacity of the current. The likelihood of a balance between these two fluxes (Rd and Rs) is small, and the concentrated layer will thicken where the flux of clasts supplied to the high-concentration shearing layer exceeds the depositional flux (i.e. $Rs > Rd$ at sites 2–3 on Fig. 6.8). For example, at a lessening (concave) slope and/or where the current encounters a topographic barrier, an initially thin modified grainflow layer may thicken rapidly in a downcurrent direction, and flow increasingly according to its own gravitational impetus (e.g. site 4 on Fig. 6.8), rather than as a result of shear exerted by the overriding less concentrated parts of the current (as with a traction carpet). In this way, high concentrations may come to dominate the entire current thickness and the current has effectively 'transformed' along a reach from a fully dilute current, in which most clasts were supported by fluid turbulence, to a granular fluid-based current entirely dominated by grain interactions and/or fluid escape (site 4 on Fig. 6.8). The resultant granular fluid-based current is likely to develop its own density stratification, for example by gravitational segregation and turbulent ingestion of air along its upper flow boundary. It may transform again according to its flow path, for example it may revert to a fully dilute current in an accumulative reach (Fig. 6.9A).

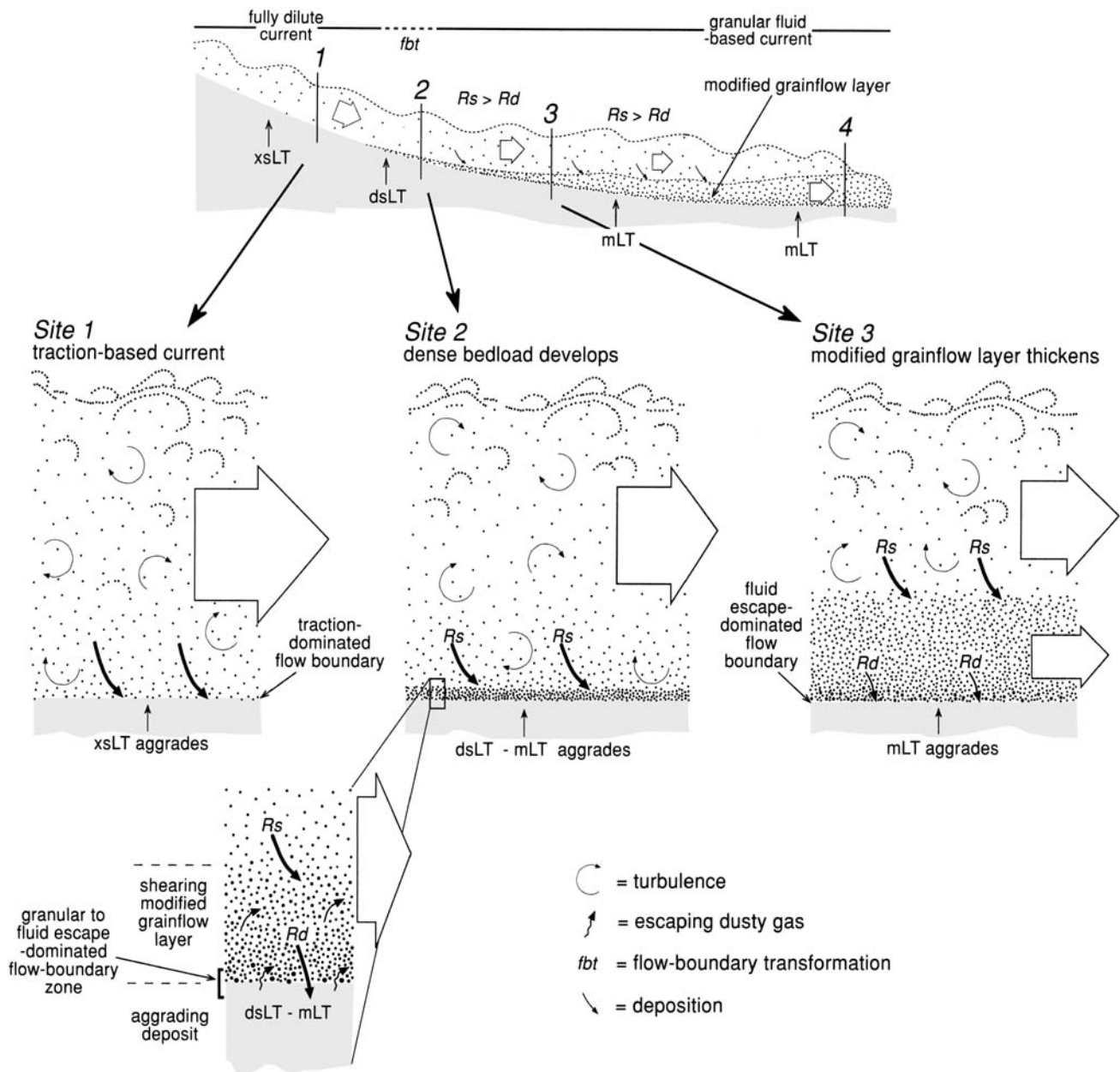


Fig. 6.8. Downcurrent changes from a fully dilute current (site 1) to a granular fluid-based current (sites 2–4). This constitutes a *flow-boundary zone transformation*. Site 1: proximal fully dilute current deposits stratified lithofacies. Site 2: the current develops a concentrated bedload (e.g. traction carpet); inset shows detail. Rate of deposition, R_d , is the mass flux of pyroclasts into the deposit per unit area of the flow boundary. Rate of supply, R_s , is the mass flux of pyroclasts per unit area, supplied to the top of the lowermost concentrated part of the current. The situation at site 2 is unstable because R_d is limited by processes and conditions that cause hindered settling (fluid escape, permeability; see p. 33), whereas R_s is controlled by depletive capacity (p. 2) of the overriding dilute parts of the current. The bed load may pinch out, be swept away by a turbulent eddy or thicken downcurrent as a result of $R_s > R_d$, as depicted for site 3. In some cases the concentrated lower part of the current may thicken sufficiently to dominate the current thickness, as depicted for site 4.

Distal lithofacies changes from massive to stratified

A downcurrent change along a deepochron from massive (mLT) to stratified (sT) lithofacies is interpreted as recording a flow-boundary zone transformation from a proximal, granular fluid-based current with a fluid escape-dominated flow-boundary zone to a distal, fully dilute current. In this case, clast concentrations in lowermost levels of the proximal current are sufficiently high for grain interactions and fluid escape to be important, even at sites where they are unimportant at higher levels in the current. The thickness of the lower concentrated part of the current decreases

downcurrent where $R_s < R_d$. Where this thickness decreases to zero, the flow-boundary zone changes to traction-dominated (e.g. Fig. 6.9). There are two alternative ways this may occur (Fig. 6.9A and B). (1) Turbulence intensity increases in an accumulative reach of the current so that turbulent eddies increasingly impinge down to the flow boundary, and reduce the concentration of the lowermost part of the current. In this case R_s is negative in that there is a net transfer of pyroclasts from the modified-grainflow layer to those parts of the current that are dominated by fluid turbulence (e.g. Fig. 6.9A). (2) In a distal, depletive reach of the current the pyroclast population of a modified-grainflow part of the current may deposit

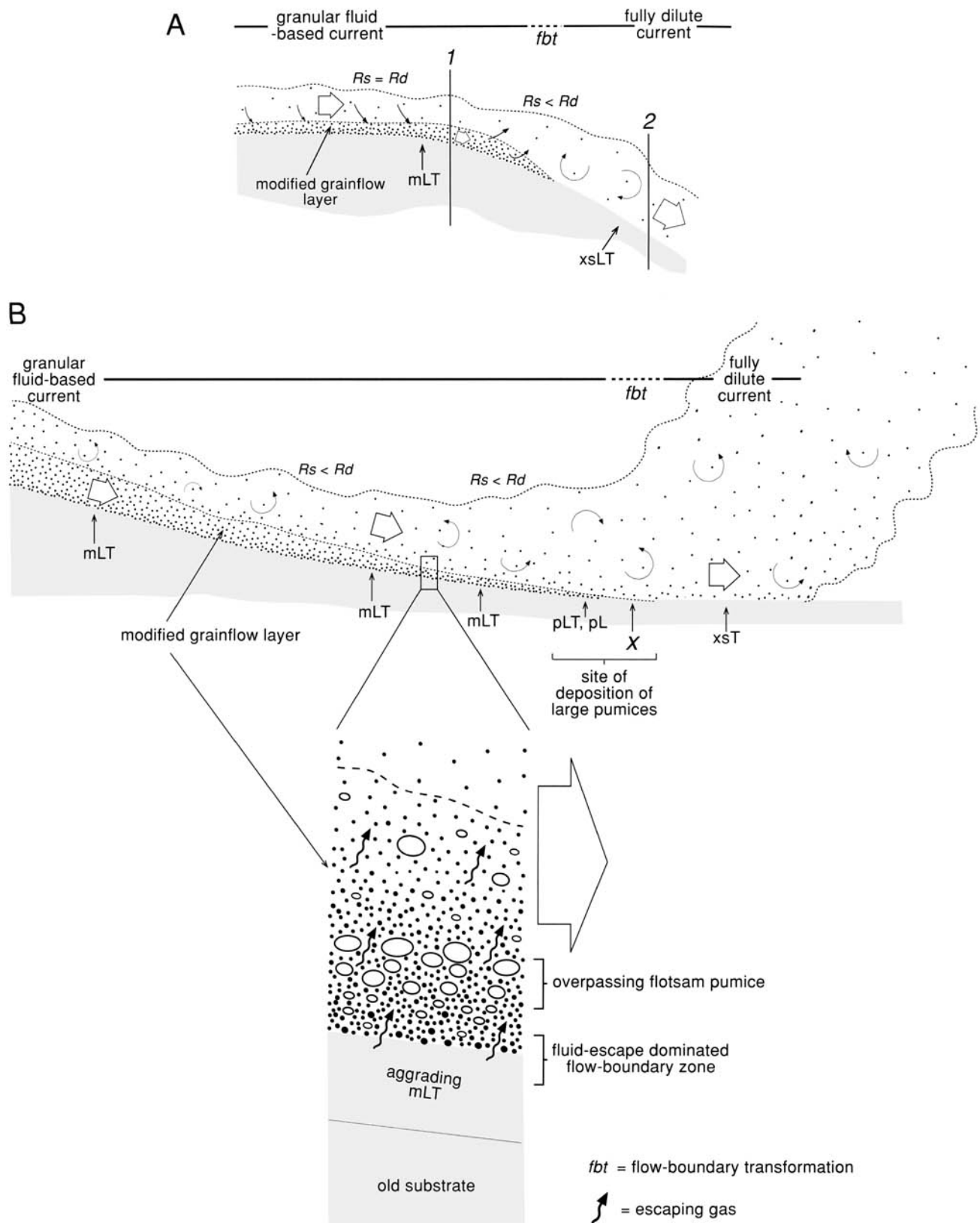


Fig. 6.9. Two ways of producing downcurrent changes from massive to stratified ignimbrite. (A) Accumulative flow at an increase in slope may cause a flow-boundary zone transformation from fluid escape- or granular fluid-dominated (at site 1) to traction-dominated (at site 2) as a result of accumulative velocity and increased turbulence intensity. Clasts within lower parts of the current are increasingly entrained by turbulence and form lower concentrations due to mixing with air. R_s is negative and, even if R_d decreases to zero, the lower concentrated part of the current thins and ultimately pinches out as clasts transfer to dilute overriding parts of the current. In comparison with the results of mechanism (B), the tractional lithofacies may be coarser grained (e.g. rich in lithic lapilli) and associated with scour surfaces. (B) Change from massive to stratified lithofacies caused by depletive capacity in the distal reach of a current. Lower modified-grainflow levels of the current thin downcurrent ($R_s < R_d$). Distal tractional facies are deposited only in cases where the dilute part of the current remains sufficiently dense to maintain contact with the ground beyond point x . If the most distal part of the current was granular fluid-based, no distal tractional lithofacies would be deposited. Pumice flotsam, supported dominantly by buoyancy and grain interactions, is dumped around x , forming pumice-rich lithofacies (see Figs 4.7 and 5.10). Distal tractional lithofacies deposited in this scenario are finer grained than those formed in the scenario depicted in (A).

more rapidly than it is replenished ($R_s < R_d$). In cases where the tractional, distal part of the current remains sufficiently dense to maintain contact with the ground (i.e. not fully lofted) beyond the distal limit of the fluid escape-dominated flow boundary (Fig. 6.9B), distal fine-grained stratified lithofacies (sT; xsT) are deposited, and their sorting and stratification reflect tractional segregation processes such as winnowing. In some cases the approximate location of this flow-boundary zone transformation may be recorded by accumulations of pumice-rich lithofacies (e.g. pL, pmLT, pmBr, plens). This is because pumice flotsam, which is supported predominantly by buoyancy and dispersive pressure at levels within the current characterized by modified-grainflow, will be deposited where the modified-grainflow levels thin and terminate. Here the lowermost levels of the current become too dilute for these support mechanisms to be effective (see Fig. 6.9B; p. 47). Some pumices, however, may travel beyond this limit by traction and/or saltation. Distal stratified lithofacies thus indicate that the pyroclastic density current persisted as a ground-hugging fully dilute current beyond the main distal pumice accumulations (Fig. 6.9B). Other currents may loft predominantly at, or even sourceward of, the place where the modified-grainflow layer terminates and the pumice flotsam is deposited. In such instances the most distal lithofacies are massive (mLT, pL) and the distal limits of the current are predominantly modified grainflows.

Longitudinal facies sequences that show downcurrent transitions from mLT (sometimes with inverse grading) into distal sT or xsT have been determined in several small-volume pyroclastic deposits (Sigurdsson *et al.* 1987; Sohn & Chough 1989; Lajoie *et al.* 1992; Colella & Hiscott 1997), and are consistent with a downcurrent change from a fluid escape-dominated to a traction-dominated flow-boundary zone, as described above. Few detailed studies of longitudinal lithofacies variations have yet been undertaken in large ignimbrite sheets. Some of these sheets have poor preservation of the distal edges, and the tracing of internal time-lines may prove difficult. In some cases, topography may affect longitudinal facies changes more than distance from source.

Interpreting vertical lithofacies variations

Vertical variations of lithofacies in an ignimbrite (Fig. 6.10) record temporal changes in the flow-boundary zone of a current. Causes of the temporal changes may: (1) result from changes in the eruption, for example mass flux, composition or temperature at source; or (2) result from the current modifying the environment through which it passes, for example by modifying the topography or the nature of the substrate, by erosion, burial or heating; or (3) originate within the flow-boundary zone itself, for example by development of strength in lowermost parts of the current or by a reduction of strength in the substrate due to liquefaction and/or changes in granular temperature (see pp. 71–74). Variations in welding intensity with height through an ignimbrite sheet may record temporal variations in the temperature and/or composition of the erupting dispersion, and/or changes in the initial porosity of the ignimbrite with height, reflecting changes in clast supply and mode of deposition (see p. 83).

Gradational versus sharp lithofacies variations

Gradational vertical changes (grading) in ignimbrites indicate gradual changes in flow-boundary zone conditions with time, whereas sharp changes in grain-size (i.e. bedding planes) or in lithofacies indicate that either the conditions changed abruptly and/or that an erosional phase of the current has removed part of the record. Some gradational vertical changes in lithofacies include a zone of alternating intercalated lithofacies that indicate fluctuating or oscillatory flow-boundary conditions during the temporal transition from one type to another.

Bedding and flow-unit boundaries

Bedding surfaces separate massive (mLT) divisions in some ignimbrite sheets. A bedding surface comprises a sharp change in grain-size and may record either: (1) a brief or extended pause (hiatus) between two successive currents; that is, it separates two ignimbrite flow-units (Ross & Smith 1961); or (2) an abrupt change (unsteadiness) in flow-boundary zone conditions during sustained flow, for example caused by a sudden change in current velocity and/or concentration, or in the particle population being supplied to the flow boundary. In this second case the bedding surface is not a flow-unit boundary. Rather, the unsteadiness may have caused an abrupt change in the size of particles being deposited, or a brief period of non-deposition or erosion during sustained passage of a current. Distinction of genuine flow-unit boundaries from bedding surfaces that record unsteadiness during sustained passage of a current is important. Both are likely to be present and they may resemble one another.

Many pyroclastic fans are known to have aggraded cumulatively from a succession of separate pyroclastic density currents, and thus comprise a succession of flow-units (e.g. at Mount St Helens, Rowley *et al.* 1981; Montserrat, Cole *et al.* 2002). The terms 'flow-unit' and 'flow-unit boundary' are genetic, and to be used only where it can somehow be established that passage of the current at that location stopped, albeit briefly. This may, for example, be by direct observation of successive currents during an eruption. Evidence in the deposit for a brief cessation might be the presence of a thin pumice-fall layer or a co-ignimbrite ashfall layer, whereas a soil, a reworked horizon or a water-rilled scour surface might indicate a longer break. In the absence of any of these, inferences that pauses separated discrete currents must be made with caution. A pyroclastic density current advancing over an ignimbrite still loose from a previous current may not leave a distinct record of the depositional hiatus. Fine ash from the succeeding current may percolate down into interstitial spaces around underlying uppermost pumice lapilli and/or only a thin inverse-graded (mLT_(i)) division may form at the contact between the two flow-units. However, seamless depositional amalgamation of successive flow-units to produce a single mLT division has yet to be demonstrated, and this interpretation may be difficult to sustain where good evidence is lacking.

Unsteadiness during sustained deposition from a single current has long been invoked to account for bedding surfaces that separate massive divisions in other types of sediment-gravity flow deposits; for example Carter (1975) noted 'If the depositional surface migrates upwards more spasmodically ... then the bed might consist of several superposed subunits; each subunit would be bounded below by a plane at which the upward migrating depositional surface paused briefly while transport continued in the sediments above'.

Variations in steadiness of a sustained pyroclastic current may result in brief periods of non-deposition and/or erosion, each recorded by a bedding surface or scour within the resultant ignimbrite sheet. Bedding surfaces of this type may persist extensively within an ignimbrite sheet where the unsteadiness of the current is substantial and where it originates at the eruptive source. Less extensive bedding surfaces may record more localized unsteadiness. Thus, lateral persistence or impersistence is not in itself a reliable criterion for distinction of a flow-unit boundary from a bedding surface of another origin. An extensive bedding surface may represent either a hiatus between currents or a momentary fluctuation (e.g. a turbulent or erosive pulse) caused by an unsteady emission at source that passed along the length of the current.

Flow-unit boundaries can be persistent or impersistent, because as a sustained current recedes and advances, and as its flow path migrates, one locality may experience sustained passage of a current while another location may experience interrupted flow (see Fig. 6.5). An abrupt change in ignimbrite composition with height does

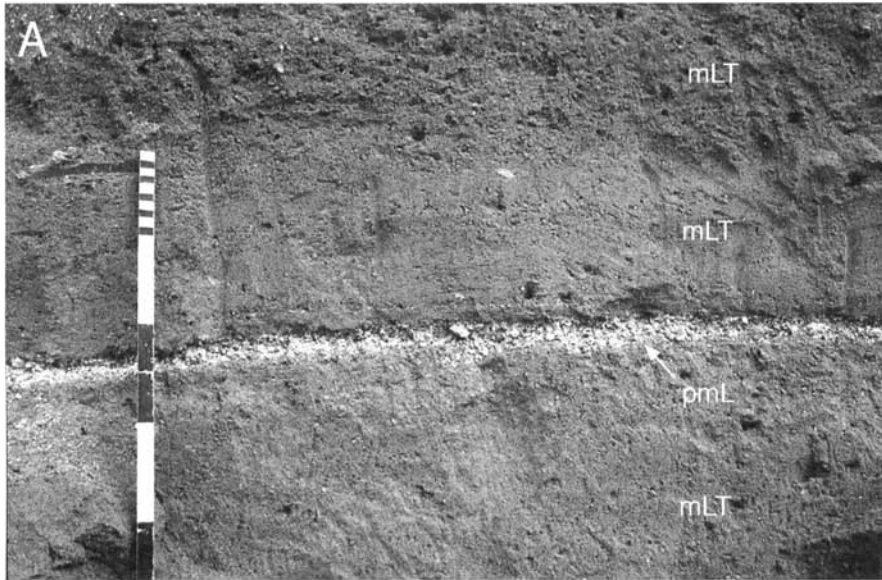
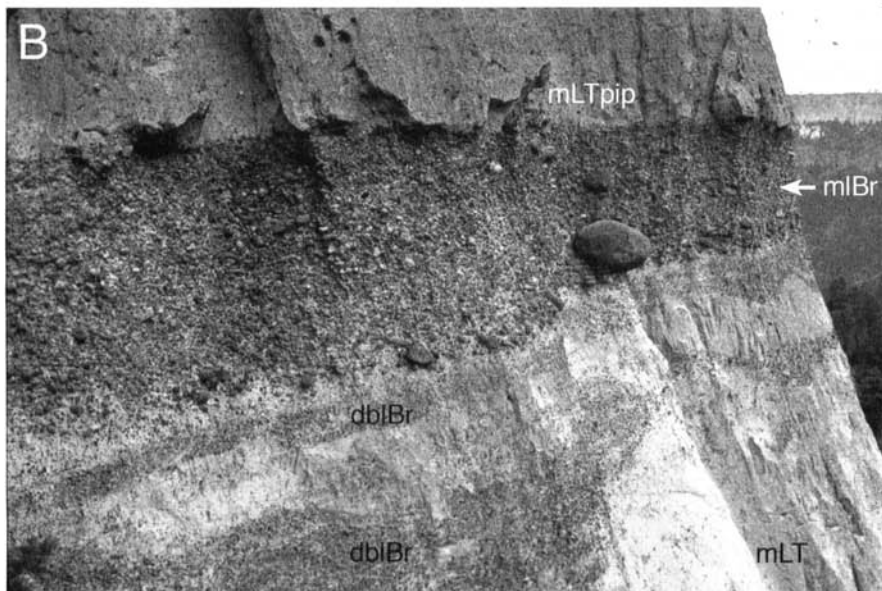
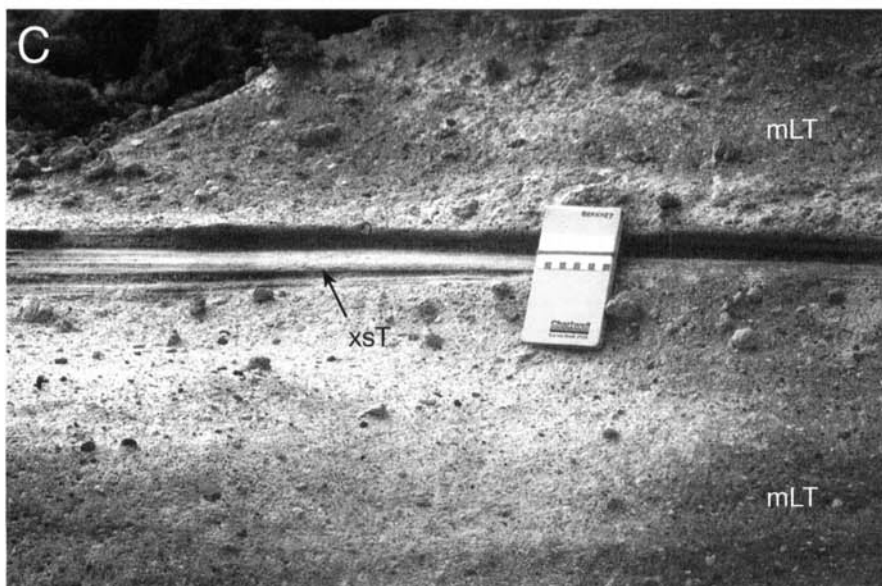


Fig. 6.10. Contrasting vertical lithofacies successions within ignimbrite sheets.

(A) A thin well-sorted pumice lapilli layer (pmL) of Plinian-fall origin intercalated within non-graded massive lapilli-tuff (mLT) represents a flow-unit boundary, i.e. a hiatus in flow between successive pyroclastic density currents, within the ignimbrite sheet. The current may have been sustained elsewhere during the time interval represented by this fall layer. Climactic 15 June 1991 ignimbrite of Pinatubo volcano, Philippines. End of ruler shows centimetres.



(B) Massive lithic breccia (mlBr) layer intercalated with lapilli-tuff, marking an abrupt short-lived increase in the competence of the sustained pyroclastic density current and/or a short-lived influx of lithic blocks at the eruptive source (e.g. due to conduit-wall erosion and/or caldera subsidence). Large block is >2 m in diameter. The laterally impersistent diffuse thin-bedded lithic breccias intercalated with mLT below the main mlBr layer may record unsteady deposition from granular flow-dominated flow-boundary zones. Proximal Lower Bandelier Tuff ignimbrite at Cat Mesa, Valles caldera, New Mexico, USA.



(C) Layer of cross-stratified tuff lithofacies (xsT) enclosed by massive lapilli-tuff lithofacies (mLT) records a temporary change in flow-boundary zone conditions from fluid escape-dominated to traction-dominated. It is not clear whether or not this unsteadiness was accompanied by a pause in flow at this site. Arico ignimbrite, SE Tenerife.

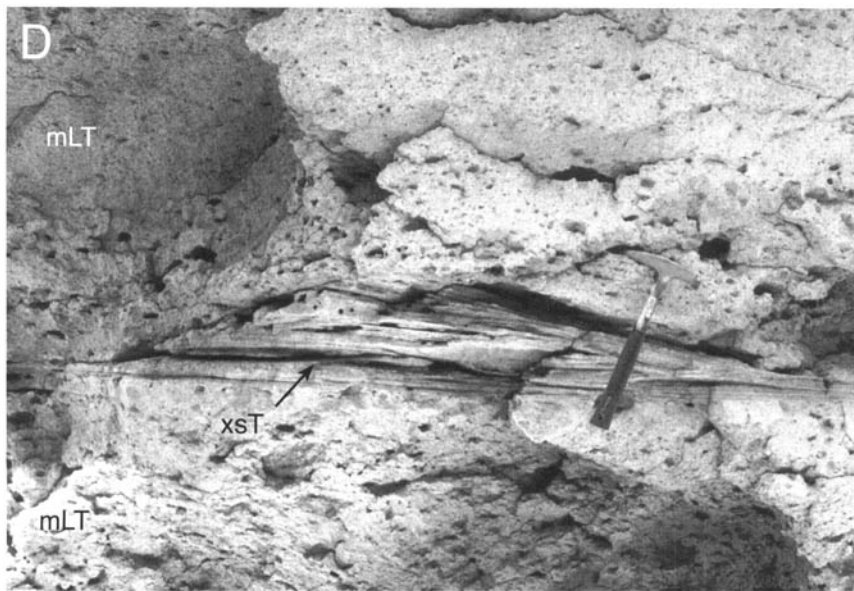
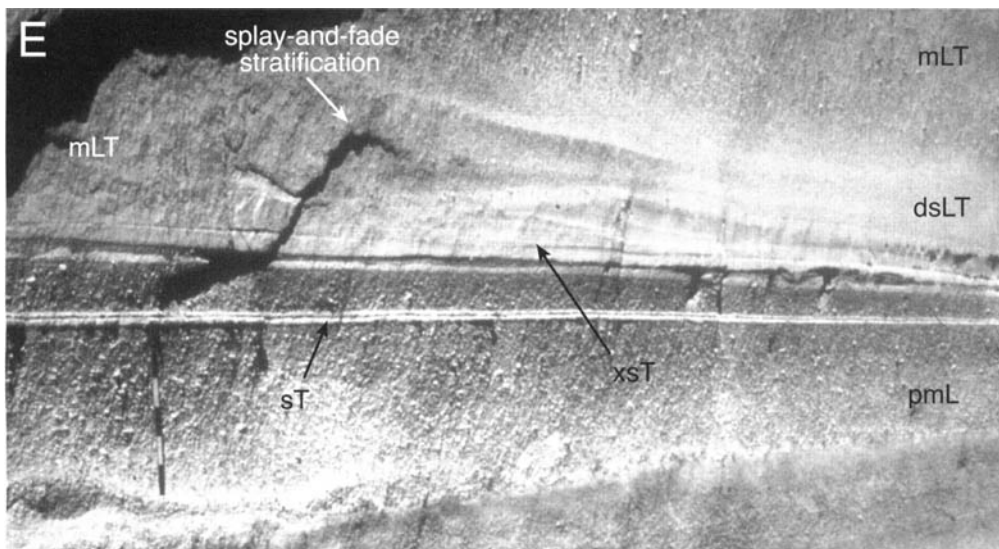


Fig. 6.10. (continued)

(D) Layer of dune cross-stratified tuff (xsT), rich in crystals, between thick divisions of massive lapilli-tuff lithofacies (mLT). As in (C), this records a temporary change in flow-boundary zone conditions from fluid escape-dominated to traction-dominated and it is not clear whether or not this was accompanied by a pause in flow at this site. Upper Bandelier Tuff ignimbrite near Los Alamos, New Mexico, USA.



(E) Intergradation of lithofacies within the base of an ignimbrite sheet. The Upper Bandelier tuff, Jemez Mountains, New Mexico, USA. The well-sorted massive pumice lapilli layer (pmL) of Plinian-fall origin is overlain by cross-stratified tuff (xsT) that grades both vertically and horizontally into massive lapilli-tuff (mLT), locally via splay-and-fade stratification (see p. 109). The presence of all gradations between cross-stratified tuff (xsT), diffuse-stratified lapilli (dsLT) and massive lapilli-tuff (mLT) indicates that flow-boundary zone conditions at the base of the sustained current varied gradationally both with location and with time. The metre ruler is for scale.

not alone establish the presence of a flow-unit boundary (cf. Freundt & Schmincke 1985), because it may simply record (1) a sudden change in the composition of material erupted during aggradation from a sustained current; or (2) a temporary depositional hiatus of a sustained current, the composition of which changed gradually with time.

The interpretation of thin inverse-graded ($mLT_{(i)}$) divisions is central to the problem of distinguishing flow-units. Their common occurrence at bases of massive ignimbrites led to an assumption that they only form at bases of ignimbrite flow-units, and hence to their early designation as 'basal layers' (Sparks *et al.* 1973; Sparks 1976). This genetic field term led to circular reasoning in which their presence within a succession of massive divisions was used to define flow-unit boundaries. Thin $mLT_{(i)}$ layers form due to unsteadiness during deposition in a granular flow-dominated flow-boundary zone (see pp. 43, 66 and 71) and do not necessarily represent a shearing layer at the base of a thicker laminar or plug flow that halted en masse (p. 13). The inverse grading develops as a result of granular segregation (pp. 29–31 and 66–71) and/or temporarily waxing flow (i.e. migration into field 1 of Fig. 1.1C from an erosional field such as 3). These conditions seem to characterize early deposition from a pyroclastic density current as it initially passes by (i.e. tending to form the distinctive layer(s) at the base of a flow-unit; see p. 108), but they may also readily develop

intermittently during unsteady phases of a sustained current (i.e. not marking a flow-unit boundary) whenever current behaviour favours development of a granular flow-dominated flow-boundary zone. Consider a sustained current depositing mLT at a fluid escape-dominated flow-boundary zone (see pp. 39–40). A temporary increase in flow-boundary shear (e.g. due to an increase in current velocity) can change the flow-boundary zone temporarily to granular flow-dominated (Fig. 4.1E to D). Larger clasts (e.g. pumice and lithic lapilli) in this flow-boundary zone are now subjected to higher dispersive forces, and granular segregation processes selectively prevent them from depositing so that a finer grained layer starts to form (see pp. 29–31; Fig. 3.6). If the shear rate then decreases, dispersive forces in the flow-boundary zone decrease so that larger clasts are increasingly able to deposit (changing selective filtering; see pp. 42 and 43) and an inverse-graded layer aggrades (Fig. 3.7). As the shear rate decreases, the flow-boundary zone gradually reverts to being dominated by fluid escape (Fig. 4.1E) and deposition of a second thick layer of mLT thus begins. The inverse-graded layer was formed during sustained flow in response to a velocity fluctuation, and so in this case does not mark the base of a flow-unit.

Temporary fluctuations in velocity and flow-boundary concentration may variously stack thin sT, dbLT and $mLT_{(i)}$ divisions between successive thick mLT divisions, even including erosion

surfaces (indicating temporary migrations into an erosive field of Fig. 1.1C), all within a single ignimbrite flow-unit. Such successions would also exhibit overall coarse-tail grading patterns that reflect how the competence of the current waxed and waned (see pp. 66–71).

Repetitious and rhythmic lithofacies successions

Many ignimbrites include repetitious rhythmic or cyclic successions of divisions, the recognition of which can be valuable in the interpretation of current behaviour.

One common repetitious succession is a thin (centimetres thick) inverse-graded division ($mLT_{(i)}$) that passes up into a thicker (decimetres to metres thick) division with normal coarse-tail graded lithic lapilli and inverse coarse-tail-graded pumice lapilli ($mLT_{(nl, ip)}$; Fig. 5.6A and E). This succession was termed ‘Layer 2’ by Sparks *et al.* (1973). We interpret it as recording flow-boundary deposition during the passage of a single surge of a current, and its abundance within ignimbrites suggests that surging flow is a common feature of pyroclastic density currents. A surge comprises a waxing phase followed by a waning phase (Fig. 1.1A), and a pyroclastic density current may constitute a single surge or it may comprise several surges during sustained passage. If the rate of aggradation remained constant during waxing and waning flow each surge of the current would be recorded as a division of $mLT_{(i)}$ overlain by an equally thick division of $mLT_{(nl, ip)}$. This assumes that the maximum size of lithic clasts at each level in the ignimbrite reflects the competence of the current. However, if the rate of deposition during waning flow is higher than it is during waxing flow (see p. 2), the upper $mLT_{(nl, ip)}$ division will be thicker than the subjacent $mLT_{(i)}$ division, which will be relatively condensed. Moreover, depending on currentwise acceleration (depletive or accumulative flow; see p. 2), non-deposition or even erosion may accompany a significant duration of each waxing phase. The result is a marked asymmetry in the deposit, with relatively thin $mLT_{(i)}$ divisions each overlain by considerably thicker $mLT_{(nl, ip)}$ divisions. In addition to this skewing effect, the waxing–waning patterns of the current surges themselves may be asymmetric, with a short rapidly waxing phase marking the relatively abrupt arrival of each surge, followed by a more protracted waning phase. The combined effects account for the predominance of normal coarse-tail grading of lithics in mLT . The normal coarse-tail grading of lithics is sometimes accompanied by inverse coarse-tail grading of pumice ($mLT_{(nl, ip)}$), which also records waning flow (see pp. 44–45 and Fig. 4.6).

Recognition of rhythmic or cyclic sequences is best achieved by sequence analysis. This quantifies, within a vertical succession, the frequency with which each division passes up into each other type of division (see review by Reading 1986). Surprisingly, few studies of this type have been undertaken on ignimbrites and, as a result, data on the abundance and variety of various sequences are lacking. In the absence of objective sequence analysis there has been a tendency for workers to look for and record $mLT_{(i)}$ – $mLT_{(nl, ip)}$, which is a sequence (Fig. 5.6A) adopted as a ‘standard’, sometimes at the expense of recording variations, other patterns (e.g. Figs 5.6B–F and 5.8) or occurrences of disordered successions (see below).

Disordered lithofacies successions

Many, if not most, ignimbrites show departures from the simple $mLT_{(i)}$ – $mLT_{(nl, ip)}$ sequence described above (e.g. see Figs 5.6, 5.8 and 6.10). Such departures are to be expected, because the $mLT_{(i)}$ – $mLT_{(nl, ip)}$ sequence results from one specific type of current when there are 13 potential types (it is essentially a single-surge waning depletive current; field 11 of Fig. 1.1C). Moreover, most currents evolve from one of the 13 types to another with time (i.e. their position on Fig. 1.1C changes). In the case of sustained currents, all sorts of waxing–waning histories are likely as vent

emissions vary, and as crater rims and substrate topographies are modified by erosion and deposition during the course of an eruption. Therefore, because most large-magnitude pyroclastic density current eruptions are sustained (see p. 7), disordered vertical sequences in ignimbrites are to be anticipated. Their documentation is best achieved using an objective lithofacies system based on physical features (Table 5.1), rather than a genetic numeric system based on a so-called ‘standard’ sequence. In analogous deposits of sustained turbidity currents it is increasingly recognized that turbidites generally do not show systematically ordered sequences of divisions (Leszczynski 1986; ‘disordered turbidites’ of Branney *et al.* 1990; Normark & Piper 1991; Kokelaar 1992), and that the ‘Bouma sequence’ and its ordered variants (e.g. Lowe 1982) are only applicable to a specific (single-surge waning depletive) type of current (Kneller & Branney 1995).

Intercalated massive and stratified divisions

Thinly interstratified massive and stratified divisions may occur due to periodic impingement of turbulent eddies onto the lower flow boundary (see Fig. 4.5A). However some occurrences within ignimbrite sheets of traction-stratified tuff layers intercalated with massive (mLT and $pmLT$) layers (Fig. 6.10C and D) may arise from larger scale current unsteadiness during which the distal limit of a sustained unsteady current advances and recedes. Possible examples include thin cross-stratified fine-ash layers within the Arico ignimbrite (Fig. 6.10C) and the thin crystal-rich cross-stratified tuff (xsT) layers interstratified with mLT in the Bandelier Tuff (Fig. 6.10D), referred to by Fisher (1979) as ‘ash-cloud surge deposits’. In principle, several alternations between mLT and xsT could form within a single flow-unit, for example where deposition has occurred from a single, sustained but unsteady current in which the lower flow-boundary zone varied periodically from traction-dominated to granular flow-dominated or fluid escape-dominated, possibly as a result of unsteady emissions at source. The presence of cross-stratified layers in ignimbrite sheets thus cannot reliably be used to infer a flow-unit boundary.

The position of successive forming pumice-rich dams constantly shifts during waxing and waning flow as the distal limit of a sustained current advances and retreats, so that pumice-rich facies become interstratified with mLT . During unsteady flow, the downcurrent limit of proximal tractional deposition (between sites 1 and 2 on Fig. 6.8A) also migrates back and forth and, in this way, proximal traction-stratified lithofacies ($xsLT$, sLT , $slBr$) may also become interstratified with mLT (Fig. 6.11). Proximal stratified lithofacies may be distinguished from distal stratified lithofacies (sT , xsT ; see Fig. 6.11) by the presence of coarser pumice and lithic lapilli and blocks, and, where there is compositional zoning, by tracing the stratified lithofacies longitudinally along entrachrons to determine whether they pass into mLT upcurrent or downcurrent.

Complex longitudinal architectures

Figure 6.11 depicts a hypothetical architecture aggraded from a sustained current that waxed and waned several times. Distally it comprises several flow-units, each with an inverse-graded pumice top. Medially there are fewer flow-units, and some layers with inverse-graded pumice lapilli record depositional fluctuations of successive surges during sustained unsteady flow (see multiple grading on p. 66). Some of these layers are not individual flow-units (see pp. 95–98), but they may closely resemble them. The varying limits of lithic breccia development record the interplay of current-competence variations and variations in lithic supply at source. In practice, even apparently simple ignimbrite sheets may exhibit great diversity in their longitudinal architectures when their arrangement of depochrons is revealed (see Fig. 6.12A–I). This is because the proximal and distal limits of deposition may change radically during the life-span of a single current, as can the locations of

bypass zones (areas where the current passes without depositing) and the locations of erosion and re-entrainment. All these locations can shift upcurrent or downcurrent either gradually or at rates even faster than the current velocity. In addition, the current may variously bifurcate or shift laterally (consider the three-dimensional interplay of various geometries depicted in Figs 6.6 and 6.12), and several discrete currents may be recorded. The possible permutations show how difficult it might be to correctly interpret the history of a pyroclastic density current by analysis of only a couple of vertical sections through an ignimbrite sheet.

By defining unconformity-bounded units in ignimbrites at Roccamonfina volcano, Italy, De Rita *et al.* (1998) documented forestepping-backstepping sequences and interpreted them to record waxing followed by waning phases of eruptions.

Interpreting lithofacies successions at bases of ignimbrites

Lowermost parts (centimetres–decimetres) of many ignimbrites have lithofacies associations that differ from those higher in the sheet. In this section, we explore some alternative ways they may be interpreted.

The lowermost part of an ignimbrite may or may not record the initial encroachment of a current. This is because density currents initially wax, and waxing flow may be accompanied by deposition, non-deposition or erosion (contrast fields 1, 2 and 3–5 of Fig. 1.1C). Erosion is reflected in occurrences of basal scour surfaces (e.g. Fig. 6.13A–D) (Rowley *et al.* 1981; Walker *et al.* 1981a; Bacon 1983; Wilson 1985; Kieffer & Sturtevant 1988; Sparks *et al.* 1997b; Bryan *et al.* 1998b), sometimes with erosional furrows and flow-parallel grooves (Fig. 6.13 C and D), percussion or impact marks (Davies *et al.* 1978; Ratté 1989; Sparks *et al.* 1997b), which are closely analogous variously to gutter casts, flutes, grooves and prod marks at the bases of turbidites. Where deposition does occur during initial waxing, it generally results from depletive capacity (field 1 in Fig. 1.1C), where the current fans out and/or flows down a lessening (concave) slope. The waxing competence may be recorded by gradual or more abrupt increases in grain size with height in the deposit (e.g. inverse grading; Figs 5.2C, E and F, 5.6B, C and F and 6.14A and B).

A wide variety of variously stratified and sorted layers and lenses (e.g. plensL, llensL, fpoorL; mLT_(i), dsLT, xsT) occur at bases of ignimbrites. Some have been classified genetically as 'ground layers' or 'layer 1', and 'basal layers' or '2a' (Sparks 1976; Wilson 1985). They may record the initial advance of the current across the landscape, and they do show that flow-boundary conditions near the flow-front commonly evolve rapidly prior to stabilizing into more or less persistent streaming, with quasi-steady deposition of mLT. As the leading parts of the current pass a fixed location, different and transitional flow-boundary conditions are recorded as a vertical succession of lithofacies. Diversity in leading parts of different pyroclastic density currents is indicated by the wide range of lithofacies successions in lowermost parts of ignimbrites (e.g. Figs 5.2C, E and F, 5.4C; 5.6A, E and F, 5.10C and F, 6.10E; 6.14 and 6.16; and accounts in Sparks *et al.* 1973; Fisher 1979; Wilson 1985; Huppert *et al.* 1986; Valentine *et al.* 1989; Schumacher & Mues-Schumacher 1996). The common presence in ignimbrites of lenses and scour surfaces, and of spatial impersistences of basal lithofacies, indicates that flow-boundary processes in leading parts are distinctly non-uniform, with low and variable rates of deposition, possible development of starved bed forms, and frequent and irregular scouring.

The lowermost lithofacies may pass up into the overlying parts (commonly mLT) sharply or gradationally. Some genetic classifications of ignimbrite layering (Druitt & Sparks 1982; Wilson & Walker 1982; Walker 1985) relate lithofacies below a sharp contact to flow-head processes ('ground layer' *sensu* Walker *et al.* 1981a) and those above to the flow body that halted en masse ('Layer 2' of Sparks *et al.* 1973; Valentine & Fisher 1986). Although aspects of these interpretations may be true, general application of such

classifications would be oversimplistic because: (1) continua of processes and conditions probably occur between a flow head and body; (2) deposition from the flow body is now thought to be by progressive aggradation, as well as that from the flow head; (3) 'flow-head' processes are only one of six ways (listed below) that conditions in leading parts of currents can differ from those further behind; and (4) the nature of any contact(s) separating lowermost lithofacies from overlying parts of the ignimbrite simply records whether changes in deposition were gradual, abrupt or interrupted by an erosional phase. We therefore classify the lowermost lithofacies of ignimbrites in much the same way as other ignimbrite lithofacies (see Chapter 5 and p. 120), and interpret them similarly in terms of evolving flow-boundary zone processes.

Lower flow-boundary conditions of leading parts of a current may differ from those further behind for the following six reasons. (1) In some currents ingestion, mixing and thermal expansion of air may result in more vigorous turbulence and dilution near the leading edge (flow-head model, Walker *et al.* 1981a). (2) Similarly, expanding gases generated by rapid combustion of vegetation and/or flashing of surface water to steam may cause more turbulence and/or fluidization at the lower flow boundary of the leading parts of the current. (3) Initial heating, destruction of vegetation and deposition of loose ash may rapidly change the shape and the physical properties of the substrate. The leading part of the current, for example, may encounter a lithified, cold and irregular pre-ignimbrite substrate, or one which is vegetated and/or wet, whereas moments later after the current has variously felled, buried and/or burnt vegetation, heated the substrate and eroded or infilled minor topographic irregularities the following parts of the current override a smoother, dry surface of loosely packed, hot and degassing ignimbrite, which engenders different flow-boundary conditions. (4) Large/dense clasts in the current may travel faster (Walker *et al.* 1981a) or slower (Hand 1997) than the leading parts of the current and so may be, respectively, concentrated or absent in the leading parts. (5) Turbulent, higher levels of a density-stratified current may advance faster than lower more concentrated levels, and thus arrive at a location somewhat earlier (Fig. 2.3B). (6) Eruptive conditions, such as mass-flux, may change at source (e.g. waxing eruption) so that the concentration, capacity and/or turbulence intensity of the current change with time and hence also spatially while conditions change along the length of the current. For example, the initial current may be fully dilute (e.g. Sparks *et al.* 1973; Fisher 1979), but as eruptive conditions change the current may become granular fluid-based, with the flow-boundary zone transformation migrating towards the current's leading edge. Several of these mechanisms may continue to cause changes for some time after the head of the current has passed by.

A wave of compressed air, displaced by the density current, may precede the leading edge of some pyroclastic density currents, causing erosion, particularly of vegetation and soil. Some ignimbrite eruptions may start with an explosively expanding blast (Wohletz *et al.* 1984; Valentine *et al.* 1989; see p. 8), although unambiguous examples of deposits from such a blast occurring at the base of an ignimbrite are unknown to us.

Stratified bases

Stratified lithofacies (sT; xsT; sLT), from a few millimetres to over one metre thick at the base of an ignimbrite (Figs 5.2F, 5.9B, 6.10E, 6.14A, B and C, and 6.17C), show that initial deposition at that location was from a traction-dominated flow-boundary zone (p. 74). This indicates that lowermost parts of the current were initially turbulent, with a sharp interface at the flow boundary along which clasts rolled or saltated (see pp. 37–39). Such initial conditions may be involved in some of the six mechanisms listed in the previous section.

Near the leading edge of a current, traction is facilitated by flow-boundary zone turbulence, by low rates of deposition favoured by waxing flow and by the sharp rheological interface provided by the

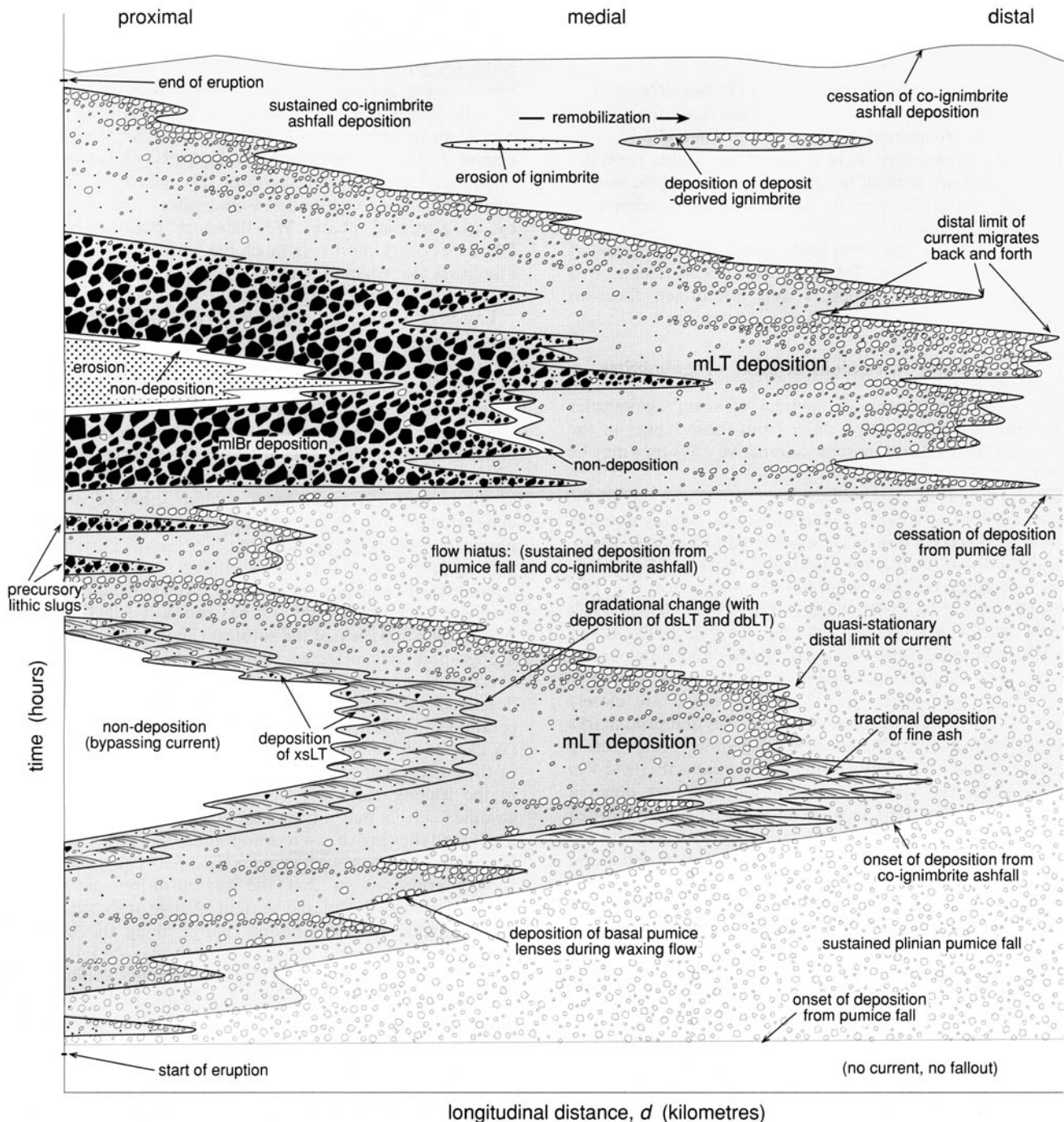


Fig. 6.11. A time-distance plot showing longitudinal lithofacies architecture of an ignimbrite sheet deposited by a depletive current that waxed and waned several times (see p. 99). Depochrons are horizontal and have been omitted for clarity. Horizontal changes reflect non-uniformity of deposition; vertical changes represent unsteadiness. Note that rates of deposition and erosion, and thus deposit thicknesses, are not indicated. The two major advances (progradations) record waxing flow, for example caused by increasing eruptive flux. The second of these carried abundant lithic breccias, perhaps recording a caldera-collapse event. Note that pumice accumulations occur distally along each depochron, and that flow-units bifurcate (several flow unit-boundaries die out proximally). A vertical section through the main proximal lithic breccias (top left) would comprise mLT passing up into a thin lithic-rich layer, which is sharply overlain by a much thicker lithic breccia with a basal erosion surface. Successions of this type previously have been labelled 'Layer 1L' and 'Layer 2L'.

pre-ignimbrite land surface. Further back in the current, however, flow-boundary turbulence intensity may decrease as a result of increased clast concentrations within the lowermost part of the current (Fig. 2.3B), increased rates of deposition (as the initial waxing phase declines), and the development of a new substrate of uncompacted and degassing ignimbrite. These conditions increasingly favour a fluid escape-dominated flow-boundary zone (see pp. 39–41), with gradational velocity and rheology profiles between

the lowermost part of the current and the new substrate (Fig. 4.1E). Consequently, as the current advances, mLT commonly is deposited on top of the lowermost stratified layer. The upward transition from the basal stratified division to the overlying mLT may grade via a zone of diffuse-stratified lapilli-tuff (e.g. Fig. 6.10E) or it may be sharp, this indicating whether the change from a traction-dominated to a fluid escape-dominated flow-boundary zone was gradational or abrupt. Some basal facies are diffuse

stratified (dsLT; or dbLT) rather than well stratified, indicating that initial deposition was not fully tractional. In some cases a basal stratified division may record a separate, preceding discrete fully dilute current in which case the sharp top of the stratified division represents a flow-unit boundary.

Basal pumice lenses

Layers and discontinuous lenses, from 1 cm to over 1 m thick and rich in rounded pumice lapilli, occur in lowermost parts of some ignimbrites (e.g. Fig. 5.10F; 6.14C; Taupo ignimbrite, Wilson 1985; Walker *et al.* 1980; Peach Springs Tuff, Valentine *et al.* 1989; Upper and Lower Bandelier Tuffs, Cas & Wright 1987, p. 245). Most are massive (mpL), although some show diffuse stratification (dspL) and they can be variously graded (e.g. pL_(i-n)) or non-graded. They range from matrix-supported (pLT) to clast-supported and fines-poor (pL), in some cases grading from the former into the latter upwards (e.g. 'Layer 1P' to 'FDI' of Wilson 1985) or downwards (e.g. 'Layer 1C' of Valentine *et al.* 1989). Their thickness and lateral impersistence seem to be influenced by topography, apart from within individual dune-like lenses.

We interpret pumice-rich lithofacies at bases of ignimbrites to be deposited at lower flow boundaries in essentially the same way as pumice-rich lithofacies found at other levels in ignimbrites (see pp. 76–77); their position reflects the temporal evolution of the current (Fig. 6.7B), rather than some special process (such as 'jetting', see below).

Pumice flotsam, supported by granular interactions and buoyancy, overpasses (Fig. 4.3) toward the distal edge of the current, where it is deposited (see p. 95; Figs 4.4 and 6.9). During quasi-steady flow, the distal limit of the current remains stationary (advance is limited by sedimentation and lofting) and the pumice clasts accumulate to form distal pumice-rich snouts or dams (see pp. 47–49; Figs 4.4, 4.7B and 6.7A). During waxing flow, however, the current leading edge and the corresponding position at which successive pumice snouts form both advance so that a layer (or lenses) of pumice-rich lithofacies progrades across the landscape and becomes buried by mLT (Figs 5.10F and 6.7B). In a similar way, basal pumice layers and lenses also can form by lateral accretion of pumice levees during transverse thalweg migration (see p. 111). In practice, a complex pattern of bifurcating and overlapping lobes may develop as the current thalwegs shift laterally and dams frequently become unstable and are breached. Secondary (deposit-sourced; Fig. 2.1F) pyroclastic density currents may deposit new ignimbrite lobes beyond the original limit of the primary current (see p. 49). During waxing stages of an eruption, the current gradually advances across the early-formed distal pumice dams close to source, either burying or reworking them. Thickness variations in pumice lenses may reflect variations in the rate of advance of the current; thicker developments record pauses in the advance of the current, and locations where basal pumice-rich lithofacies are absent may record sites where the current advanced abruptly or where initially deposited pumices were re-entrained.

Some pumice lenses at bases of ignimbrites, therefore, are sheared and buried remnants of ephemeral pumice snouts and levees formed during the initial advance of the current across the landscape. Others may be starved low-angle, or remnant, bars or dunes of tractional (lagan) pumice lapilli, deposited from a traction-dominated flow-boundary zone where turbulence winnowed away much of the fine ash. Other massive pumice-rich basal deposits may form from a fluid escape-dominated flow-boundary zone where elutriation was enhanced by hot gases expanding from burning vegetation or from boiling groundwater. The paucity of lithic lapilli in many basal pumice-rich deposits may be due to: (1) delayed arrival time of saltating and rolling lithics relative to pumice flotsam (see pp. 66–67); (2) depletive capacity as the current waxes; and/or (3) the lesser tendency of lithic lapilli to overpass all

the way to distal or lateral margins of the current. In some basal deposits, some of the pumice lapilli may have been entrained locally from remnant Plinian fallout layers. An intriguing hypothesis, not yet modelled, is that pumice-rich material may be 'jetted' forward out of a rapidly advancing flow head (Wilson & Walker 1982; Wilson 1985), although it is not clear that the field relations and granulometry of basal pumice lenses require this mechanism in preference to the others.

Fines-poor bases

Basal lithofacies of some ignimbrites locally include layers and lenses of tuff (Fig. 6.14D) and lapilli-tuff (Fig. 6.14C) that are better sorted than overlying mLT, in that they contain less fine-grained ash (e.g. σ_{ϕ} 1–3 in Walker 1971; Walker *et al.* 1981b; Druitt & Sparks 1982; Wilson 1985; Freundt & Schmincke 1985; Suzuki-Kamata 1988). Some of these are traction-stratified (as considered in the previous section), whereas others are massive and some vary from massive to stratified (Fig. 6.14C). Some basal tractional stratified facies may be difficult to distinguish where they are only thin and/or where there has been disruption by vegetation or escaping gas. The contact between these better-sorted lithofacies and the overlying lithofacies can be sharp (Fig. 6.14C; e.g. erosional), diffuse or gradational (Fig. 6.14D).

Fines-poor lithofacies may be formed in various ways, including turbulent winnowing around the lower flow boundary (see p. 24), granular segregation (see pp. 29–31), elutriation associated with vigorous sedimentation fluidization (see p. 34), or by deposition from a current that contained little fine ash. They can occur at any level in an ignimbrite sheet, but common occurrences at bases of ignimbrites indicate the involvement of leading parts of the current and/or interactions between the current and the pre-ignimbrite substrate. Five effects may play a role. (1) Surface roughness (e.g. abundant rills, vegetation or coarse regolith) may enhance flow-boundary turbulence, air ingestion and winnowing. (2) Combustion of vegetation may add to the upflow of gas, enhancing current turbulence and/or enhancing elutriation in the current or in the deposit. (3) Thermal expansion of steam derived from surface or ground water may have similar effects to (2) (e.g. see Sigurdsson & Carey 1989), as may thermal expansion of air partly trapped beneath compacting vegetation. These effects may diminish abruptly or gradually as vegetation is felled, compacted and destroyed, and as an irregular or wet substrate is buried by a more uniform layer of loose ignimbrite. This would be recorded by burial of the fines-poor lithofacies by mLT with a higher content of fine ash. Pipes or pods of fines-poor tuff, the sorting of which (see p. 61) closely resembles that of the basal fines-poor lithofacies, sometimes occur in mLT that encloses incompletely burned wood and provide evidence for more persistent localized segregation. (4) The current may initially have contained a relatively low proportion of fine ash, either because the initial phase of the eruption only generated a low content of fine ash or because a significant proportion of fine ash erupted was lost during transport, for example at the upper mixing layer of an initial supercritical current (Bursik & Woods 1996). (5) Ingestion and thermal expansion of cold air into the front of a turbulent flow 'head' (Fig. 2.3) also can cause a loss of fine ash. The genetic terms 'ground layer' and 'Layer 1H' (*sensu* Walker *et al.* 1981a) assign fines-poor lithofacies to this latter mode of formation, but this is only justified where it can somehow be established that this mechanism occurred rather than any of the other four.

Fine-grained layers at the base of ignimbrites

Fine-grained layers are common at bases of ignimbrites (Fig. 6.14A and B). Many have inverse grading of lithics and pumices, most commonly of the coarse-tail but sometimes affecting a larger part of

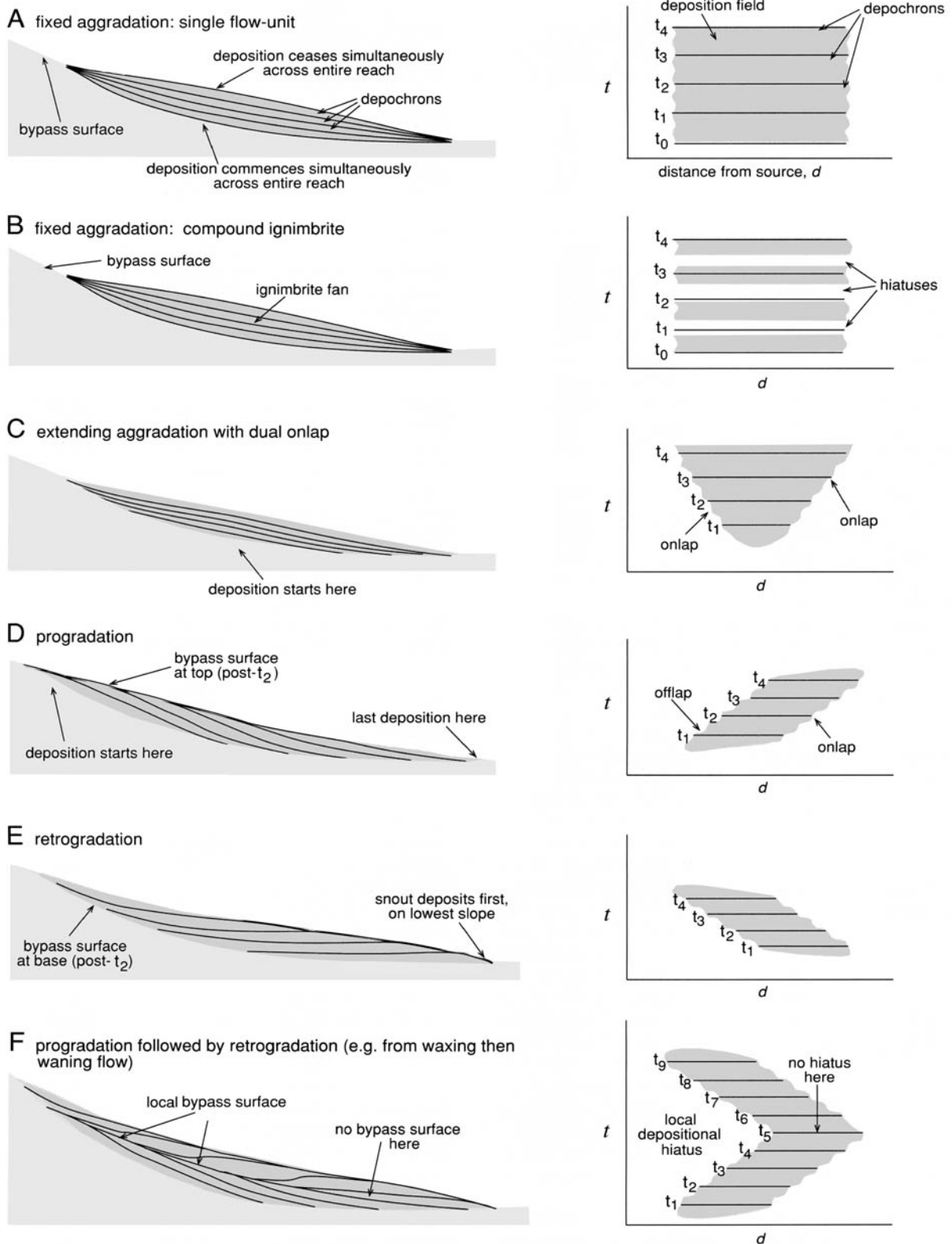


Fig. 6.12. Longitudinal depochron architectures in cross-section (see p. 98). These architectures may occur on all scales and are shown with vertical exaggeration. In the left column depochron spacing is proportional to deposition rate. The same depochron architectures are plotted against time in the right-hand column to show when and where deposition occurred. The plots on the right show hiatuses but not rates of deposition. In (A) deposition was steady. The depochrons will be invisible within massive ignimbrite. In (B) the deposit geometry is identical to (A), but the sheet contains three flow-unit boundaries (not shown) that correspond to depositional hiatuses (right). (A) and (B) are unrealistic because deposition started and stopped simultaneously everywhere along the depositional reach. In (C), however, deposition more realistically started at a point source and extended with time. If massive, this ignimbrite would appear identical to (A), even though its base is markedly diachronous. In (D) the ignimbrite progrades. This may result from the modification of topography by deposition, or from waxing flow conditions. Later deposited material bypassed the top surface of the proximal ignimbrite. In (E) deposition first occurred distally on the lowest slope and the deposit surface retrograded sourcewards. This may occur in the case of a single small ignimbrite lobe with a terminal pumice dam, or in a much larger ignimbrite fan deposited during waning flow conditions. In contrast to (D), the bypass surface underlies the proximal ignimbrite. In (F) deposition was sustained, but a localized bypass surface occurs proximally and corresponds with a proximal hiatus (see right) corresponding to the time when deposition occurred furthest from source.

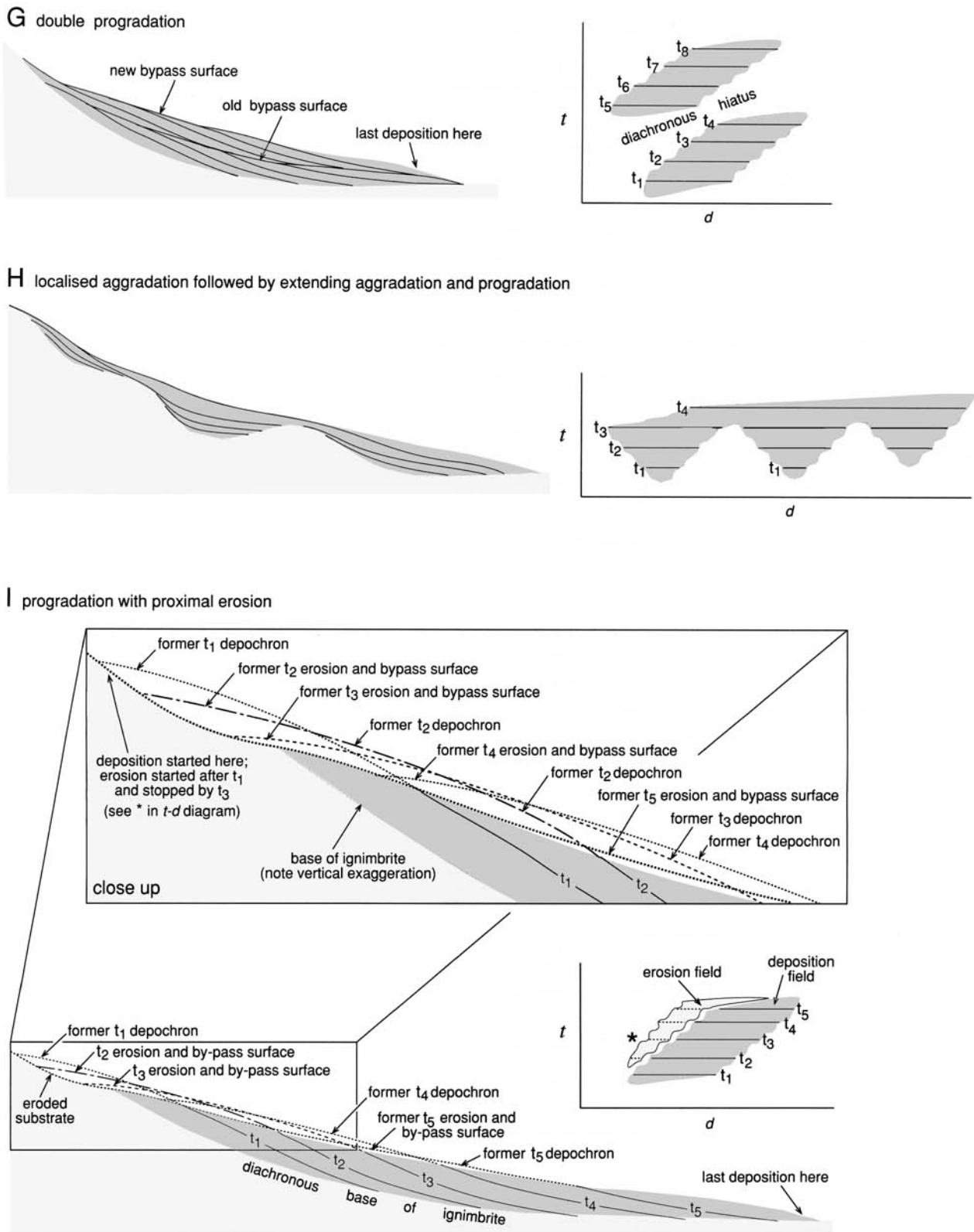


Fig. 6.12. (cont.) (G) The ignimbrite records two progradational events (each as in D), for example from two connected or discrete current surges. A single *diachronous* bypass surface traces along the entire length of the ignimbrite, even though deposition occurred throughout the history of the current (for a short period, around $t = 4.5$, distal deposition occurred simultaneously with proximal deposition). In (H) deposition commenced at two separate locations almost simultaneously, and extended with time so that the separate depocentres merged. The base of the ignimbrite is markedly diachronous with overlap. In (I) progradation was accompanied by proximal erosion (of substrate and of just-deposited ignimbrite) and (re-)entrainment. The location of erosion advances downcurrent with time producing a scour surface that is diachronous. The situation may result from waxing flow. Inset shows how the proximal depochrons, and erosion and bypass surfaces changed with time (most of the record of this has been removed by erosion).

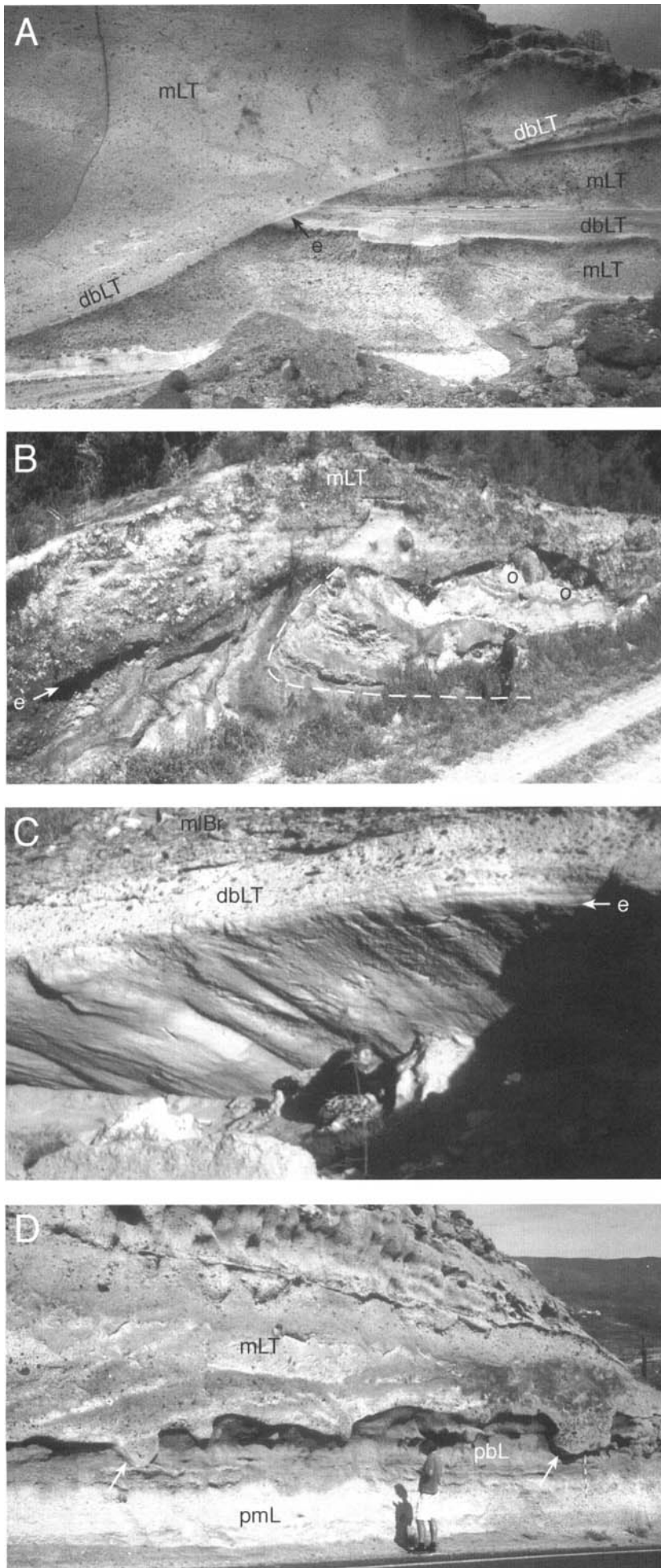


Fig. 6.13. Effects of substrate erosion, shear and fluidization (see pp. 99 and 108).

(A) Inclined erosional surface cut into earlier deposits of the same ignimbrite sheet is draped by diffuse-bedded lapilli-tuff (dbLT) that grades into massive lapilli-tuff (mLT). Poris ignimbrite at La Caleta, southern Tenerife. A metre rule is right of centre. (Photograph: Richard Brown).

(B) Ignimbrite (mLT) on an erosional surface (e) cut into recumbent-folded substrate, comprising tephra layers and soils, with overturned limb (o). Folding and erosion are thought to have been caused by the pyroclastic density current that deposited the ignimbrite, because some ignimbrite tephra is preserved in the fold core (Houghton & Wilson 1986). The overturning may have been facilitated by trees that, when knocked over by the current, overturned cohesive tephra and soil attached to the roots, now rotted away (there are abundant small-scale soft-state faults in the substrate). Approximately 12 km south of the inferred vent. The inferred current direction is left to right. Taupo ignimbrite, New Zealand.

(C) Casts of erosional furrows, analogous to flute or gutter casts in turbidites, pointing downslope. Inferred current direction is away from viewer and to the right. Poris ignimbrite, Tajao, southern Tenerife.

(D) Parallel gutter casts (arrows) at the base of the Arico ignimbrite, SE Tenerife, caused by pyroclastic density current erosion into soils and Plinian fall deposits. The inferred current direction is towards the viewer.

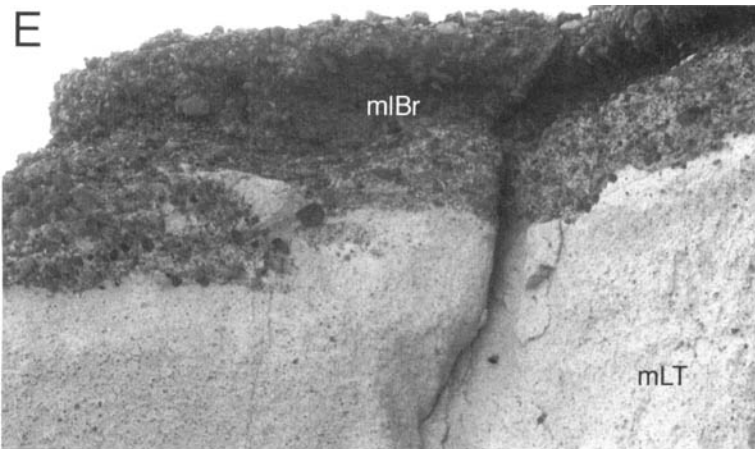
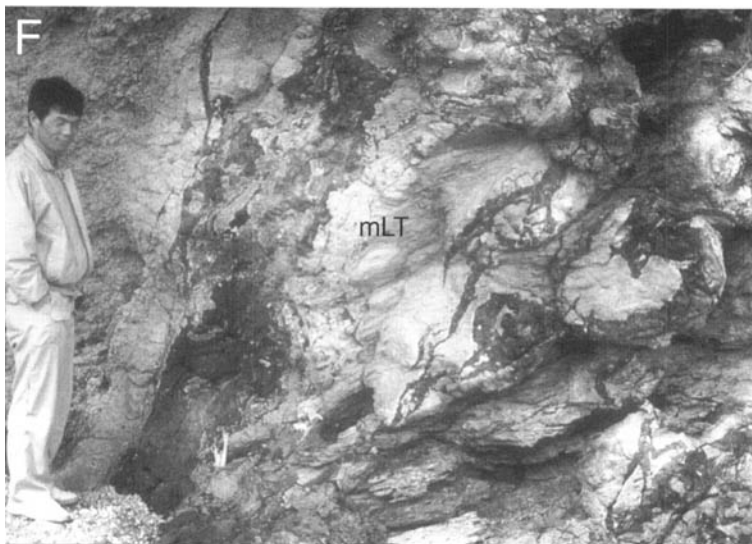


Fig. 6.13. (continued)

(E) Sheared flames of massive lapilli-tuff (mLT) that penetrated into overlying, massive lithic breccia (mlBr) during loading. Poris ignimbrite, southern Tenerife. The height of the section is 4 m.



(F) Ramifying dykes of fluidized black siltstone and mudstone within the basal 5 m of a thick massive, non-welded ignimbrite (mLT). They record hot-state fluidization and injection of wet sediment substrate, forming a type of peperite. Miocene ignimbrite, Mogpo coast, South Korea.



(G) Soft-state deformed ramifying dyklets of stratified ash (sT) in massive lapilli-tuff, inferred to have formed by liquefaction and steam-fluidization where a hot pyroclastic density current flowed onto wet coastal sediments. Matahina ignimbrite, Bay of Plenty coast, New Zealand (Bailey & Carr 1994). End of ruler shows cm.

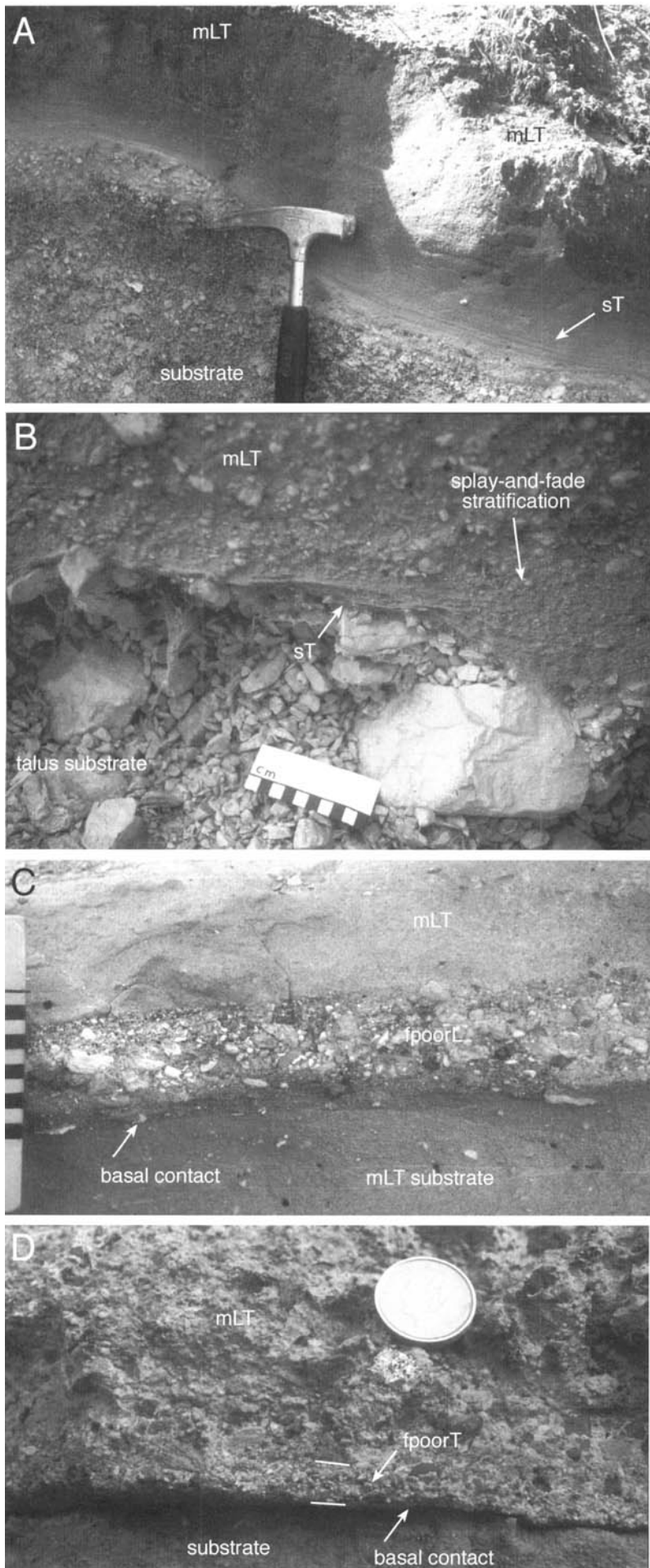


Fig. 6.14. Lithofacies at bases of ignimbrites and along their steep contacts.

(A) Fine-grained ash with subtle stratification (sT) grades up into coarser grained massive lapilli-tuff (mLT). This indicates that initial tractional deposition rapidly but gradationally changed to deposition dominated by fluid escape. See the text for interpretation of the inverse coarse-tail grading. Base of the proximal Campanian ignimbrite at Procida, Italy.

(B) Massive lapilli-tuff (mLT) deposited on a talus slope. Basal fine ash (sT) with ramifying cross-lamination grades up into mLT (with inverse coarse-tail grading) and passes downslope into massive lapilli-tuff via splay-and-fade stratification (see the subsection describing this stratification in this chapter). Campanian ignimbrite, Italy.

(C) Lens of fines-poor, pumice and lithic-rich lapilli (fpoorL) sharply overlain by massive lapilli-tuff (mLT) at the base of an ignimbrite: Member B of the Huckleberry Ridge Tuff, eastern Idaho, USA. Pumice lapilli have been rounded by abrasion. When traced laterally the lens develops low-angle cross-stratification (xsL; not shown). Scale shows cm.

(D) Fines-poor, crystal-rich coarse-ash layer (fpoorT) at the base of the Arico ignimbrite, southern Tenerife. This layer grades up into overlying massive lapilli-tuff (mLT). Coin is 1.5 cm.

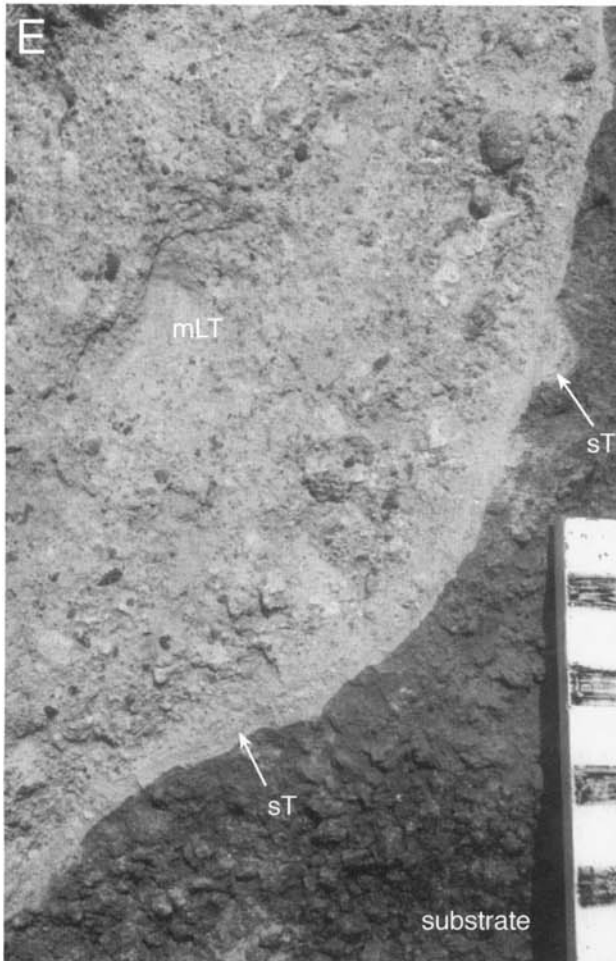
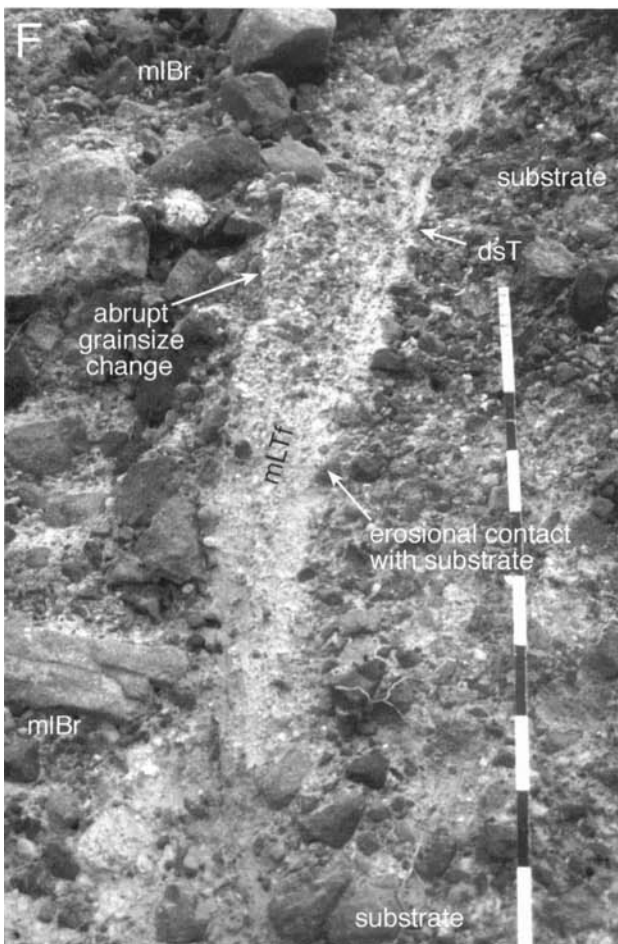


Fig. 6.14. (continued)

(E) Fine-grained ash layer (sT) lies against a steep substrate topography and grades away from the contact into massive lapilli-tuff (mLT). The fine ash is locally stratified (cross-laminae are visible in the field). Minoan ignimbrite at Phira Quarry, Santorini. The scale is in centimetres.



(F) Proximal massive lithic breccia (mlBr) deposited against a steep slope, with an 8–15-cm thick layer of finer grained lapilli-tuff (mLTf) that in places shows grain fabrics and diffuse stratification (dsT) parallel to the substrate slope. This fine-grained layer does not grade into the overlying lithic breccia. Cape Loumaravi, Santorini (Druitt & Sparks 1982). The metre rule is for scale.

the grain-size distribution. Fine-grained layers with inverse grading (mLT_(i)) are sometimes referred to as a 'basal layer' (e.g. Sparks 1976; Francis 1993), but, since originally defined, this usage has been extended somewhat indiscriminately from inverse grading just of the lowermost few millimetres of mLT (e.g. Sparks *et al.* 1973) (Fig. 6.14A), or of a few centimetres–decimetres of mLT (e.g. fig. 11 of Sparks 1976) (Figs 5.2E and F, and 5.6F), to include a wide variety of types of fine-grained layers. These include fine-grained layers in which inverse grading is poorly developed (Figs 5.2C and 6.14C and F), inverse graded layers with subtle diffuse stratification (dsLT_(i)), in places with low-angle truncations (Wilson 1986, p 13; fig. 10.21 of Francis 1993) (Figs 5.2F, 5.6E, and 6.14 A, B and E), stacked, multiple inverse-graded beds or laminations, in some cases with low-angle truncations (Minoan ignimbrite of Sparks 1976; Cas & Wright 1987, fig. 8; Buesch 1992; Cole *et al.* 1993) (Figs 5.2C, 6.13A and 6.16A), and fine-grained, sometimes inverse-graded, lower parts of ignimbrites that span several divisions (e.g. of mT, sT, dsT, mTacc, mLT; e.g. fig. 10.20 of Francis 1993) (Fig. 5.2D). These are unlikely all to have the same origin. Some fine-ash layers at the base of ignimbrites may represent deposits of low-concentration ash clouds that advanced ahead of slower, more concentrated and more competent parts of the pyroclastic current, which deposited overlying mLT. Such ash layers can be massive (see p. 37) or traction stratified (see p. 99).

We interpret both fine-grained layers and inverse-graded layers at the base of ignimbrites in essentially the same ways as when these occur at other levels in ignimbrites (see pp. 66–71 and pp. 95–98) and at the sides of ignimbrites where they lie on pre-ignimbrite slopes that exceed repose angles (Sparks 1976; Druitt & Sparks 1982) (Fig. 6.14E and F). All types of inverse grading at bases of ignimbrites must record some form of unsteadiness, in which changing flow-boundary conditions increasingly let larger clasts pass down to the rising deposit surface (e.g. Fig. 3.7). However, the wide range of inverse-grading types seen indicates that there are various mechanisms (pp. 43–45 and p. 111 and pp. 66–71 and Table 5.2). A similar range of inverse-grading types occurs at bases of some deposits of lahars and of high-density turbidity current deposits (e.g. Leszczynski 1986; Smith & Lowe 1991).

The common occurrence of inverse grading at ignimbrite bases indicates that unsteadiness characterizes a current's initial moments of deposition at a particular location. The unsteadiness probably relates to waxing flow, proximity to the leading edge of the current and/or changing substrate properties as the ground is initially buried by loose ash.

Inverse grading produced by waxing flow competence or delays in the initial arrival of successively larger saltating clasts (see pp. 66–71) may affect the lowermost centimetres, decimetres or even metres of an ignimbrite, in some cases including several lithofacies. For example, a succession of sT, dsLT and mLT may be inversely graded overall. Inverse-graded layers that are only millimetres to a couple of centimetres thick may reflect granular segregation in a granular flow-dominated flow-boundary zone during the onset of deposition (mechanisms described in the sections on pp. 29–31 and 66–71).

Some common successions of basal lithofacies

A common succession of lithofacies in lowermost parts of ignimbrites is sT–mLT_(i)–mLT (Figs 5.2F, 6.10E, 6.14A and B). This is consistent with the initial waxing of a current and the associated evolution of the flow-boundary zone from traction-dominated (sT), through granular flow-dominated (mLT_(i)) to fluid escape-dominated (mLT). The path that such evolving flow-boundary conditions follows may be plotted in the cube of Fig. 4.2, and corresponds with increasing rates of deposition, increasing development of density stratification in the current, decreasing turbulence in the lower flow-boundary zone and a change in substrate from a hard to loose, which favours development of more

diffuse shear within the flow-boundary zone. A phase of granular flow-dominated deposition of relatively long duration will be recorded by a relatively thick division of diffuse thin bedding (dbLT), with several thin inverse or inverse-to-normal graded layers (see Figs 5.6D, 5.8A, F and G, 6.10E, 6.13C, 6.16A and B). Such diffuse thin bedding indicates that a granular flow-dominated type of flow-boundary zone is sensitive to subtle fluctuations in the current (Fig. 4.5B), whereas the overlying thick mLT indicates that subtle fluctuations in the current become increasingly dampened within the flow-boundary zone as it changes to fluid escape-dominated (Fig. 4.5C; see explanation on p. 43). Absences of sT at the base of an ignimbrite indicate instances where an initial traction-dominated flow-boundary zone did not deposit, because of waxing flow (see Fig. 1.1C) or instances in which a granular flow-dominated or fluid escape-dominated flow-boundary zone temporarily extended right to the leading edge of the current, so that even in the leading part of the current high particle concentrations near the base inhibited traction (Fig. 2.3C). In other cases initial tractional deposits may have been scoured away by succeeding parts of the current.

Sheared or loaded substrate

One of the reasons why the lower flow-boundary zone of a pyroclastic density current is taken to include the uppermost part of the substrate as well as the lowermost part of the current (see p. 2) is that the current can modify the top of the substrate in various ways. It may exert shear stress on the substrate, load the substrate, transmit shock waves through the substrate (p. 35), heat the substrate causing pore water to expand, liquefy the substrate, or fluidize the substrate by loading or by steam generation (Fig. 6.13F and G). It may also raise the granular temperature and hence dilate the substrate by causing clasts in it to vibrate (pp. 29–31). This vibration may disaggregate loosely agglomerated fine-ash particles (see Santana *et al.* 1999). Combinations of these effects can lower the strength of the substrate and may be important in promoting erosion by pyroclastic density currents. Erosion is widely recorded by scour surfaces at the base of, and within, ignimbrites (Figs 6.13A–D and 6.14F), and by the presence in the ignimbrite of substrate-derived lithics, intraclasts, or vegetation fragments. With progressive aggradation, the substrate at first comprises the pre-ignimbrite substrate, and then comprises the loose, hot and degassing, aggrading deposit, which is readily remobilized and re-entrained. Evidence for substrate modification and remobilization may be found at all levels within an ignimbrite, as well as at its base.

Loading coupled with loss of substrate strength is recorded by load-and-flame structures at the base of some ignimbrites (e.g. base of the Cerro Galan ignimbrite; Sparks *et al.* 1985) and at the base of ignimbrite breccias (see pp. 57–61; Fig. 5.3C). These develop when Rayleigh–Taylor instabilities perturb the surface between an upper dense layer of deposit and an underlying less dense layer of deposit or substrate. Load-and-flame structures may form during or shortly after deposition. Those formed during deposition have a growth geometry in which the deformation gradually decreases upwards through the deposit. Some examples show evidence of downslope soft-state shear deformation (Figs 5.7B and 6.13E). Elutriation pipes rising from some lithic breccias (e.g. Allen & Cas 1998) may record fluid escape enhanced by loading of mLT by the dense breccia (see Fig. 5.7B). Spectacular load structures that penetrate down more than 10 m into the substrate and in some cases have become detached 'load balls' occur at the base of welded ignimbrites in Wales, where heating and fluidization of the wet sediment was involved (Capel Curing Volcanic Formation; Francis & Howells 1973; Kokelaar 1982; Howells *et al.* 1985; Branney 1986).

Discrete or ramifying granular shear zones can record soft-state shear deformation caused by pyroclastic density currents. These are

marked by undulose fine-grained laminations formed by granular segregation (e.g. Fig. 6.14B). Strictly speaking, substrate undergoing shear momentarily becomes part of the flow. Other examples of substrate shear deformation caused by pyroclastic currents are indicated by overturned strata beneath the Upper Merihuaca ignimbrite in Argentina (Sparks *et al.* 1985) and beneath the Taupo ignimbrite (Fig. 6.13B) (Houghton & Wilson 1986), and by subhorizontal tongues of ImBr intercalated with substrate pumice fall deposit in the Cape Riva Member of Santorini. This intercalation indicates that the substrate was sheared and lifted into the pyroclastic current as semi-coherent slabs (Druitt & Sparks 1982). It is also indicated by soil schlieren and low-angle finger-like tephra dyklets in non-lithified pumiceous substrate at the base of deposits of the blast-initiated pyroclastic density currents of Mount St Helens ('layer AO' or 'GL' of Fisher 1990a) and Bezmianny (Belousov 1996). Laminar shear in just-deposited ignimbrite beneath a pyroclastic current is inferred from deformed load structures and elutriation pipes at Roccamonfina volcano (Cole *et al.* 1993). Substrate shearing is also indicated by soft-state slide surfaces preserved in shales beneath subaqueously emplaced deposits of a Miocene pyroclastic density current (Kano *et al.* 1988).

Interpreting lithofacies at the top of ignimbrites

Lithofacies at the top of an ignimbrite sheet may be interpreted in essentially the same way as those lower in the sheet. Unless there has been erosion, the top surface of an ignimbrite records the last increment of deposition from the lower flow-boundary of a pyroclastic density current at that location. Stratified deposits at the top of an ignimbrite sheet record tractional deposition from the lower flow boundary of the last part of the ignimbrite-forming density current during its waning phase (e.g. the low-concentration wake, or 'tail', of the current; see p. 10). Such a fully dilute current may be a low-concentration ash cloud. When the tractional deposit was forming, the ash cloud must have been travelling across a stationary surface (i.e. the already deposited ignimbrite). Had it been riding above a denser flow (e.g. as inferred by Fisher 1979; Wilson & Walker 1982; Wilson 1985), its deposit would settle down into the moving flow, mix and thus not be preserved as a discrete layer. Stratified deposits at the top of an ignimbrite alternatively may record a subsequent pyroclastic current (see below).

In cases where the distal limit of a sustained density current retreats back towards the source during the waning stages of the eruption, the top of the ignimbrite sheet may record distal-tip deposition as the retreating edge passes by (see Fig. 6.2C and p. 98). For example, thickness variations of pumice-rich layers and lenses at the top of an ignimbrite may record how distal pumice-rich accumulations (see pp. 47–49 and 76–77) were deposited successively closer to source during the waning history of the current.

Dilute last stages of some pyroclastic density currents may not deposit on the main ignimbrite sheet, because the thermal output from the deposited ignimbrite sheet cause them to loft. Lofted, low-concentration phoenix clouds or co-ignimbrite ash plumes, rich in elutriated fine-grained ash, are most likely to deposit fine ash on top of hot ignimbrite if the ash is agglomerated into clusters or pellets. Powerful inward draughts driven by large-scale thermal convection may even erode the upper loose ash surface, sometimes leaving a thin 'lag' deposit of open-work lithic lapilli and large pumices. However, lapilli-rich lag deposits can also form long after ignimbrite emplacement by the removal of fine ash by normal wind winnowing of the upper surface of the unlithified ignimbrite.

Where an ignimbrite is rapidly buried before compaction and degassing is complete the succeeding deposit may founder into the loose, fluidal ('quick') just-formed deposit, forming load structures (Fig. 6.15).

Uppermost layers of some ignimbrite sheets record rootless

explosions that occurred in hot ignimbrite where it interacted with groundwater, surface water, rainwater or ice. Such 'secondary' rootless explosions commonly form craters in the upper surface of the ignimbrite sheet and produce short-lived fully dilute pyroclastic density currents that locally deposit lenses, tens to hundreds of metres long, of fine stratified ash (sT, xsT, bT), lapilli (sL) and/or lapilli-tuff (xsLT) (Fig. 6.15B). These may be difficult to distinguish from 'primary' deposits of the waning stages of the main pyroclastic density current, although they are typically restricted in extent and associated with localized ashfall layers and ballistic clasts also derived from the rootless explosion (Moyer & Swanson 1987). Such deposits may interfinger and merge with: (1) similar lenses from adjacent rootless explosions; (2) ash layers derived from plumes that rise above 'secondary' collapse scars (Torres *et al.* 1996); and/or (3) deposits from minor postclimactic eruptions of the volcano. Examples include the May and June 1980 ignimbrites of Mount St Helens (Rowley *et al.* 1981; Moyer & Swanson 1987) and at the top of the main 1991 ignimbrite of Mount Pinatubo (Scott *et al.* 1996). In ancient ignimbrites, such deposits usefully indicate that the original upper surface of an ignimbrite sheet is preserved (e.g. Side Pike ignimbrite, UK; Branney 1988).

Transverse lithofacies variations

Transverse sections through ignimbrites show lithofacies changes on all scales, ranging from a few centimetres to those that occur across entire regional-scale sheets. Tracing depochrons or entachrons along transverse sections through ignimbrites will show the extent of lateral diachroneity of deposition. We describe and interpret transverse lithofacies variations below, in order of increasing scale.

Splay-and-fade stratification (new term)

Transverse sections through ignimbrites commonly show sharp or diffuse stratification (sT dsT), with strata from millimetres to centimetres thick (sT to bLT) that gradually splay (thicken and diverge) and become diffuse, eventually fading out completely into mLT when traced laterally across decimetres to several metres of ignimbrite (Figs 5.6E, 5.10d, 6.10E, 6.16A and D, and 6.17C). We refer to this as *splay-and-fade stratification*. It occurs in both current-transverse and current-parallel sections. The stratification may be diffuse or sharply defined, picked out by fine-grained tuff and overlain by thin mLT layers, some with an inverse-graded base. Typically, each surface becomes increasingly diffuse (dbLT) and gradually becomes imperceptible (mLT) when traced laterally.

We interpret splay-and-fade stratification as recording small-scale non-uniformity in flow-boundary conditions. At the location where the ignimbrite is massive (mLT), deposition was quasi-steady from a fluid escape-dominated flow-boundary zone (see pp. 39–41 and 56). Simultaneously, deposition just a short distance to one side of this was unsteady (bLT) and from a flow-boundary zone that fluctuated between granular flow-dominated and fluid escape-dominated (see pp. 41 and 71–74), in some cases with traction (dsT). The divergence (splay) of stratification shows that the net rate of deposition varied locally, being higher where the mLT was deposited than it was nearby where the bLT aggraded. The localized lithofacies variations show that flow-boundary conditions varied across small distances. The fact that the stratification becomes more widely spaced (i.e. it splays) as it fades towards the mLT indicates that mLT characteristically aggrades more rapidly than bLT or sLT (see Fig. 4.2). We infer that splay-and-fade stratification forms where the flow-boundary zone is locally affected by passage of current surges, while steadier flow conditions occur nearby. The sustained current may widely have been unsteady (e.g. with passing turbulent vortices and/or minor surges), but at the majority of the locations, where the homogeneous mLT was rapidly

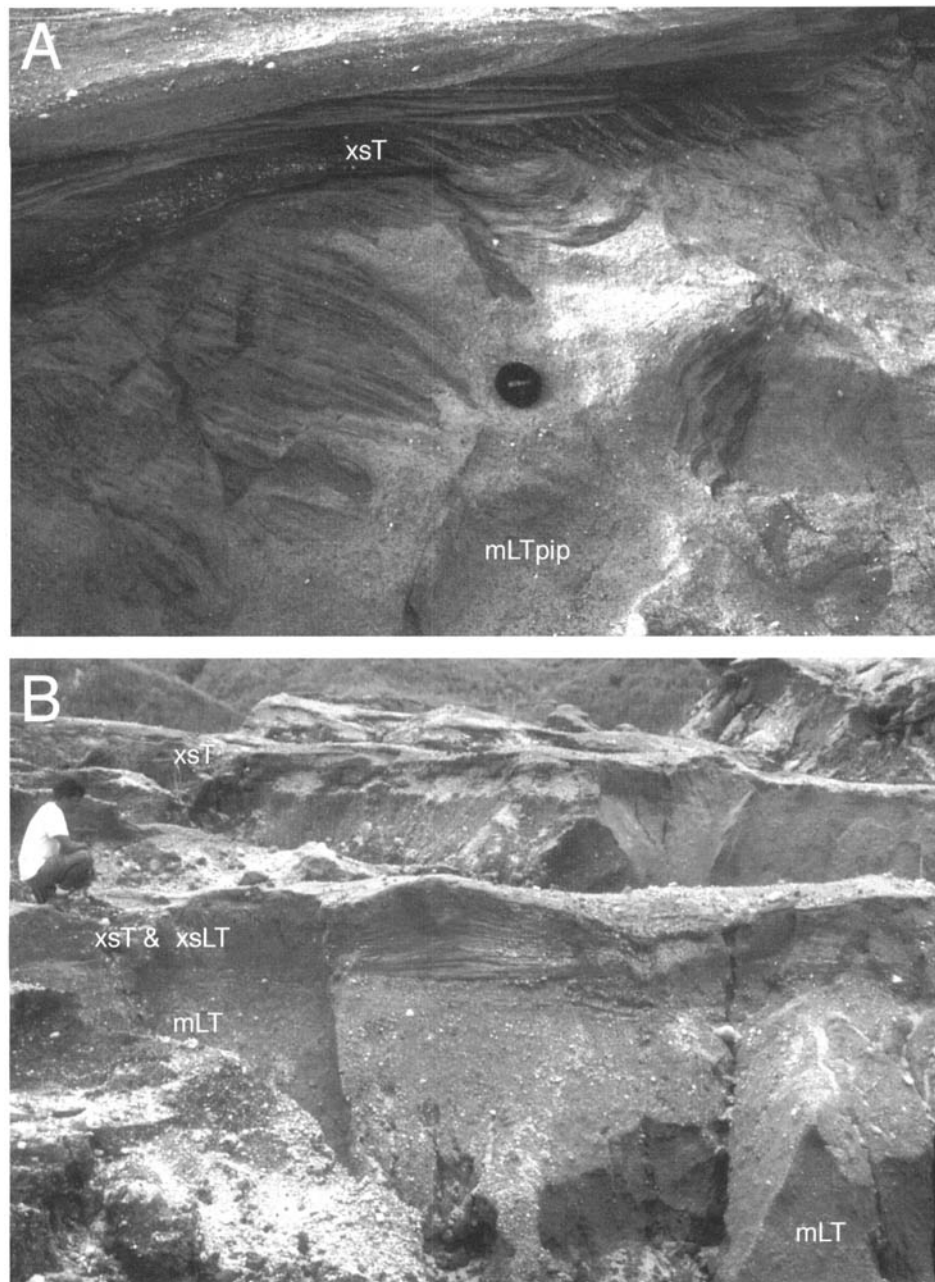


Fig. 6.15. Lithofacies at the top of ignimbrite sheets. **(A)** Load structures in the top of the Wolverine Creek Tuff ignimbrite, eastern Idaho, USA. A layer of tractional cross-stratified tuff (xsT) overlies the top of the ignimbrite and has locally foundered into it. The growth geometry of the deformation, which only affects lower parts of the xsT, suggests that deposition of the xsT from a fully dilute current occurred while the massive lapilli-tuff (mLTpip; elutriation pipes not clearly visible here, but see Fig. 5.5D) was still loose, fluidal and degassing. **(B)** The relatively flat top of the 15 June 1991 Pinatubo ignimbrite (mLT) is overlain by thin lenses of cross-stratified tuff (xsT) and lapilli-tuffs (xsLT) formed from short-lived fully dilute pyroclastic density currents derived from rootless phreatic explosions when rain and surface water gained access to the hot ignimbrite. The phreatic deposits trace for several tens of metres and interfinger with those from adjacent rootless vents. The deposits have since been deeply incised by ephemeral streams.

deposited, the fluctuations were dampened-out within a fluid escape-dominated flow-boundary zone (see explanation on p. 43).

Scour splay-and-fade stratification (new term)

Transverse sections through some ignimbrites exhibit intersecting concave-up scour surfaces, each of which (if not itself scoured) traces laterally into splay-and-fade stratification (Figs 6.16B and C). We refer to this as *scour splay-and-fade stratification*. The scour surfaces may be overlain by dbLT or mLT, with an inverse-graded base, and vary from subhorizontal, wavy surfaces to asymmetric furrow or flute-like scours that in some cases steepen to vertical.

They can occur near the base and/or high within an ignimbrite flow-unit. The position of successive stacked scours typically shifts a few centimetres, decimetres or metres laterally, most commonly in the direction opposite to that in which the stratification fades (Fig. 6.16C). Scour splay-and-fade stratification may go unnoticed where the transverse variations occur across a scale larger than individual exposures, in which case the sub-horizontal scour surface overlain by an inverse-graded layer and mLT could easily be mistaken for a flow-unit boundary (see pp. 95–98).

Scour splay-and-fade stratification traces laterally into homogeneous mLT that apparently records quasi-steady deposition from a fluid escape-dominated flow-boundary zone (see pp. 39–41). This

lateral transition indicates that momentary erosion of just-deposited ash occurs during sustained flow. Scour splay-and-fade stratification is inferred to form in a similar way to splay-and-fade stratification, except that the stacked, laterally impersistent scours indicate that the current locally became intermittently erosional, whilst deposition occurred steadily nearby (mLT). The localized erosion most probably records passage of current surges and/or localized vortex impingement directly onto the deposit surface. The deposit surface must have risen steadily (mLT) at one location (location 1 in Fig. 6.16C) while a few metres to one side (locations 2 and 3 on Fig. 6.16C) it rose and fell alternately (the stacked scours) as aggradation was punctuated briefly by erosional re-entrainment.

The coherence of the steep scour surfaces, which commonly have a near-vertical inverse-graded layer against them, indicates that the eroded deposit was briefly supported by material of closely similar concentration within the basal part of the pyroclastic current. We infer that the densities of the just-deposited and just-remobilized materials were closely similar, so that collapse of the rapidly formed steep scour was prevented.

Splay-and-fade and scour splay-and-fade stratification also occurs in sediments deposited from high-density turbidity currents (Leszczynski 1986; Branney *et al.* 1990; Kokelaar 1992) and lahars (e.g. 1991 Cerro Hudson lahar deposits, Chile), commonly at locations transitional between areas dominated by bypass (non-deposition) and areas dominated by rapid and thick deposition. These transitional locations are characterized by momentary remobilization of just-deposited sediment. We infer that splay-and-fade and scour splay-and-fade stratification mark sites where overall rates of ignimbrite aggradation are less than at locations (e.g. downcurrent and/or on lower slopes) where the ignimbrite is entirely massive (mLT).

We propose that significant variations in flow across small distances are common in catastrophic density currents, but that they are sensitively recorded by lithofacies only at locations where the current only just becomes depositional so that most of the current load bypasses and overall aggradation rates are relatively low. In these conditions the current variations are recorded in the ignimbrite, for example as splay-and-fade stratification. In contrast, where currents are predominantly dumping their load and overall aggradation rates are relatively high, lithofacies (e.g. mLT) do not so sensitively record flow fluctuations. Hence, splay-and-fade lithofacies tend to register flow variations while massive deposits can give a misleading impression of current homogeneity and uniformity.

Effects of current thalwegs and braiding

Laterally uniform ignimbrite sheets with near-horizontal depositions (Fig. 6.6A) may form from unconfined short-lived, very large mass-flux currents that move as laterally uniform sheet-flows. However, with sustained flow there is a tendency for currents to develop thalwegs (p. 19), and initial subtle transverse variations of current behaviour may affect the later pattern of sedimentation and erosion, with development of an aggradational topography that further accentuates the transverse organization of the current. As thalwegs develop and dissipate, migrate, braid and meander, during sustained aggradation of ignimbrite across a plain, the positions of successive coarse-grained pumiceous channels and levees, and snouts or dams (see pp. 47–49), will migrate laterally. Thalwegs may become channelled, diverted or abandoned, and coarse pumice accumulations may become successively overridden or broken through by deepening ponds of ‘quick’ mLT. These processes can give rise to pumice lenses (p. 76), various grading patterns (pp. 66–71), impersistent scours and lithic trains, as well as diachronous layers of various lithofacies dispersed widely within a thick and extensive ignimbrite. Such features are well known from cross-sections through ignimbrites (Wright 1981; Druitt 1985; Cole *et al.* 1993; Bryan *et al.* 1998a; Fig. 5.10C), but exposure limitations normally prevent their internal three-dimensional organization

being fully resolved.

Consider a sustained large-volume pyroclastic current that radiates across a plain from a central vent. Proximally the current may initially move as a circumferentially uniform sheet-flow and may deposit relatively homogeneous, simple massive ignimbrite (e.g. Ito ignimbrite; Aramaki 1984) with few internal subdivisions, layers or lenses. With increasing radial distance and consequent spreading, the current mass flux becomes less than it was more proximally until the current is insufficient to inundate the landscape evenly. Here, flow between thalwegs may be minor and the current may increasingly divide into separate ribbon-like elements. Through time and with lateral migrations of the thalwegs the ignimbrite in distal areas will aggrade with considerable lateral variability. The resultant sheet here may comprise numerous layers (as in a ‘compound’ ignimbrite; Wright 1981), including variously graded beds and pumice-rich lithofacies that record former pumice levees and dams (see pp. 76–77). Even when the supply is quasi-steady at source, such layering may develop, because shifting pumiceous bars, dams and levees cause intermittent diversions of the current so that flow at a particular location is highly unsteady.

As a sustained eruption gradually waxes and then wanes, the outer limit of any circumferentially uniform sheet-flow may advance and then retreat. Thus, in medial reaches, the ignimbrite sheet can have layers and lenses near its base, then pass up into laterally uniform homogeneous massive ignimbrite marking the phase of peak flow, and then pass up into ignimbrite with numerous internal layers and lenses towards the top.

Gradations between massive valley-filling ignimbrite and stratified topographic veneers

Many ignimbrites show transverse gradational changes from stratified lithofacies on topographic highs to massive lithofacies in valleys: for example in the Taupo ignimbrite (Wilson 1985), the 1991 Pinatubo ignimbrite (Scott *et al.* 1996), the Valley of Ten Thousand Smokes ignimbrite (Fierstein & Hildreth 1992) and the Fasnía ignimbrite of Tenerife (see Fig. 6.17C). These indicate that traction-dominated flow-boundary zones occur on higher ground, while fluid escape-dominated or granular flow-dominated flow-boundary zones exist at valley bottoms. Six mechanisms may contribute to the implicit higher basal concentrations along the valley floors. (1) The current develops lateral (transverse) density segregation with high-concentration thalwegs and less concentrated intervening parts. Once formed, the thalwegs tend to funnel preferentially along valley axes (thalweg capture). (2) The pyroclastic density current is density-stratified on a vertical scale similar to the topographic relief so that its more concentrated levels occur at valley floors, while hills project through these levels into less concentrated upper levels of the current. The general decrease in current concentration with height is reflected by decreasing flow-boundary concentrations with height up each valley side (see Branney & Kokelaar 1997). (3) Lower, concentrated levels of a density-stratified current are topographically confined, whereas upper, less concentrated levels rise across hills (flow-stripping; see the subsection on ‘Effects of topography’). (4) During passage of a sustained pyroclastic current, loose material aggrading on valley sides continues to move, or remobilizes, downslope (Wilson 1985) as modified grain flows in which basal concentrations are sufficient to suppress tractional segregation in the flow-boundary zone at the valley floor. This is the transverse equivalent of the mechanism explained in ‘Downcurrent lithofacies changes from stratified to massive’ in Chapter 6. (5) Flow down a concave slope causes depletive current capacity and a localized valley-bottom increase in the density stratification. (6) Partial restriction of the exit from topographic lows, causing partial blocking of the current, may cause the current capacity to become markedly depletive, which decreases the shear rate in the flow-boundary zone and/or causes the current to develop increased concentrations in its lowermost parts ($R_s > R_d$; p. 93), thus favouring the formation of massive

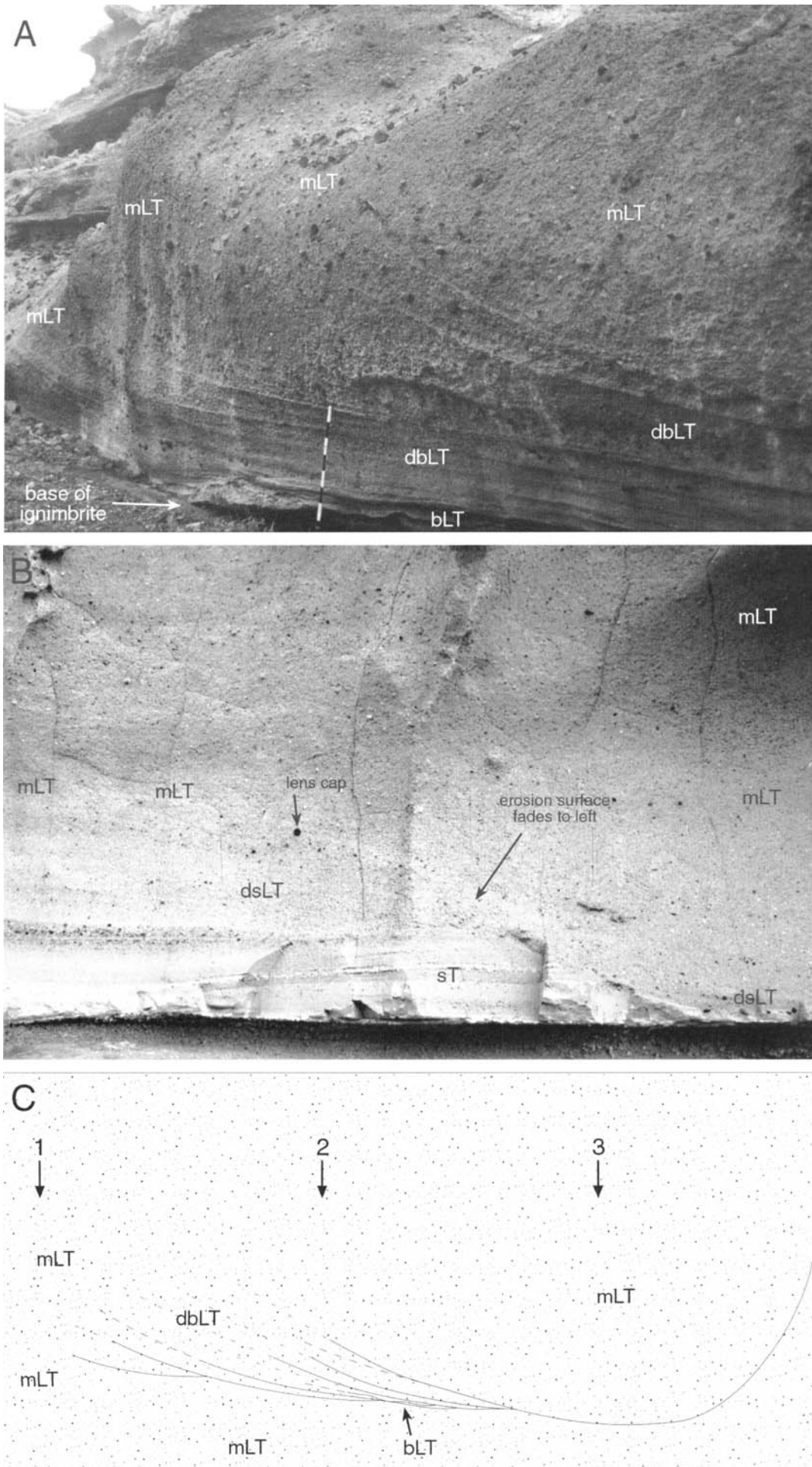


Fig. 6.16. Splay-and-fade and scour splay-and-fade stratification.

(A) Splay-and-fade stratification. Diffuse thin bedding (dbLT) splays and fades leftwards, and grades laterally into homogeneous massive lapilli-tuff (mLT) that lacks any stratification. Massive ignimbrite aggraded quasi-steadily on the left from a fluid escape-dominated flow-boundary zone at the same time as diffuse thin-bedded ignimbrite aggraded unsteadily on the right, possibly from a granular flow-dominated flow-boundary zone. The inferred current direction is away from viewer and to the right. Arico ignimbrite, southeastern Tenerife. The metre ruler is for scale.

(B) Scour splay-and-fade stratification. An erosion surface forms the base of the ignimbrite on the right, but it splays and fades leftwards where it gradually becomes imperceptible within homogeneous massive lapilli-tuff. Scouring occurred on the right while ignimbrite was progressively aggrading on the left. The inferred current direction is to the right and away from the viewer. La Caleta ignimbrite, southern Tenerife. Lens cap is 6 cm.

(C) Typical transverse arrangement of scour splay-and-fade stratification. Successive flute-like scours cut earlier scours and migrate in the direction opposite to that of splaying and fading. Sharp bedding surfaces fade out completely within homogeneous massive lapilli-tuff (mLT) and the splay (fanning out) indicates that the mLT aggraded more rapidly than the thin-bedded lithofacies. Flow-boundary conditions varied laterally between locations 1 (quasi-steady aggradation from a fluid escape-dominated flow-boundary zone), 2 (fluctuating aggradation and intermittent erosion) and 3 (record of early depositional history removed by erosion followed by gradual aggradation of mLT from a fluid escape-dominated flow-boundary zone). A thin inverse-graded layer may overlie the scour surface on the right, but this does not mark a flow-unit boundary. The scale can vary from centimetres to tens of metres.

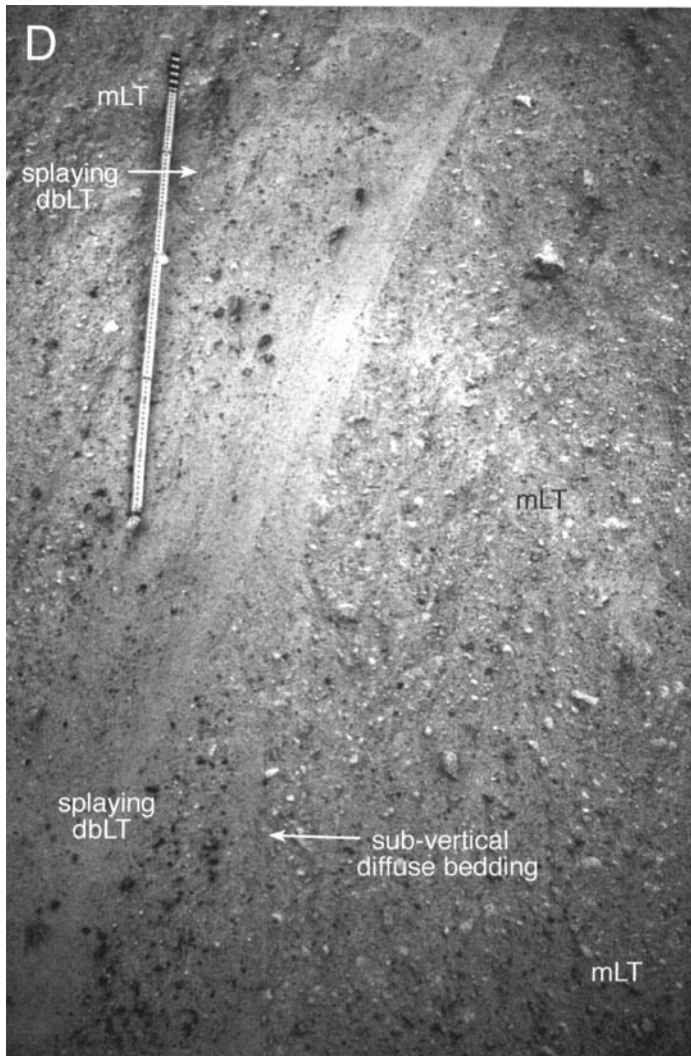


Fig. 6.16. (continued)

(D) Steep splay-and-fade stratification enclosed within thick massive lapilli-tuff. Xáltipan ignimbrite, Pueblo, Mexico. This structure suggests that a pyroclastic density current deeply scoured just-deposited loose ignimbrite on the right (mLT) and almost immediately deposited diffuse bedded (dbLT) and massive ignimbrite (mLT) against the scour surface. Bedding splays and fades downslope. The steep contact at top right extends upwards a further 5 m before fading.

ignimbrite (see p. 39).

Massive ignimbrite in valleys is sometimes referred to loosely as 'valley ponded' (e.g. Wilson & Walker 1982) to distinguish it from thinner deposits of stratified ignimbrite on hills. However, it is rarely fully surrounded, as is a pond, in that most of the topographic depressions occupied by the ignimbrite have downslope exits. Both the base and the top surfaces of massive 1991 ignimbrite in valleys that radiate down from Pinatubo volcano (Fig. 6.17A) generally dip away from source (Scott *et al.* 1996). Here the massive ignimbrite aggraded as a result of depletive current capacity, which was in response to overall radial spreading and the decrease of valley-floor slope with distance from source (Fig. 6.19A). True ponding applies to ignimbrites that were emplaced in a caldera, or within restricted valleys from which the pyroclastic current was unable to exit as rapidly as it entered.

Relatively thin deposits of ignimbrite are common on topographic highs, which they drape and on which they thin upslope. Such ignimbrite is commonly stratified or diffuse-bedded (sT, xsT dsLT, bLT lithofacies) and thus was deposited from traction-dominated flow-boundaries zones, although massive (mLT) layers or lenses also occur. We advocate that the term 'ignimbrite veneer' should be used for any thin ignimbrite layer, of any lithofacies, that drapes or partially drapes topographic highs. There should be no implication of deposition from the 'tail' of a pyroclastic flow, as was originally inferred (Walker *et al.* 1981b; Wilson 1985). Deposits previously termed 'pyroclastic surge deposits' (e.g. those emplaced from El Chichón in 1982; Sigurdsson *et al.* 1987) mostly form veneers. Stratified veneers of ignimbrite may be deposited from any

tractional reach of a current, and they may or may not pass into thick valley fills of mLT. Those that do are commonly deposited simultaneously with, but at a slower rate than, the valley-filling mLT (Figs 5.11C, 6.6F and 6.17C). On a local scale (tens of metres) stratified veneers laterally grade into valley-filling massive facies via 'splay-and-fade' stratification (see above).

Radially symmetrical ignimbrite distributions

Near-symmetrical, circular distributions of ignimbrite around central vent(s) are common, for example the Mazama ignimbrite (Bacon 1983), the Taupo ignimbrite (Wilson 1985), the 1991 Pinatubo ignimbrite (Scott *et al.* 1996), the Bandelier ignimbrites (Self *et al.* 1986) and the Carpenter Ridge Tuff (Steven & Lipman 1976). They may develop in two ways. (1) The pyroclastic density current may have flowed radially from source simultaneously in all directions, irrespective of topography, and deposited a thin circular ignimbrite sheet that aggraded evenly with time (Fig. 6.18D). (2) The pyroclastic current may have flowed in a particular direction (azimuth), initially depositing a radial ribbon (e.g. valley-filling) or fan-shaped deposit, and then spilt over into adjacent ground so that eventually the successive radial lobes merged to form a more or less circular ignimbrite apron (Fig. 6.18C). Discrimination between these two mechanisms may be difficult where the ignimbrite appears homogeneous, but each mechanism produces a distinctive depochron architecture. In ignimbrites formed by the first mechanism only, depochron surfaces trace concentrically in the sheet (and would resemble Fig. 6.6A in transverse section). A sheet formed by

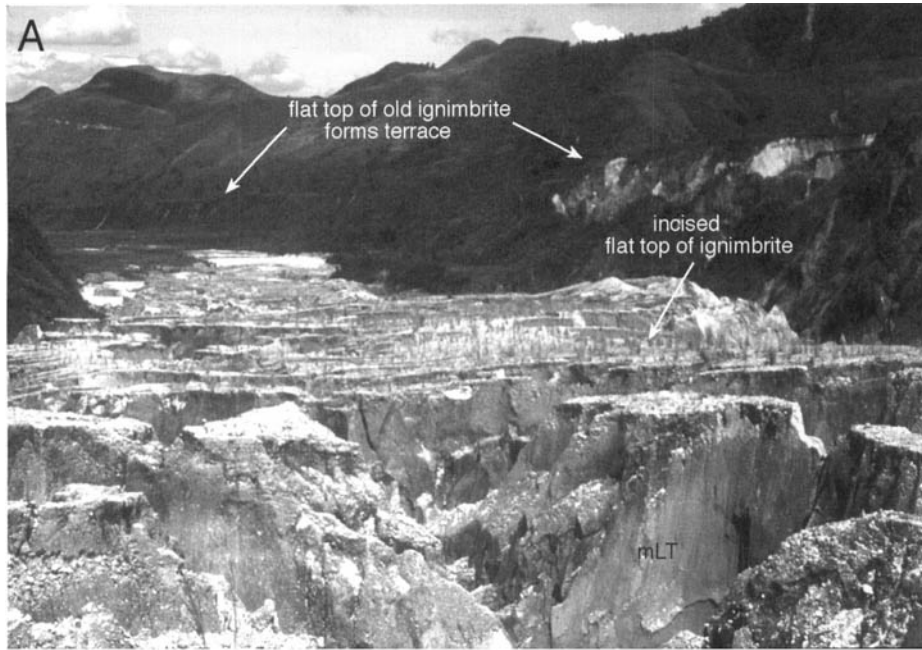
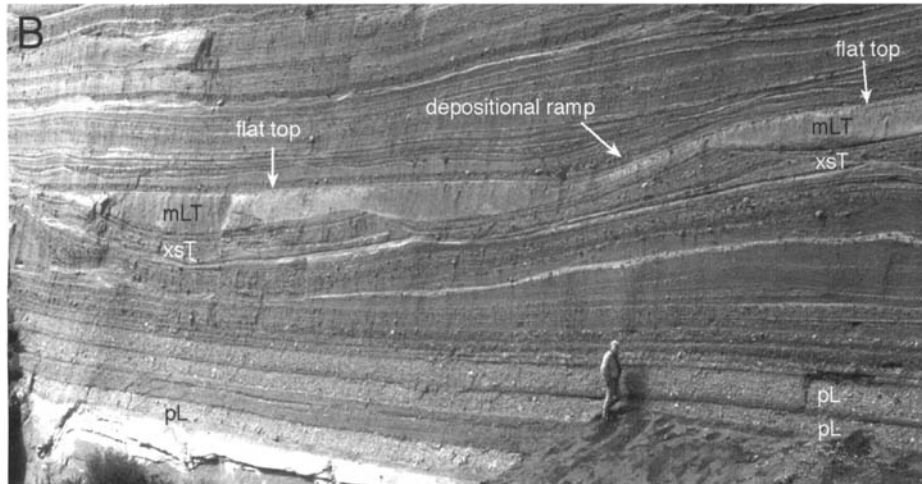
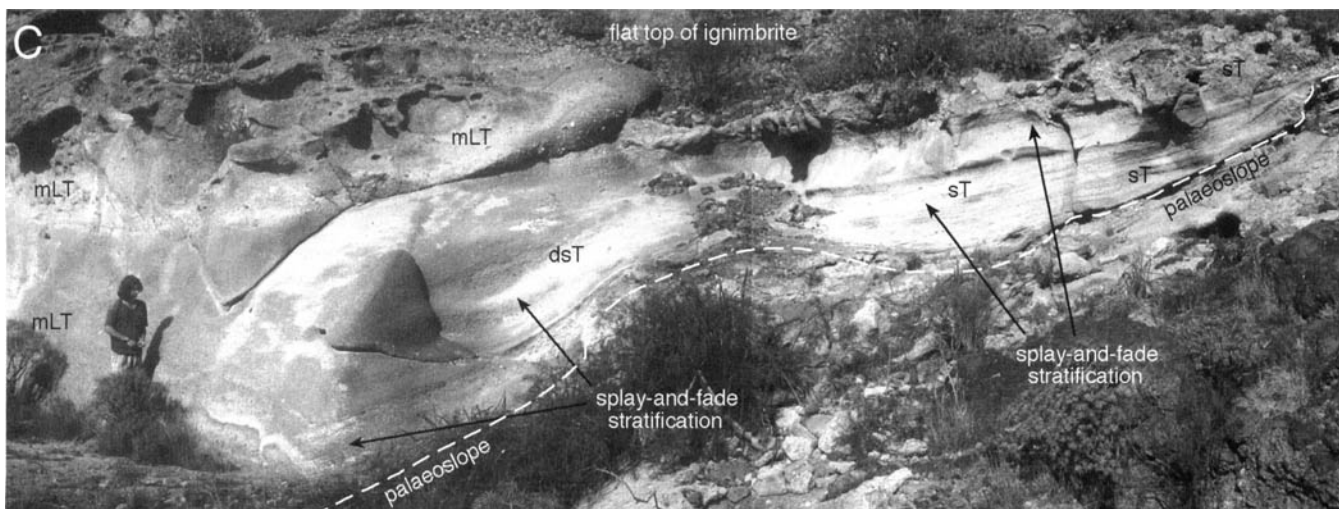


Fig. 6.17. Valley-filling and slope-draping ignimbrites.

(A) Massive lapilli-tuff (mLT) of the 15 June 1991 Pinatubo ignimbrite partially fills this steep-sided valley to a thickness of about 200 m. Its flat top, now deeply eroded by streams, is subhorizontal in transverse section, and slopes gently away to the ignimbrite's distal feather-edge. The current flowed away from the viewer. A closely similar, but much larger, older ignimbrite forms the dark vegetated terrace behind.



(B) Massive lapilli-tuff (mLT) partially fills dune-topography in underlying cross-stratified tuffs (xsT) and locally has flat subhorizontal upper surfaces (transverse section). Above the geologist it mantles the sloping topography (depositional ramp) and its top slopes nearly parallel to the substrate slope. The flat tops suggest that some of the loose lapilli-tuff depositing at a fluid escape-dominated flow-boundary zone is fluidal ('quick') and capable of down-slope flow. In contrast, the stratified deposits (xsT) from a traction-dominated flow-boundary zone have strength immediately they are deposited and so are able to deposit on slopes (e.g. foresets). Layers of well-sorted pumice lapilli (pL) are fallout deposits. Laacher See, Eifel, Germany.



(C) Stratified ignimbrite (sT) draping the palaeoslope on the right grades laterally into entirely massive valley-filling ignimbrite (mLT) on the left. The thickness variations and onlap architecture of the splay-and-fade stratification indicate that massive ignimbrite (mLT) aggraded in the valley at the same time as stratified ignimbrite was being deposited upslope, and that the rate of mLT aggradation was higher than the rate of sT aggradation. This indicates that the flow-boundary zone of the current varied laterally and gradationally from fluid escape-dominated in the valley to granular flow-dominated upslope, and that the location of this transition shifted transversely, from left to right (upslope), with time as the valley gradually filled. Ignimbrite of the Fasnja Formation, SE Tenerife.

lateral shifting of current pathways will have a petal-like architecture, which in transverse (circumferential) cross-section may exhibit an imbricate depochron pattern (like Fig. 6.6B). If the radial direction of the current fluctuated to and fro sideways, stacked flow-units would result at some sites, even though the current was sustained at source (see the first section of this chapter). The 1991 Pinatubo ignimbrite is an example of an incompletely merged radial deposit that locally fills radial valleys and locally overtops radial ridges (Scott *et al.* 1996; Figs 6.6F and 6.19A). This would have produced a circular ignimbrite apron had the eruption and aggradation continued. Larger volume ignimbrites may bury substantial substrate topography to form shields (see below).

Ignimbrite fans and asymmetric ignimbrite distributions

Ignimbrites commonly have markedly asymmetric, ribbon or fan-shaped regional distributions, for example being largely confined to a single valley, as with the Valley of Ten Thousand Smokes ignimbrite (Fierstein & Hildreth 1992).

Markedly asymmetric distributions may arise: (1) where a pyroclastic density current debouches asymmetrically from the volcano, for example by derivation from a directed or inclined pyroclastic fountain (Lagmay *et al.* 1999; see p. 7), by flowing through a low point in a crater or caldera wall, or by being channelled proximally down prominent valleys; or (2) where the general topographic relief of the region across which the ignimbrite is distributed has pronounced asymmetry, in which case ignimbrites tend to occupy the basinal areas.

During a sustained large-volume eruption, successive asymmetric fans of ignimbrite may develop in different locations as a result of: (1) changing vent dynamics; (2) modification of the proximal topography by aggradation of ignimbrite; (3) proximal subsidence, tilting and fault-scarp growth during caldera collapse (e.g. Branney & Kokelaar 1992; Valentine *et al.* 1992; Moore & Kokelaar 1998), sometimes accompanied by; (4) vent migration or multiplication. Sequentially developed regional fans may be difficult to distinguish within an extensive ignimbrite sheet, but can be revealed by detailed fieldwork coupled with petrographic analysis in cases where the composition of the eruption or included lithic clasts changed with time (e.g. Bishop Tuff; Wilson & Hildreth 1997) (Fig. 6.19B).

Interpreting the shape of ignimbrites

When ignimbrites were interpreted as pyroclastic flows that stopped and deflated en masse, their shapes were being interpreted rather simply in terms of flow parameters such as runout, rheology and velocity (Wilson & Head 1981; Hayashi & Self 1992). The preceding sections have explored how internal architectures are constructed bit by bit through time from sustained, variable and shifting pyroclastic density currents, with varying rates and locations of aggradation commonly involving lateral accretion and remobilization. The overall shape of an ignimbrite can now be seen to be the result of a history of changing flow conditions and directions, which may be deciphered from the internal architecture.

Ignimbrites have commonly been regarded as tapering wedges that are thickest near the vent and thin with distance towards a distal limit (e.g. Fig. 6.2A) (Smith 1960; Ross & Smith 1961; Fisher *et al.* 1983; Wilson 1985). Some depositional models of currents on horizontal surfaces also produce wedge-shaped deposits that thin with distance from source (Bursik & Woods 1996). In nature, however, ignimbrites depart from a simple wedge shape for the following reasons. (1) Proximal reaches of currents are commonly non-depositional and/or erosional, so many ignimbrites have feather-edges towards source as well as distally; that is, they have a lens-shaped longitudinal profile, as in the valleys on Mount Pinatubo (Figs 6.17A and 6.19A) and in the Krakatau ignimbrite, which thickens into offshore marine basins (Mandeville *et al.* 1996). (2) Ignimbrite thickness variations are profoundly affected by slope changes in the downcurrent topographic profile, which cause

depletive or accumulative flow and thus control the locations and rates of deposition. Localized changes in current behaviour caused by slope changes, such as hydraulic jumps, turbulent mixing, flow-stripping, blocking and/or reflection, all affect ignimbrite shape. (3) Transverse topographic irregularities (e.g. hills and valleys) may variously channel or divert pyroclastic currents, for example causing flow-line divergence or convergence. (4) Ignimbrite shape fundamentally depends on how the ignimbrite architecture was constructed through time (see Fig. 6.12); for example, deposition is rarely sustained at all locations for the entire aggradation history. With progressive aggradation, the volume of an ignimbrite is cumulative and is unrelated to current volume at any time, so no simple relationship between ignimbrite volume and runout distance is anticipated.

A classification of ignimbrite shapes

Shapes of ignimbrites can be broadly classified into six intergradational categories (Fig. 6.18). Many ignimbrites have characteristics that span more than one category.

- (1) *Ignimbrite lobes*, hundreds of metres to kilometres in length and generally less than 10 m thick, have convex pumiceous snouts and lateral margins, and are ribbon-like with 'cat's-paw' terminations (Fig. 4.7) and marginal levees (Fig. 6.6E). They are small-volume deposits from short-lived, low mass-flux currents (e.g. 12 June, 22 July and 7 August 1980 deposits of Mount St Helens; Rowley *et al.* 1981).
- (2) *Ignimbrite fans*, generally hundreds of metres to several kilometres in length and tens to hundreds of metres thick, typically fan out from a canyon or vent onto a plain or valley floor, and thin to a distal feather-edge (e.g. pumiceous fans formed by the 18 May 1980 eruption of Mount St Helens; Rowley *et al.* 1981). Fans may be formed from asymmetric moderate to large mass-flux eruptions, and/or from the merging of successive small volume ignimbrite fans, ribbons and lobes over extended periods (Fig. 6.6D).
- (3) *Ignimbrite aprons*, typically kilometres to tens of kilometres in radial length, are laterally extensive bodies that thin at feather-edges both proximally and distally, and form by the merging together of adjacent, either simultaneously formed or successive, radial fans. They may completely encircle a volcano. Many silicic caldera volcanoes (e.g. Santorini, Valles, Crater Lake) have ignimbrite aprons.
- (4) *Thin circular ignimbrite sheets* comprise ignimbrite that is much thinner than the vertical relief of topographic irregularities, which it drapes and only partly infills. They have near-circular distributions, typically tens to hundreds of kilometres in diameter and symmetrically distributed around a central source, and they typically include some ribbon-like thick ignimbrite in valleys (e.g. Taupo and Kidnappers ignimbrites; Wilson *et al.* 1995). They are interpreted to result from short-duration, large mass-flux eruptions.
- (5) *Ignimbrite shields* also have a near-circular distribution around a central source, but they are sufficiently thick to have completely buried all topographic irregularities so that the distribution of uppermost levels of the ignimbrite is little affected by palaeotopography, apart from at the distal feather-edges. In distal parts the ignimbrite is thinner and it may extend further down palaeovalleys. Ignimbrite shields have a low-angle convex-up profile and are generally from large-magnitude, long-duration eruptions. Some may develop from the merging of successive radial fans, but no examples of this are known. Their shape may be modified by caldera collapse and/or resurgent uplift. True shields are scarce.
- (6) *Topographically confined ignimbrites*. These ignimbrites have the shape of the topographic depression that they occupy, and so may be shoestring-shaped where they fill a valley or series of valleys, rectangular wedge-shaped where they occupy a graben, or a more complex basinal shape where they occupy a regional drainage basin. They may initiate as small fans or aprons, but their shape rapidly assumes that of the depression as it is filled

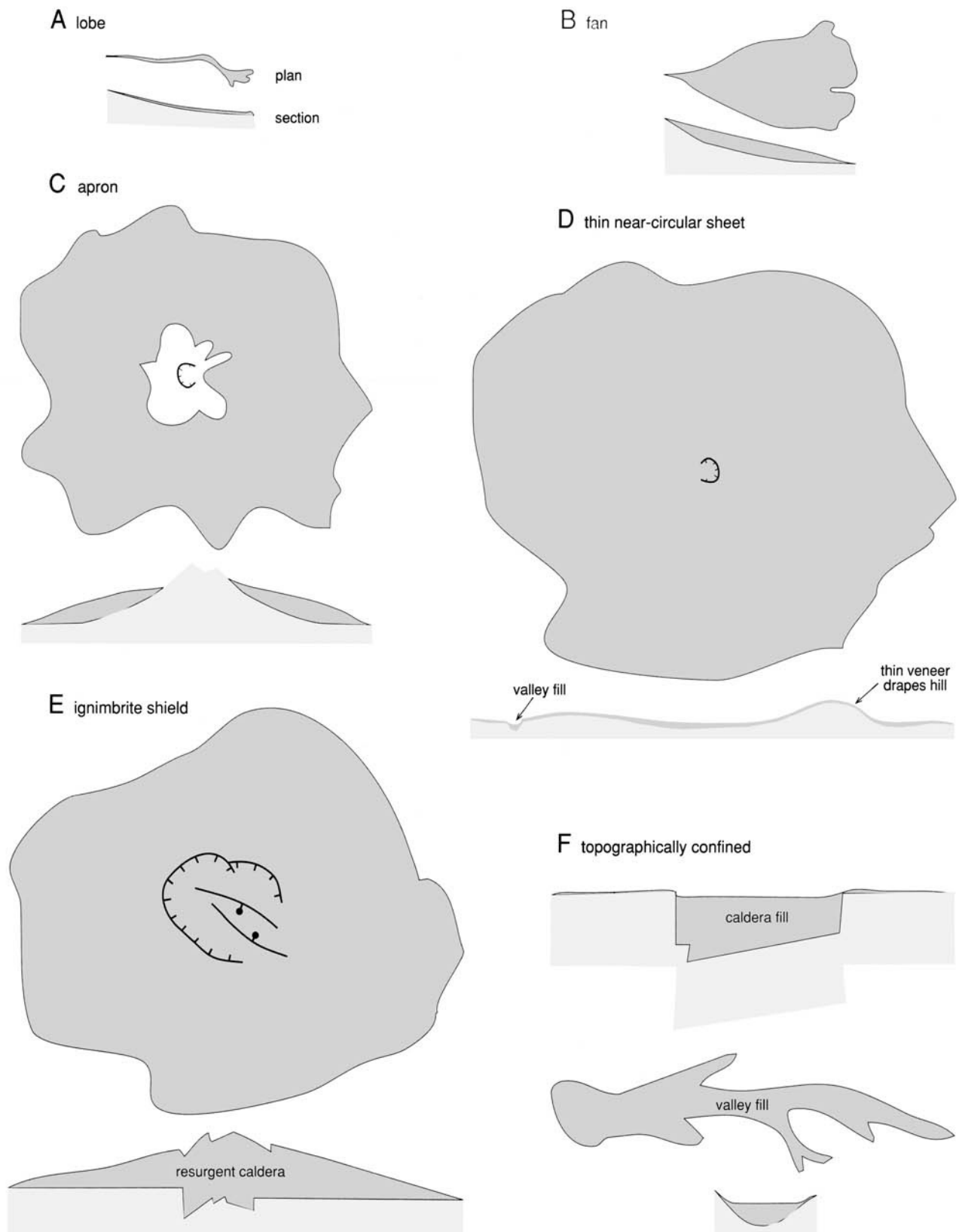


Fig. 6.18. A classification of ignimbrite shapes. Note all categories are intergradational. Examples and scales given in the text.

(Valley of Ten Thousand Smokes ignimbrite; Fierstein & Hildreth 1992). Caldera-filling ignimbrites are of this type; they may be as thick as 2 km (Lipman 1984), may have various shapes depending on the shape of the caldera (graben-shaped,

bowl-shaped, asymmetric trapdoor-fill, complex piecemeal or funnel) and may have complementary thin outflow sheets (aprons or fans). Outflow sheets are exact time-equivalents of caldera fills *only* if the pyroclastic density currents constantly

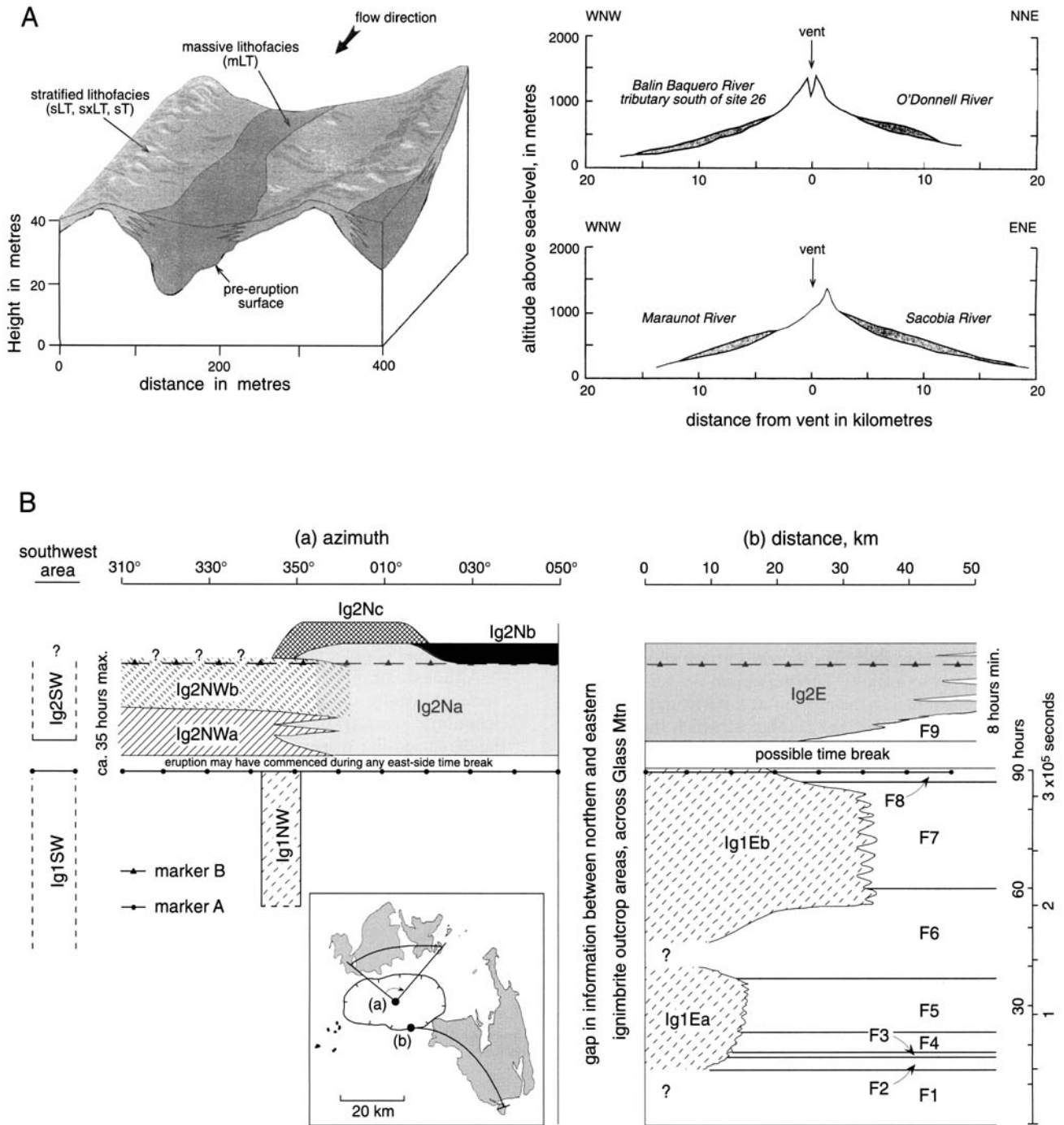


Fig. 6.19. Ignimbrite architectures: two case studies. (A) Block model and longitudinal cross-sections through the 1991 ignimbrite of Mount Pinatubo, Philippines (from Scott *et al.* 1996). (B) Timings of fall and ignimbrite units of the Bishop Tuff, California, USA. Inset map shows location of transverse (a) and proximal to distal (b) sections. In the transverse section (a) the labelled ignimbrite 'subpackages' (e.g. Ig2Na) are drawn to represent their projected dispersal arcs and relative stratigraphic positions. In the longitudinal section (b) the earlier phase of the eruption is scaled for time and fallout deposits are labelled. Two inferred time markers, defined by upsection appearances of distinctive lithics, link the northern and southeastern sections (redrawn from Wilson & Hildreth 1997, fig. 19). Such markers constitute a type of entrachron (see p. 88).

spilled outside the caldera limits whilst the caldera fill aggraded. Most outflow sheets probably correlate to only some fraction(s) of the collapse history. Resolution of depochron architecture could reveal the subsidence history of a caldera, for example by distinguishing the times before, during or just after subsidence, when the pyroclastic current was able to flow beyond the developing caldera walls. It may also be possible to distinguish successive incremental subsidence geometries during progressive caldera collapse (e.g. due to tilting, downsag, horst and

graben development, or growth faulting in the caldera floor; Branney & Kokelaar 1994b; Moore & Kokelaar 1998).

Significance of aspect ratio

The aspect ratio of an ignimbrite sheet is the ratio of average sheet thickness to the diameter of a circle that covers the same area as the sheet (Walker 1983; Wilson *et al.* 1995). Average thickness is difficult to derive for most ignimbrites. Ignimbrite aspect ratios

range across a spectrum between two end-members (Walker 1983); *high aspect-ratio ignimbrites* are thick and geographically restricted, for example the Valley of Ten Thousand Smokes ignimbrite, Alaska (Fierstein & Hildreth 1992), and *low aspect-ratio ignimbrites* are thin and extensive, for example the Taupo and the Kidnappers ignimbrites of New Zealand (Wilson *et al.* 1995), the Peach Springs ignimbrite, USA (Buesch 1992) and the Rattlesnake ignimbrite, USA (Streck & Grunder 1995).

It has been proposed that the spectrum of aspect ratios reflects different velocities of the pyroclastic currents, with low aspect-ratio ignimbrites being emplaced more violently than are high aspect-ratio ignimbrites (Walker 1983). This interpretation warrants reappraisal in the light of the progressive aggradation model for ignimbrite emplacement.

First, the *thickness* of progressively aggraded ignimbrite at a location reflects both the rate and the duration of aggradation at that location (minus modifications due to compaction). The rate of aggradation may vary with time (unsteadiness) and, because of bypassing and depositional diachroneity, the duration of aggradation at any location may not be the same as the duration of the current. Much of an ignimbrite's thickness may have been deposited at a time when the current did not reach its maximum extent, so thickness has no direct relation to current properties at the time of maximum runout. Several known ignimbrite sheets are the net result of shifting patterns of deposition and fan-merging (see above; e.g. Figs 6.6, 6.12 and 6.19), and even massive flow-units may have complicated internal deepochron architectures (see pp. 87–91 and 98) that record rapidly shifting, diachronous deposition.

Secondly, ignimbrite *length* (maximum runout distance) is only a measure of the maximum distance that the current travelled along the ground (e.g. prior to lofting). This maximum is a function of the eruptive mass flux supplying the current at a particular time in the current's history (p. 16) and of the manner in which the current at that time was variously divergent or channelled from the volcano. The length of a pyroclastic current is also affected by topography (which changes as ignimbrite aggrades) and admixture of air (see Woods & Bursik 1994).

We conclude that ignimbrite aspect ratio has little directly to do with current velocity. There appears to be a general tendency for low aspect-ratio ignimbrites to aggrade during short-lived and/or high mass-flux eruptions, and high aspect-ratio ignimbrites tend to aggrade during long-lived and/or lower mass-flux eruptions (also

see Freundt 1999). However, for the reasons given above, it can be misleading to infer overall properties of a pyroclastic current by simple reference to overall ignimbrite shape (e.g. length and thickness). Current behaviour may only be deciphered properly when the ignimbrite architecture has been resolved, for example by tracing the internal pattern of entrachrons (p. 88).

Top surfaces of ignimbrites

Ignimbrite sheets have flat upper surfaces that vary from subhorizontal to sloping at up to approximately 5° (Fig. 6.17). Ignimbrite plateaux (e.g. Marshall 1935; see back cover) are dissected parts of widespread ignimbrite fans, aprons or topographically confined sheets. Pristine top surfaces may exhibit small-scale (usually <2 m) topography due to the presence of last-deposited pumiceous lobes and levees, and may exhibit phreatic explosion craters with related deposits (see 'Interpreting lithofacies at the top of ignimbrites' on p. 109).

The angle of slope of top surfaces of unconfined ignimbrites is partly the product of the internal stacking architecture of the sheet (e.g. Figs 6.4, 6.5, 6.6 and 6.12) and the subjacent buried topography. For example, top surfaces may be relatively steep where the distal depositional limit of the current(s) retreated only slowly during waning stages of the eruption, so that substantial thicknesses of ignimbrite were deposited proximally with no medial or distal time-equivalents (see Fig. 6.4C). Conversely, more gently sloping tops form when the depositional limit of the parent current(s) retreated rapidly. Thus, the slope of the top of an ignimbrite sheet can be controlled by the temporal evolution of the current, and is not simply a function of overall current rheology.

Although stratified ignimbrite can drape topography, with top surfaces locally dipping at up to 30°, top surfaces of massive ignimbrite generally have much lower slopes. This indicates that the hindered-settling dispersions that sediment through fluid escape-dominated flow-boundary zones (and deposit mLT; see pp. 39–41 and 56) are unstable on slopes steeper than a few degrees and consequently drain downslope until they encounter lower slopes or topographic dams. In contrast, dispersions from other types of flow-boundary zones have more strength (quasi-static frictional grain contacts; see p. 35) and can remain perched on slopes, unless these are oversteepened by aggradation or undercutting, in which case they are remobilized as deposit-sourced downslope flows (see p. 49).

Chapter 7

Overview, key implications and future research

Overview and key implications

The vast extent of many ignimbrites shows that eruptions have occurred on almost unimaginable scales, well beyond any modern human experience. Evidence is emerging that plumes derived from large pyroclastic currents have impacted climate and biota on a global scale, whilst certain types of ignimbrites (e.g. extensive rheomorphic ignimbrites) indicate particularly awesome styles of eruption and emplacement that are regionally devastating and which we do not fully comprehend. Such unimaginable eruptions are bound to occur again. If we are to interpret such catastrophic events correctly, and possibly even anticipate the impact of future occurrences, it is essential that ignimbrite sheet architectures are studied further in order to understand the mechanisms, rates and durations of the fundamental processes. Of particular importance in risk mitigation will be the understanding of early stages of such devastating eruptions. The new approaches and descriptive schemes presented in this Memoir are intended to stimulate and facilitate such future work.

Below, we summarize the fourteen main points and key implications of our analysis of pyroclastic density current deposition. Many of the ideas are also directly applicable to the interpretation of other types of sediment gravity flow deposits, such as those from turbidity currents, debris flows and lahars.

- (1) We have reviewed significant recent advances in the understanding of particle transport, segregation and deposition. Valuable insights derive from laboratory experiments and computer models, from analogous processes in nature and in industry, and from observations of volcanic eruptions and their deposits.
- (2) Clasts in pyroclastic density currents are supported by combinations of fluid turbulence, grain collisions, fluid escape during hindered settling, buoyancy and by an interface, as in saltation, rolling and sliding. Each support mechanism is influenced by the local particle concentration and shear intensity, both of which change with height in the current (stratified flow), with time (unsteady flow), with location (non-uniform flow) and with clast type (polydisperse flow). Clasts segregate during both transport and deposition, according to their various settling velocities, buoyancy, aerodynamic drag and diverse interactions with other clasts during granular shear and fluid escape. Their different rates of downward movement (sedimentation) and/or upward migration (e.g. elutriation) relative to the lower boundary of the current vary with location, with height in the current and with time.
- (3) We have developed a *conceptual framework* for investigating the deposition of all types of ignimbrite from pyroclastic density currents. This treats ignimbrite sedimentation as a sustained process in which the mechanisms of deposition, and hence the sorting and bed-form characteristics, are ultimately determined by the nature of the *flow-boundary zone*. This zone spans the basal part of the current and the uppermost part of the incrementally aggrading deposit.
- (4) We have described and illustrated the most common ignimbrite lithofacies with reference to numerous examples from ignimbrites around the world. Ignimbrite lithofacies, distinguished by sorting and bed-form characteristics, are diverse and spatially intergradational. A non-genetic scheme for classification of ignimbrite lithofacies is presented, and is amenable to further development. Some new lithofacies (e.g. *diffuse-stratified lapilli-tuff*) and structured lithofacies associations (e.g. *splay-and-fade* stratification and *scour splay-and-fade* stratification) have been described and interpreted in terms of flow-boundary zone conditions and processes. We interpret lithofacies associations as recording various and temporally changing types of flow-boundary zone (see summary on Table 7.1).
- (5) We have proposed four main intergradational types of flow-boundary zone: those dominated by *direct fallout*, by *traction*, by *granular flow* and by *fluid escape*. The abundant intergradational types of lithofacies that occur in ignimbrites record transitions between these types. As lithofacies are controlled primarily by flow-boundary zone processes, they provide only limited information about bulk properties of the current at that location.
- (6) We have presented a new twofold classification for pyroclastic density currents. *Fully dilute pyroclastic density currents* are those in which interactions between clasts have little effect on particle support, segregation and current rheology, even toward the current base. Such currents have flow-boundary zones dominated by direct fallout or by traction. *Granular fluid-based currents* are those in which clast interactions and/or fluid escape significantly affect clast transport and support, at least in lowermost levels of the current. Their lower flow-boundary zones are dominated by granular flow or by fluid escape. The two types of current are entirely intergradational. Ignimbrite lithofacies architectures suggest that an individual pyroclastic density current can differ in type along different reaches, or laterally, and with time.
- (7) In a fully dilute pyroclastic density current, a steep shear gradient exists near a sharply defined deposit surface. If the shear is sufficient, this facilitates traction with production of a stratified and relatively well-sorted deposit (traction-dominated flow-boundary zone). In granular fluid-based currents, on the other hand, basal parts are at least hyperconcentrated, and turbulence is increasingly suppressed with proximity to the lower flow boundary while clast contacts and frictional interactions increase. Where the flow-boundary zone is dominated by fluid escape, particle settling is hindered by escaping fluid in both the lowermost part of the current and in the uppermost part of the compacting deposit, and the shear velocity *gradually* diminishes to zero at the flow boundary. Absence of a sharp rheological interface inhibits traction so that a non-stratified deposit forms, sometimes with orientated grain fabrics and/or elutriation pipes. Where the flow-boundary zone is dominated by granular flow, high rates of granular shear induce various granular segregation processes.
- (8) As each sedimenting clast settles through a density-stratified flow-boundary zone, it is subjected to changing combinations of segregation effects. As a result of this, the zone acts as a *selective filter* in which some clasts, such as dense lithic lapilli, pass downwards more easily than others, such as larger pumices, which therefore travel further downcurrent (*overpassing*) and may form terminal pumiceous snouts, dams or levees. However, selective filtering in the flow-boundary zone varies with time (during current unsteadiness) so that different clast populations may be deposited successively at a single location.
- (9) As a result of the various segregation processes that occur

Table 7.1. Summary of alternative interpretations of common ignimbrite features (see Chapters 4 and 5 for full explanations). Previous interpretations are as reviewed in Carey (1991); Francis (1993), and references therein.

Observation	Previous interpretation	Alternative interpretations (this Memoir)
Poor sorting	The current was of high concentration	Absence of tractional sorting. Fine ash agglomerated. Interlocking in high-concentration parts of the flow-boundary zone may have limited segregation during deposition. Concentration at higher levels in the current not indicated
Vertical grading patterns (e.g. of grain size or clast type)	The current was stratified with respect to clast sizes in the same way as occurs in the deposit	Sizes of depositing clasts changed with time due to current unsteadiness (e.g. waxing and waning flow competence, changing clast supply, and/or changing selective filtering). Provides no information about current stratification
Grading absent	Highly unsteady en masse deposition of an homogeneous (non-stratified) pyroclastic current	Steady aggradation from steady current. Provides no information about presence or absence of current stratification
Inverse coarse-tail grading of pumice	The pyroclastic current was denser than the pumices, which floated to the top of the (laminar to plug-like) semi-fluidized current	Selective filtering resulting from buoyancy and granular flow processes in a high-concentration flow-boundary zone prevented deposition of larger pumices until the current waned. Overall density of the current is not indicated
Absence of stratification	En masse deposition from an extremely unsteady, waning pyroclastic flow	Aggradation was quasi-steady. Traction prevented by high concentrations in a fluid escape-dominated flow-boundary zone that lacked a sharp rheological interface
Thickness of a massive layer	Proportional to current thickness	A function of rate and duration of deposition. Provides no information about current thickness
Diffuse, localized stratification within a flow-unit	Shearing within a current (semi-fluidized plug flow) as it finally comes to a halt en masse	Small-scale unsteadiness within the lower flow-boundary zone of a quasi-steady granular fluid-based current causes unsteady segregation and deposition. Flow-boundary zone was transitional between granular flow-dominated and fluid escape-dominated
Laterally traceable tops and bases of stacked massive divisions	Flow-unit boundaries, representing pauses between successive currents or overlapping current lobes	Records either pauses between successive currents, or records flow unsteadiness resulting in momentary phases of erosion, non-deposition, or traction, during the sustained passage of a single depositing current
Ignimbrite length (distance from source to the distal termination of the sheet)	A measure of current velocity and runout; short deposits record sluggish currents, long deposits record highly energetic currents	Records how far the current travelled whilst depositing, prior to wholesale lofting; a high-velocity current may loft close to source forming a short deposit. Largely controlled by current mass flux
Ignimbrite aspect ratio (AR)	Records current velocity; High Aspect Ratio Ignimbrite (HARI) from low-velocity current; Low Aspect Ratio Ignimbrite (LARI) from high-velocity current	Aspect ratio records transport distance prior to lofting (see above), and the rate and duration of deposition (see thickness, above)
Matrix-supported blocks	The current had a high yield-strength that supported the blocks, or the blocks sank slowly through a viscous laminar Newtonian current during transport	The blocks were at least intermittently supported (e.g. in rolling, sliding, saltation) along a rising deposit surface during progressive aggradation. Current competence and deposit yield strength are indicated, rather than current yield strength
Convex, lobate shape of deposit terminations	Current had high viscosity and/or yield strength, and moved as a plug with marginal dead zones	Levee deposits and pumice dams had high yield strength; overall rheology of the transporting current is not indicated
Vertical elutriation pipes	Caused by segregation within the current. Indicate fluidization-enhanced current mobility	Newly formed <i>deposit</i> underwent segregation during hindered settling and degassing. High gas-flux channelled through deposit. No indicator of current mobility
Inverse-graded layer at base of ignimbrite	The grading developed in response to dispersive forces in a former shearing layer at the base of a non-shearing plug	Records flow-boundary zone changes during initial deposition just behind the leading edge of the current due to waxing flow competence, larger clasts trailing behind the current's leading edge and/or clast percolation within a flow-boundary zone that changed with time from granular flow-dominated to fluid escape-dominated
Stacked thin inverse-graded layers	Record multiple flow-units, or shearing levels within the decelerating current	Record current unsteadiness; clast percolation and interlocking during unsteady deposition from granular flow-dominated flow-boundary zone. Possible influence of eddies on traction carpets (Fig. 4.5). Multiple flow-units also possible
Proximal lithic-breccia	Energetic deposition in a turbulent proximal 'deflation zone' wherein an expanded, dilute current transforms wholesale with distance into a laminar, high-concentration giant fluidized flow	Deposited by similar mechanisms to ignimbrite, but more energetically. Fines were elutriated during rapid deposition and sedimentation-fluidization. Current does not deflate, but segregates gravitationally along its length, becoming concentrated toward the deposit and more buoyant in its upper parts

before and during deposition, the clast population of an ignimbrite lithofacies at any one location is likely to be dissimilar to any erupted population, or even the population of any reach of the density current at a particular moment. For example, a pyroclastic density current that is relatively poor in dense clasts can in some circumstances produce a

deposit rich in dense clasts as a result of selective filtering in the flow-boundary zone and overpassing of other clasts. This principle of clast-population segregation, and the consequent non-equivalence of a batch of particles in a deposit to any batch in the original dispersion, is fundamental to understanding how we may use ignimbrites to infer current

dynamics and how we may use ignimbrite zoning to infer the nature of zonation in a subvolcanic magma chamber.

- (10) The flow-boundary zone approach ascribes vertical lithofacies sequences in ignimbrites to the temporal evolution of variously sustained currents. A single pyroclastic current can produce several (stacked) massive divisions of ignimbrite with intervening bedding surfaces or layers that record changes or pauses in deposition, or even temporary erosional phases of the current. Evidence for current cessation is required for any stacked divisions to be distinguished as the products of successive discrete flows (flow-units). This is important in using deposit stratigraphy to determine eruptive history. The formation of grading patterns vertically and laterally in ignimbrites involves *gradual* changes in the competence or composition of a current, or in the selective filtering properties of its flow-boundary zone.
- (11) We introduce *deposchrons* and *entrachrons* to help describe and interpret architectures of ignimbrite sheets in terms of current depositional histories. These are time-surfaces that enable the visualization of spatial and temporal variations in deposition across a wide area, and in well-exposed ground they can aid reconstruction of current behaviour. Lateral variations of lithofacies along individual deposchrons record instantaneous downcurrent and transverse variations of a flow-boundary zone. Vertical variations within the current (e.g. density stratification), however, can be less easy to infer from the deposit.
- (12) Poor sorting in ignimbrites is partly a result of high particle concentration in the flow-boundary zone, which causes particle interlocking and limits segregation. Also contributing to the poor sorting are: (1) an initially poorly sorted particle supply from the eruption; (2) generation of fine ash by attrition, involving both breakage and abrasion of pumice clasts during hyperconcentrated flow; (3) agglomeration (adherence and clustering of fine ash particles); and (4) simultaneous deposition of diverse clasts transported by different mechanisms. For example, lithic blocks set in ash matrix some distance above the base of a massive ignimbrite are likely to have rolled or saltated along the top of the aggrading deposit, and are unlikely to have been fully supported by the current during most of their transport (i.e. they neither 'floated' nor were 'passively rafted' within the current). In comparison, the ash comprising the matrix enclosing the blocks would have had a very different transport history. Vertical, lithic and crystal-rich elutriation pipes in ignimbrites record segregation in a compacting, degassing *deposit* rather than recording fluidization of the current.
- (13) In a sustained current, deposition generally accompanies transport rather than the current undergoing transport first, followed by a phase of deposition. This means that transport may be affected by deposition. For example, modification of substrate slopes by ignimbrite deposition, or by erosion, can cause changes of flow paths, local flow velocities, mobility, and/or runout distance. Conditions in the current flow-boundary zone also can affect current runout distance. For example, in granular fluid-based currents, the rate of deposition can be significantly reduced by the upward escape of interparticle fluid through the settling dispersion (hindered settling). Unless such a current is ponded, it will continue to spread (flow) until the hindered settling is completed. In addition, the upward flow of gas displaced by settling clasts will lower the effective viscosity of lower parts of the current and supply fine ash back to higher levels.
- (14) With progressive aggradation, the thickness of an ignimbrite

depends on the rate *and* the duration of deposition, and is not directly related to the thickness or volume of the current at any instant. This has implications for the interpretation of ignimbrite aspect ratio; that is, the ratio between thickness (a function of the rate and duration of deposition) and length (the transport distance, determined by the eruptive mass flux versus the rate of deposition). Therefore, ignimbrite aspect ratio is not simply a measure of current velocity.

Future research

A considerable gap in understanding remains between models of pyroclastic density currents and the documented character of ignimbrite lithofacies, such as their sorting, fabric and sedimentary structures. To close this gap will require both fieldwork and experimental modelling.

Experimentation is required to learn about the physics of density-stratified hyperconcentrated and granular flows that have polydisperse clast populations and a gaseous fluid phase (dusty gas). Investigating deposition in steady conditions would be a useful start. The main four types of flow-boundary zone proposed in this Memoir require experimental investigation to quantify the controlling parameters and to constrain the physical processes, such as segregation and attrition, via which distinctive lithofacies are produced. Also requiring investigation are the important links between flow-boundary zone conditions and the conditions in the overriding parts of the current; little is known about the nature of flow stratification in granular fluid-based currents, and how this stratification responds to changes in current velocity and capacity, and to deposition. Until the links are understood it will continue to be difficult to infer whole-current behaviour from the lithofacies in an ignimbrite. As most experimental work to date has used aqueous analogues for pyroclastic density currents, it will be useful to explore attributes of pneumatic polydisperse systems: for example, to investigate the effects of gas compressibility, rheology and thermal expansion upon transport, segregation and deposition.

Rapid advances in particle technology and in computer simulation are making it easier to model aspects of pyroclastic transport, segregation and deposition. It seems likely that modelling will soon outstrip the study of natural deposits. Very few ignimbrite sheets have been analysed in real detail, and funding for such work can be scarce. However, both field-based and modelling approaches are required if we are ever to use deposits realistically to constrain what happens during these remarkable and devastating eruptions. With the realization that ignimbrite sheets have complex architectures that are assembled through time comes the requirement to analyse sheet architectures with respect to a precise temporal framework (i.e. using deposchrons and entrachrons) to determine how large sustained pyroclastic density currents can evolve in time and space. Without this, estimates of the flow properties, velocities and durations may be misleadingly inaccurate, whilst our understanding of magma chamber stratification and how large explosive eruptions evolve (e.g. during caldera collapse) will remain speculative. Many ignimbrite sheets have insufficient three-dimensional exposure, so case studies should focus on the best-exposed ignimbrites that exhibit complex compositional zoning so that the position of entrachrons can be traced throughout. Geophysical methods, such as ground-penetrating radar (e.g. Cagnoli & Ulrych 2001), may usefully be employed to constrain the three-dimensional morphology of distinctive lithofacies, such as lithic breccias and pumice lenses, and the substrate topography between exposures.

Finally, if we are to mitigate the risks attributable to large ignimbrite-forming eruptions in the future, it will be important to analyse the opening stages of past eruptions, linking possible precursor styles of activity to the initial stages of the main ignimbrite emplacement. Determining the characteristics and durations of the early phases of catastrophic eruptions may not be easy, not least because of problems of material preservation, but it may offer some hope of minimizing the loss of life and property.

This page intentionally left blank

Definitions of terms used

- accumulative*. A downstream increase in a current parameter, such as velocity, concentration or capacity (see p. 2). For example, accumulative velocity is downstream spatial acceleration. Term coined by Kneller & Branney (1995).
- agglomerate*. Welded or non-welded coarse-grained deposit formed mainly of juvenile pyroclasts (typically spatter, scoria, pumice, or obsidian 'bombs' or lapilli) whose shapes and/or external surface textures indicate that they were partly fluidal during transport. Agglomerates can be deposited by pyroclastic density currents (p. 61), by pyroclastic fall or ballistically. Those within ignimbrite sheets commonly contain subordinate lithic blocks, pumice lapilli and pumiceous ash, and grade into pumiceous ignimbrite and/or massive lithic breccia (p. 57). In powder technology, loosely bonded clusters or clumps of fine cohesive particles are referred to as 'agglomerates'.
- agglomeration*. Adherence and clustering together of ash particles to form agglomerations: i.e. loose or firm clumps, pellets and/or accretionary lapilli. Fine ash may agglomerate within an eruption plume or in a pyroclastic density current initially due to electrostatic effects or (when moist) surface tension effects, and the agglomerations may be rapidly cemented by precipitation of salts as water evaporates (p. 83).
- agglutination*. Very rapid, syn-depositional welding of hot, fluidal pyroclasts prior to burial by aggrading ignimbrite (p. 84). Agglutination results in a welded tuff in which former clast outlines are still visible (cf. *coalescence* in which they are not).
- amalgamation*. Inferred seamless joining of deposits from successive discrete depositional events to produce a single bed with no trace of a hiatus (p. 95).
- architecture*. The overall structure of an ignimbrite, including its distribution, thickness variations, the three-dimensional arrangement of lithofacies and of 'time-lines' (depositional isochrons or entrainment isochrons), the geometry of any internal or bounding scour surfaces, and the relations of all these features to topography and substrate (see p. 4 and Chapter 6).
- ash-flow tuff*. Ignimbrite.
- aspect ratio*. The ratio of average thickness of an ignimbrite sheet to the diameter of a circle that covers the same area as the whole sheet (Walker 1983; Wilson *et al.* 1995). High aspect-ratio ignimbrites are thick and geographically restricted, and low aspect-ratio ignimbrites are thin and extensive (p. 117). Average thickness may be difficult to determine.
- basal avalanche*. A rather imprecise term sometimes used for a basal part of a pyroclastic density current that flows downslope in a manner inferred to be like an avalanche. However, avalanches encompass a wide variety of flow phenomena, and are commonly themselves partly turbulent and density stratified: i.e. more like entire pyroclastic density currents than just their basal parts. We prefer to use more precise terms like basal *modified grainflow* and/or *debris fall*, or simply 'lower levels of the stratified current', as appropriate (p. 15).
- bedding plane/bedding surface*. A generally planar surface within a deposit picked out by a sharp change in grain size or grain type. It typically records an abrupt change (unsteadiness) in deposition, a hiatus in deposition, and/or erosion (p. 95).
- block-and-ash flow*. A pyroclastic density current in which most of the juvenile component comprises dense, non-vesicular to moderately vesicular blocks, lapilli, and non-pumiceous (poorly vesicular) ash of similar composition, rather than pumiceous pyroclasts and bubble-wall shards (p. 1). Their deposits are usually of small volume and differ from ignimbrites in that they are not pumiceous, although several aspects of their sedimentation may be similar (p. 47).
- bypassing*. When all clasts in a current pass a location without depositing there (cf. *overpassing*).
- capacity*. A measure of the overall sediment load that a current is able to transport, by all mechanisms of support (Chapter 3). Relates to current size, velocity and concentration.
- coalescence*. Merging of hot, fluidal pyroclasts (droplets) to form a homogeneous liquid in which remnant clast outlines are obliterated, for example during the formation of lava-like tuff and clastogenic lava.
- cohesive debris flow*. A high-concentration gravity flow of materials that incline to stick together, for example owing to the presence of clay minerals or interstitial liquid, providing cohesive strength. Many are predominantly laminar (p. 35).
- competence*. A measure of the ability of a current to transport clasts of particular sizes and/or densities, by any mechanism, expressed in terms of maximum potentially transportable grain size. Relates to current velocity and concentration.
- depletive*. Downstream decrease in a current parameter, such as velocity, concentration or capacity (p. 2). Term from Kneller & Branney (1995).
- deposchiron* (new term). Depositional isochron: a notional surface within an ignimbrite sheet that connects clasts deposited at the same instant in time (pp. 87–88). (See *entrainment isochron*).
- dispersion*. Particles dispersed within a fluid (gas or liquid). A dispersion may be of any solids concentration up to a maximum near that of a deposit: for example, formed from deposit by shear-induced vibration. The particles may be undergoing transport or deposition (Chapter 3).
- division*. Informal descriptive term for any specified architectural portion of a deposit (ignimbrite or turbidite), usually a layer or lens that has some common characteristics and/or bounding surface(s). A division may comprise one or several lithofacies (Chapter 6).
- entrainment isochron* (new term). Entrainment isochron: a notional surface within an ignimbrite sheet that connects the lowermost clasts that were entrained in the current together at the same instant in time. For example, they may be clasts of a distinct composition, such as when a new layer of a stratified magma chamber is first tapped or when lithic debris collapses into a vent or current (p. 88). (See *deposchiron*).
- eutaxitic*. Planar fabric of deformed vitroclastic ash shards and fiamme, typically formed by hot-state compaction in welded ignimbrites and fall deposits. The fabric commonly is oblate, although in rheomorphic tuffs it typically contains an elongation lineation (p. 83).
- fiamme*. Lens or flame-shaped object, such as typically forms from a flattened pumice lapillus in a welded ignimbrite (p. 83). Fiamme also occur in welded fall deposits, and may form in other ways (e.g. tectonic deformation, sheared lava autobreccia, non-welded pumice diagenetically altered to clay and compacted during burial).
- finer-poor*. The characteristic of having a significantly lower proportion of fine ash than has the majority of the ignimbrite (pp. 61 and 101). Typically better sorted (σ_ϕ 1–3) than the finer-rich massive lapilli-tuff (σ_ϕ 2–5) of the same ignimbrite. 'Finer-poor' is preferred to the term 'finer-depleted', which has genetic connotations and derives from the early idea that facies with conspicuously little fine ash must have originated from a dispersion with a 'normal' proportion of fines but which became 'depleted' in fines by some process. What constituted the initial reference proportion of fines is not clear (fine ash is constantly both generated within, and lost from, a pyroclastic current), and the implied process of depletion cannot always be inferred.
- flotsam*. Clasts (e.g. of pumice) that do not sink to the base of a shearing granular dispersion, as a net result of their positive buoyancy and/or the effects of surrounding vibrating and/or shearing clasts (pp. 34, 41 and 94). Flotsam travels at some level

- above the base of a stratified current, in the extreme case towards the top (antonym: *lagan*).
- flow*. Fluid motion, irrespective of particulate density and motive force. Not used for an entire flowing entity (i.e. current) or for any type of deposit.
- flow acceleration/deceleration*. Ambiguous terms best avoided unless the user specifies whether they mean: (1) a temporal change of speed with reference to a fixed location that the current passes, i.e. waxing or waning velocity in an unsteady current; or (2) a spatial change of flow velocity with reference to a point moving with the flow: i.e. accumulative or depletive velocity in a non-uniform current (see pp. 2–3).
- flow boundary*. Top, base or marginal contact of a current, typically with ambient fluid (atmosphere or hydrosphere) or the substrate. The lower flow boundary, i.e. the base of the current in contact with the substrate or aggrading deposit, may be sharp or indistinct. It may be indistinct, for example, where it lies between a concentrated, slowly shearing mass of grains in the current and a similar but stationary mass of grains (uncompacted deposit) beneath. In this case the top of the deposit is defined as the level beneath which there is no net downstream movement of grains. Settling and fluid escape may occur both above and below this level (pp. 4 and 39; Fig. 4.1E).
- flow-boundary zone*. A loosely delineated zone that includes the lowermost part of the current and the uppermost part of the forming deposit (Fig. 1.2), where lithofacies characteristics are largely determined. As the deposit aggrades, the flow-boundary zone rises (Fig. 1.2A) with the deposit surface. We propose that most flow-boundary zones are transitional between four end-member types (pp. 37–41): (1) fallout-dominated; (2) traction-dominated; (3) granular flow-dominated; and (4) fluid escape-dominated.
- flow-boundary zone transformation*. Downcurrent or transverse change in flow-boundary zone conditions (e.g. laminar or turbulent) of a current. We prefer this to '*flow transformation*' (a downstream change in flow behaviour from laminar to turbulent or vice versa; Fisher 1983), because: (1) of the difficulty in inferring whole-current behaviour from a deposit, the lithofacies of which reflect the conditions and behaviour of the flow-boundary zone rather than the rest of the current (which can have different properties and behaviour); and (2) a current can exhibit transitional behaviour between laminar and turbulent (p. 13) particularly when density stratified (pp. 14–16) and/or non-uniform transverse to the flow direction (p. 109).
- flow-stripping*. The consequence of partial blocking of a density-stratified current by topography, in which higher levels of the current travel further and/or in a different direction compared with lower levels of the current, which are topographically confined (pp. 18–19).
- flow-unit*. A genetic term meaning the deposit of a discrete current. A 'simple' ignimbrite sheet comprises one flow-unit, but many ignimbrite sheets are 'compound' and comprise two or more flow-units. Recognition of a flow-unit boundary requires evidence for cessation of a current, otherwise breaks or bedding surfaces in a deposit that has aggraded progressively may just record impersistent or unsteady deposition during the passage of a sustained current (see pp. 95–98).
- fluidization*. Transformation of a particulate framework to a slightly expanded dispersion with fluidal properties (or the maintenance of such a fluidal dispersion) as a result of particle separation and support caused by an interstitial flow of gas or liquid through it (pp. 31–33).
- Froude number (Fr)*. A dimensionless expression of the ratio of the inertial to the gravitational forces in an open-channel current (pp. 16–17). When $Fr = 1$ the total flow energy is a minimum for a given discharge, and the flow is said to be critical. A subcritical flow ($Fr \leq 1$) is thicker and slower moving (more 'tranquil') than its supercritical ($Fr > 1$) ('rapid') counterpart. A *densimetric Froude number* takes account of modification of the gravitational force according to the density difference between a density current and the ambient fluid.
- fully dilute pyroclastic density current*. A pyroclastic density current in which fluid turbulence dominates transport down to the lower flow boundary and in which interactions between transported clasts have little effect upon particle support, segregation and current rheology, even toward the current base (see pp. 20–21). Transport by bed-load traction and saltation may occur (pp. 24–28), and the deposits typically exhibit tractional sedimentary structures (pp. 74–76) (cf. *granular fluid-based pyroclastic density current*).
- giant fluidized flow model*. Conceptual pyroclastic density current that comprised a dense, semi-fluidized, granular mass that travelled predominantly as a laminar to plug flow, deflated during (and after) transport, and halted en masse to form a single, massive layer of ignimbrite (p. 1 and Fig. 2.2A). Such a current would be a type of granular fluid-based pyroclastic density current (p. 20).
- grainflow*. A true grainflow is a type of rapid granular flow in which the effects of interstitial fluid are negligible, and which moves gravitationally down near-repose slopes (generally 30–38°), without shear stress from an overriding current. Grainflow is common in the finer detritus near apices of talus (scree) slopes and on foresets of sand dunes (pp. 26–29).
- granular flow*. Any flow predominantly of non-cohesive particles. Granular flows include 'quasi-static granular flows', which shear slowly at low granular temperatures, and 'rapid granular flows', which include: (1) 'debris falls', that move in the kinetic or streaming mode wherein clast collisions are not crucial to flow; and (2) 'cohesionless grainflows', which move in the collisional mode wherein momentum is transferred between clasts during frequent collisions (high *granular temperature*). Cohesionless grainflows can be subdivided into 'true' grainflows and 'modified' grainflows, the latter being modified by effects of interstitial fluid and/or drag exerted from overriding parts of a current (pp. 29–31 and 42–43). Gradations exist between cohesive and non-cohesive granular flows.
- granular fluid-based pyroclastic density current*. Pyroclastic density current in which clast concentrations towards the lower flow boundary are sufficiently high for particle support to be dominated by collisional momentum transfer between moving grains and/or fluid escape (pp. 20–21). Higher levels of a granular fluid-based pyroclastic density current also may be dominated by clast interactions, or they may be of lower concentration and dominated by fluid turbulence. Near the lower flow boundary turbulence is typically dampened and traction is reduced, so that mainly massive or diffuse-bedded ignimbrite forms (cf. *fully dilute pyroclastic density current*). Lithofacies deposited from such a current do not record how the concentration of the current varied with height.
- granular temperature*. Shear-induced random vibrations of clasts in a granular mass, and the resultant dilation of that mass. Analogous to the heat-induced random motion of molecules in a gas and accompanying gas expansion (p. 29).
- head* (of a density current). Used for the leading part of a current in cases when this is significantly thicker than the succeeding part (the 'body'), partly as a result of resistance by ambient fluid and by the substrate, partly due to the ingestion of ambient fluid, and partly due to the development of billows on the upper surface (p. 10 and Fig. 2.3). Morphologically distinct heads in hot pyroclastic density currents are less well documented than they are in aqueous gravity currents (e.g. Simpson 1997).
- hindered settling*. The reduction in settling velocity of particles in a dispersion caused by (1) upward movement of fluid displaced by the sedimenting particles, (2) collisions with other particles, and/or (3) the fluid wakes of surrounding particles. The effect starts to become measurable at concentrations as low as 1 vol. % (p. 33).
- hydraulic equivalence*. Clasts that have similar settling velocities in liquid (e.g. water) are said to be hydraulically equivalent. It

- depends on particle size, density and shape (see *pneumatic equivalence*).
- ignimbrite*. The deposit of a pyroclastic density current rich in pumice and pumiceous ash shards (e.g. bubble wall, cusped). Ignimbrites are commonly, but not necessarily, dominated by poorly sorted massive lapilli-tuff (mLT), although the architecture of a typical ignimbrite sheet is made up of various massive and stratified pumiceous lithofacies, as well as some subordinate pumice-poor lithofacies (e.g. lithic breccia and/or massive agglomerate).
- interlocking*. Applies where clasts become trapped by, or 'locked' together with, adjacent clasts, whether moving relative to one another or not. It mostly occurs in high-concentration dispersions.
- lagan*. Clasts that preferentially sink towards the base of a shearing or stationary dispersion as a net result of negative buoyancy forces and/or granular segregation processes such as percolation (pp. 34, 41–42 and 91–95). (antonym: *flotsam*).
- leading part* (of a current). The most distal section of an advancing current. It usually has a leading edge with an overhanging 'nose', and it may or may not have a morphologically distinct (i.e. thicker) 'head'.
- liquefaction*. Reduction of the strength of a deposit such that it deforms as a liquid, involving disruption of a loose-packed framework of particles with static or quasi-static grain contacts to form a temporary dispersion, through which fluid is displaced. A more densely packed particulate framework reforms subsequently (pp. 108–109).
- lithofacies*. Refers to the character of a part of a deposit that is distinct according to some combination of stratification, grain size, grain shape, sorting, fabric and composition. It is descriptive, non-genetic and non-stratigraphic. Some common ignimbrite lithofacies are listed in Table 5.1 (p. 51).
- lithofacies association*. A recognized repeated association of two or more lithofacies, which may be linked on the basis of mutual proximity, intergradation, or some other spatial organization (p. 51 and Chapter 6).
- massive*. A lithofacies that lacks internal stratification. It may exhibit a grain fabric, grading or compositional zoning (pp. 52–61). Commonly rapidly deposited by quasi-steady (gradual) progressive aggradation.
- modified grainflow*. Rapid granular flow in which clast support is modified by buoyancy effects of interstitial fluid, fluid escape (hindered settling), and/or shear stress exerted by overriding, less concentrated parts of a current. Can move on slopes less steep than those required by true grainflows (p. 29). See *traction carpet* (pp. 42–43; see Fig. 2.8C).
- monodisperse*. Applies to a population of identical particles (see p. 23).
- non-cohesive debris flow*. Synonymous with 'cohesionless grainflow' (see *granular flow*).
- overpassing*. Applies where certain clasts pass a location, because they are unable to deposit there, while others are doing so (cf. *bypassing*) (pp. 28 and 41–42).
- percolation*. The relative downward movement of some clasts between other clasts in a shearing or vibrating granular dispersion. Percolation generally enables smaller clasts to 'sink' to the base of a moving mass of larger clasts (pp. 29–31).
- pneumatic equivalence*. Clasts with similar settling velocities in gas are pneumatically equivalent. It depends on particle size, density and shape (Chapter 3).
- polydisperse*. Applies to a population of clasts that includes particles of diverse sizes, densities and/or shapes (p. 23).
- progressive aggradation*. Increase in deposit thickness with time as a result of deposition on its upper surface (such as occurs during fallout deposition), irrespective of the rate or manner at which this occurs (steady, unsteady, gradual, stepwise) and irrespective of the depositional mechanism (pp. 2 and 87). Branney & Kokelaar (1992) proposed that this is the way that most ignimbrites are deposited.
- pyroclastic density current*. A general term for a ground-hugging current of pyroclasts and gas (including air) that moves because it is denser than the surrounding atmosphere (or water): i.e. an underflow. It may have any concentration up to about 45 vol. % solids, any vertical concentration gradient and any mechanism(s) of particle support.
- pyroclastic flow*. A conceptual type of pyroclastic density current envisaged to be mainly of high concentration and non-turbulent (see *giant fluidized flow model*), and formerly envisaged to account for ignimbrite emplacement (Chapter 1). Not to be used for a deposit. We propose that ignimbrites are predominantly deposited from *granular fluid-based pyroclastic density currents* (pp. 20–21 and 56).
- pyroclastic surge*. A conceptual dilute pyroclastic density current that deposits thin cross-stratified and stratified, typically small-volume, topography-draping pyroclastic deposits (p. 1; see *pyroclastic surge deposits*). This is contrary to the more general use in fluid dynamics of the term 'surge', which means a short-lived fluctuation or pulse in any type of current. Moreover, pyroclastic currents that deposit stratified lithofacies can be sustained and even quasi-steady for periods of time (pp. 2 and 37–39). Because of this, and because stratified lithofacies commonly grade laterally into massive ignimbrite, we prefer the term '*fully dilute pyroclastic density current*' (see pp. 20–21).
- pyroclastic surge deposits*. Widely used for small-volume deposits of pyroclastic density currents comprising parallel-stratified, cross-stratified and massive layers. Although similar layers occur in ignimbrites, pyroclastic surge deposits have been distinguished from ignimbrites on the basis of a predominance of the tractionally stratified (non-massive) lithofacies. In fact, all the types of deposit are intergradational. We propose that the stratified lithofacies of what have been called pyroclastic surge deposits are formed from *fully dilute pyroclastic density currents* (pp. 20–21 and 74–76), whereas some of the massive layers are formed from *granular fluid-based pyroclastic density currents* (pp. 20–21 and 56–75).
- quasi-steady*. Nearly steady. Approximating to time invariant, or in depositional terms leading to aggradation of vertically uniform (not necessarily massive) deposit (see p. 2).
- rapid flow*. Supercritical flow (see *Froude number*) (pp. 16–17).
- reach*. A longitudinal section of a current of given length and location.
- Richardson number (Ri)*. A dimensionless expression of the ratio of the inertial to the gravitational forces that influence mixing along the shearing contact of two fluids (see p. 16). A high density contrast confers gravitational stability and inhibits mixing, whereas a low contrast with high shear facilitates mixing by interfacial development of 'breaking-wave' vortices (Kelvin-Helmholtz instability). The *gradient Richardson number (Ri_g)* concerns local density gradients within density currents with concentration stratification, and is a measure of stratification stability.
- runout distance*. Distance that a pyroclastic density current travels along the ground. Because the runout distance of a sustained current will vary with time, inference of runout from a deposit should involve measurement along a time line (*deposchron*). The distance from the vent to the most distal tip of an ignimbrite sheet indicates the *maximum* runout distance, which normally only relates to a relatively brief period in a protracted history of a current. Runout distance is a function of eruptive mass flux (see pp. 16 and 18).
- selective filtering*. A process in which there is (selective) hindering of deposition of certain sizes or types of clast, while deposition of others occurs at the same site. It results from various particle segregation processes (involving buoyancy, and aerodynamic or granular effects) in a current flow-boundary zone, and it causes the pyroclast population of the aggrading deposit to differ from that of the arriving current (pp. 41–42).

sillar. Ignimbrite, or part of an ignimbrite, that is non-welded but indurated as a result of vapour-phase crystallization, typically including tridymite, cristobalite and alkali feldspar. Term first coined by Fenner (1948).

sorting. The distribution of clast sizes in a polydisperse population, often given as a graphical standard deviation, $\sigma_\phi = \phi_{84} - \phi_{16}$ (Inman 1952), where: 0–1 very well sorted; 1–2 well sorted; *c.* 2 moderately sorted; 2–4 poorly sorted; > 4 very poorly sorted (after Walker 1971). Pyroclastic deposits that appear to be poorly sorted in terms of size may be well sorted in terms of *pneumatic equivalence*. (Chapter 3).

steady. Time invariant.

stratified flow, stratified current. A current in which density or another parameter (e.g. grain size or composition) varies with height, irrespective of whether the gradient is continuous or has discrete interfaces (p. 14). Most natural gravity currents are density stratified to some extent. Mechanisms of particle support may vary with height in stratified currents, particularly when concentrations in lower levels are sufficiently high for clast interactions to be frequent (pp. 21 and 25).

stratified lithofacies. Lithofacies that exhibit near-parallel fine, and possibly diffuse, stratification (sT, dsT; 'horizontal discontinuous lamination' or 'transcurrent lamination' of Allen (1984)) and low- to high-angle cross-stratification (xsT; p. 74). Inferred to record tractional deposition, respectively in plane-beds and sand-waves. Stratified tuffs differ from parallel-laminated tuffs (//sT; commonly formed by ash fallout; p. 83) in the impersistent nature of the laminae observed by detailed examination. Thin-bedded lithofacies (e.g. bT; bLT; p. 71) are less finely stratified.

surge. A peak in the velocity, mass flux, capacity, concentration, etc. of an unsteady current. A sustained current may have any number of surges, sometimes referred to as pulses.

suspension. Some authors use 'suspension' for clasts supported by fluid turbulence, and 'dispersion' where transport occurs involving any support (e.g. dispersive pressure).

traction carpet. A thin (probably discontinuous) modified-grainflow layer within the basal part of some stratified currents, in which the motion of the layer partly derives from shear stress exerted from overriding, more turbulent levels of the current. By preference not used for either a particular mode of deposition or a type of deposit stratification (pp. 42–43).

tractional stratification. Fine, typically discontinuous, subparallel stratification and/or cross-stratification inferred to have been formed by tractional segregation and deposition of saltating and/or rolling clasts at the base of a turbulent fully dilute current (pp. 37 and 74). Subparallel tractional stratification (e.g. sT; often termed 'transcurrent lamination' or 'horizontal discontinuous lamination'; Allen 1984) can superficially resemble ash-fall lamination (e.g. //sT), but, whereas ash-fall laminae are laterally persistent, each component lamina (which can be as thin as a single clast diameter) within a tractionally stratified unit generally shows some thickness changes or impersistence within a few metres, and can have a well-developed grain fabric.

tractional transport. Fluid-driven rolling, sliding or saltating of clasts along the lower flow boundary of a current (pp. 24–28). Commonly produces stratified and cross-stratified lithofacies (p. 74).

tranquil flow. Subcritical flow (see *Froude number*).

underflow. All pyroclastic density currents are underflows in being denser than the atmosphere and so travelling along the ground underneath it (in contrast to co-ignimbrite or phoenix plumes, which loft upwards through atmosphere). High-concentration lower levels of density-stratified pyroclastic currents are best described in terms of what they are (e.g. 'basal modified grainflow part') rather than using the loose terms 'underflow' or 'basal avalanche' (p. 15).

uniform. Spatially invariant.

veneer (of deposit). Architectural term for a thin layer of deposit that drapes topographic highs and proximal steep slopes (typically no more than about 30°). Veneers may be formed of fallout deposits, stratified deposits previously called 'pyroclastic surge deposits', and parts of ignimbrites. Some ignimbrite veneers are stratigraphically condensed correlatives of thicker, massive valley-filling ignimbrite, into which they may grade (pp. 111–114). They are commonly composed of stratified or bedded lithofacies with pumice lenses, although they may be of any lithofacies. We use the term veneer purely descriptively and imply no particular origin (cf. Wilson & Walker 1982).

waning. Decrease of a flow parameter through time, with respect to a fixed geographic location (see p. 2 and Fig. 1.1A).

waxing. Increase of a flow parameter through time, with respect to a fixed geographic location (see p. 2 and Fig. 1.1A).

References

- ALEXANDER, J. & MORRIS, S. 1994. Observations on experimental, nonchannelized, high-concentration turbidity currents and variations in deposits around obstacles. *Journal of Sedimentary Petrology*, **A64**, 899–909.
- ALIDIBIROV, M. & DINGWELL, D. B. 1996. Magma fragmentation by rapid decompression. *Nature*, **380**, 146–148.
- ALIDIBIROV, M. & DINGWELL, D. B. 2000. Three fragmentation mechanisms for highly viscous magma under rapid decompression. *Journal of Volcanology and Geothermal Research*, **100**, 413–421.
- ALLEN, E. & UHLHERR, P. H. T. 1989. Nonhomogeneous sedimentation in viscoelastic fluids. *Journal of Rheology*, **33**, 627–638.
- ALLEN, J. R. L. 1972. Intensity of deposition from avalanches and the loose packing of avalanche deposits. *Sedimentology*, **18**, 105–111.
- ALLEN, J. R. L. 1984. *Sedimentary Structures: Their Character and Physical Basis*. Developments in Sedimentology. Elsevier, Amsterdam.
- ALLEN, J. R. L. 1985. *Principles of Physical Sedimentology*. Chapman and Hall, London.
- ALLEN, J. R. L. 1994. Fundamental properties of fluids and their relation to sediment transport processes. In: PYE K. (ed.) *Sediment Transport and Depositional Processes*. Blackwell Scientific Publications, Oxford, 25–60.
- ALLEN, S. R. & CAS, R. A. F. 1998. Lateral variations within coarse cognimbrite lithic breccias of the Kos Plateau Tuff, Greece. *Bulletin of Volcanology*, **59**, 356–377.
- ALTINAKAR, M. S., GRAF, W. H. & HOPFINGER, E. J. 1996. Flow structure in turbidity currents. *Journal of Hydraulic Research*, **34**, 713–718.
- ANDERSON, T. & FLETT, J. S. 1903. Report of the Soufriere in St. Vincent, in 1902, and on a visit to Montagne Pelée, in Martinique, Part 1. *Philosophical Transactions of the Royal Society, London*, **A200**, 353–553.
- ANILKUMAR, A. V., SPARKS, R. S. J. & STURTEVANT, B. 1993. Geological implications and applications of high velocity two-phase flow experiments. *Journal of Volcanology and Geothermal Research*, **56**, 145–160.
- ARAMAKI, S. 1984. Formation of the Aira caldera, southern Kyushu, ~22,000 years ago. *Journal of Geophysical Research*, **B89**, 8485–8501.
- ARAMAKI, S. & UI, T. 1966. The Aira and Ata pyroclastic flows and related caldera depressions in southern Kyushu, Japan. *Bulletin Volcanologique*, **29**, 29–47.
- ARNOTT, R. W. C. & HAND, B. M. 1989. Bedforms, primary structures and grain fabric in the presence of suspended sediment rain. *Journal of Sedimentary Petrology*, **59**, 1062–1069.
- BACON, C. R. 1983. Eruptive history of Mount Mazama and Crater Lake caldera, Cascade range, USA. *Journal of Volcanology and Geothermal Research*, **18**, 57–115.
- BAER, E. M., FISHER, R. V., FULLER, M. & VALENTINE, G. 1997. Turbulent transport and deposition of the Ito pyroclastic flow: determinations using anisotropy of magnetic susceptibility. *Journal of Geophysical Research*, **B102**, 22 565–22 586.
- BAGNOLD, R. A. 1954. Experiments on a gravity-free dispersion of large solid spheres in a Newtonian fluid under shear. *Proceedings of the Royal Society, London*, **A225**, 49–63.
- BAGNOLD, R. A. 1955. Some flume experiments on large grains but little denser than the transporting fluid, and their implications. *Proceedings of the Institution of Civil Engineers*, **3**, 174–205.
- BAGNOLD, R. A. 1956. The flow of cohesionless grains in fluids. *Philosophical Transactions of the Royal Society, London*, **A249**, 235–297.
- BAGNOLD, R. A. 1973. The nature of saltation and of 'bed-load' transport in water. *Proceedings of the Royal Society, London*, **A332**, 473–504.
- BAILEY, R. A. & CARR, R. G. 1994. Physical geology and eruptive history of the Matahina ignimbrite, Taupo Volcanic Zone, North Island, New Zealand. *New Zealand Journal of Geology and Geophysics*, **37**, 319–344.
- BAINES, P. G. 1995. *Topographic Effects in Stratified Flows*. Cambridge University Press, Cambridge.
- BARDINTZEFF, J. M. 1984. Merapi volcano (Java, Indonesia) and Merapi-type nuée ardente. *Bulletin of Volcanology*, **47**, 433–446.
- BATCHELOR, G. K. & VAN RENSBURG, R. W. 1986. Structure formation in bidisperse sedimentation. *Journal of Fluid Mechanics*, **166**, 379–407.
- BATTAGALIA, M. 1993. On pyroclastic flow emplacement. *Journal of Geophysical Research*, **B98**, 22 268–22 272.
- BELOUSOV, A. 1996. Deposits on the 30 March 1956 directed blast at Bezymianny volcano, Kamchatka, Russia. *Bulletin of Volcanology*, **57**, 649–662.
- BERTRAN, P., HÉTU, B., TEXIER, J.-P. & VAN STEIN, H. 1997. Fabric characteristics of subaerial slope deposits. *Sedimentology*, **44**, 1–16.
- BEST, J. L. 1989. Fluidization pipes in volcanoclastic mass flows, Volcán Hudson, southern Chile. *Terra Nova*, **1**, 203–208.
- BEST, J. L. 1992. Sedimentology and event timing of a catastrophic volcanoclastic mass-flow, Volcán Hudson, Southern Chile. *Bulletin of Volcanology*, **54**, 299–318.
- BEST, J. L., KIRKBRIDE, A. & PEAKALL, J. 2001. Mean flow and turbulence structure of sediment-laden gravity currents: new insights using ultrasonic Doppler velocity profiling. In: MCCAFFREY, W. D., KNELLER, B. C. & PEAKALL, J. (eds) *Particulate gravity currents*. International Association of Sedimentologists, Special Publications, **31**, 159–172.
- BEST, M. G. & CHRISTIANSEN, E. H. 1997. Origin of broken phenocrysts in ash-flow tuffs. *Geological Society of America Bulletin*, **109**, 63–73.
- BOGOYAVLENSKAYA, G. E., BRAITSEVA, O. A., MELEKETSEV, I. V., KIRIANOV, V. Y. & MILLER, C. D. 1985. Catastrophic eruptions of the directed-blast type at Mount St. Helens, Bezymianny and Shiveluch volcanoes. *Journal of Geodynamics*, **3**, 189–218.
- BOND, A. & SPARKS, R. S. J. 1976. The Minoan eruption of Santorini, Greece. *Journal of the Geological Society, London*, **132**, 1–16.
- BOTTERILL, J. S. M. & HALIM, B. H. 1978. The flow of fluidized solids. In: DAVIDSON, J. F. & KEAIRNS, D. L. (eds) *Fluidization. Proceedings of the 2nd Engineering Foundation Conference, Trinity College, Cambridge England*, 2–6 April 1978. 122–127, Cambridge University Press, Cambridge.
- BOTTERILL, J. S. M. & HALIM, B. H. 1979. The open-channel fluid flow of fluidized solids. *Powder Technology*, **27**, 7–12.
- BOUDON, G., CAMUS, G., GOURGAUD, A. & LAJOIE, J. 1993. The 1984 nuée-ardente deposits of Merapi volcano, Central Java, Indonesia: stratigraphy, textural characteristics and transport mechanisms. *Bulletin of Volcanology*, **55**, 327–342.
- BRANNEY, M. J. 1986. Isolated pods of subaqueous welded ash-flow tuff – a distal facies of the Capel Curig Volcanic Formation (Ordovician), North Wales. *Geological Magazine*, **123**, 589–590.
- BRANNEY, M. J. 1988. The subaerial setting of the Ordovician Borrowdale Volcanic Group, English Lake District. *Journal of the Geological Society, London*, **145**, 887–890.
- BRANNEY, M. J. 1991. Eruption and depositional facies of the Whorneyside Tuff Formation, English Lake District – an exceptionally large-magnitude phreatoplinian eruption. *Geological Society of America Bulletin*, **103**, 886–897.
- BRANNEY, M. J. & KOKELAAR, B. P. 1992. A reappraisal of ignimbrite emplacement: progressive aggradation and changes from particulate to non-particulate flow during emplacement of high-grade ignimbrite. *Bulletin of Volcanology*, **54**, 504–520.
- BRANNEY, M. J. & KOKELAAR, B. P. 1994a. A reappraisal of ignimbrite emplacement: progressive aggradation and changes from particulate to non-particulate flow during emplacement of high-grade ignimbrite – Reply. *Bulletin of Volcanology*, **56**, 138–143.
- BRANNEY, M. J. & KOKELAAR, B. P. 1994b. Rheomorphism and soft-state deformation of tuffs induced by volcanotectonic faulting at a piecemeal caldera, English Lake District. *Geological Society America Bulletin*, **106**, 507–530.
- BRANNEY, M. J. & KOKELAAR, B. P. 1997. Giant bed from a sustained catastrophic density current flowing over topography: Acatlán ignimbrite, Mexico. *Geology*, **25**, 115–118.
- BRANNEY, M. J. & SPARKS, R. S. J. 1990. Fiamme formed by diagenesis and burial-compaction in soils and subaqueous sediments. *Journal of the Geological Society, London*, **147**, 919–922.
- BRANNEY, M. J., KNELLER, B. C. & KOKELAAR, B. P. 1990. Disordered turbidite facies – a product of continuous surging density currents. (Abstract). *Proceedings 23rd International Association of Sedimentologists, Nottingham, UK, August 1990*, Volume 2, 38, Utrecht State University, Utrecht.
- BRANNEY, M. J., KOKELAAR, B. P. & MCCONNELL, B. J. 1992. The Bad Step Tuff: a lava-like rheomorphic ignimbrite in a calcalkaline piecemeal caldera, English Lake District. *Bulletin of Volcanology*, **54**, 187–199.

- BRENNEN, C. E., SIECK, K. & PASLASKI, J. 1983. Hydraulic jumps in granular material flow. *Powder Technology*, **35**, 31–37.
- BRIDGEWATER, J., FOO, W. S. & STEPHENS, D. J. 1985. Particle mixing and segregation in failure zones – theory and experiment. *Powder Technology*, **41**, 147–158.
- BRITTER, R. E. & LINDEN, P. F. 1980. The motion of the front of a gravity current travelling down an incline. *Journal of Fluid Mechanics*, **99**, 531–543.
- BROWN, R. J. 2001. *Eruption history and depositional processes of the Poris ignimbrite of Tenerife and the Glaramara Tuff of the English Lake District*. PhD thesis, Leicester.
- BROWN, R. J., BARRY, T. L., BRANNEY, M. J., PRINGLE, M. S. & BRYAN, S. E. 2003. The Quaternary pyroclastic succession of southern Tenerife, Canary Islands: explosive eruptions, related caldera subsidence, and sector collapse. *Geological Magazine*, in press.
- BRYAN, S. E., CAS, R. A. F. & MARTI, J. 1998a. Lithic breccias in intermediate volume phonolitic ignimbrites, Tenerife (Canary Islands): constraints on pyroclastic flow depositional processes. *Journal of Volcanology and Geothermal Research*, **81**, 269–296.
- BRYAN, S. E., MARTI, J. & CAS, R. A. F. 1998a. Stratigraphy of the Bandes del sur Formation: an extracaldera record of Quaternary phonolitic explosive eruptions from the Las Cañadas edifice, Tenerife (Canary Islands). *Geological Magazine*, **135**, 605–636.
- BUESCH, D. C. 1992. Incorporation and redistribution of locally derived lithic fragments within a pyroclastic flow. *Geological Society of America Bulletin*, **104**, 1193–1207.
- BÜRGER, R., CONCHA, F., FJELDE, K.-K. & HVIStENDAHL KARLSEN, K. 2000. Numerical simulation of the settling of polydisperse suspensions of spheres. *Powder Technology*, **113**, 30–54.
- BURSIK, M. I. 1989. Effects of the drag force on the rise height of particles in the gas-thrust region of volcanic eruption columns. *Geophysical Research Letters*, **16**, 441–444.
- BURSIK, M. I. & WOODS, A. W. 1996. The dynamics and thermodynamics of large ash flows. *Bulletin of Volcanology*, **58**, 175–193.
- BURSIK, M. I., KURBATOV, A. V., SHERIDAN, M. F. & WOODS, A. W. 1998. Transport and deposition in the May 18, 1980, Mount St Helens blast flow. *Geology*, **26**, 155–158.
- BUSBY-SPERA, C. J. 1986. Depositional features of rhyolitic and andesitic volcanoclastic rocks of the Mineral King submarine caldera complex, Sierra Nevada, California. *Journal of Volcanology and Geothermal Research*, **27**, 43–76.
- CAGNOLI, B. & TARLING, D. H. 1997. The reliability of anisotropy of magnetic susceptibility (AMS) data as flow direction indicators in friable base surge and ignimbrite deposits: Italian examples. *Journal of Volcanology and Geothermal Research*, **75**, 309–320.
- CAGNOLI, B. & ULRYCH, T. J. 2001. Ground penetrating radar images of unexposed climbing dune-forms in the Ubehebe hydrovolcanic field (Death Valley, California). *Journal of Volcanology and Geothermal Research*, **109**, 279–298.
- CALDER, E. S., SPARKS, R. S. J. & GARDEWEG, M. C. 2000. Erosion, transport and segregation of pumice and lithic clasts in pyroclastic flows inferred from ignimbrite at Lascar Volcano, Chile. *Journal of Volcanology and Geothermal Research*, **104**, 201–235.
- CAMPBELL, C. S. 1986. The effect of microstructure development on the collisional stress tensor in a granular flow. *Acta Mechanica*, **63**, 61–72.
- CAMPBELL, C. S. 1989. Self-lubrication for long runout landslides. *Journal of Geology*, **97**, 653–665.
- CAMPBELL, C. S. 1990. Rapid granular flows. *Annual Review of Fluid Mechanics*, **22**, 57–92.
- CAMPBELL, C. S. & BRENNEN, C. E. 1983. Computer-simulation of shear flows of granular material. In: JENKINS, J. T. & SATAKE, M. (eds) *Mechanics of Granular Materials: New Models and Constitutive Relations*. Elsevier, Amsterdam, 313–326.
- CAMPBELL, C. S. & BRENNEN, C. E. 1985. Computer-simulation of granular shear flows. *Journal of Fluid Mechanics*, **151**, 167–188.
- CAMPBELL, C. S. & GONG, A. 1986. The stress tensor in a two-dimensional granular shear flow. *Journal of Fluid Mechanics*, **164**, 107–125.
- CAMPBELL, C. S., CLEARY, P. W. & HOPKINS, M. 1995. Large-scale landslide simulations: global deformation, velocities and basal friction. *Journal of Geophysical Research*, **B100**, 8267–8283.
- CAPACCIONI, B. & SAROCCHI, D. 1996. Computer-assisted image-analysis on clast shape fabric from the Ovierto-Bagnoregio ignimbrite (Vulsini district, central Italy): implications on the emplacement mechanisms. *Journal of Volcanology and Geothermal Research*, **70**, 75–90.
- CAPACCIONI, B., NAPPI, G. & VALENTINI, L. 2001. Directional fabric measurements: an investigative approach to transport and depositional mechanisms in pyroclastic flows. *Journal of Volcanology and Geothermal Research*, **107**, 275–292.
- CAREY, S. N. 1991. Transport and deposition of tephra by pyroclastic flows and surges. In: FISHER, R. V. & SMITH, G. A. (eds) *Sedimentation in Volcanic Settings*. SEPM, Special Publications, **45**, 39–57.
- CAREY, S. N., SIGURDSSON, H., MANDEVILLE, C. & BRONTO, S. 1996. Pyroclastic surges and flows over water: an example from the 1883 Krakatau eruption. *Bulletin of Volcanology*, **57**, 493–511.
- CAREY, S. N., SIGURDSSON, H. & SPARKS, R. S. J. 1988. Experimental studies of particle-laden plumes. *Journal of Geophysical Research*, **B93**, 1514–1528.
- CARRASCO-NÚÑEZ, G. & ROSE, W. I. 1995. Eruption of a major Holocene pyroclastic flow at Citlatépetl volcano (Pico de Orizaba), Mexico, 8.5–9.0 ka. *Journal of Volcanology and Geothermal Research*, **69**, 197–215.
- CARTER, R. M. 1975. A discussion and classification of subaqueous mass-transport with particular application to grain-flow, slurry flow and fluxo-turbidites. *Earth Science Reviews*, **11**, 145–177.
- CAS, R. A. F. & WRIGHT, J. V. 1987. *Volcanic Successions: Modern and Ancient*. Allen and Unwin, London.
- CHAPIN, C. E. & LOWELL, G. R. 1979. Primary and secondary flow structures in ash-flow tuffs of the Gribbles Run palaeovalley, central Colorado. In: CHAPIN, C. E. & ELSTON, W. E. (eds) *Ash-flow Tuffs*. Geological Society of America, Special Papers, **180**, 137–154.
- CHEPIL, W. S. 1961. The use of spheres to measure lift and drag on wind-eroded soil grains. *Proceedings of the Soil Science Society of America*, **25**, 343–345.
- CHUN, S. S. & CHOUGH, S. K. 1992. Depositional sequences from high-concentration turbidity currents, Cretaceous Uhangri Formation (SW Korea). *Sedimentary Geology*, **77**, 225–233.
- CLARK, S. 1984. The relevance of hydraulic jumps to pyroclastic flows. (Abstract.) *Eos Transactions of the American Geophysical Union*, **65**, 1142.
- COLE, P. D. 1991. Migration direction of sand-wave structures in pyroclastic surge deposits – implications for depositional processes. *Geology*, **19**, 1108–1111.
- COLE, P. D. & SCARPATI, C. 1993. A facies interpretation of the eruption and emplacement mechanisms of the upper part of the Neapolitan Yellow Tuff, Campi-Flegrei, Southern Italy. *Bulletin of Volcanology*, **55**, 311–326.
- COLE, P. D., CALDER, E. S., DRUITT, T. H., HOBLITT, R., ROBERTSON, R., SPARKS, R. S. J. & YOUNG, S. R. 1998. Pyroclastic flows generated by gravitational instability of the 1996–97 lava dome of Soufriere Hills Volcano, Montserrat. *Geophysical Research Letters*, **25**, 3425–3428.
- COLE, P. D., CALDER, E. S., SPARKS, R. S. J., CLARKE, A. B., DRUITT, T. H., YOUNG, S. R., HERD, R. A., HARFORD, C. L. & NORTON, G. E. 2002. Deposits from dome-collapse and fountain-collapse pyroclastic flows at Soufriere Hills Volcano, Montserrat. In: DRUITT, T. H. & KOKELAAR, B. P. (eds) *The Eruption of Soufriere Hills Volcano, Montserrat, From 1995 to 1999*. Geological Society, London, Memoirs, **21**, 231–262.
- COLE, P. D., GUEST, J. E. & DUNCAN, A. M. 1993. The emplacement of intermediate volume ignimbrites – a case study from Roccamonfina Volcano, Southern Italy. *Bulletin of Volcanology*, **55**, 467–480.
- COLELLA, A. & HISCOTT, R. N. 1997. Pyroclastic surges of the Pleistocene Monte Guardia sequence (Lipari island, Italy): depositional processes. *Sedimentology*, **44**, 47–66.
- COLEMAN, N. L. 1969. A new examination of sediment suspension in open channels. *Journal of Hydraulic Research*, **7**, 67–82.
- COLLINS, J. D. 1986. Alluvial sediments. In: READING, H. G. (ed.) *Sedimentary Environments and Facies*, Volume 2. Blackwell Scientific, Oxford, 20–62.
- COULSEN, J. M. & RICHARDSON, J. F. 1990. *Chemical Engineering*. Pergamon, Oxford, UK.
- CROWE, B. M. & FISHER, R. V. 1973. Sedimentary structures in base surge deposits with special reference to cross bedding, Ubehebe Craters, Death Valley, California. *Geological Society of America Bulletin*, **84**, 663–682.
- DADE, W. B. & HUPPERT, H. E. 1996. Emplacement of the Taupo ignimbrite by a dilute, turbulent flow. *Nature*, **381**, 509–512.
- DAVIES, D. K., QUEARRY, M. W. & BONIS, S. B. 1978. Glowing avalanches from the 1974 eruption of volcano Fuego, Guatemala. *Geological Society*

- of *America Bulletin*, **89**, 369–384.
- DAVIES, R. & KAYE, B. H. 1971. Experimental investigations into the settling behaviour of dispersions. *Powder Technology*, **5**, 61–68.
- DAVIS, R. H. & ACRIVOS, A. 1985. Sedimentation of noncolloidal particles at low Reynolds numbers. *Annual Reviews in Fluid Mechanics*, **17**, 91–119.
- DELLINO, P., FRAZZETTA, G. & LA VOLPE, L. 1990. Wet surge deposits at La Fossa di vulcano: depositional and eruptive mechanisms. *Journal of Volcanology and Geothermal Research*, **43**, 215–233.
- DENLINGER, R. P. 1987. A model for generation of ash clouds by pyroclastic flows, with application to the 1980 eruptions at Mount St. Helens, Washington. *Journal of Geophysical Research*, **B92**, 10284–10298.
- DE RITA, D., GIORDANO, G. & MILLI, S. 1998. Forestepping-backstepping stacking pattern of volcanoclastic successions: Roccamonfina volcano, Italy. *Journal of Volcanology and Geothermal Research*, **80**, 155–178.
- DE SILVA, S. L. 1989. Geochronology and stratigraphy of the ignimbrites from the 21°30'S to 23°30'S portion of the central Andes of northern Chile. *Journal of Volcanology and Geothermal Research*, **37**, 93–131.
- DINGWELL, D. B. 1998. Recent experimental progress in the physical description of silicic magma relevant to explosive volcanism. In: GILBERT, J. S. & SPARKS, R. S. J. (eds) *The physics of explosive volcanic eruptions*. Geological Society, London Special Publications, **145**, 9–26.
- DOBBINS, W. E. 1944. Effects of turbulence on sedimentation. *Transactions of the American Society of Civil Engineers*, Paper 2218, 629–678.
- DOBTRAN, F., NERI, A. & MACEDONIO, G. 1993. Numerical simulation of collapsing volcanic columns. *Journal of Geophysical Research*, **B98**, 4231–4259.
- DOHEIM, M. A., ABU-ALI, M. H. & MABROUK, S. A. 1997. Investigation and modelling of sedimentation of mixed particles. *Powder Technology*, **91**, 43–47.
- DOLAN, J. F., BECK, C. & OGAWA, Y. 1989. Upslope flow of extremely distal turbidites: an example from the Tiburon Rise, west-central Atlantic. *Geology*, **17**, 990–994.
- DOLGUNIN, V. N. & UKOLOV, A. A. 1995. Segregation of particle rapid gravity flow. *Powder Technology*, **83**, 95–103.
- DOLGUNIN, V. N., KUDY, A. N. & UKOLOV, A. A. 1998. Development of the model of segregation of particles undergoing granular flow down an inclined chute. *Powder Technology*, **96**, 211–218.
- DRAHUN, J. A. & BRIDGEWATER, J. 1983. The mechanism of free surface segregation. *Powder Technology*, **36**, 39–53.
- DRUITT, T. H. 1985. Vent evolution and lag breccia formation during the Cape Riva Eruption of Santorini, Greece. *Journal of Geology*, **93**, 439–454.
- DRUITT, T. H. 1992. Emplacement of the 18 May 1980 lateral blast deposit ENE of Mount St. Helens, Washington. *Bulletin of Volcanology*, **54**, 554–572.
- DRUITT, T. H. 1995. Settling behavior of concentrated dispersions and some volcanological applications. *Journal of Volcanology and Geothermal Research*, **65**, 27–39.
- DRUITT, T. H. 1998. Pyroclastic density currents. In: GILBERT, J. S. & SPARKS, R. S. J. (eds) *The Physics of Explosive Volcanic Eruptions*. Geological Society, London, Special Publications, **145**, 145–182.
- DRUITT, T. H. & BACON, C. R. 1986. Lithic breccia and ignimbrite erupted during the collapse of Crater Lake Caldera, Oregon. *Journal of Volcanology and Geothermal Research*, **29**, 1–32.
- DRUITT, T. H. & SPARKS, R. S. J. 1982. A proximal ignimbrite breccia facies on Santorini volcano, Greece. *Journal of Volcanology and Geothermal Research*, **13**, 147–171.
- DRUITT, T. H., CALDER, E. S., COLE, P. D., HOBLITT, R. P., NORTON, G. E., RITCHIE, L. J., SPARKS, R. S. J. & VOIGHT, B. 2002. Small-volume, highly mobile pyroclastic flows formed by rapid sedimentation from pyroclastic surges at Soufrière Hills Volcano, Montserrat: an important volcanic hazard. In: DRUITT, T. H. & KOKELAAR, B. P. (eds) *The eruption of Soufrière Hills Volcano, Montserrat, From 1995 to 1999*. Geological Society, London, Memoirs, **21**, 263–280.
- DRUITT, T. H., MELLORS, R. A., PYLE, D. M. & SPARKS, R. S. J. 1989. Explosive volcanism on Santorini, Greece. *Geological Magazine*, **126**, 95–126.
- DUNCAN, A. M., QUEIROZ, G., GUEST, J. E., COLE, P. D., WALLENSTEIN, N. & PACHECO, J. M. 1999. The Povoção ignimbrite, Furnas volcano, São Miguel, Azores. *Journal of Volcanology and Geothermal Research*, **92**, 55–65.
- DUYVERMAN, H. J. & ROOBOL, M. J. 1981. Gas pipes in Eocambrian volcanic breccias. *Geological Magazine*, **118**, 265–270.
- DZULYNSKI, S. & SANDERS, J. E. 1962. Current marks on firm mud bottoms. *Proceedings of the Connecticut Academy of Arts and Science*, **42**, 57–96.
- EDWARDS, D. A., LEEDER, M. R., BEST, J. L. & PANTIN, H. M. 1994. On experimental reflected density currents and the interpretation of certain turbidites. *Sedimentology*, **41**, 437–461.
- EINSTEIN, N. H. & CHIEN, N. 1955. Effects of heavy sediment concentration near the bed on velocity and sediment distribution. *US Army Corps of Engineers, Missouri River Division, Sedimentology Series*, **8**, 1–76.
- ELLWOOD, B. B. 1982. Estimates of flow direction for calc-alkaline welded tuffs and paleomagnetic data reliability from anisotropy of magnetic susceptibility measurements – Central San Juan Mountains, Southwest Colorado. *Earth and Planetary Science Letters*, **59**, 303–314.
- ELSTON, W. E. & SMITH, E. I. 1970. Determination of flow direction of rhyolitic ash-flow tuffs from fluidal textures. *Geological Society of America Bulletin*, **81**, 3393–3406.
- ENOS, P. 1977. Flow regimes in debris flow. *Sedimentology*, **24**, 133–142.
- FELIX, M. 2001. A two-dimensional numerical model for a turbidity current. In: McCAFFREY, W. D., KNELLER, B. C. & PEAKALL, J. (eds) *Particulate Gravity Currents*. International Association of Sedimentologists, Special Publications, **31**, 71–82.
- FENNER, C. N. 1948. Incandescent tuff flows in southern Peru. *Geological Society of America Bulletin*, **59**, 879–893.
- FERRIZ, H. & MAHOOD, G. A. 1984. Eruption rates and compositional trends at Los Humeros Volcanic Center, Puebla, Mexico. *Journal of Geophysical Research*, **B89**, 8511–8524.
- FIERSTEIN, J. & HILDRETH, W. 1992. The Plinian eruptions of 1912 at Novarupta, Katmai National Park, Alaska. *Bulletin of Volcanology*, **54**, 646–684.
- FINK, J. H. & KIEFFER, S. W. 1993. Estimate of pyroclastic flow velocities resulting from explosive decompression of lava domes. *Nature*, **363**, 612–615.
- FISHER, R. V. 1966. Mechanism of deposition from pyroclastic flows. *American Journal of Science*, **264**, 350–363.
- FISHER, R. V. 1979. Models for pyroclastic surges and pyroclastic flows. *Journal of Volcanology and Geothermal Research*, **6**, 305–318.
- FISHER, R. V. 1983. Flow transformations in sediment gravity flows. *Geology*, **11**, 273–274.
- FISHER, R. V. 1989. Large volume pyroclastic flows: if they can weld, how can they flow? (Abstract.) *New Mexico Bureau of Mines and Mineral Resources Bulletin*, **131**, 91.
- FISHER, R. V. 1990a. Transport and deposition of a pyroclastic surge across an area of high relief – the 18 May 1980 eruption of Mount St. Helens, Washington. *Geological Society of America Bulletin*, **102**, 1038–1054.
- FISHER, R. V. 1990b. Terminology and the transform from flow to surge, and surge to flow. *International Association of Volcanology and Chemistry of the Earth's Interior, Commission on Explosive Volcanism Newsletter*, **18** July 1990, 4–5.
- FISHER, R. V. & HEIKEN, G. 1982. Mt. Pelee, Martinique – May 8 and 20, 1902, pyroclastic flows and surges. *Journal of Volcanology and Geothermal Research*, **13**, 339–371.
- FISHER, R. V. & SCHMINCKE, H.-U. 1984. *Pyroclastic Rocks*. Springer, Berlin.
- FISHER, R. V. & WATERS, A. C. 1970. Base surge bed forms in maar volcanoes. *American Journal of Science*, **268**, 157–180.
- FISHER, R. V., ORSI, G., ORT, M. & HEIKEN, G. 1993. Mobility of a large volume pyroclastic flow – emplacement of the Campanian ignimbrite, Italy. *Journal of Volcanology and Geothermal Research*, **56**, 205–220.
- FISHER, R. V., SCHMINCKE, H.-U. & VAN BOGAARD, P. 1983. Origin and emplacement of a pyroclastic flow and surge unit at Laacher See, Germany. *Journal of Volcanology and Geothermal Research*, **17**, 375–392.
- FOO, W. S. & BRIDGEWATER, J. 1983. Particle migration. *Powder Technology*, **36**, 271–273.
- FORTERRE, Y. & POULIQUEN, O. 2001. Longitudinal vortices in granular flows. *Physical Review Letters*, **86**, 5886–5889.
- FRANCIS, E. H. & HOWELLS, M. F. 1973. Transgressive welded ash-flow tuffs among the Ordovician sediments of north-east Snowdonia. *Journal of the Geological Society, London*, **129**, 621–641.
- FRANCIS, P. W. 1993. *Volcanoes: a planetary perspective*. Oxford University Press, Oxford.
- FRANCIS, P. W., ROOBOL, M. J., WALKER, G. P. L., COBBOLD, P. R. & COWARD, M. 1974. The San Pedro and San Pablo volcanoes and their hot

- avalanche deposits. *Geologische Rundschau*, **63**, 357–388.
- FRANCOU, B. 1991. Pentes, granulométrie et mobilité des matériaux le long d'un talus d'éboulement en milieu alpin. *Permafrost and Periglacial Processes*, **2**, 175–186.
- FRAZZETTA, G., LA VOLPE, L. & SHERIDAN, M. F. 1989. Interpretation of emplacement units in recent surge deposits on Lipari, Italy. *Journal of Volcanology and Geothermal Research*, **37**, 339–350.
- FREUNDT, A. 1998. The formation of high-grade ignimbrites – Part I: Experiments on high- and low-concentration transport systems containing sticky particles. *Bulletin of Volcanology*, **59**, 414–435.
- FREUNDT, A. 1999. Formation of high-grade ignimbrites – Part II. A pyroclastic suspension current model with implications also for low-grade ignimbrites. *Bulletin of Volcanology*, **60**, 545–576.
- FREUNDT, A. & SCHMINCKE, H.-U. 1985. Lithic-enriched segregation bodies in pyroclastic flow deposits of Laacher See Volcano (East Eifel, Germany). *Journal of Volcanology and Geothermal Research*, **25**, 193–224.
- FREUNDT, A. & SCHMINCKE, H.-U. 1986. Emplacement of small-volume pyroclastic flows at Laacher See (East Eifel, Germany). *Bulletin of Volcanology*, **48**, 39–59.
- FREUNDT, A. & SCHMINCKE, H.-U. 1995. Eruption and emplacement of a basaltic welded ignimbrite during caldera formation on Gran Canaria. *Bulletin of Volcanology*, **56**, 640–659.
- FREUNDT, A., WILSON, C. J. N. & CAREY, S. N. 2000. Ignimbrites and block-and-ash flow deposits. In: SIGURDSSON, H., HOUGHTON, B. F., McNUTT, S. R., RYMER, H. & STIX, J. (eds) *Encyclopedia of Volcanoes*. Academic Press, London, 581–600.
- FUJII, T. & NAKADA, S. 1999. The 15 September 1991 pyroclastic flows at Unzen Volcano (Japan): a flow model for associated ash-cloud surges. *Journal of Volcanology and Geothermal Research*, **89**, 159–172.
- GARCÍA, M.H. 1993. Hydraulic jumps in sediment-driven bottom currents. *Journal of Hydraulic Engineering*, **119**, 1094–1117.
- GARCÍA, M. H. 1994. Depositional turbidity currents laden with poorly sorted sediment. *Journal of Hydraulic Engineering*, **120**, 1240–1263.
- GARCÍA, M. H. & PARKER, G. 1989. Experiments on hydraulic jumps in turbidity currents near a canyon-fan transition. *Science*, **245**, 393–396.
- GARCÍA, M. H. & PARKER, G. 1993. Experiments on the entrainment of sediment into suspension by a dense bottom current. *Journal of Geophysical Research*, **B98**, 4793–4807.
- GHOSH, J. K., MAZUMDER, B. S., SAHA, M. R. & SENGUPTA, S. 1986. Deposition of sand by suspension currents – experimental and theoretical studies. *Journal of Sedimentary Petrology*, **56**, 57–66.
- GIANNETTI, B. & DE CASA, G. 2000. Stratigraphy, chronology and sedimentology of ignimbrites from the white trachytic tuff, Roccamonfina Volcano, Italy. *Journal of Volcanology and Geothermal Research*, **96**, 243–295.
- GIORDANO, G. 1998. Facies characteristics and magma-water interaction of the White Trachytic Tuffs (Roccamonfina Volcano, southern Italy). *Bulletin of Volcanology*, **60**, 10–26.
- GLUCKMAN, M. J., YERUSHALMI, J. & SQUIRES, A. M. 1976. Defluidization characteristics of sticky or agglomerating beds. In: KEAIRNS, D. L. (ed.) *Fluidization Technology Volume 2*. McGraw-Hill, New York, 395–422.
- GRUNEWALD, U., SPARKS, R. S. J., KEARNS, S. & KOMOROWSKI, J. C. 2000. Friction marks on blocks from pyroclastic flows at the Soufrière Hills Volcano, Montserrat: implications for flow mechanisms. *Geology*, **28**, 827–830.
- GUARINOS, J. & GUARINOS, A. 1993. Contribution à l'étude de l'éruption du volcan Lascar (Chili) d'Avril 1993. *Archives des Sciences Genève*, **46**, 303–319.
- HAFF, P. K. 1983. Grain flow as a fluid-mechanical phenomenon. *Journal of Fluid Mechanics*, **134**, 401–430.
- HAND, B. M. 1974. Supercritical flow in density currents. *Journal of Sedimentary Petrology*, **44**, 637–648.
- HAND, B. M. 1997. Inverse grading resulting from coarse-sediment transport lag. *Journal of Sedimentary Research*, **67**, 124–129.
- HANES, D. M. & BOWEN, A. J. 1985. A granular-fluid model for steady intense bed-load transport. *Journal of Geophysical Research*, **B90**, 9149–9158.
- HARLAND, W. B., HEROD, K. N. & KRINSLEY, D. H. 1966. The definition and identification of tills and tillites. *Earth Science Reviews*, **2**, 255–256.
- HAYASHI, J. N. & SELF, S. 1992. A comparison of pyroclastic flow and debris avalanche mobility. *Journal of Geophysical Research*, **B97**, 9063–9071.
- HAZEN, A. 1904. On sedimentation. *Transactions of the American Society of Civil Engineering*, **3**, 45–88.
- HEIN, F. J. 1982. Depositional mechanisms of deep-sea coarse clastic sediments, Cap Enragé Formation, Quebec. *Canadian Journal of Earth Sciences*, **19**, 267–287.
- HILLHOUSE, J. W. & WELLS, R. E. 1991. Magnetic fabric, flow directions, and source area of the Lower Miocene Peach Springs Tuff in Arizona, California, and Nevada. *Journal of Geophysical Research*, **B96**, 12443–12460.
- HISCOTT, R. N. 1994a. Loss of capacity, not competence, as the fundamental process governing deposition from turbidity currents. *Journal of Sedimentary Research Section A*, **64**, 209–214.
- HISCOTT, R. N. 1994b. Traction-carpet stratification in turbidites – fact or fiction? *Journal of Sedimentary Research Section A*, **64**, 204–208.
- HISCOTT, R. N. & MIDDLETON, G. V. 1979. Depositional mechanics of thick-bedded sandstones at the base of a submarine slope, Tourelle Formation (Lower Ordovician) Quebec, Canada. In: DOYLE, L. J. & PILKEY, O. H. (eds) SEPM Special Publications, **27**, 303–326.
- HISCOTT, R. N. & MIDDLETON, G. V. 1980. Fabric of coarse deep-water sandstones, Tourelle Formation (Lower Ordovician) Quebec, Canada. *Journal of Sedimentary Petrology*, **50**, 703–722.
- HOBLITT, R. P. 1986. Observations of the eruptions of July 22 and August 7, 1980, at Mount St. Helens, Washington. US Geological Survey, Professional Paper, **1335**, 1–44.
- HOBLITT, R. P. & MILLER, C. D. 1984. Mount St Helens 1980 and Mount Pelée 1902 – flow or surge – comment. *Geology*, **12**, 692–694.
- HOFFMANN, A. C. & ROMP, E. J. 1991. Segregation in a fluidized powder of a continuous size distribution. *Powder Technology*, **66**, 119–126.
- HOUGHTON, B. F. & WILSON, C. J. N. 1986. Explosive rhyolitic volcanism: the case studies of Mayor Island and Taupo volcanoes. In: *Guide to the Earth's Interior, International Volcanological Congress, New Zealand. New Zealand Geological Survey Record*, **12**, 33–100.
- HOWELLS, M. F., CAMPBELL, S. D. G. & REEDMAN, A. J. 1985. Isolated pods of subaqueous welded ash-flow tuff: a distal facies of the Capel Curig volcanic formation (Ordovician), North Wales. *Geological Magazine*, **122**, 175–180.
- HÜS, K. J. 1959. Flute and groove casts in the pre-alpine flysch, Switzerland. *American Journal of Science*, **257**, 529–536.
- HUGHES, S. R. & DRUITT, T. H. 1998. Particle fabric in a small, type-2 ignimbrite flow unit (Laacher See, Germany) and implications for emplacement dynamics. *Bulletin of Volcanology*, **60**, 125–136.
- HUNT, J. N. 1969. On the turbulent transport of a heterogeneous sediment. *Quarterly Journal of Mechanical and Applied Mathematics*, **22**, 235–246.
- HUPPERT, H. E., TURNER, J. S., CAREY, S. N., SPARKS, R. S. J. & HALLWORTH, M. A. 1986. A laboratory study of pyroclastic flows down slopes. *Journal of Volcanology and Geothermal Research*, **30**, 179–199.
- HURWITZ, S. & NAVON, O. 1994. Bubble nucleation in rhyolitic melts: experiments at high pressure, temperature and water content. *Earth and Planetary Science Letters*, **122**, 267–280.
- IBAD-ZADE, Y. A. 1987. *Movement of Sediment in Open Channels*. Balkema, Rotterdam.
- IMRAN, J., PARKER, G. & KATOPODES, N. 1998. A numerical model of channel inception on submarine fans. *Journal of Geophysical Research*, **B103**, 1219–1238.
- INMAN, D. L. 1952. Measures for describing the size distribution of sediments. *Journal of Sedimentary Petrology*, **22**, 125–145.
- ISHIDA, M. & HATANO, H. 1983. The flow of solid particles in an aerated inclined channel. In: *Advances in the Mechanics and Flow of Granular Materials, Volume 2*. Trans Tech Publications, Houston, TX, 565–575.
- IVERSON, R. M. & VALLANCE, J. W. 2001. New views of granular mass flows. *Geology*, **29**, 115–118.
- IVERSON, R. M., REID, M. E. & LAHUSEN, R. G. 1997. Debris-flow mobilization from landslides. *Annual Reviews of Earth and Planetary Sciences*, **25**, 85–138.
- JACKSON, R. G. 1976. Sedimentological and fluid dynamic implications of the turbulent bursting phenomenon in geophysical flows. *Journal of Fluid Mechanics*, **77**, 531–560.
- JAHNS, R. H. 1949. Desert floods. *Engineering Science Monthly*, May, v. 12, 10–14.
- JENKINS, J. T. & ASKARI, E. 1991. Boundary-conditions for rapid granular flows – phase interfaces. *Journal of Fluid Mechanics*, **223**, 497–508.
- JIANG, Z. 1995. The motion of sediment-water mixtures during intense

- bedload transport: computer simulations. *Sedimentology*, **42**, 935–945.
- JO, H. R., RHEE, C. W. & CHOUGH, S. K. 1997. Distinctive characteristics of a streamflow-dominated alluvial fan deposit: Sanghori area, Kyongsang Basin (Early Cretaceous), southeastern Korea. *Sedimentary Geology*, **110**, 51–70.
- JOHNSON, A. M. 1970. *Physical Processes in Geology*. Freeman, San Francisco, CA.
- JOHNSON, A. M. & RODINE, J. R. 1984. Debris flow. In: BRUNSDEN, D. & PRIOR, D. B. (eds) *Slope instability*. Wiley, Chichester, 257–361.
- KALMAN, H. 1999. Attrition control by pneumatic conveying. *Powder Technology*, **104**, 214–220.
- KAMATA, H. & MIMURA, K. 1983. Flow directions inferred from imbrication in the Handa pyroclastic flow deposit in Japan. *Bulletin Volcanologique*, **46**, 277–282.
- KANO, K., NAKANO, S. & MIMURA, K. 1988. Deformation structures in shale bed indicate flow direction of overlying Miocene subaqueous pyroclastic flow. *Bulletin of Volcanology*, **50**, 380–385.
- KASTENS, K. A. & SHOR, A. N. 1985. Depositional processes of a meandering channel on Mississippi fan. *AAPG Bulletin*, **69**, 190–202.
- KEEFER, D. K. & JOHNSON, A. M. 1983. Earth flows; morphology, mobilization and movement. US Geological Survey, Professional Paper, **1264**, 1–56.
- KENT, P. E. 1966. The transport mechanism in catastrophic rock falls. *Journal of Geology*, **74**, 79–83.
- KIEFFER, S. W. 1981. Fluid dynamics of the May 18 blast at Mount St. Helens. In: LIPMAN, P. W. & MULLINEAUX, D. R. (eds) *The 1980 Eruption of Mount St Helens, Washington*. US Geological Survey, Professional Papers, **1250**, 379–400.
- KIEFFER, S. W. & STURTEVANT, B. 1984. Laboratory studies of volcanic jets. *Journal of Geophysical Research*, **B89**, 8253–8268.
- KIEFFER, S. W. & STURTEVANT, B. 1988. Erosional furrows formed during the lateral blast at Mount St Helens, May 18, 1980. *Journal of Geophysical Research*, **B93**, 14 793–14 816.
- KJAER, K. H. & KRUGER, J. 1998. Does clast size influence fabric strength? *Journal of Sedimentary Research*, **68**, 746–749.
- KNELLER, B. C. & BRANNEY, M. J. 1995. Sustained high-density turbidity currents and the deposition of thick massive sands. *Sedimentology*, **42**, 607–616.
- KNELLER, B. & BUCKEE, C. 2000. The structure and fluid mechanics of turbidity currents: a review of some recent studies and their geological implications. *Sedimentology*, **47**, (Suppl. 1), 62–94.
- KNELLER, B. C. & McCAFFREY, W. D. 1999. Depositional effects of flow non-uniformity and stratification within turbidity currents approaching a bounding slope: deflection, reflection and facies variation. *Journal of Sedimentary Research*, **69**, 980–991.
- KNELLER, B. C., BENNETT, S. J. & McCAFFREY, W. D. 1997. Velocity and turbulence structure of gravity currents and internal solitary waves: potential sediment transport and formation of wave ripples in deep water. *Sedimentary Geology*, **112**, 235–250.
- KNELLER, B., EDWARDS, D., McCAFFREY, W. & MOORE, R. 1991. Oblique reflection of turbidity currents. *Geology*, **19**, 250–252.
- KNIGHT, J. B., JAEGER, H. M. & NAGEL, S. R. 1993. Vibration-induced size separation in granular media: the convection connection. *Physical Review Letters*, **70**, 3728–3731.
- KNIGHT, M. D., WALKER, G. P. L., ELLWOOD, B. B. & DIEHL, J. F. 1986. Stratigraphy, paleomagnetism, and magnetic fabric of the Toba Tuffs – constraints on the sources and eruptive styles. *Journal of Geophysical Research*, **B91**, 10 355–10 382.
- KOKELAAR, B. P. 1982. Fluidization of wet sediment during the emplacement and cooling of various igneous bodies. *Journal of the Geological Society, London*, **139**, 21–33.
- KOKELAAR, B. P. 1992. Ordovician marine volcanic and sedimentary record of rifting and volcanotectonism: Snowdon, Wales, United Kingdom. *Geological Society of America Bulletin*, **104**, 1433–1455.
- KOKELAAR, B. P. & KÖNIGER, S. 2000. Marine emplacement of welded ignimbrite: the Ordovician Pitts Head Tuff, North Wales. *Journal of the Geological Society, London*, **157**, 517–536.
- KOKELAAR, B. P., BEVINS, R. E. & ROACH, R. A. 1985. Submarine silicic volcanism and associated sedimentary and tectonic processes, Ramsey Island, SW Wales. *Journal of the Geological Society, London*, **142**, 591–613.
- KOKELAAR, P. & BRANNEY, M. J. 1996. On pyroclastic flow emplacement – Comment. *Journal of Geophysical Research*, **B101**, 5653–5655.
- KOLBUSZEWSKI, J. 1950. Notes on the deposition of sands. *Research*, **3**, 478–483.
- KRUYT, N. P. & VERËL, W. J. T. 1992. Experimental and theoretical study of rapid flows of cohesionless granular materials down inclined chutes. *Powder Technology*, **73**, 109–115.
- KUNII, D. & LEVENSPIEL, O. 1991. *Fluidization Engineering*. Butterworth-Heinemann, Boston, MA.
- KUNO, H. 1941. Characteristics of deposits formed by pumice flows and those formed by ejected pumice. *Tokyo University Earthquake Research Institute Bulletin*, **19**, 144–149.
- KWAUK, M., LI, J. & LUI, D. 2000. Particulate and aggregative fluidization – 50 years in retrospect. *Powder Technology*, **111**, 3–18.
- KYNCH, G. J. 1952. A theory of sedimentation. *Transactions of the Faraday Society*, **48**, 166–176.
- LAGMAY, M. A., PYLE, D. M., DADE, B. & OPPENHEIMER, C. 1999. Control of crater morphology on flow path direction of Soufrière-type pyroclastic flows. *Journal of Geophysical Research*, **B104**, 7169–7181.
- LAIRD, M. G. 1970. Vertical sheet structures – a new indicator of sedimentary fabric. *Journal of Sedimentary Petrology*, **40**, 428–434.
- LAJOIE, J., LANZAFAMA, G., ROSSI, P. L. & TRANNE, C. A. 1992. Lateral facies variations in hydromagmatic pyroclastic deposits at Linosa, Italy. *Journal of Volcanology and Geothermal Research*, **54**, 135–143.
- LAOUAR, S. & MOLODTSOF, Y. 1998. Experimental characterization of the pressure drop in dense phase pneumatic transport at very low velocity. *Powder Technology*, **95**, 165–173.
- LEAT, P. T. & SCHMINCKE, H.-U. 1993. Large-scale rheomorphic shear deformation in Miocene peralkaline ignimbrite E, Gran Canaria. *Bulletin of Volcanology*, **55**, 155–165.
- LEGROS, F. & KELFOUN, K. 2000. On the ability of pyroclastic flows to scale topographic obstacles. *Journal of Volcanology and Geothermal Research*, **98**, 235–241.
- LESZCZYNSKI, S. 1986. Excursion Guide for the International Association Sedimentologists' 7th European Regional Meeting, Kraków, Poland. **B7**.
- LEVINE, A. H. & KIEFFER, S. W. 1991. Hydraulics of the August 7, 1980, pyroclastic flow at Mount St Helens, Washington. *Geology*, **19**, 1121–1124.
- LI, M. Z. & KOMAR, P. D. 1992. Selective entrainment and transport of mixed size and density sands – flume experiments simulating the formation of black-sand placers. *Journal of Sedimentary Petrology*, **62**, 584–590.
- LIPMAN, P. W. 1967. Mineral and chemical variations within an ash-flow sheet from Aso caldera, south-western Japan. *Contributions to Mineralogy and Petrology*, **16**, 300–327.
- LIPMAN, P. W. 1976. Caldera collapse breccias in the western San Juan Mountains, Colorado. *Geological Society of America Bulletin*, **87**, 1397–1410.
- LIPMAN, P. W. 1984. The roots of ash flow calderas in Western North America: windows into the tops of granitic batholiths. *Journal of Geophysical Research*, **B89**, 8801–8841.
- LOCKETT, M. J. & AL-HABBOOBY, H. M. 1974. Relative particle velocities in two-species settling. *Powder Technology*, **10**, 67–71.
- LORENZ, V. 1974. Vesiculated tuffs and associated features. *Sedimentology*, **21**, 273–291.
- LOUGHLIN, S. C., BAXTER, P. J., ASPINALL, W. P., DARROUX, B., HARFORD, C. L. & MILLER, A. D. 2000a. Eyewitness accounts of the 25 June 1997 pyroclastic flows and surges at Soufrière Hills Volcano, Montserrat, and implications for disaster mitigation. In: DRUITT, T. H. & KOKELAAR, B. P. (eds) *The Eruption of Soufrière Hills Volcano, Montserrat, From 1995 to 1999*. Geological Society, London, Memoirs, **21**, 211–230.
- LOUGHLIN, S. C., CALDER, E. S., CLARKE, A. B., COLE, P. D., LUCKETT, R., MANGAN, M., PYLE, D., SPARKS, R. S. J., VOIGHT, B. & WATTS, R. B. 2000b. Pyroclastic flows and surges generated by the 25 June 1997 dome collapse, Soufrière Hills Volcano, Montserrat. In: DRUITT, T. H. & KOKELAAR, B. P. (eds) *The Eruption of Soufrière Hills Volcano, Montserrat, From 1995 to 1999*. Geological Society, London, Memoirs, **21**, 191–210.
- LOWE, D. R. 1975. Water escape structures in coarse-grained sediments. *Sedimentology*, **22**, 157–204.
- LOWE, D. R. 1976. Grain flow and grain flow deposits. *Journal of Sedimentary Petrology*, **46**, 188–199.
- LOWE, D. R. 1979. Sediment gravity flows: their classification and some

- problems of application to natural flows and their deposits. In: DOYLE, L. J. & PILKEY, O. H. Jr. (eds) *Geology of Continental Slopes*. SEPM Special Publications, **27**, 75–82.
- LOWE, D. R. 1982. Sediment gravity flows: II. Depositional models with special reference to the deposits of high-density turbidity currents. *Journal of Sedimentary Petrology*, **52**, 279–298.
- LOWE, D. R. 1988. Suspended-load fallout rate as an independent variable in the analysis of current structures. *Sedimentology*, **35**, 765–776.
- MACDONALD, W. D. & PALMER, H. C. 1990. Flow directions in ash-flow tuffs: a comparison of geological and magnetic susceptibility measurements, Tshirege Member (upper Bandelier Tuff), Valles caldera, New Mexico, USA. *Bulletin of Volcanology*, **53**, 45–59.
- MACÍAS, J. L., ESPÍNDOLA, J. M., BURSÍK, M. & SHERIDAN, M. F. 1998. Development of lithic-breccias in the 1982 pyroclastic flow deposits of El Chichón Volcano, Mexico. *Journal of Volcanology and Geothermal Research*, **83**, 173–196.
- MADER, H. M., PHILLIPS, J. C., SPARKS, R. S. J. & STURTEVANT, B. 1996. Dynamics of explosive degassing of magma: Observations of fragmenting two-phase flows. *Journal of Geophysical Research*, **B101**, 5547–5560.
- MAHOOD, G. A. 1980. Geological evolution of a Pleistocene rhyolitic center: the Sierra La Primavera, Jalisco, Mexico. *Journal of Volcanology and Geothermal Research*, **8**, 199–230.
- MAHOOD, G. A. 1984. Pyroclastic rocks and calderas associated with strongly peralkaline volcanic rocks. *Journal of Geophysical Research*, **89**, 8540–8552.
- MAHOOD, G. A. & HILDRETH, W. 1986. Geology of the peralkaline volcano at Pantelleria, Strait of Sicily. *Bulletin of Volcanology*, **48**, 143–172.
- MANDENVILLE, C. W., CAREY, S. & SIGURDSSON, H. 1996. Sedimentology of the Krakatau 1883 submarine pyroclastic deposits. *Bulletin of Volcanology*, **57**, 512–529.
- MARSELLA, M., PALLADINO, D. M. & TRIGILA, R. 1987. The Onano Pyroclastic Formation (Vulsini volcanoes): depositional features, distribution and eruptive mechanisms. *Periodico di Mineralogia*, **56**, 225–240.
- MARSHALL, P. 1935. Acid rocks of the Taupo-Rotorua volcanic district. *Transactions of the Royal Society of New Zealand*, **64**, 323–366.
- MASSEY, B. S. 1989. *Mechanics of fluids*. Van Nostrand Reinhold (International), London.
- MCGUIGAN, S. J. & PUGH, R. R. 1976. The flow of fluidized solids in an open channel. In: *Proceedings of the 3rd International Conference on Pneumatic Transport of Solids in Pipes*, BHRA, UK, Paper E2, 17.
- MCPHIE, J. 1986. Primary and redeposited facies from a large-magnitude rhyolitic, phreatomagmatic eruption: Cana Creek Tuff, late-Carboniferous, Australia. *Journal of Volcanology and Geothermal Research*, **28**, 319–350.
- MCTAGGART, K. C. 1960. The mobility of nuées ardentes. *American Journal of Science*, **258**, 369–382.
- MELLORS, R. A. & SPARKS, R. S. J. 1991. Spatter-rich pyroclastic flow deposits on Santorini, Greece. *Bulletin of Volcanology*, **53**, 327–342.
- MELLORS, R. A., WAITT, R. B. & SWANSON, D. A. 1988. Generation of pyroclastic flows and surges by hot-rock avalanches from the dome of Mount St Helens volcano, USA. *Bulletin of Volcanology*, **50**, 14–25.
- MELOSH, H. J. 1979. Acoustic fluidization: a new geologic process? *Journal of Geophysical Research*, **B84**, 7513–7520.
- MELOSH, H. J. 1987. The mechanics of large rock avalanches. *Geological Society of America Reviews in Engineering Geology*, **7**, 41–49.
- MIDDLETON, G. V. 1967. Experiments on density and turbidity currents III. Deposition of sediment. *Canadian Journal of Earth Sciences*, **4**, 474–505.
- MIDDLETON, G. V. 1970. Experimental studies related to the problems of flysch sedimentation. *Geological Association of Canada Special Paper*, **7**, 253–272.
- MIDDLETON, G. V. & SOUTHARD, J. B. 1984. *Mechanics of Sediment Movement*. Short Course Notes: 3. Society of Economic Paleontologists and Mineralogists, Tulsa.
- MILLER, T. P. & SMITH, R. L. 1977. Spectacular mobility of ash flows around Aniakchak and Fisher calderas, Alaska. *Geology*, **5**, 173–176.
- MIMURA, K. 1984. Imbrication, flow direction and possible source areas of the pumice-flow tuffs near Bend, Oregon, USA. *Journal of Volcanology and Geothermal Research*, **21**, 45–60.
- MİYABUCHI, Y. 1999. Deposits associated with the 1990–1995 eruption of Unzen volcano, Japan. *Journal of Volcanology and Geothermal Research*, **89**, 139–158.
- MÖBIUS, M. E., LAUDERDALE, B. E., NAGEL, S. R. & JAEGER, H. M. 2001. Size separation of granular particles. *Nature*, **414**, 270.
- MOORE, I. & KOKELAAR, P. 1998. Tectonically controlled piecemeal caldera collapse: a case study of Glencoe volcano, Scotland. *Geological Society of America Bulletin*, **110**, 1448–1466.
- MOORE, J. G. & MELSON, W. G. 1969. Nuées ardentes of the 1968 eruption of Mayon volcano, Philippines. *Bulletin Volcanologique*, **33**, 600–620.
- MOORE, J. G. & RICE, C. J. 1984. Chronology and character of the May 18, 1980, explosive eruptions of Mount St Helens. *Studies in Geophysics. Explosive Volcanism: inception, evolution and hazards*. National Academy Press, Washington D.C., 133–142.
- MORRISON, H. L. & RICHMOND, O. 1976. Application of Spencer's ideal soil model to granular flow. *Journal of Applied Mechanics*, **43**, 49–53.
- MOYER, T. C. & SWANSON, D. A. 1987. Secondary hydroeruptions in pyroclastic-flow deposits: examples from Mount St. Helens. *Journal of Volcanology and Geothermal Research*, **32**, 299–319.
- MRÓZ, Z. 1980. On hypoelasticity and plasticity approaches to constitutive modelling of inelastic behaviour of soils. *International Journal of Numerical Analytical Methods for Geomechanics*, **4**, 45–55.
- MUCK, M. T. & UNDERWOOD, M. B. 1990. Upslope flow of turbidity currents – a comparison among field observations, theory, and laboratory models. *Geology*, **18**, 54–57.
- MULDER, T. & ALEXANDER, J. 2001. Abrupt change in slope causes variation in the deposit thickness of concentrated particle-driven density currents. *Marine Geology*, **175**, 221–235.
- MURAI, I. 1961. A study of the textural characteristics of pyroclastic flow deposits in Japan. *Tokyo University Earthquake Research Institute Bulletin*, **39**, 133–248.
- MURPHY, P. J. & HOOSHIARI, H. 1982. Saltation in water dynamics. *Journal of the Hydraulics Division, Proceedings of the ASCE*, **108**, 1251–1267.
- NAVON, O. & LYAKHOVSKY, V. 1998. Vesiculation in silicic magmas. In: GILBERT, J. S. & SPARKS, R. S. J. (eds) *The Physics of Explosive Volcanic Eruptions*. Geological Society, London, Special Publications, **145**, 27–50.
- NELSON, C. S., KAMP, P. J. J. & MILDENHALL, D. C. 1989. Late Pliocene distal silicic ignimbrites, Port Waikato, New Zealand: implications for volcanism and sea-level changes in South Auckland. *New Zealand Journal of Geology and Geophysics*, **32**, 357–370.
- NEMEC, W. 1990. Aspects of sediment movement on steep delta slopes. In: COLELLA, A. & PRIOR, D. B. (eds) *Coarse grained deltas*. International Association of Sedimentology, Special Publications, **10**, 29–73.
- NIR, A. & ACRIVOS, A. 1990. Sedimentation and sediment flow on inclined surfaces. *Journal of Fluid Mechanics*, **212**, 139–153.
- NISHIMURA, K. & ITO, Y. 1997. Velocity distribution in snow avalanches. *Journal of Geophysical Research-Solid Earth*, **B102**, 27 297–27 303.
- NORMARK, W. R. & PIPER, D. J. W. 1991. Initiation processes and flow evolution of turbidity currents: implications for the depositional record. In: OSBORNE, R. H. (ed.) *From Shoreline to Abyss: contributions of Marine Geology in Honour of Francis Parker Shepard*. SEPM, Special Publication **5**, 207–230.
- OGAWA, S. 1978. Multi-temperature theory of granular materials. In: *Proceedings US–Japan Seminars on Continuum-Mechanics and Statistical Approaches to Mechanical Granular Materials*, Gukunjutsu bunken Fukuyukai, Tokyo, 208–217.
- PALLADINO, D. M. & VALENTINE, G. A. 1995. Coarse-tail vertical and lateral grading in pyroclastic flow deposits of the Latera Volcanic Complex (Vulsini, Central Italy): origin and implications for flow dynamics. *Journal of Volcanology and Geothermal Research*, **69**, 343–364.
- PAPANICOLAOU, P. N. & LIST, E. J. 1988. Investigations of round vertical turbulent buoyant jets. *Journal of Fluid Mechanics*, **195**, 341–391.
- PERROTTA, A., SCARPATI, C., GIACOMELLI, L. & CAPOZZI, A. R. 1996. Proximal depositional facies from a caldera-forming eruption: the Parata Grande Tuff at Ventotene Island (Italy). *Journal of Volcanology and Geothermal Research*, **71**, 201–228.
- PICKERING, K. T., HISCOTT, R. N. & HEIN, F. J. 1989. *Deep marine environments: clastic sedimentation and tectonics*. Unwin Hyman, London.
- PICKERING, K. T., UNDERWOOD, M. B. & TAIRA, A. 1992. Open ocean to trench turbidity current flow in the Nankai Trough – flow collapse and reflection. *Geology*, **20**, 1099–1102.
- PIERSON, T. C. 1981. Dominant particle support mechanisms in debris flows at Mt. Thomas, New Zealand, and implications for flow mobility. *Sedimentology*, **28**, 49–60.
- PIERSON, T. C. 1986. Flow behaviour of channelized debris flows, Mount St.

- Helens, Washington. In: ABRAHAMS, A. D. (ed.) *Hillslope Processes*. Allen and Unwin, Boston, MA, 269–296.
- PIPER, D. J. W. & NORMARK, W. R. 1983. Turbidite depositional patterns and flow characteristics, Navy Submarine Fan, California Borderland. *Sedimentology*, **30**, 681–694.
- POSTMA, G. 1986. Classification for sediment gravity flow deposits based on flow conditions during sedimentation. *Geology*, **14**, 291–294.
- POSTMA, G., NEMEC, W. & KLEINSPEHN, K. L. 1988. Large floating clasts in turbidites – a mechanism for their emplacement. *Sedimentary Geology*, **58**, 47–61.
- POTAPOV, A. V. & CAMPBELL, C. S. 1997. Computer simulation of shear-induced particle attrition. *Powder Technology*, **94**, 109–122.
- POTTER, D. B. & OBERTHAL, C. M. 1987. Vent sites and flow directions of the Otowi ash flows (Lower Bandelier Tuff), New Mexico. *Geological Society of America Bulletin*, **98**, 66–76.
- POULIQUEN, O. & VALLANCE, J. W. 1999. Segregation induced instabilities of granular fronts. *Chaos*, **9**, 621–630.
- PRIOR, D. B., BORNHOLD, B. D. & JOHNS, M. W. 1984. Depositional characteristics of a submarine debris flow. *Journal of Geology*, **92**, 707–727.
- PUGH, F. J. & WILSON, K. C. 1999. Role of the interface in stratified slurry flow. *Powder Technology*, **104**, 221–226.
- RATTÉ, J. C. 1989. Direction-to-source indicators in the Bloodgood Canyon Tuff and tuff of Triangle C Ranch at Coyote Well. In: CHAPIN, C. E. & ZIDEK, J. (eds) *Field Excursions to Volcanic Terranes in the Western United States, Vol. 1: Southern Rocky Mountain Region*. New Mexico Bureau of Mines and Mineral Resources, **46**, 111–114.
- READING, H. G. 1986. Facies. In: READING, H. G. (ed.) *Sedimentary Environments and facies*, Volume 2. Blackwell, Oxford, 4–13.
- REES, A. I. 1966. The effect of depositional slopes on the anisotropy of magnetic susceptibility of laboratory deposited sands. *Journal of Geology*, **74**, 856–867.
- RICHARDSON, J. F. & ZAKI, W. N. 1954. Sedimentation and fluidisation: Part 1. *Transactions of the Institution of Chemical Engineers*, **32**, 35–53.
- RIDGEWAY, K. & RUPP, R. 1971. The mixing of powder layers on a chute: the effect of particle size and shape. *Powder Technology*, **4**, 195–202.
- RIEHLE, J. R. 1973. Calculated compaction profiles of rhyolitic ash-flow tuffs. *Geological Society of America Bulletin*, **84**, 2194–2216.
- RIEHLE, J. R., MILLER, T. F. & BAILEY, R. A. 1995. Cooling, degassing and compaction of rhyolitic ash flow tuffs – a computational model. *Bulletin of Volcanology*, **57**, 319–336.
- RITCHIE, L. J., COLE, P. D. & SPARKS, R. S. J. 2002. Sedimentology of deposits from the pyroclastic density current of 26 December 1997 at Soufrière Hills Volcano, Montserrat. In: DRUITT, T. H. & KOKELAAR, B. P. (eds) *The Eruption of Soufrière Hills Volcano, Montserrat, From 1995 to 1999*. Geological Society, London, Memoirs, **21**, 435–456.
- ROBIN, C., EISSEN, J. P. & MONZIER, M. 1994. Ignimbrites of basaltic andesite and andesite compositions from Tanna, New Hebrides arc. *Bulletin of Volcanology*, **56**, 10–22.
- ROCO, M. C. & SHOOK, C. A. 1984. A model for turbulent slurry flow. *Journal of Pipelines*, **4**, 3–13.
- RODINE, J. D. & JOHNSON, A. M. 1976. The ability of debris, heavily freighted with coarse clastic materials, to flow on gentle slopes. *Sedimentology*, **23**, 213–234.
- ROOBOL, M. J., SMITH, A. L. & WRIGHT, J. V. 1987. Lithic breccias in pyroclastic flow deposits on St. Kitts, West Indies. *Bulletin of Volcanology*, **49**, 694–707.
- ROSE, W. I., PEARSON, T. & BONIS, S. 1977. Nuée ardente eruption from the foot of a dacite lava flow, Santiaguito volcano, Guatemala. *Bulletin Volcanologique*, **40**, 23–38.
- ROSI, M. 1992. A model for the formation of vesiculated tuff by the coalescence of accretionary lapilli. *Bulletin of Volcanology*, **54**, 429–434.
- ROSI, M., VEZZOLI, L., ALEOTTI, P. & DE CENSI, M. 1996. Interaction between caldera collapse and eruptive dynamics during the Campanian ignimbrite eruption, Phlegraean Fields, Italy. *Bulletin of Volcanology*, **57**, 541–554.
- ROSS, C. S. & SMITH, R. L. 1961. *Ash-flow Tuffs, Their Origin, Geological Relations and Identification*. US Geological Survey, Professional Papers, **366**.
- ROTTMAN, J. W., SIMPSON, J. E. & HUNT, J. C. R. 1985. Unsteady gravity currents flows over obstacles: some observations and analysis related to Phase II trials. *Journal of Hazardous Materials*, **11**, 325–340.
- ROUSE, H. 1937. Modern conceptions of the mechanics of fluid turbulence. *Transactions of the American Society of Civil Engineering*, **102**, 436–505.
- ROUSE, H. 1939. Experiments on the mechanics of sediment suspension. In: *Fifth International Congress of Applied Mechanics, Cambridge, Massachusetts*, 550–505.
- ROWLEY, P. D., KUNTZ, M. A. & MACLEOD, N. S. 1981. Pyroclastic flow deposits. In: LIPMAN, P. W. & MULLINEAUX, D. R. (eds) *The 1980 Eruptions of Mount St Helens, Washington*. US Geological Survey, Professional Papers, **1250**, 489–512.
- ROWLEY, P. D., MACLEOD, N. S., KUNTZ, M. A. & KAPLAN, A. M. 1985. Proximal bedded deposits related to pyroclastic flows of May 18, 1980, Mount St Helens, Washington. *Geological Society of America Bulletin*, **96**, 1373–1383.
- SADJADPOUR, M. & CAMPBELL, C. S. 1999. Granular chute flow-regimes: mass flow rates, flow rate limits and clogging. *Advanced Powder Technology*, **10**, 175–185.
- SANTANA, D., RODRÍGUEZ, J. M. & MACÍAS-MACHÍN, A. 1999. Modelling fluidized bed elutriation of fine particles. *Powder Technology*, **106**, 110–118.
- SAVAGE, S. B. 1979. Gravity flow of cohesionless granular materials in chutes and channels. *Journal of Fluid Mechanics*, **92**, 53–96.
- SAVAGE, S. B. 1983. Granular flows down rough inclines – review and extension. In: Jenkins, J.T. & Satake, M. (eds) *Mechanics of Granular Materials: New Models and Constitutive Relations*. Elsevier, Amsterdam, 261–281.
- SAVAGE, S. B. 1984. The mechanics of rapid granular flows. *Advances in Applied Mechanics*, **24**, 289–366.
- SAVAGE, S. B. & LUN, C. K. K. 1988. Particle size segregation in inclined chute flow of dry cohesionless granular solids. *Journal of Fluid Mechanics*, **189**, 311–335.
- SCHAAFSMA, S. H., VONK, P., SEGERS, P. & KOSSEN, N. W. F. 1998. Description of agglomerate growth. *Powder Technology*, **97**, 183–190.
- SCHAFLINGER, U., ACRIVOS, A. & ZHANG, K. 1990. Viscous resuspension of a sediment within a laminar and stratified flow. *International Journal of Multiphase Flow*, **16**, 567–578.
- SCHWEILLER, T. 1986. Dynamics of powder-snow avalanches. *Mitteilungen der versuchsanstalt für Wasserbau, Hydrologie und Glaziologie, Zurich*, **81**, 115.
- SCHMINCKE, H.-U. 1974. Volcanological aspects of peralkaline silicic welded ash-flow tuffs. *Bulletin Volcanologique*, **38**, 594–636.
- SCHMINCKE, H.-U. & SWANSON, D. A. 1967. Laminar viscous flowage structures in ash-flow tuffs from Gran Canaria, Canary Islands. *Journal of Geology*, **75**, 641–664.
- SCHMINCKE, H.-U., FISHER, R. V. & WATERS, A. C. 1973. Antidune and chute and pool structures in the base surge deposits of the Laacher See area, Germany. *Sedimentology*, **20**, 553–574.
- SCHUMACHER, R. & MUES-SCHUMACHER, U. 1996. The Kizilkaya ignimbrite – an unusual low-aspect-ratio ignimbrite from Cappadocia, central Turkey. *Journal of Volcanology and Geothermal Research*, **70**, 107–121.
- SCHUMACHER, R. & SCHMINCKE, H.-U. 1990. The lateral facies of ignimbrites at Laacher See volcano. *Bulletin of Volcanology*, **52**, 271–285.
- SCHUMACHER, R. & SCHMINCKE, H.-U. 1995. Models for the origin of accretionary lapilli. *Bulletin of Volcanology*, **56**, 626–639.
- SCHÜGERL, K. 1971. Rheological behaviour of fluidized systems. In: DAVIDSON, J. F. & HARRISON, D. (eds) *Fluidization*. Academic Press, London, 261–292.
- SCOTT, A. M. & BRIDGEWATER, J. 1975. Interparticle percolation: a fundamental solids mixing mechanism. *Industrial and Engineering Chemistry: Fundamentals*, **14**, 22–27.
- SCOTT, W. E., HOBLITT, R. P., TORRES, R. C., SELF, S., MARTINEZ, M. L. & NILLOS, T. J. 1996. Pyroclastic flows of the June 15, 1991, climatic eruption of Mount Pinatubo. In: NEWHALL, C. G. & PUNONGBAYAN, S. (eds) *Fire and Mud: Eruptions of Mount Pinatubo, Philippines*. Philippine Institute Volcanology and Seismology, Quezon City & University of Washington Press, Seattle, 545–570.
- SELF, S. 1983. Large-scale silicic phreatomagmatism; a case study from New Zealand. *Journal of Volcanology and Geothermal Research*, **17**, 433–469.
- SELF, S. & SYKES, M. L. 1996. Field guide to the Bandelier Tuff and Valles caldera. *New Mexico Bureau of Mines and Mineral Resources Bulletin*, **134**, 5–57.
- SELF, S., GOFF, F., GARDNER, J. N., WRIGHT, J. V. & KITE, W. M. 1986. Explosive rhyolitic volcanism in Jemez mountains: vent locations, caldera

- development and relation to regional structure. *Journal of Geophysical Research*, **B91**, 1779–1798.
- SELIM, M. S., KOTHARI, A. C. & TURIAN, R. M. 1983. Sedimentation of multisized particles in concentrated suspensions. *American Institute of Chemical Engineers Journal*, **29**, 1029–1038.
- SEVILLE, J. P. K., SILOMON-PFLUG, H. & KNIGHT, P. C. 1998. Modelling of sintering in high temperature gas fluidisation. *Powder Technology*, **97**, 160–169.
- SHARP, R. P. 1942. Mudflow levees. *Journal of Geomorphology*, **5**, 222–227.
- SHERIDAN, M. F. 1971. Particle-size characteristics of pyroclastic tuffs. *Journal of Geophysical Research*, **B76**, 5627–5634.
- SHERIDAN, M. F. 1979. Emplacement of pyroclastic flows: a review. In: CHAPIN, C. E. & ELSTON, W. E. (eds) *Ash-flow Tuffs*. Geological Society of America Special Paper, **180**, 125–136.
- SHERIDAN, M. F. & RAGAN, D. M. 1976. Compaction of ash-flow tuffs. In: CHILINGARIAN, G. V. & WOLFF, K. H. (eds) *Compaction of coarse-grained sediments, II, Developments in Sedimentology*. Elsevier, Amsterdam, 677–713.
- SHOOK, C. A. & DANIEL, S. M. 1965. Flow of suspensions of solids in pipelines, Part 1. Flow with a stable stationary deposit. *Canadian Journal of Chemical Engineering*, **43**, 56–61.
- SHOOK, C. A., GILLIES, R., HAAS, D. B., HUSBAND, W. H. W. & SMALL, M. 1982. Flow of coarse and fine sand slurries in pipelines. *Journal of Pipelines*, **3**, 13–21.
- STIGURDSSON, H. & CAREY, S. 1989. Plinian and co-ignimbrite tephra fall from the 1815 eruption of Tambora volcano. *Bulletin of Volcanology*, **51**, 243–270.
- STIGURDSSON, H., CAREY, S. N. & FISHER, R. V. 1987. The 1982 eruption of El Chichon volcano, Mexico 3: Physical properties of pyroclastic surges. *Bulletin of Volcanology*, **49**, 467–488.
- SIMONS, S. R. J. 1996. Modelling of agglomerating systems: from spheres to fractals. *Powder Technology*, **87**, 29–41.
- SIMPSON, J. 1997. *Gravity Currents in the Environment and the Laboratory*, 2nd edition, Cambridge University Press, Cambridge.
- SISSON, T. W. 1995. Blast ashfall deposit of May 18, 1980 at Mount St Helens, Washington. *Journal of Volcanology and Geothermal Research*, **66**, 203–216.
- SMITH, G. A. 1986. Coarse-grained nonmarine volcanoclastic sediment – terminology and depositional process. *Geological Society of America Bulletin*, **97**, 1–10.
- SMITH, G. A. & LOWE, D. R. 1991. Lahars: volcano-hydrological events and deposition in the debris flow – hyperconcentrated flow continuum. In: FISHER, R. V. & SMITH, G. A. (eds) *Sedimentation in Volcanic Settings*. Special Publication, Society of Economic Paleontologists and Mineralogists, **45**, 59–70.
- SMITH, R. L. 1960. Zones and zonal variations in welded ash flows. *US Geological Survey, Professional Papers*, **354-F**, 149–159.
- SOHN, Y. K. 1995. Traction-carpet stratification in turbidites – fact or fiction? – Discussion. *Journal of Sedimentary Research*, **A65**, 703–705.
- SOHN, Y. K. 1997. On traction-carpet sedimentation. *Journal of Sedimentary Research*, **67**, 502–509.
- SOHN, Y. K. & CHOUGH, S. K. 1989. Depositional processes of the Suwobong Tuff Ring, Cheju Island (Korea). *Sedimentology*, **36**, 837–855.
- SOHN, Y. K. & CHOUGH, S. K. 1993. The Udo Tuff Cone, Cheju Island, South Korea – transformation of pyroclastic fall into debris fall and grain flow on a steep volcanic cone slope. *Sedimentology*, **40**, 769–786.
- SPARKS, R. S. J. 1975. Stratigraphy and geology of the ignimbrites of Vulcini volcano, central Italy. *Geologische Rundschau*, **64**, 497–523.
- SPARKS, R. S. J. 1976. Grain size variations in ignimbrites and implications for the transport of pyroclastic flows. *Sedimentology*, **23**, 147–188.
- SPARKS, R. S. J. 1978. Gas release rates from pyroclastic flows: an assessment of the role of fluidization in their emplacement. *Bulletin of Volcanology*, **41**, 1–9.
- SPARKS, R. S. J. 1997. Causes and consequences of pressurisation in lava dome eruptions. *Earth and Planetary Science Letters*, **150**, 177–189.
- SPARKS, R. S. J. & WALKER, G. P. L. 1977. The significance of vitric-enriched air-fall ashes associated with crystal-enriched ignimbrites. *Journal of Volcanology and Geothermal Research*, **2**, 329–341.
- SPARKS, R. S. J., BURSIK, M. I., CAREY, S. M., GILBERT, J. S., GLAZE, L. S., SIGURDSSON, H. & WOODS, A. W. 1997a. *Volcanic Plumes*. Wiley, Chichester.
- SPARKS, R. S. J., FRANCIS, P. W., HAMER, R. D., PANKHURST, R. J., O'CALLAGHAN, L. O., THORPE, R. S. & PAGE, R. 1985. Ignimbrites of the Cerro Galán Caldera, NW Argentina. *Journal of Volcanology and Geothermal Research*, **24**, 205–248.
- SPARKS, R. S. J., GARDEWEG, M. C., CALDER, E. S. & MATTHEWS, S. J. 1997b. Erosion by pyroclastic flows on Lascar volcano, Chile. *Bulletin of Volcanology*, **58**, 557–565.
- SPARKS, R. S. J., SELF, S. & WALKER, G. P. L. 1973. Products of ignimbrite eruptions. *Geology*, **1**, 115–118.
- SPARKS, R. S. J., TAIT, S. R. & YANEV, Y. 1999. Dense welding caused by volatile resorption. *Journal of the Geological Society, London*, **156**, 217–225.
- SPARKS, R. S. J., WILSON, L. & HULME, G. 1978. Theoretical modelling of the generation, movement and emplacement of pyroclastic flows by column collapse. *Journal of Geophysical Research*, **B83**, 1727–1739.
- SPENCER, A. J. M. 1981. Deformation of ideal granular materials. In: HOPKINS, H. G. & SWELL, M. J. (eds) *Mechanics of Solids*. Pergamon Press, Oxford, 607–651.
- STEIN, M., SEVILLE, J. P. K. & PARKER, D. J. 1998. Attrition of porous glass particles in a fluidised bed. *Powder Technology*, **100**, 242–250.
- STEVEN, T. A. & LIPMAN, P. W. 1976. *Calderas of the San Juan Volcanic Field, South-western Colorado*. US Geological Survey, Professional Papers, **958**, 1–35.
- STEVENS, D. J. & BRIDGEWATER, J. 1978. The mixing and segregation of cohesionless particulate materials: Part 1, Failure zone formation; Part 2, Microscopic mechanisms for particles differing in size. *Powder Technology*, **21**, 17–44.
- STOW, D. A. V. & WETZEL, A. 1990. Hemiturbidite: a new type of deep-water sediment. In: COCHRAN, J. R. & STOW, D. A. V. (eds) *Proceedings of the Ocean Drilling Programme, Scientific Results*, **116**, 25–34.
- STRAUB, S. 1994. *Rapid granular flow in subaerial pyroclastic flows*. Dissertation thesis, University of Würzburg (in German), 404 pp.
- STRAUB, S. 1996. Self-organization in the rapid flow of granular material: evidence for a major flow mechanism. *Geologische Rundschau*, **85**, 85–91.
- STRECK, M. J. & GRUNDER, A. L. 1995. Crystallization and welding variations in a widespread ignimbrite sheet – the Rattlesnake Tuff, Eastern Oregon, USA. *Bulletin of Volcanology*, **57**, 151–169.
- SUGIOKA, I. & BURSIK, M. 1995. Explosive fragmentation of erupting magma. *Nature*, **373**, 689–692.
- SUMNER, J. M. & BRANNEY, M. J. 2002. The emplacement history of a remarkable heterogeneous, chemically zoned, rheomorphic and locally lava-like ignimbrite: 'TL' on Gran Canaria. *Journal of Volcanology and Geothermal Research*, **115**, 109–138.
- SUZUKI-KAMATA, K. 1988. The ground layer of Ata pyroclastic flow deposit, southwestern Japan – evidence for the capture of lithic fragments. *Bulletin of Volcanology*, **50**, 119–129.
- SUZUKI-KAMATA, K. & KAMATA, H. 1990. The proximal facies of the Tosu pyroclastic flow deposit erupted from Aso Caldera, Japan. *Bulletin of Volcanology*, **52**, 325–333.
- SUZUKI-KAMATA, K. & UI, T. 1982. Grain orientation and depositional ramps as flow direction indicators of a large scale pyroclastic flow deposit in Japan. *Geology*, **10**, 429–432.
- TALBOT, J. P., SELF, S. & WILSON, C. J. N. 1994. Dilute gravity current and rain-flushed ash deposits in the 1.8 ka Hatepe Plinian deposit, Taupo, New Zealand. *Bulletin of Volcanology*, **56**, 538–551.
- TODD, S. P. 1989. Stream-driven, high-density gravelly traction carpets – possible deposits in the Trabeg Conglomerate Formation, SW Ireland and some theoretical considerations of their origin. *Sedimentology*, **36**, 513–530.
- TORRES, R. C., SELF, S. & MARTINEZ, M. L. 1996. Secondary pyroclastic flows from the June 15, 1991, ignimbrite of Mount Pinatubo. In: NEWHALL, C. G. & PUNONGBAYAN, S. (eds) *Fire and Mud: Eruptions of Mount Pinatubo, Philippines*. Philippine Institute of Volcanology and Seismology, Quezon City, University of Washington Press, Seattle, 665–678.
- TRIGILIA, R. & WALKER, G. P. L. 1986. The Onano spatter flow, Italy: evidence for a new ignimbrite depositional mechanism. (Abstract.) *International Volcanological Congress, New Zealand 1986*.
- TRITTON, D. J. 1988. *Physical Fluid Dynamics*. Clarendon Press, Oxford.
- TURNER, J. S. 1979. *Buoyancy Effects in Fluids*. Cambridge University Press, Cambridge.
- UI, T. 1973. Exceptionally far-reaching thin pyroclastic flows in southern Kyushu, Japan. *Bulletin of the Volcanological Society of Japan*, **18**, 153–

- 168.
- UI, T., KOBAYASHI, T. & SUZUKI-KAMATA, K. 1992. Calderas and pyroclastic flows in southern Kyushu. In: KATO, H. & NORO, H. (eds) *29th International Geological Congress Field Trip Guide Book, Volume 4. Volcanoes and Geothermal Fields of Japan*. Geological Survey of Japan, 245–276.
- UI, T., MATSUWO, N., SUMITA, M. & FUJINAWA, A. 1999. Generation of block and ash flows during the 1990–1995 eruption of Unzen volcano, Japan. *Journal of Volcanology and Geothermal Research*, **89**, 123–137.
- UI, T., SUZUKI-KAMATA, K., MATSUSUE, R., FUJITA, K., METSUGI, H. & ARAKI, M. 1989. Flow behavior of large-scale pyroclastic flows – evidence obtained from petrofabric analysis. *Bulletin of Volcanology*, **51**, 115–122.
- VALENTINE, G. A. 1987. Stratified flow in pyroclastic surges. *Bulletin of Volcanology*, **49**, 616–630.
- VALENTINE, G. A. & FISHER, R. V. 1986. Origin of layer-1 deposits in ignimbrites. *Geology*, **14**, 146–148.
- VALENTINE, G. A. & GIANNETTI, B. 1995. Single pyroclastic beds deposited by simultaneous fallout and surge processes – Roccamonfina Volcano, Italy. *Journal of Volcanology and Geothermal Research*, **64**, 129–137.
- VALENTINE, G. A. & WOHLLETZ, K. H. 1989. Numerical models of Plinian eruption columns and pyroclastic flows. *Journal of Geophysical Research*, **B94**, 1867–1887.
- VALENTINE, G. A., BUESCH, D. C. & FISHER, R. V. 1989. Basal layered deposits of the Peach Springs Tuff, Northwestern Arizona, USA. *Bulletin of Volcanology*, **51**, 395–414.
- VALENTINE, G. A., WOHLLETZ, K. H. & KIEFFER, S. W. 1992. Effects of topography on facies and compositional zonation in caldera-related ignimbrites. *Geological Society of America Bulletin*, **104**, 154–165.
- VOIGHT, B. 1978. *Rockslides and avalanches: 1. Natural Phenomena*. Elsevier, Amsterdam.
- VROLIJK, P. J. & SOUTHARD, J. B. 1998. Experiments on rapid deposition of sand from high-velocity flows. *Geoscience Canada*, **24**, 45–54.
- WALKER, G. P. L. 1971. Grain-size characteristics of pyroclastic deposits. *Journal of Geology*, **79**, 696–714.
- WALKER, G. P. L. 1972. Crystal concentration in ignimbrites. *Contributions to Mineralogy and Petrology*, **36**, 135–146.
- WALKER, G. P. L. 1981. Characteristics of two phreatoplinian ashes, and their water flushed origin. *Journal of Volcanology and Geothermal Research*, **9**, 395–407.
- WALKER, G. P. L. 1983. Ignimbrite types and ignimbrite problems. *Journal of Volcanology and Geothermal Research*, **17**, 65–88.
- WALKER, G. P. L. 1984. Characteristics of dune-bedded pyroclastic surge bedsets. *Journal of Volcanology and Geothermal Research*, **20**, 281–296.
- WALKER, G. P. L. 1985. Origin of coarse lithic breccias near ignimbrite source vents. *Journal of Volcanology and Geothermal Research*, **25**, 157–171.
- WALKER, G. P. L. & MCBROOME, L. A. 1983. Mount St. Helens 1980 and Mount Pelee 1902 – flow or surge. *Geology*, **11**, 571–574.
- WALKER, G. P. L., HAYASHI, J. N. & SELF, S. 1995. Travel of pyroclastic flows as transient waves – implications for the energy line concept and particle-concentration assessment. *Journal of Volcanology and Geothermal Research*, **66**, 265–282.
- WALKER, G. P. L., SELF, S. & FROGGATT, P. C. 1981a. The ground layer of the Taupo ignimbrite – a striking example of sedimentation from a pyroclastic flow. *Journal of Volcanology and Geothermal Research*, **10**, 1–11.
- WALKER, G. P. L., WILSON, C. J. N. & FROGGATT, P. C. 1980. Fines depleted ignimbrite in New Zealand – the product of a turbulent pyroclastic flow. *Geology*, **8**, 245–249.
- WALKER, G. P. L., WILSON, C. J. N. & FROGGATT, P. C. 1981b. An ignimbrite veneer deposit – the trail-marker of a pyroclastic flow. *Journal of Volcanology and Geothermal Research*, **9**, 409–421.
- WALTON, O.R. 1983. Particle-dynamics calculations of shear flow. In: JENKINS, J. T. & SATAKE, M. (eds) *Mechanics of Granular Materials: New Models and Constitutive Relations*. Elsevier, Amsterdam, 327–338.
- WASP, E. J., KENNY, J. P. & GANDHI, R. L. 1977. *Solid-Liquid Flow Slurry Pipeline Transportation, Volume 1*. Series on Bulk Materials Handling. Trans Tech Publications, Houston, TX.
- WATERS, A. C. & FISHER, R. V. 1971. Base surges and their deposits: Capelinhos and Taal volcanoes. *Journal of Geophysical Research*, **B76**, 5596–5614.
- WEILAND, R. H., FESSAS, Y. P. & RAMARAO, B. V. 1984. On instabilities arising during sedimentation of 2-component mixtures of solids. *Journal of Fluid Mechanics*, **142**, 383–389.
- WEN, C.-Y. & SIMONS, H. P. 1959. Flow characteristics in horizontal fluidized solids transport. *American Institute of Chemical Engineers Journal*, **5**, 257–264.
- WILLIAMS, G. 1964. Some aspects of the aeolian saltation load. *Sedimentology*, **3**, 257–287.
- WILLIAMS, J.C. 1976. The segregation of granular materials: a review. *Powder Technology*, **15**, 245–251.
- WILSON, C. J. N. 1980. The role of fluidisation in the emplacement of pyroclastic flows: an experimental approach. *Journal of Volcanology and Geothermal Research*, **8**, 231–249.
- WILSON, C. J. N. 1984. The role of fluidization in the emplacement of pyroclastic flows 2. Experimental results and their interpretation. *Journal of Volcanology and Geothermal Research*, **20**, 55–84.
- WILSON, C. J. N. 1985. The Taupo eruption, New-Zealand: II. The Taupo ignimbrite. *Philosophical Transactions of the Royal Society of London Series A*, **314**, 229–310.
- WILSON, C. J. N. 1986. Pyroclastic flows and ignimbrites. *Science Progress*, **70**, 171–207.
- WILSON, C. J. N. 1997. Emplacement of the Taupo ignimbrite. *Nature*, **385**, 306–307.
- WILSON, C. J. N. & HILDRETH, W. 1997. The Bishop Tuff: new insights from eruptive stratigraphy. *Journal of Geology*, **105**, 407–439.
- WILSON, C. J. N. & HILDRETH, W. 1998. Hybrid fall deposits in the Bishop Tuff, California: A novel pyroclastic depositional mechanism. *Geology*, **26**, 7–10.
- WILSON, C. J. N. & WALKER, G. P. L. 1982. Ignimbrite depositional facies – the anatomy of a pyroclastic flow. *Journal of the Geological Society, London*, **139**, 581–592.
- WILSON, C. J. N., HOUGHTON, B. F., KAMP, P. J. J. & MCBROOME, M. O. 1995. An exceptionally widespread ignimbrite with implications for pyroclastic flow emplacement. *Nature*, **378**, 605–607.
- WILSON, L. & HEAD, J. W. 1981. Morphology and rheology of pyroclastic flows and their deposits, and guidelines for future observations. In: LIPMAN, P. W. & MULLINEAUX, D. R. (eds) *The 1980 Eruptions of Mount St Helens, Washington, USA*. US Geological Survey, Professional Papers, **1250**, 513–524.
- WOHLLETZ, K. H. & SHERIDAN, M. F. 1979. A model of pyroclastic surge. In: CHAPIN, C. E. & ELSTON, W. E. (eds) *Ash-flow Tuffs*. Geological Society of America, Special Papers, **180**, 177–194.
- WOHLLETZ, K. H. & VALENTINE, G. A. 1990. Computer simulations of explosive volcanic eruptions. In: RYAN, M. P. (ed.) *Magma Storage and Transport*. Wiley, Chichester, 113–135.
- WOHLLETZ, K. H., MCGETCHIN, T. R., SANDFORD, M. T. & JONES, E. M. 1984. Hydrodynamic aspects of caldera-forming eruptions: numerical models. *Journal of Geophysical Research*, **B89**, 8269–8285.
- WOLFF, J. A. & WRIGHT, J. V. 1981. Rheomorphism of welded tuffs. *Journal of Volcanology and Geothermal Research*, **10**, 13–34.
- WOODS, A. W. & BURSİK, M. I. 1994. A laboratory study of ash flows. *Journal of Geophysical Research*, **B99**, 4375–4394.
- WOODS, A. W., BURSİK, M. I. & KURBATOV, A. V. 1998. The interaction of ash flows with ridges. *Bulletin of Volcanology*, **60**, 38–51.
- WOODS, A. W., SPARKS, R. S. J., RITCHIE, L. J., BATEY, J., GLADSTONE, C. & BURSİK, M. I. 2002. The explosive decompression of a pressurized volcanic dome: the 26 December 1997 collapse and explosion of Soufrière Hills Volcano, Montserrat. In: DRUITT, T. H. & KOKELAAR, B. P. (eds) *The Eruption of Soufrière Hills Volcano, Montserrat, From 1995 to 1999*. Geological Society, London, Memoirs, **21**, 457–466.
- WRIGHT, J. V. 1981. The Rio Caliente ignimbrite: analysis of a compound intraplinian ignimbrite from a major late Quaternary Mexican eruption. *Bulletin of Volcanology*, **44**, 189–212.
- WRIGHT, J. V. & WALKER, G. P. L. 1981. Eruption, transport and deposition of ignimbrite – a case-study from Mexico. *Journal of Volcanology and Geothermal Research*, **9**, 111–131.
- YAMAMOTO, T., TAKARADA, S. & SUTO, S. 1993. Pyroclastic flows from the 1991 eruption of Unzen volcano, Japan. *Bulletin of Volcanology*, **55**, 166–175.
- YIH, C.-S. 1980. Stratified flows. Academic Press, New York, 103–141.
- YOKOYAMA, S. 1974. Flow and emplacement mechanism of the Ito pyroclastic flow from Aira caldera, Japan. *Tokyo Kyoiku Daigaku Scientific Report*, **C12**, 17–62.

- ZALASIEWICZ, J. A., HUDSON, J. D., BRANNEY, M. J. & BÖHM, M. F. 1997. Emplacement of catastrophic submarine gravity flow deposit (Scheck Breccia, Austria): insights from matrix exceptionally preserved by early cementation. (Abstract.) *In: 18th International Association of Sedimentologists Regional Meeting of Sedimentology, Heidelberg, Germany, GAEA, Heidelbergensis*, **3**, 370, Heidelberg, Germany.
- ZHANG, Y. & CAMPBELL, C. S. 1992. The interface between fluid-like and solid-like behaviour in two-dimensional granular flows. *Journal of Fluid Mechanics*, **237**, 541–568.
- ZHANG, Y. & REESE, J. M. 2000. The influence of the drag force due to the interstitial gas on granular flows down a chute. *International Journal of Multiphase Flow*, **26**, 2049–2072.
- ZIMMELS, Y. 1983. Theory of hindered sedimentation of polydisperse mixtures. *American Institute of Chemical Engineers Journal*, **29**, 669–676.
- ZINGG, A. W. 1953. Some characteristics of aeolian sand movement by saltation process. *Centre Nationale de la Recherche Scientifique*, **13**, 197–208.

Index

References to the page numbers of figures are given in *italic*, tables in **bold** and definitions are highlighted by a star*

- Acatlán ignimbrite, Mexico 49, 58, 59, 61, 63–64, 91
accretion 77
 adhesion-enhanced 74, 76
 lateral 90, 101, 115
accumulative flow 47, 123*
accumulative velocity 91, 123*
acoustic fluidization *see* acoustic mobilization
acoustic mobilization 35
aerodynamic drag 119
agglomerate lithofacies, massive 61, 62–63, 123*
agglomeration 1, 83–84, 121, 123* *see also* electrostatic agglomeration; moist agglomeration
agglutination 84, 123*
aggradation 16, 23, 37, 39, 88, 88, 93, 95, 98, 102, 109, 114, 115, 117, 119–121
 adhesion-enhanced 76, 76
 quasi-steady 74
 rate of 2, 16, 41, 48, 56, 74, 88
 surface 87
 see also progressive aggradation; stepwise aggradation
aggregate fluidization 31, 34, 84
air ingestion, effects on flow 2, 84, 91, 118
Aira caldera, Japan 73
amalgamation 123*
AMS *see* magnetic susceptibility, anisotropy
architecture 123*
 conceptualizing 87–91
Arico ignimbrite, Tenerife 55, 79, 82, 96, 98, 104, 106, 112
ash
 finest-poor 106
 generation by attrition 121
ash-cloud
 ground-hugging 41
 low-concentration 108–109
 surge deposits 98
 turbulent 28, 49
ash-fall
 lamination 74, 83
 layers 1, 76, 80–81, 109
ash-flow tuff *see* ignimbrite
Aso caldera ignimbrite, Japan 58
aspect ratio 1, 117–118, 120, 121, 123*
Ata ignimbrite, Japan 18, 20, 91
attenuation structures 46
attrition 85, 121
autosuspending slab model 3
avalanches 12, 35, 57, 60, 66 *see also* basal avalanches; debris avalanches

Bandelier Tuffs, USA 7, 52, 54, 61, 71, 79, 84, 96–97, 98, 101, 113
basal avalanches 15, 123*
basal concentration layer 42, 92, 111
basal ignimbrite layer 97, 99–109
basal shear layer 1, 9, 46
bed form 34, 37, 60, 66, 74, 77, 99, 104–105, 108 *see also* dunes; erosion; load-and-flame structures; load balls; scour; shoals
bed-load
 concentration 41
 transport 74, 93
bedding plane/surface 123*
Bezymianny, Kamchatka, Russia, 30 March 1956 8, 109
billows *see* transverse vortices

Bingham-type plug flow 1
Bishop Tuff, USA 7, 56, 71, 91, 115, 117
block-and-ash flow deposits 1–2, 27, 28, 123* *see also* Merapi-type block-and-ash flow
body transformation of current 10, 20
bore 19, 20
Bouma sequence 98
boundary-layer shear 15
braiding, effects on transverse lithofacies 111
bubbling 32–33
buoyancy 29, 30, 34, 39, 42, 46–49, 66, 101
 forces 16–18, 77
 of density currents 13, 15–16, 21
 segregation by 14, 29, 34, 41, 76
 support by 60, 94, 119
 thermally-induced 37
 see also clasts
burial compaction 57, 61, 83
bypassing 111, 123*

caldera 57, 61, 115–117
 collapse 7, 100, 115, 117, 121
Campanian Tuff, Italy 9, 18, 20, 106
Campi Flegrei, Italy 61
canyon-to-fan transition 16
capacity 123*
Cape Riva ignimbrite, Santorini, Greece 65, 75, 109
Cape Loumaravi, Santorini, Greece 107
Capel Curig Volcanic Formation, Wales 108
Carpenter Ridge Tuff, USA 113
cataclastic textures 28
cat's paw terminations 47, 48, 115
Cerro Galan ignimbrite, Argentina 108
Cerro Hudson lahar deposit, Chile, 1991 111
channelling 18, 24, 32–33, 66, 91
chemical zonation, massive ignimbrites 12–13, 46, 84, 87
chute-and-pools 17, 74
clasts
 abrasion and breakage 2, 29, 56
 buoyancy 23, 24–25, 34, 42
 comminution 29
 concentration 8, 20, 29, 33–34, 37–39, 41, 43, 46–47, 49, 67, 92–93, 100
 profiles 2, 4
 diversity 2, 23
 interactions/collisions 29, 33, 39, 46
 support by 20, 25, 25, 28
 population 14, 29, 120
 size 28, 56
 support *see* support
 see also grain; particles; segregation; suspension clast population
co-ignimbrite ash plume 1, 9, 10, 15–16, 29, 82–83, 91, 95, 100, 109
co-ignimbrite lag breccia 9
coalescence 123*
coarse-particle dispersion 46
cohesionless debris flow 29, 39, 46, 49, 125* *see also* grainflow; modified grainflow; true grainflow
cohesionless grainflow 124*
cohesionless solid-gas systems 35
cohesive debris flows 12, 35, 45–46, 123* *see also* cohesionless debris flow; flow; grainflow; modified grainflow; true grainflow
combustion of vegetation 101

- competence 123*
- composition 5, 51
zonation 2, 46
- compressed air 99
- compressional structures 46
- concentration profiles 37, 39, 40
- condensed sequence 90, 98
- convective processes 30 *see also* thermal convection
- Coulomb friction 47
- Crater Lake, USA 91, 115
- craters
morphology, effect on gas thrusts 7
rim 98
- cross-stratification 1, 20, 28, 37, 57, 69, 74–76, 83, 97, 98, 106–107
upcurrent-dipping 17
- cross-stratified tuffs 97, 110
- cryptic deposit surface 39, 88–89, 90
- current 2–4, 9–11, 49, 77
accumulative 47, 122*
competence 98
concentration/density 8–10, 12, 14, 16, 23, 111
depletive 2–3, 3, 59, 60
dynamics, constraints on 87–116
heterogeneity 23–24
high-concentration 16, 20, 21, 31–32, 34
leading part 125* *see also* leading-edge advance; leading-edge morphologies
low-concentration (dilute) 1, 15–16, 18, 20, 21, 84
low mass-flux 115
mobility 29, 32
modelling 20, 29, 121
non-uniformity 3, 3
rate of advance 101
rheology 118
single surge 2–4, 45, 70, 98
steadiness 2–4, 95, 97
stratified 14–15, 18, 126*
unsteadiness 43–47, 95, 98, 119, 120
quasi-steady flow 2, 3, 37, 91, 92, 125*
waxing and waning 2–4, 24, 30, 37, 43–46, 49, 66–67, 67, 68, 70–71, 76, 77, 88–89, 92, 98–100, 102–103, 108, 126*
velocity 11, 16, 20, 38, 40, 98, 118, 121
turbulence intensity 11–13
profiles 4, 10–13, 21, 46, 100
see also density currents, pyroclastic; density-stratified currents; depletive currents; hyperconcentrated currents/flow; turbidity currents
- debris avalanches 32–33, 35
- debris fall 28, 47, 56, 71, 76, 124*
blocks 10, 26–27, 28
transport 28
- debris flow 119 *see also* cohesionless debris flow; cohesive debris flow
- decompression 7, 8, 56, 84
fluidization 3
- deflation 10, 115
- deflation zone 9, 10, 60
- degassing 33, 57, 66, 70, 84, 101, 120, 121
- density contrast 31, 34
- density currents, pyroclastic 67, 101, 108, 119
behaviour of 16–20
classification of 20, 21, 33
concentrated 34
definition of 1, 125*
deposit-derived 31–32, 101
- deposits 1–2
conceptual framework for 119
head of 124*
- high-concentration 12–13
key concepts in 2–5
laminar 66
lateral migration of 18
mixing zone 10, 11, 15, 24
nature of 10–16
turbulent 7–8, 10, 14, 84
velocity of 41
see also buoyancy; currents; density-stratified currents; flow; fully dilute pyroclastic density currents; granular fluid-based pyroclastic density currents; topography; turbulence
- density-stratified currents 1–2, 9, 10–11, 11, 13–18, 20, 21, 29, 34–35, 39, 41, 48, 60, 77, 92, 108, 111, 117, 121, 126*
- depletive
capacity 99, 101, 123*
competence 91, 92
current 20, 45, 47, 88, 92, 92–93, 100, 115
velocity 17–18, 91, 123*
- depochnons 87–93, 98, 100, 102–103, 109, 113, 121, 123*
architecture 117
petaloid 115
- deposit morphology, lobate 8–9
- deposition 66, 87–91, 98, 111, 115, 119
deceleration-induced 46
during unsteadiness 43–47, 75
effect on current behaviour 49
en masse 39, 45–47
fluctuating 43, 44
from steady currents 37–43
hiatuses in 102
non-uniform 47–49
progradational 89, 100, 102–103
ramp 114
rates of 33–34, 40, 41, 43, 67, 101, 108, 120, 121
see also aggradation; bypass; stratigraphy; retrogradation
- depositional history 121
- depositional isochrons *see* depochrons
- depositional system, dense mobile layer 15–16
- diachroneity 87–88, 87–89, 102–103, 109, 111, 118
- diamicts 84
- diffuse-stratified lithofacies 43, 69, 71–74, 78–79, 87, 96–97, 100–101, 104, 107, 108–110, 112–113, 119
- dilation 29, 47
- direct fallout-dominated deposition 37, 82
- direct fallout-dominated flow-boundary zone 21, 37, 38, 40, 41–43, 44, 57, 60, 76, 80, 83, 108, 119
- direct-suspension sedimentation 37, 40
- disaggregation 108
- disordered lithofacies associations 98
- dispersion 7, 31, 47, 49, 118, 123*
concentration 35
density 11, 30
density stratified 11, 46
dilated 29, 39
high-concentration 34, 46, 56
stationary fluidized 34
see also coarse-particle dispersion; dispersive pressure; particulate dispersions; quick dispersion
- dispersive pressure 29–31, 34, 39, 47, 77
- divisions, ignimbrite 87, 123*
- drag *see* aerodynamic drag; fluid drag
- dunes 37, 57, 60, 74, 76–77, 97, 101 *see also* migrating dunes; starved dunes
- dusty gas 20, 29, 39, 60, 70, 93
- eddies 37, 42–43, 44, 74
development of 13, 19, 20, 21, 25
velocity of 24
- El Chichón, Mexico, 1982 28, 113

- electrostatic agglomeration 56, 84
- elutriation 4, 9, 10, 15–16, 17, **23**, 23, 24, 33–34, 49, 56, 59, 60, 66, 84, 101, 109, 119
- effects on flow 2
- lithofacies 61, 66
- pipes 1, 9, 31, 33, 33, 39, 57, 61, 64–65, 66, 70, 84, 108–109, 119–121, **120**
- entrachrons 87–88, 87–88, 91, 98, 109, 121, 123*
- entrainment 11, 17, 18, 23–25, 32–33, 37, 87 *see also* re-entrainment
- entrainment isochrons *see* entrachrons
- erosion 45, 49, 71, 85, 95, 98–99, 103–104, 108, 112 *see also* channelling; substrate
- eruption
- conditions 99
- conduit 2, 57, **67**
- history 121
- rates 16
- styles
- boil over explosive 7, 8
- collapsing lava domes 1, 8, 8
- fountain-like collapse 1, 4, 10
- lateral blasts 1, 8, 8, 31, 99
- pyroclastic fountaining 1, 7–8, 8, 10, 32
- Soufrière-type 7
- eutaxitic 123*
- lithofacies 82–84, 82
- expansion of air 10–11, 11, 23, 47
- exsolution 84
- fabric 57
- anisotropy 5
- development of 43, 57
- strength 71
- see also* grain fabrics
- Fasnia Formation, Tenerife 69, 71, 111, 114
- fault-scarp growth 115
- fiamme 123*
- finer-depleted pipes, sheets or pods 31, 61, 64–65, 66
- finer-poor 123*
- lithofacies 1, 108
- Fisher ignimbrite, USA 19
- flotsam, pumice 34, 45, 47, 76–77, 94, 95, 101, 123–124*
- flow 2, 12, 18, 20, 37, 91, 124*
- acceleration/deceleration 124*
- axes *see* thalwegs
- laminar 13, 34, 39, 42
- lines 18, 46
- stratification 121
- stripping 18, 111, 115, 124*
- transformations 2, 13, 92, 95
- units 71, 89–90, 91–92, 95, 97, 115, 124*
- boundary 95–97, 100, 103
- see also* air ingestion; cohesionless debris flow; debris flow; elutriation; grainflow; granular flow; gravity flow; interaction with substrate; liquefied flow; modified grainflow; open-channel flow; polydisperse flow; sedimentation; shear flow; slope changes
- flow boundary 124*
- flow-boundary zones 2, 4, 12, 15–16, 19–20, 23, 30–32, 57, 59, 60, 66, 68, 70, 71, 74, 76, 84, 91, 95, 111, 114, 119–121, 124*
- approach to conceptualizing deposition 37–49, 119
- concentration 97
- conditions in 56, 71, 91–92, 96–97, 99, 109, 119, 121
- evolution 4–5, 108
- segregation at 24–25, 24, 41–42
- shear 97
- transformation 92–93, 93–94, 124*
- turbulence 99
- unsteadiness 5, 95
- see also* direct fallout-dominated flow-boundary zone; fluid escape-dominated flow-boundary zone; granular flow-dominated flow-boundary zone; lower flow-boundary zone; traction-dominated flow-boundary zone
- flow-front advance 31, 99
- flow-head
- model 99
- processes 99, 101
- fluid
- density, effects of changes in 16–18, 19
- drag 37
- escape 29–34, 42–43, 47–49, 56, 61, 74, 92–93
- segregation by 24, 34, 66
- support by 15, 21, **23**, 25, 119
- lift 24, 25, 28, 37, 42
- turbulence 13, **23**, 24–25, 37, 39, 45, 48, 74, 92–93
- segregation of clasts in 24–25
- support by 1, 15, 20, 21, 24, 119
- fluid escape-dominated deposition 39–41, 106
- fluid escape-dominated flow-boundary zone 21, 37–47, 56–57, 60, 66, 70, 71, 76–77, 92–97, 100–101, 109, 112, 114, 118–119
- fluidization 31–33, 66, 108, 124* *see also* acoustic fluidization; aggregate fluidization; decompression; gas fluidization; partial fluidization; sedimentation fluidization; stationary fluidization; steam fluidization
- folds 82, 83, 104
- fragmentation 7, 85
- freezing up from the base 35, 39–40
- frictional freezing 43
- frictional interlocking 35, 39, 48–49, 74
- Froude number 16, 124*
- fully dilute pyroclastic density currents 20, 21, **23**, 24, 37, 43, 49, 92–93, 93, 95, 101, 110, 119, 124–125*
- gas 84, 101
- compressibility 10, 121
- escape structures 61, 70
- flow velocity 33
- interactions support mechanism 28
- thrust 7, 8, 10–11
- volume flux 66
- see also* compressed air; dusty gas
- giant fluidized bed/flow 20, 33–34, 45–46, 124*
- gradational flow-boundary deposition 41
- grading patterns 1, 3, 30–31, 31, 43, 45, 56, 71, **120**, 121
- coarse-tail 1, 9, 13, 33, 45, 46, 66–67, 68–69, 77, 91–92, 98
- downcurrent 59
- inverse 3, 9, 13–14, 26–27, 29–30, 30, 34, 43, 45–47, 66–67, **67**, 68–69, 74, 77, 79, 92, 97–98, 101, 108, 110, 112
- inverse coarse-tail 98, 101, 106, **120**
- inverse-to-normal 66, 71, 74
- mirror 69
- normal 67, **67**
- normal-to-inverse 66, 71
- reverse 67, 91
- see also* vertical grading patterns
- grain
- contacts 35
- frictional 118
- quasi-static 35, 47–49
- fabrics 12, 20, 37–39, 41, 51, 56, 74, 119
- directional 74
- imbrication 43, 54–55, 56–57, 60–61
- see also* AMS fabrics; particle fabrics
- interactions/collisions 13, 15, 21, 28–29, 43, 48, 92–93, 94, 101
- support by **23**, 46, 119
- self-fluidization 31, 32
- size 35, 43, 49, 51, 60, 66, 83–84, 92, 95
- grainflow 23, 26, 28–29, 47, 74, 124*

- shearing modified 93
 - see also* cohesionless grainflow
- Granadilla Formation, Tenerife 55, 69, 71, 72, 78
- granular-convective motions 29
- granular flow 1, 17, 26, 29–30, 56, 74, 124*
 - computer simulations 14, 29
 - deposition 39
 - high-concentration 92
 - models 29, 39
 - quasi-static regime 37
 - rapid flow regime 35
 - segregation in 24, 26–28, 29–31, 41, 43, 46, 119
 - theory 29
 - see also* grain flow; modified grain flow
- granular flow-dominated flow-boundary zone 21, 28, 37–39, 40, 43–47, 57, 67, 71, 76, 77, 84, 92, 93, 96, 97–98, 108–109, 112, 114, 119, 121
- granular fluid-based pyroclastic density currents 14, 20, 21, 23, 25, 29, 30, 34–35, 43, 49, 92–93, 93–94, 119, 121, 124*
- granular interactions 101
- granular jumps 16–18, 24
- granular mass 30
- granular segregation 66, 74, 77, 97, 101, 109
 - models 30
 - processes 34, 47
- granular shear 67, 109, 119
- granular temperature 23, 29–35, 39, 41, 47, 74, 95, 108, 124*
- granulometry 2, 5, 11, 16, 24, 49
- gravitational segregation *see* segregation
- gravity flows 37, 62, 119
- Green Tuff ignimbrite, Pantelleria, Italy 82
- ground layers 99, 108
- ground-penetrating radar 75, 121

- Hazen's Law 21, 37
- hemiturbidites 37
- hindered settling 13, 21, 29, 32–34, 39, 41–42, 44, 46–47, 56, 66, 118–121, 124*
 - modelling 33–34
 - support by 23
- Huckleberry Ridge Tuff, USA 106
- Hudson volcano, Chile, lahars 77
- humidity, effects of 33, 76, 108–109
- hydraulic equivalence 120, 124–125*
- hydraulic jumps 2, 16–18, 24, 60, 74, 115 *see also* granular jumps
- hydrodynamic coupling 34
- hydrothermal fluids 59, 61, 66
- hyperconcentrated currents/flow 10, 20, 45, 56, 60, 66, 77, 119–121

- ignimbrite 1–2, 40, 84, 95, 99, 111, 115, 118, 125*
 - aprons 115–116, 116
 - architecture 4–5, 18, 49, 87–118, 121
 - basal layer 108
 - caldera-filling 116–117
 - centre of gravity 33
 - compositionally zoned 87
 - emplacement 3, 9, 12
 - fans 1, 18, 90, 102, 115–116, 116, 118
 - features, interpretation 120
 - lithofacies 51–85, 91–115, 119
 - lobes, dams and levees 18, 47–49, 90, 115, 116, 118
 - plateaux 118
 - poor sorting in 84–85
 - shape of 115–119
 - sheets 1–2, 20, 46, 49, 88, 89, 98, 104, 109, 110, 113, 115–117, 119, 121
 - shields 18, 115, 116
 - shoestring-shaped 115
 - veener deposits 1, 111, 113, 116, 126*
- wedge 88, 88
- zonation 121
 - see also* chemical zonation; Fisher ignimbrite; radial ignimbrite fans and sheets; ribbon ignimbrites; topographically-confined ignimbrites; valley-filling ignimbrites; welded ignimbrites
- ingestion of air 10–12, 16, 23, 47, 101
- interaction with substrate, effects on flow 2, 10
- interlocking *see* particle interlocking
- internal waves 16–18, 19
- interstitial fluids 39, 42
- intra-Plinian ignimbrite 73
- isothermal sheets 83–84
- Ito ignimbrite, Japan 52, 111

- jet model 11, 101
- jumps *see* granular jumps; hydraulic jumps

- Kaimondake volcano, Japan 26
- Kelvin-Helmholtz billows *see* transverse vortices
- Kidnappers ignimbrite, New Zealand 115, 118
- kinematic sieving 30
- kinetic energy 29
- kinetic modelling 29
- Kos Plateau Tuff, Greece 9
- Koya ignimbrite, Japan 9
- Krakatau ignimbrite, Indonesia 9, 115

- La Caleta Formation ignimbrite, SE Tenerife 53, 64, 72, 80–81, 112
- Laacher See ignimbrites, Germany 11, 80, 114
- lag 25, 60, 109
- lagan 33–34, 41, 76–77, 125*
- lahars 77, 119 *see also* Cerro Hudson lahar deposit, Chile
- lapilli deposits, massive and parallel-bedded 44, 77, 79–81, 80–82
- lapilli-tuff
 - lithic-rich 42, 106
 - lithofacies, massive 41, 47, 51, 52–55, 56–57, 58–59, 67, 68–70, 70–71, 74, 78–81, 83, 93, 96–97, 97–98, 100, 100–101, 104–107, 108–111, 112–114, 113, 117
 - welded 83
- lava-like lithofacies 83–84
- leading-edge advance 10–11, 88
- leading-edge morphologies 10, 11, 31
- lee waves 17, 19, 20
- life-raft structures 60–61, 62
- liquefaction 74, 105, 125*
- liquefied flow 34
- lithic blocks 25
 - matrix-supported 9, 46, 120
- lithic breccia 1, 10, 17, 91, 107, 120
- lithic breccia lithofacies, massive to stratified 57, 58–59, 59, 60–61, 70, 96, 100, 105
- lithic lapilli settling 119
- lithic slugs 100
- lithofacies 2, 23, 37, 45, 51, 51–85, 95, 99, 119, 125*
 - architecture 2, 4–5, 100
 - associations 51, 119, 125*
 - at top of ignimbrites 109–110
 - basal 99–109
 - description of 5, 51
 - ideal sequences 51
 - lateral variations of 121
 - longitudinal variations 91–95, 98–111
 - models 51
 - standard sequence 98
 - stratified to massive changes 91–95, 98–99, 126*
 - system 98
 - transverse variations 109–111, 121 *see also* braiding
 - vertical variations 95–99, 121

- see also* agglomerate lithofacies; cross-stratified tuffs; diffuse-stratified lithofacies; disordered lithofacies associations; elutriation; eutaxitic lithofacies; fines-depleted pipes, sheets or pods; fines-poor lithofacies; ignimbrite; lapilli deposits, massive and parallel-bedded; lapilli-tuff lithofacies; lava-like lithofacies; lithic breccia lithofacies; pipes, pods and sheets lithofacies; rheomorphic lithofacies; rhythmic lithofacies associations; stratified and cross-stratified tuffs; thin-bedded lithofacies
- load-and-flame structures 108–109
- load balls 70, 108
- load-welding 84
- loading-liquefaction 70
- lobate terminations 29, 46
- lofting 16–17, 17, 24, 47, 49, 77, 91, 101, 109, 118
- lower flow-boundary zones 2, 4, 9–10, 11–12, 20, 24, 25, 28, 34, 37, 45, 57, 99, 122*
- Lower Pumice 1, Santorini, Greece 57
- magma chamber stratification 121
- magnetic susceptibility, anisotropy 12, 56, 74
- Magnus effect 24
- mass flux 7, 20, 25, 33, 40, 41, 82, 84, 117
- of ignimbrite eruptions 7, 95, 118
- partitioning in density-stratified currents 15–16, 18
- mass transport, models 15–16
- massive 125*
- Matahina ignimbrite, New Zealand 64, 105
- Mayor Island, New Zealand 68
- Mazama ignimbrite, USA 87, 113
- Merapi collapsing lava dome eruption 8
- Merapi-type block-and-ash flow 28
- Mesa Falls Tuff, USA 81
- mesostasis 8
- migrating dunes 43
- Minoan ignimbrite, Santorini, Greece 71, 72, 107, 108
- Miocene ignimbrite, South Korea 105, 109
- models 121
- modified grainflow 12, 20, 21, 28–29, 39, 42–45, 74, 92–93, 93–94, 125*
- Mohr-Coulomb model 33
- moist agglomeration 56
- monodisperse 125*
- Montserrat 92, 95
- Montserrat, 25 June 1997 eruption 8, 18
- Montserrat, 26 December 1997 eruption 62
- Mount St Helens, USA, eruption 35, 48, 49, 71, 74, 95, 109
- Mount St Helens, USA, 18 May 1980 eruption 2, 8, 11, 15, 18, 20, 75, 92, 109
- Mount St Helens, USA, 12 June 1980 ignimbrite 28, 109, 115
- Mount St Helens, USA, 22 July 1980 ignimbrite 48, 115
- Mount St Helens, USA, 7 August 1980 ignimbrite 115
- Mount Pinatubo *see* Pinatubo volcano, Philippines
- Mount Uzen, Japan, 3 June 1991 eruption 8, 15, 18, 28
- Mt Pelée, Martinique, 1902 eruption 15, 18
- Mud Springs Creek, USA 27
- Neapolitan Yellow Tuff, Italy 74
- nepheloid flow 37
- non-cohesive debris flow *see* cohesionless debris flow
- open-channel flow 14, 15
- overburden pressure 35
- overhanging nose 10, 11
- overpassing 32, 42, 44, 45, 47, 49, 60–61, 66, 76–77, 84, 92, 94, 101, 119, 125*
- during deposition 41–42
- of particles 28, 119
- segregation by 24, 26, 28, 28, 30, 30–31, 39
- palaeoslope 114
- palaeotopography 115, 118
- palaeovalleys 116
- partial fluidization 34
- particle
- concentration 2, 20, 37, 41, 71, 108, 119, 121
- profiles 14–16, 14, 21
- fabrics 1
- fractionation 23
- interlocking 35, 56, 84, 120, 121, 125*
- mixing 23
- support 14, 28
- particles, friction between 35
- particulate dispersions 32
- Pavey Arc Breccia, Scafell caldera, UK 63, 63
- Peach Springs Tuff ignimbrite, USA 54, 101, 118
- peperite 105
- percolation 24, 30–32, 34, 39, 41, 47, 74, 76–77, 120, 125*
- permeability 84
- Phira Quarry, Santorini, Greece 68
- phoenix cloud 1, 9, 11, 16, 83, 109
- phreatomagmatism 20, 35, 37, 41, 61, 83
- ash-fall deposit 8, 82
- explosivity 2, 118
- fountaining 7–8
- see also* rootless phreatic explosions
- Pinatubo volcano, Philippines, 15 June 1991 26, 49, 56, 59, 74, 75, 78, 91, 96, 109–111, 113, 117
- pipes, pods and sheets lithofacies 61, 64–65, 66
- plastered base-surge deposits 74
- Plinian eruption fountain 7, 8, 10
- Plinian pumice fallout deposit 55, 77, 79, 82, 84, 89, 91, 96–97, 100, 101, 104
- plug flow 9, 10, 13, 13–14, 23, 34, 43, 46–47 *see also* Bingham-type plug flow
- plug zone 13, 46
- plume 9, 11, 47, 82–83, 109 *see also* co-ignimbrite ash plume
- pneumatic equivalence 14, 28, 28, 124–125*
- polydisperse sedimentation 15, 24, 29, 125*
- polydisperse flow 29, 125*
- ponding 24
- pore fluid pressure, support by 23
- Poris Formation ignimbrite, Tenerife 54–55, 58–59, 71, 73, 104–105
- progressive aggradation 1–2, 9, 11–12, 21, 25, 34, 45–46, 56, 77, 84, 90, 99, 112, 118, 121, 125*
- rate of 4
- pumice 76, 106, 119
- dams 46–49, 77, 98, 120
- fall layers 1, 7, 82, 91
- lapilli 29, 34, 114
- rafts 23, 77, 121
- pumice-rich layers, lenses and pods 42, 46–47, 76, 77–78, 109
- pumiceous snouts, dams and levees 14, 24, 46, 48–49, 48, 56–57, 66, 77, 101, 102, 111, 119, 120
- pyroclast diversity 13, 23–24
- pyroclastic
- flows 13–14, 20, 125*
- flux 93
- fountaining 91, 115
- surges 1–2, 13–15, 17, 20, 39, 42, 74, 88, 98, 109, 113, 125*
- transport across water 9–10
- pyroclastic surge deposits 113, 125*
- quasi-static zones 29, 39
- quick bed 42, 47, 66, 67, 70, 77, 109, 111
- quick dispersion 47
- radial ignimbrite fans and sheets 113, 115–117

- radial spreading 113
radiating flow 24
rain flushing 82–83
rapid flow 125*
Rayleigh-Taylor instabilities 108 *see also* leading edge morphologies
Rattlesnake ignimbrite, USA 118
re-entrainment 29, 103, 111
remobilization, postdepositional 49, 92, 101, 115, 118
research 121
retrogradation 88–89, 102
Reynolds number 12
rheology 4, 7–10, 12, 25, 29–30, 34, 37, 38, 47, 84, 99, 100, 115, 119, 120, 121 *see also* current rheology
rheomorphic lithofacies 57, 83–84, 82, 119
rhythmic lithofacies associations 98
ribbon ignimbrites 113, 115
Richardson number 16, 125*
Rio Caliente ignimbrite, Mexico 68, 73
Robins effect 24
Roccamonfina volcano, Italy 99, 109
rolling and sliding, of particles 25, 56, 100–101, 119
rootless phreatic explosions 109, 110
Rouse number 14–15
 runout
 direction 5
 distance 11, 11, 16, 17, 18, 32–34, 49, 88, 115, 118, 121, 125*
saltation, of particles 15, 20, 24, 24–25, 28, 32, 101, 119, 121
sand waves 28
Santiaguito collapsing lava dome eruption 8
Santorini volcano, Greece 115 *see also* Cape Riva ignimbrite; Cape Loumaravi; Lower Pumice 1; Minoan ignimbrite; Phira Quarry; Upper Scoria 1 Member; Upper Scoria 2 Member
scour 43, 74, 95, 99, 108
 bounding surfaces 4–5
scour splay-and-fade stratification 111, 112–113, 119
sedimentary structures 1, 120
sedimentation 101, 119
 effects on flow 2, 12, 23
 fluidization 32–34, 101
 unsteady 45
 see also direct-suspension sedimentation; polydisperse sedimentation
segregation 2, 4, 10, 14–15, 23–35, 37, 39, 60–61, 66, 67, 70, 76, 84, 101, 113, 119–121
 flow-boundary zone 24, 24–25, 41–42
 gravitational 92
 lateral (transverse) 111
 longitudinal 42
 structures 57, 59
 tractional 56, 111
 see also acoustic mobilization; buoyancy; fluid escape; fluid turbulence; fluidization; granular flow; granular segregation; hindered settling; overpassing; turbulence; vertical segregation
selective filtering 30, 32, 41–45, 45, 47, 60, 66–67, 77, 119–121, 120, 125*
semi-fluidized flow 1, 23, 29, 31
sequence analysis 98
shear 33, 39, 56–57, 59, 66–67, 70, 84, 119
 deformation 108–109
 flow 13
 gradient 29, 71, 119
 intensity 30, 37, 39, 56, 119
 profiles 29, 37
 rates 2, 21, 29–30, 32, 34–35, 40, 41, 47, 49, 92, 97, 111
 see also flow-boundary zones; granular shear; laminar shear
shear-stress 39, 42–43, 44, 108
 profiles 15–16, 43
shear-strain 39, 67
shearing layer 92 *see also* basal shear layer
shearing mass 29–30, 41, 43
shoals, hogs-back 77
Side Pike ignimbrite, UK 109
sieve deposit 46
sillar 126*
sinter-neck 84
slope changes, effects on flow 2, 16, 113 *see also* topography, effects on pyroclastic density currents
slug-flow regime 77
soil schlieren 109
sorting 18, 25, 31, 34, 37, 39, 43–44, 56, 66, 84–85, 120, 121, 126*
Soufrière Hills Volcano, Montserrat 27
source variability 23
splay-and-fade stratification 1, 41, 56, 78, 97, 106, 109–113, 113, 119
squeeze expulsion 30
standard ignimbrite flow-unit 1–4, 69, 91, 98
starved dunes 74
stationary fluidization 32–34, 84
stationary waves 17
steady 126*
steam fluidization 105
stepwise aggradation 30, 37, 43, 44, 74
stratification 1, 5, 43, 51, 57, 60, 83, 101, 120
 bands 71, 74
 current 60, 125*
 horizontal discontinuous 74
 on-lap relationships 56
 pinch-and-swell 74
 spaced 42, 109
 see also cross-stratification; current stratification; flow stratification; magma chamber stratification; scour splay-and-fade stratification; sequence analysis; splay-and-fade stratification; traction stratification
stratified and cross-stratified tuffs 74–76, 116
stratified topographic veneers 111, 113–115
stratigraphy, fall 82
strength, support by 35
Strombolian cone, SE Tenerife 27
Strombolian spatter 61
subcritical currents 15–17, 17, 18, 91, 125*
subsidence 115
substantive acceleration equation 70
substrate 61, 95, 98, 104, 106–107, 121
 erosion 57
 groove-marked 42
 intrusions into 61
 loaded 108–109
 remobilization of 108
 sheared 108–109
 support by 23, 60
substrate-derived lithics 108
supercritical currents 12, 15–17, 17, 19, 24, 91, 101 *see also* rapid flow
support 23, 25–28, 119 *see also* buoyancy; clast interactions; fluid-escape support; fluid turbulence; gas; grain interactions; hindered settling; pore fluid pressure; strength; substrate; traction support; yield strength
surface-roughness effect 30, 34, 101
surge 126* *see also* pyroclastic surges
suspended-load fallout rate 41
suspension clast population 21, 24–25, 25, 60, 126*
suspensions, low-concentration 1, 84, 92
Taal caldera, Philippines 61, 63
talus slopes 56

- Tambora volcano, Indonesia 61
- Taupo ignimbrite, New Zealand 7, 11, 16, 18, 71, 74, 78, 101, 104, 109, 111, 115, 118
- Teide volcano, Tenerife 26
- tephra dyklets 109
- thalwegs 18, 24, 47–48, 57, 66, 70, 76–77, 91, 101
- capture 111
 - effects on transverse lithofacies 111, 113
 - modelling 18
- thermal convection 15, 31, 109
- thermal expansion 15–16, 32, 34, 59, 101, 121
- of air 99
- thin-bedded lithofacies 44, 71–74, 72–73
- time-geometry framework 45, 87–92, 100
- time surfaces 4–5
- Toconquis Ignimbrite Formation 74
- topographic separation *see* decoupling; flow-stripping
- topographically-confined ignimbrites 115–117
- topography
- effects on pyroclastic density currents 1–2, 9, 10, 12–13, 16, 18–20, 21, 24, 37, 46, 56–57, 60, 71, 77, 80, 90, 91, 95, 107, 111, 115, 117–118
 - effects on turbulence 12, 45
 - see also* palaeotopography
- traction
- carpets 21, 42–43, 44, 77, 92, 93, **120**, 126*
 - clast population 24
 - inhibition of 108, 119
 - structures
 - absence of 12
 - sorting 21, **120**
 - stratification 21, 98, 126* - support by **23**
 - turbulence-induced 71
- traction-dominated deposition 4, 20, 24, 25, 37–39, 106, 109–110
- traction-dominated flow-boundary zone 21, 37, 38, 40, 41, 43, 44, 57, 60, 71, 74, 76, 92–93, 93, 95, 96, 98–101, 108, 114, 119
- tractional transport 126*
- tranquil flow *see* subcritical flow
- tree orientation 20
- true grainflow 29 *see also* grainflow
- tuffs 20, 29
- massive fallout 74
 - parallel-bedded and parallel-laminated 81, 83
 - traction-stratified 98
- turbidites 42–43, 74, 98–99 *see also* hemiturbidites
- turbidity currents 10, 16, 20, 25, 35, 37, 66, 111, 119
- high-density 34, 45, 71, 91
 - modelling 15, 18
 - see also* flow-stripping
- turbulence 1, 12, 14–15, 23, 29–30, 32, 66, 71, 93, 101, 108, 119
- density current 7, 10, 84
 - intensity of 43, 91, 93
 - mixing 45–46, 60, 115
 - segregation by 24, 77
 - see also* ash cloud; fluid turbulence
- underflow 15–16, 126*
- uniform 126*
- Upper Merihuaca ignimbrite, Argentina 109
- Upper Scoria 1 Member, Santorini, Greece 62
- Upper Scoria 2 Member, Santorini, Greece 62
- valley-filling ignimbrites 111, 113–118
- valley floor slope 113
- Valley of Ten Thousand Smokes ignimbrite, USA 16, 71, 74, 91, 111, 115–116, 118
- Vanuatu 61
- veener *see* ignimbrite veener deposits
- vent 111, 116
- emissions 98
 - migration 115
 - see also* caldera; eruptive conduit
- vertical grading patterns 34, 44, 66–71, 76–77, 108, **120**
- vertical segregation 30, 33
- vesicles 7, 84
- viscosity 31, 39, 49
- volatiles 2, 7, 33, 84
- volcanic hazards 1–2, 49, 119, 121
- von Kármán's coefficient 14
- vortices 43, 109
- corkscrew 31
 - impingement 109
 - longitudinal 30
 - transverse 10, 18
- Vulcanian eruptions 2, 8
- Vulsini, Italy 61
- wake 10, 11, 109
- wash load *see* suspension clast population
- water, effects of 108, 110 *see also* humidity; moist agglomeration; phreatomagmatism; rain flushing; rootless phreatic explosions
- waves 17, 20 *see also* lee waves; sand waves; stationary waves
- welded agglomerate 61
- welded ignimbrites 10, 46, 51, 82, 108
- high-grade 35
 - intensity 83–84, 95
- welding compaction 57
- postdepositional 84
- White Trachytic Tuff, Italy 78
- winning 47, 77, 109 *see also* turbulence
- Wolverine Creek Tuff ignimbrite, USA 65, 110
- Xáltipan ignimbrite, Mexico 18, 52, 113
- yield strength 13–14, 35, 39, 43, 46–48, 66, 74, **120**
- support by **23**
- Zaragoza ignimbrite, Mexico 87